CHAPTER ONE

INTRODUCTION

1.1 Background of Study

Tobacco is one of the most common addictive stimulants consumed and smoking is the most common manner of consuming tobacco. It stimulates a cocktail and invigorating feeling of wellbeing and gratifying sentiment (Ineichen, 2005). Tobacco smoking which is the practice of burning tobacco and inhaling the particle and gaseous phases (smoke) is done using either tobacco pipes or rolled cigars/cigarettes with or without filter. It was perceived as, a sacred herb by Spaniards, French and Portuguese because of the medicinal attributes (Binorkar and Jani, 2012), and the report by Monardes (1574), shows that a conservative 36 health issues can be treated using tobacco. The medicinal attributes was supported by the publication on the positive impact of tobacco by Anthony Chute which was cited by Gatley (2004). Irrespective of the fact that the nicotine contained in tobacco boosts alertness, enhances the ability to concentrate while eradicating any measure of depression or mood swings; it is implicated in the addictive potential of tobacco and its products because of the interaction between the nicotine and dopamine contained in the human brain. The smoke from a cigarette contains a cocktail of about 7000 chemical species (Cityofhope.org. 2014), and contributes directly or remotely to various health challenges people experience. Oftenly, the manifestation occurs years-on when the individual may not be able to trace the challenge to the cultivated habit. Consequently, the negative health impact of this product from its usage experienced at different degrees and in different ailments amongst direct and indirect users is of great concern.

Cigarette manufacturers, for obvious reasons, are not willing to modify their products to meet world health standards. The use of Tobacco in various forms like cigarette, come with overwhelming negative impact both to humans and the environment O'Connor (2012). The type and degree of these effects to humans or the ecosystem differs but are inter-related.

1.2 Statement of Problem

The act and practice of smoking cigarette also impacts differently amongst respective societies, cultures and ecosystems but generally can be viewed under common mitigating factors(Suhrcke et al., 2006; Townsend et al., 2006; WHO, 2004; WHO, 2011a). As reported, (ASH, 2009) estimates have it that smoking prevalence within the African region will rise by as much as 39 percent by 2030. This is an uphill from a 15.8 percent in 2010 to 21.9 percent 2012 (Blecher and Ross, 2013; Mendez et al., 2012). In Nigeria, smokers spend nearly 10 percent of gross domestic product per capita on manufactured cigarettes annually (Federal Ministry of Health, 2012a, b).

It is unarguably difficult to stop people from the age old practice of smoking cigarete and other tobacco products, even with harsh penalties and or total bans from government and concerned organizations. The size and influence of the tobacco industry globally effectively fustrates efforts targeted at completely stopping the production of tobacco products. The fact that the sector provides jobs and income for people and the governments at various stages of its production (the growing, harvesting, processing of leaves up to the product's (cigarette) manufacturing, distribution and marketing stages), makes control very complicated and challenging.

Within the sub-Saharan Africa, only Chad, Seychelles, Burkina Faso, Congo and Namibia, have put in place the framework convention on tobacco control (FCTC) conditions for establishing a

100 percent smoke-free indoor setting, (WHO, 2010c, 2013d). They have completely banned smoking in places like educational, health care, government, recreational and vulnerable facilities (WHO, 2013b) Lopez *et al.* 1994 and Shafey *et al.* 2003 opined that the sustained rise in cigarette smoking in Africa will be trailed by a sharp prevalence in tobacco linked mortality.

There are a conservative 250 women, 1 billion men and unaccounted-for number of children actively smoking globally today (Prasad, 2015). Meanwhile in every country, populations of active smokers fall within a minority but the effect of their activity creates negative geometric-ripple impact on the overall population. Indications are that more of adolescent populations particularly in developing nations like Nigeria indulge in cigarette smoking than the fully grown adults from the same population; creating the existence of an unsecured, weakening, non-viable and unsustainable work force for such a nation in the coming decades. George (2009) postulated that annually, tobacco usage directly or indirectly kills four times more people than does the combination of other drugs, AIDS, suicides, accidents (vehicular), and homicides.

Eriksen et al. (2012); Esson and Leeder, (2004) reported that most sub-Saharan African countries are still in the early stages of smoking epidemics, valuable opportunities for intervention and primary prevention is very much possible.

Sometime in June 2000, a colleague asked, “Can you device a means of making cigarette smoking safer without stopping people from smoking?” This study is targeted at answering that question thereby meeting the need of the public with regards to safety from the use of tobacco products. The active, second and third hand smokers are put into consideration in the fabrication of these molecularly imprinted polymer (MIP) materials from this research activity.

1.3 Aim and Objectives

The aim of this study is to synthesize an efficient Molecularly Imprinted Polymer (MIP) material that can be used for molecular recognition and sequestration of cancer causing agents from cigarette smoke stream such as tobacco-specific nitrosamine toxicants and their analogues.

The objectives of the study are to:

1. Determine the optimal functional monomer versus template(s) interaction ratio using Proton NMR (^{1}H NMR) and using the result in the synthesis of robust MIPs.

2. Carry out a proof-of-concept experiment using a Quartz Crystal Microbalance method to ascertain the feasibility of using Chitosan in a blend combination with Methacrylic acid.

3. Prepare and perfect the use of hybrid functional monomer materials from a combination of natural (Chitosan) and synthetic (Methacrylic acid) materials in the preparation of the MIPs by determining the functional group transmittances of the prepolymer blends by Fourier Transformed Infra-red Spectroscopy.

4. Determine the optimal individual cross linkers' amount for the MIP synthesis and evaluate their respective characteristic potentials in the recognition and sequestration of the toxicants; by the rebinding studies using HPLC analytical method.

5. Determine the particle and pore sizes, surface area and pore volume of the MIPs; using the Brunauer-Emmett-Teller (BET) and Barrett-Joyner-Halenda (BJH) methods Evaluate the thermal and microscopic attributes using Simultaneous Thermal Analysis, Scanning Electron Microscopy and Transmission Electron Microscopy.

6. Carry out rebinding studies using the synthesized MIPs with the aid of high performance liquid chromatography (HPLC) technique and UV-VIS spectroscopy.

7. Ascertain the real-life efficiency of the prepared MIPs using a machine aided smoking regime. And analyzing the filtrates using HPLC method.

1.4 Justification

Irrespective of the fact that Nigeria has one of the lowest rates of cigarette smoking, a 2012 WHO report and projection from a global tobacco survey, presented Nigeria as having a conservative 20 million (more than 7.2% of the population) active cigarette smokers (GATS, 2012). The number of adult smokers in Nigeria is 4.5million with smoking prevalence of 17.1 percent, leaving the rest active smokers of 8.5million to be adolescents from the young age of 13years to 20years with a smoking prevalence of 18.1 percent (Odukoya *et al*. 2013). They reported an average incidence of lifetime of smoking within youths in secondary schools to be 26.4 percent and this spanned a range of from 7.2 percent to 42.9 percent. This implies that by the next 30 years when the negative impact of cigarette smoking starts manifesting, the country's mature workforce will be an endangered group with consequent retardation in overall manpower input and heightened national expenditure on medical bills as well as burden to the incumbent government.

The clandestine/discrete adolescent smokers on their own pollute additional (secret) places because of the need to keep their activities discrete, with consequent expansion of the endangered environments and increased number of exposed non-smokers; this increases the impact-of-burden. The GATS 2012 reported that, four out of every five active smoker admitted knowing the harmful effect of cigarette smoking, but quitting is challenging. The inability to quit

is scientifically linked to the presence and effect of the addictive component found in tobacco (Nicotine). Contributory to that is, the existence of very weak legislature concerning tobacco and its products usage in Nigeria. As a compromised and vulnerable environment cigarette is readily available even to the underaged and exposed class of the population in Nigeria.

A conservative 0.77 billion kg of difficultly non-degradable cigarette butts are discarded into the environment as litter annually (Healton *et al*., 2011). Nigeria has only approved less than 6 out of the 14 ban types/categories on cigarette and tobacco products; this creates vulnerability potential among populations within the country.

This work will provide a biodegradable filter material which can be used in the efficient sequestration of the inherent toxic and addictive substances obtainable from smoking and thereby help in keeping the populace and the environment healthy.

1.5 Scope of Study

This study investigated the feasibility of using Chitosan in the fabrication of a filter material for the sequestration of toxic substances from the smoke of burnt tobacco product such as cigarette. The approach will be by synthesizing a molecularly imprinted polymer product selective for nicotine and analogues of tobacco specific nitrous amines particularly phenylalanine amide.

The method for determining the best monomer-template ratio using proton NMR (^{1}H NMR) is reported with particular outcome from investigating the use of two reacting ratios of 1:1 and 4:1 of the functional monomer-template systems at three different reaction temperatures of 30^{o}C, 40^{o}C and 60^{o}C. The best condition was used to synthesize a thin film biosensor using quartz crystal microbalance method. A detailed report of using chitosan and methacrylic acid as matrix and functional monomers, nicotine and 3-Phenylpyridine as templates with 1,4-bisacryloyl

pipiradine (BAP) as cross linker in the presence of ammonium persulphate as a UV induced thermal initiator is presented. The result was used as a proof of concept experiment. The preparation of molecularly imprinted polymers specific for nicotine, phenylalanine and a 50:50 blend of the templates by non-covalent bulk polymerization will be detailed.

The impact of using two different cross linkers 1,4-bisacryloyl pipiradine (BAP) and Geranic acid (synthetic and natural cross linkers) in the preparation of the MIPs and NIPs as well as reaction time and rate of heating; was studied. Other characterizations that were carried out and reported are: surface morphology, integrity of produced cavities, functional groups and confirmation of polymerization (FTIR), particle size, ionic nature, thermal stability and imprinting factor.

Assessment of the efficiency in real life sequestration of toxicants from the cigarette smoke by the prepared MIPs and NIPs was investigated and compared with commercially available filters using an adapted machine-aidded smoking regime. The performance was evaluated by HPLC-MS analysis of the resulting filtrates/eluents. This was used to evaluate the feasibility and authenticity of optimizing the fabrication of the filter materials as a more efficient approach for the sequestration of tobacco specific nitrous amines and other toxicants from tobacco smoking activities.

1.6 Significance of Study

This study will assist researchers to build up on the existing knowledge gap in the use of specialty filters for the control of toxicants from air streams irrespective of pollution source.

The feasible prospect of embarking on research where the application of template polymerization and molecular recognition approaches is required for synthesizing utility materials are still budding; this activity will be highly beneficial and directing. On another vain, this study has

stamped-in the feasibility of using bio/natural monomer materials as well as hybrids of natural and synthetic monomers in the preparation of imprinted polymer compounds for low-to-moderate temperature applications as is obtainable to the temperature of cigarette smoke.

The molecular imprinted polymers synthesized from this work can replace existing filters in the cigarette manufacturing industries as well as in other related tobacco processing industries, thereby assisting in the overall reduction and control of negative impact from tobacco consumption activities.

The technique will also provide a platform for separation, purification and concentration of specific interest compounds from crude natural product extracts for use in the manufacturing industries within our immediate environment.

Chapter Two

LITERATURE REVIEW

2.0 Conceptual Framework

Towards the end of the 1920s, German scientists associated incidence of lung cancer to smoking, leading to the first anti-smoking campaign in modern history; it is not exactly a secret that smoking can shave years off your life. Researchers at the University of Bristol figured out that one cigarette shortens a person' life span by 11 whole minutes (Husain *et al.,* 2001). The study, published in the U.S. National Institutes of Health's national library of medicine, took into account, the difference in life expectancy between male smokers and non-smokers and an estimate of the total number of cigarettes a regular male smoker may consume in his lifetime (Hayashida *et al*., 2010).

Using data provided by the office for National Statistics, the researchers found the difference in life expectancy between smokers and non-smokers to be 6.5 years. They calculated that if a man smokes the average number of 5,772 cigarettes a year from the median starting age of 17 until his death at the age of 71, he will consume a total of 311,688 cigarettes in his life-time. Assuming that each cigarette makes the same contribution to the male's death; each cigarette has cost him, on average, 11 minutes of life time.

Mathematically:

6.5 years = 2,374 days and 56,976 hours, or 3,418,560 minutes

5,772 cigarettes per year for 54 years = 311,688 cigarettes

3,418,560/311,688=11 minutes per cigarette.

The overall assumption is that smoking impacts on our health consistently as a plateau all through the life's span of an active smoker assuming that the smoker maintains an averagely

consistent volume of cigarette within this period of life. For the passive smokers, there may be variations with level of impact depending on the environment where contacts are made with cigarette smoke; nonetheless the impact is not lost on either of the parties.

When heat is given to a stick of cigarette, smoke and air combination from different points, leave or enter the cigarette product. This gives rise to different zones known as combustion and the zone of distillation, pyrolysis and pyro synthesis. The flow of product gases, by diffusion leaves the cigarette roll as side stream and mainstream smokes. Figure 2.1 shows the activities. Both streams impact the active smoker as well as the non-smoker but with different degrees of impact. At the start of smoking before getting to the middle of the roll, the non-smoker is exposed to more of the side stream smoke free of the tobacco specific nitrosamine toxicants while the active smoker is exposed to both the side stream smoke components and the mainstream components with the initial reaction products from the heating reaction from the tobacco specific nitrosamine (TSNA). The amount of the TSNA at this stage is still minimal that the tendency is for all of it to be deposited within the lungs and body parts of the active smoker without it being released to the non-smoker (a postulate). From the midpoint of the cigarette, both parties are exposed to both streams but with the active smoker having more of the TSNA than the passive smoker.

Second hand smokes have been analyzed and found to contain 250 similar toxicants and as much as 69 potential carcinogens as is found in directly inhaled cigarette smoke (WHO, 2009). Differences in physicochemical properties exist between side stream mainstream second hand smoke and the ratios of these two streams also differ depending on the make-up of the tobacco product used in manufacturing the product. The latter is directly linked to brain tumors, nasal cavity cancer, lymphoma and leukemia.

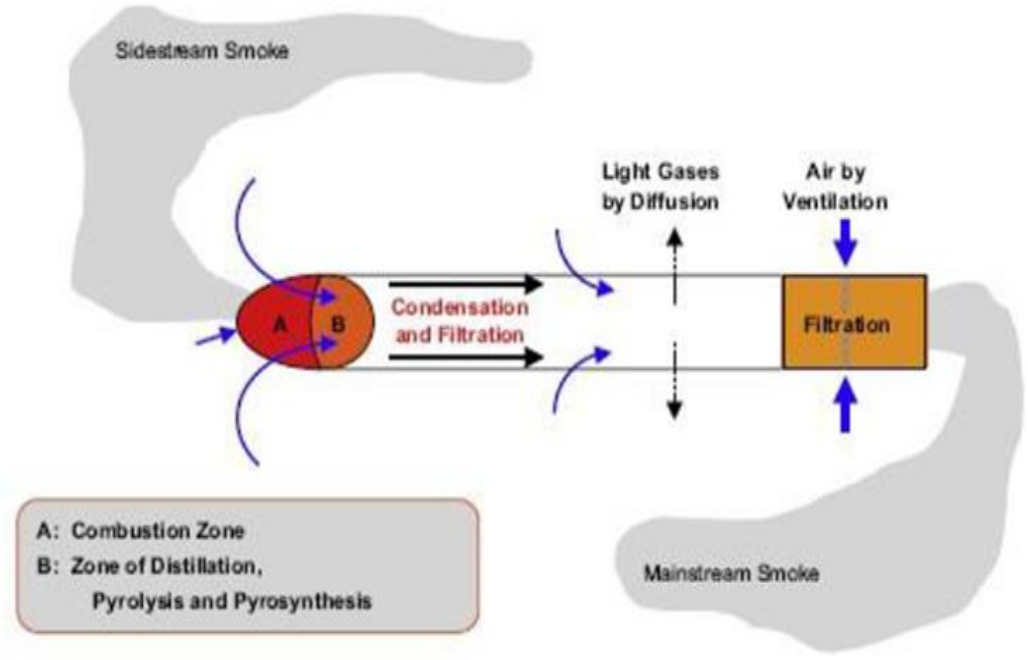

Figure 2.1: Gas and Smoke flow pathways during smoking. (Chaouachi, 2009).

Some of the toxicants substances of interest are:

1**. Nicotine; 3**-(N-Methyl-2-pyrrolidyl) pyridine **(addictive agent)**

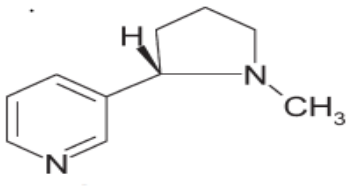

It is a tertiary amine with pyrrolidine as well as pyridine rings. It is a light to dark yellowish liquid, volatile and basic in nature. At a temperature of 15^{o}C nicotine exhibits dual pK of 10.96 (pyrrolidine ring) and 6.16 (pyridine ring) respectively in aqueous environment.

2. Ammonia

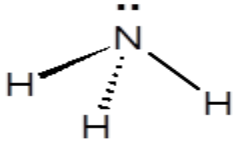

This auxiliary is included towards increasing the frequency of nicotine absorption via the blood fluid and its brain-barrier. It acts by raising the smoke's pH which yields "free nicotine" which is more easily absorbed in vivo as bound nicotine.

3. Tar

Tar is also generated. It is a cocktail of hydrocarbon compounds that are components of the cigarette product in the form of pyrolyzed oily material with mainly charred residue (figure 2.2).

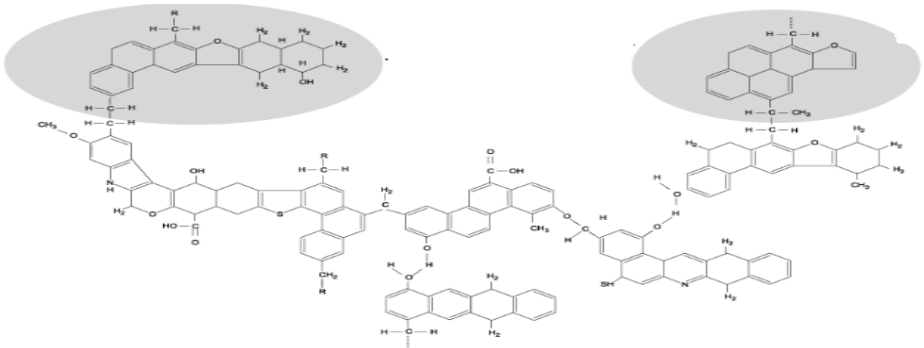

Figure 2.2: **S**tructure of Tar (Veras, Carvalho Jr. and Ferreira, 2002)

4**.** Benzo [α] pyrene (BaP), (a pre-carcinogen of the cigarette tar).

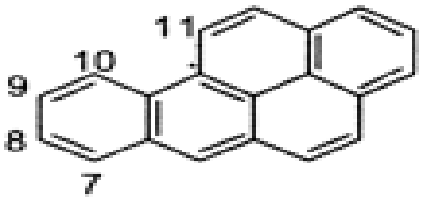

5. Respiratory irritants (acrolein, formaldehyde, phenols**)**.

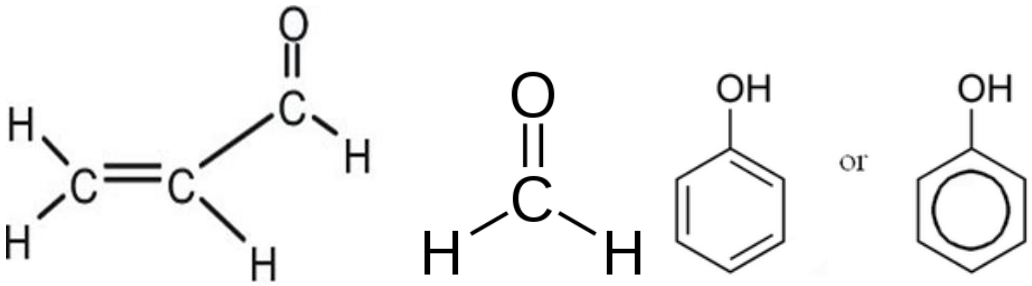

Acrolein formaldehyde and Phenols

These are formed as a result of combusting tobacco leaves and when digested in vivo in humans and animals give benzo [α] pyrene-7, 8-dihydrodiol-9, 10-epoxide.

6. Nicotine-derived nitrosamine ketone or 4-(methylnitrosamino)-1-(3-pyridyl)-1-butanone

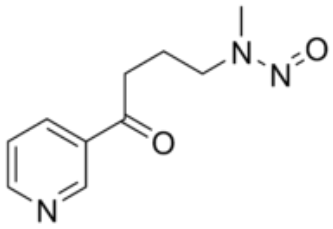

(NNK).

7. N-nitrosonornicotine (NNN),

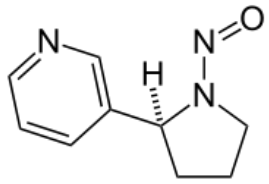

$C_9H_{11}N_3O$ (esophageal and respiratory tract carcinogen)

8. N′-nitrosoanatabine (NAT)

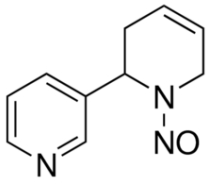

$C_{10}H_{11}N_3O$

9. N-nitrosoanabasine (NAB).

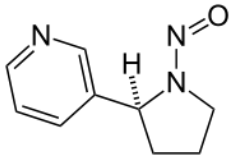

$C_9H_{11}N_3O$ (nasal cavity, liver, and pancreas tumors).

10. 4-(methylnitrosamino)-1-(3-pyridyl)-1-butanol (NNAL)

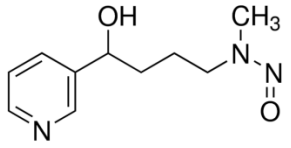

(Lung, nasal cavity, liver, and pancreas carcinogen).

Within the oral cavity of experimental rats, oral tumors occur as a result of impact of blend contact of NNN and NNK swab (Nilsson, 1994).

11. N-Nitrosodiethylamine 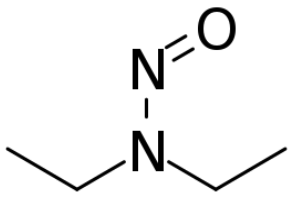

.

This substance is a group 2A carcinogen. It is a potential cancer causing agent (no sufficient human toxicity evidence). The IUPAC prefared name is N,N-Diethylnitrous amide and it is released during cigarette smoking regime.

In addition to the mentioned toxicants, there are two (2) members of the aldehyde family, three(3) of the aza-arenes, three(3) of aromatic amines, nine (9) polycyclic aromatic hydrocarbons, eight (8) heterocyclic aromatic amines, seven (7) inorganic and fifteen (15) organic carcinogenic compounds in a stream of tobacco smoke. This gives a total of 55 potent cancer causing toxicants. Nicotine and nitrosamines propagate tumor growth via activation of the nicotinic acetylcholine receptors (nAChRs) and β-adrenergic receptors (β-AdrRs). Djordjevic and Doran, (2009), reported that the content of carcinogens and the addictive nicotine in cigarettes and cigars differ considerable from brand to brand. Available nicotine ranges from 13.79 mg to 22.68 mg for every gram, dry weight of tobacco leaves for cigarettes that contain a range from 0.49 to 0.89 grms of processed tobacco material (Counts *et al*., 2005**).** For cigar, with standard tobacco (6.3 to 15.6 mg nicotine after curing), nicotine content ranges from or 5.9

to 335.2 mg for every single cigar produced with tobacco material content of not less than 21.5 grams, (Henningfield *et al.,* 1999). With this knowledge, it is not surprising that, fourteen (14) types of cancers, varied debilitating lung and heart diseases are linked directly or indirectly to smoking. Evidence also exist that, 84 % of the 1.1 million deaths due to lung cancer are attributable to cigarette smoking activity (Jha, 2009).

These toxicants also destroy vital protective anti-cancer genes within our system. Not minding the fact that the mechanistic approach to the ultimate destruction may differ, toxicants such as the nitrosamines, benzene, benzo (α) pyrene, polonium-210 and thirty-five toxicants have direct causative effect on affected parts and system while other components of tobacco smoke present indirect impact on the parts and systems; for instance, chromium enhances the stronger attachment of benzo (α) pyrene to DNA, with consequent exacerbation of its damaging potential. nickel and arsenic hinder plausible repair pathways for damaged DNA. This creates possibility of cancer development from affected cells. It is established that, DNA change with remote possibility to develop to a full blown cancerous growth occurs for every set of 15 cigarettes smoked (Munnia *et al.,* 2017). As reported by O'Brien, (2001), nicotine dependence not only ensures the continual habitual smoking activity of people but where there is a sharp decrease of up to 50% in its ingestion, signs and symptoms linked to certain uneasiness like, anxiety bradycardia, insomnia gastroenterological distress, weight gain, reduced mental concentration, increased appetite, dysphoria and depression are triggered. This creates the experienced challenge in quitting, in addition to the highlighted damages to affected human anatomy.

Strikingly, nicotine is not directly a carcinogen, but its presence and association with potential carcinogens greatly harms the host's *in vitro* environment because it is the sole causative addictive agent which thereby allows prolonged contact with tobacco smoke with constituent

carcenogens. This invariably increases the risk of incidence of cancer. Irrefutably, smoking secession is the ultimate solution to preventing the incidence of the highlighted cases of harm to health, personal as well as national economy; but regrettably, secession is nearly impossible for majority of addicts and very intrussive to the vulnerable younger population.

2.1. Tobacco-Specific Nitrosamines

During curing and processing of tobacco, nitrosation reaction takes place between nicotine and related compounds. This interaction produces nitrosamine carcinogens. These materials are called tobacco-specific nitrosamines because they are found only in tobacco products and possibly in some other nicotine-containing products. Tobacco-specific nitrosamines are present in both smokeless tobacco products such as dipping tobacco and in cigarette smoke. These products are minimally present in unfermented and pasteurized products such as the Swedish styled snuff (snus). They have been detected in American style smokeless tobacco products, though a study (Health New Zealand, 2009), expressed that these carcinogens and toxicants were present below harmful levels. They are among the most important carcinogens in cigarette smoke, along with combustion products and other carcinogens (Sunday, 2006). The formation of TSNAs from the nitrosation reactions of nicotine and its analogues during the curing process of tobacco leaves is explained in Figure 2.3.

Among the tobacco-specific nitrosamines, 4-(methylnitrosamino)-1-(3-pyridyl)-1-butanone (NNK) and N'-nitrosonornicotine (NNN) are the most carcinogenic. NNK and its metabolite, 4-(methylnitrosamino)-1-(3-pyridyl)-1-butanol (NNAL) are potent systemic lung carcinogens in rats(Nilsson, 2006). Tumors of the nasal cavity, liver, and pancreas are also observed in NNK- or NNAL-treated rats. NNN is an effective esophageal carcinogen in the rat, and induces respiratory tract tumors in mice, hamsters, and mink.

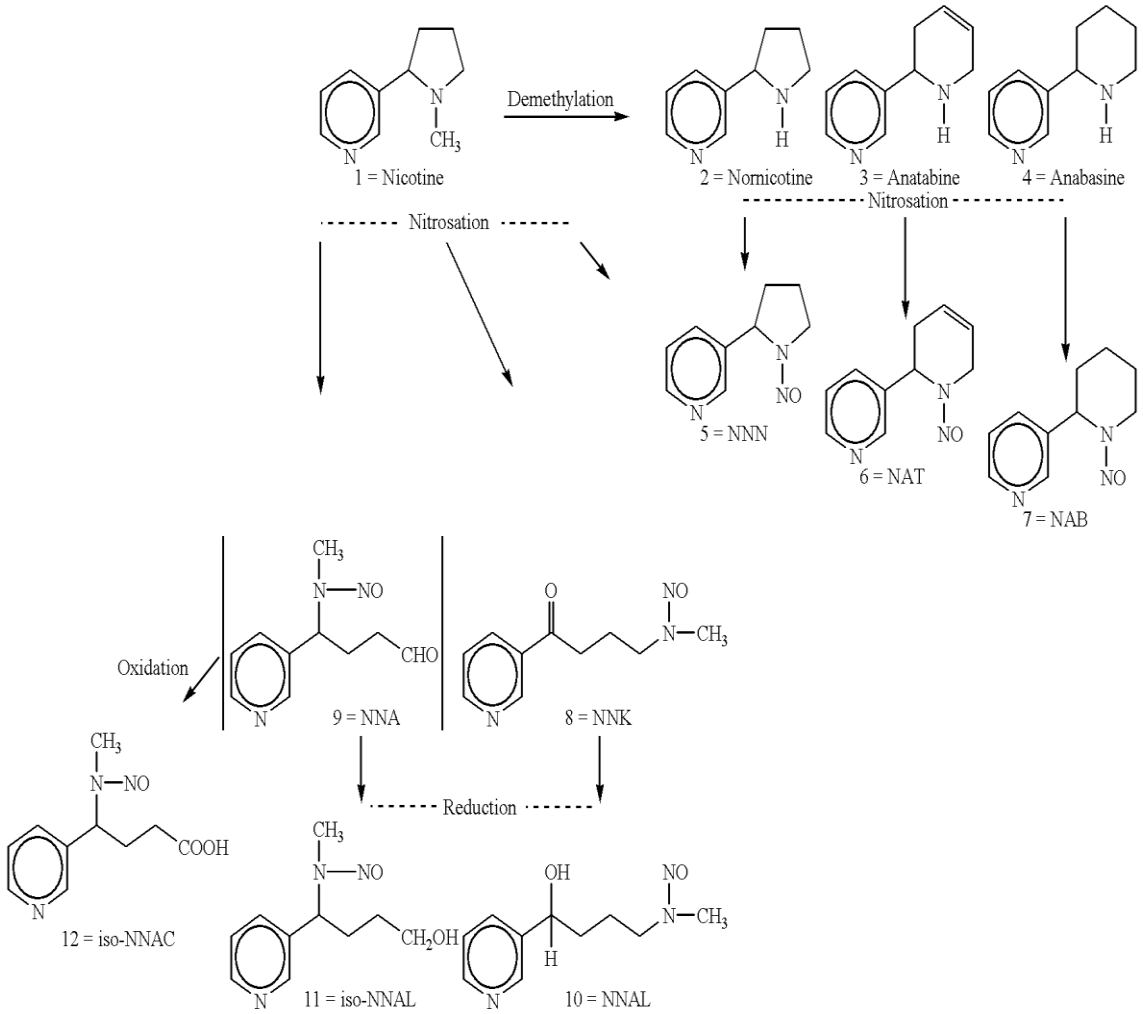

Figure 2.3: The formation of TSNAs from the nitrosation reactions of Nicotine and its analogues during the curing process of Tobacco leaves (Regent Court Technologies, 2001)

A mixture of NNK and NNN caused oral tumors when swabbed in the rat oral cavity (Nilsson, 2006). Thus, considerable evidence supports the role of tobacco-specific nitrosamines as important causative factors for cancers of the lung, pancreas, esophagus, and oral cavity in people who use tobacco products.

NNK and NNN induce cancer in humans by the mechanism of metabolic and chemical binding to DNA by adduct formation pathway. This metabolic pathway varies amongst individuals, (Silvia, 2012). Brunnemann *et al.,* (1996) identified seven TSNA within the range ≤ 25

micrograms/g in smokeless tobacco and 1.3 micrograms TSNA/cigarette in mainstream smoke of cigarettes. The authors stated that a typical indoor air that is polluted by tobacco smoke contains as much as 24 pg/L of TSNA. This substantiates the health risk fact of tobacco smoking to both active and passive smokers.

2.1.2 Remediation Approach:-Filters

An adopted approach for reducing the carcinogenic effect of tobacco products is the application of chemo-preventive agents, primarily of micronutrients (Hoffmann, 1996). But this approach has its drawbacks in the form of side reaction products. An alternative approach to the handling of smoke stream contents reaching the vulnerable areas of the body is by the use of filters. Boris Aivaz in 1925 patented the cigarette filter making process where he used crepe paper. These filters are attached to manufactured cigarette products either during the manufacturing process or at point of consumption. Cigarette filters are usually made of drag or cellulose acetate and are intended to sequester nicotine and tar, to varying amounts, as evaluated by standard smoking test method. They frequently provide ventilation that also reduces the nicotine and tar yield of cigarettes. Hoffmann *et al*., 1996.), reported that the content of the filter-cigarette is richer in nitrate than the non-filter cigarette because the smoke from filter-attached cigarettes contains lower yield of nicotine and remotely induces a desire for more intense drags from cigarettes than experienced with non fiter-attached cigarettes. This is possible because the filters are made with ventilating holes (Figure 2.4), and the holes allow air dilution of the smoke dragged from the filter. By this, manufacturers increase the level of accessible TSNAs encountered during cigarette smoking which encourages longer and deeper drags by smokers probably to compensate for the filtered fraction of nicotine.

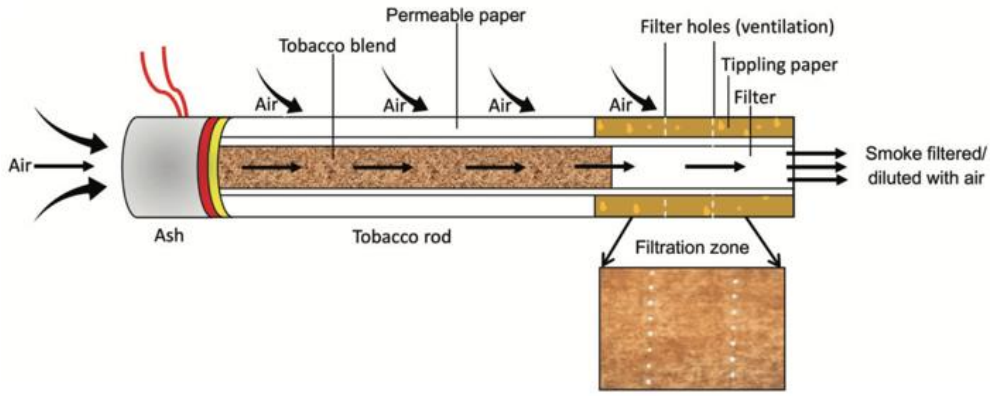

Figure 2.4: The filter of a cigarette showing the vents. Adapted from (Song et al., 2017).

This consequently exposes the victims to more lethal substances from the cigarette and this has been shown to be a trigger-route to adenocarcinoma (Song *et al.,* 2017) because it causes the peripheral lung to be exposed to higher amounts of nitrogen oxides, nitrosated compounds, and lung-specific smoke carcinogens.

2.1.3 Available filter technologies for cigarette and other tobacco based smokeable products.

Various filter products are available in the market: Nic-Out Plastic Cigarette Filters (made in Israel), Nico-Slim Cigarette Filters, Water Based Cigarette Filter ZB501 - Portable Hookah. Interestingly the past 10 decades witnessed several patented filter materials both natural and synthetics like foams, sponges, resins, paper (cotton, corn, silk and flax), cellulose esters, ethers; carbon granules and powders, salicylates and oxides of aluminium. Numerous additional filter materials like silicates have been implicated as possible alternatives but were not employed in commercially sold products. Most of these filter materials are made from synthetic materials which are not easily biodegradeable (cellulose acetate etc.). Conversely in recent time, biodegradeable ones have emerged which are meant to cater for the environmental issues surrounding biodegradation. One of such filters is Greenbuttts filter. This product is made with

organic cotton, degummed hemp with wheat flour as the binder. The greenbutt filter brand is marketed under the illusion that it is an improvement over the common cellulose acetate filter currently being used world wide. Cellulose filters sequester a bit of the particulates, very little of the volatile nitrosamines and close to eighty percent of the semi volatile phenols only. The charcoal filters sequesters selectively some compounds contained in the vapour phase but not exclusively the nitrosomes and definitely not the tar.

Evidently, all the filter types and designs, have one common shortcoming which is the inability to selectively and specifically sequester the carcinogenic TSNAs from the smoke stream alongside the nicotine and tar and because tobacco usage in different forms by people of all ages/class world over cannot be completely stopped, the urgency then exists for a method of containing the harmful products that result from its contact despite the introduction and use of the filters. This then neccesitates adoption of a technology that will cary out the desired multi-targeted sequestration of the mixed toxicants from cigarette smoke stream; hence the focus of this research activity in the development of a material with template specific and selective potentials.

2.1.4 Molecularly Imprinted Polymer (MIP).

2.1.4.1 Molecular imprinting strategy

These are polymer materials, synthetic, natural, semi-synthetic or hybrid of natural and synthetic; that possess well-defined three dimensional cavities with spatially oriented functional groups in the highly cross linked polymer network. The unoccupied recognition sites present good binding attraction, stability and selectivity towards target molecules at the molecular level. This technique thrives on the induction of receptor-like binding sites in select polymers and its

selectivity stems from the synthetic procedure adopted for its preparation (Lachová, Lehotay and Cizmárik, 2007).

Polyakov (1931), started the molecular imprinting technique. He proposed a mechanism explaining the concept based on observed silica's binding preference for any solvent in which it is prepared, whenever it is exposed to different solvent systems (Polyakov, 1931). Though the proposed mechanism was ignored by scientists at the time, Dickey (1949), working with dyes as templates, recorded that dye templated imprinted silica compounds exhibited preferencial rebinding with template dye in the presence of other dyestuffs (Dickey, 1949). Dickey's work can be said to be the first ever prepararion of a molecularly imprinted material because the template dye stuff was added to the prepolymer mix before polymerization and extraction of it and this is the exact protocol being used till date.

Lok and Son, (2009) reported that Wulff and Sarhan (1972), reignited activities within the molecular imprinting technology research while Mosbach's research group expanded the scope within the 80s (Andersson, Sellergren and Mosbach, 1984). MIPs hold a number of advantages over the conventional processes such as: high selectivity and affinity, high stability and the ease of preparation (Piletsky, Turner, and Laitenberger, 2005), repeatable usage without loss of activity, high mechanical strength and resilient to harsh chemical media, heat and pressure when compared to biological receptors (Lavignac, Allender, and Brain, 2004.).

Chemical stability studies confirmed that MIPs maintained more than 95% of their affinity even after 24h exposure to autoclaving, triethylamine, 10M HCl acid and 25% NH_3 while heat treatment revealed that they are thermally durable and retain their chemical affinity up to temperatures of 150^{o}C (Svenson and Nicholls, 2001). Consequently MIPs can be stored for years without loss of affinity for the target analyte.

A study by Wulff *et al.,* (2002) explained that, increasing the amount of cross-linking matrix increases the specific recognition by covalently imprinted polymers. A new strategy for monomer design has been studied which combines interactive monomer functionality with a cross-linking format, giving as a result, non-covalent molecular imprinted polymers with improved performance. Quantitative structure-selective relationship studies have verified a key improvement to monomer design and in the template interactive functional group in a cross-linking monomer format (Tada and Iwasawa, 2003). Molecular recognition is crucial for the functioning of living systems, where biological macromolecules, including proteins (which may serve as enzymes, antibodies, and receptors), nucleic acids, and saccharides, play decisive roles in biological activities. In order to obtain host molecules with precise recognition of guest species, the design, synthesis, and evaluation of supra molecules are being intensely investigated in laboratories throughout the world. However, the requisite multi-step preparative routes to the molecular receptors are often challenging and the overall yield of the final product is quite low. An alternative approach to the synthesis of host molecules which can recognize target guest species is a much simpler template polymerization technique called "molecular imprinting" (Severin, 2001). In this method, precise molecular design is not necessary since a cross-linked polymer is prepared in the presence of a template.

Two kinds of molecular imprinting strategies have been established based on covalence interactions between the template and functional monomers to be the major driving theories in templating within the network of a polymer matrix. They are covalent approach and non-covalent approach. In both cases, the functional monomers are chosen so as to allow interactions with the functional groups of the template molecule and are polymerized in presence of the template. The spatial binding sites are formed by covalent or, more commonly, non-covalent

interaction between the functional group of the template and the monomer, followed by a cross-linked co-polymerization (Takeda and Kobayashi, 2005).

Of the two strategies, the non-covalent approach has been used more extensively due to the following reasons:

i. Non-covalent protocol is easy to conduct, avoiding the tedious synthesis of pre-polymerization complex.
ii. Removal of the template is much easier, usually accomplished by continuous extraction, and
iii. A high variety of functionality can be introduced into the imprinted binding site using non-covalent methods (Santora and Gagne, 2000).

2.1.4.1.1 Covalent approach

The covalent or pre-organized approach which was introduced by Wulff (1972), is based on the formation of reversible covalent bonds between the template and monomer(s) before polymerization. The entrapped template is removed by cleavage of the covalent bonds induction, but is re-formed upon rebinding with the target molecule. This approach generates homogenous numerous binding sites as a result of the high stability of template-monomer interaction. An obvious disadvantage of this approach is the relatively high "energy-demand" condition for the covalent bond cleavageing. In covalent approach, the imprinted molecule is covalently coupled to a polymerisable monomer. The binding of this type of polymer relies on reversible covalent bonds. After copolymerization with cross-linker, the imprint molecule is chemically cleaved from the highly cross-linked polymer. Wulff *et al.,* (1973) first produced molecular imprinted polymers by synthesizing specific sugar or amino acid derivatives which contained a polymerisable function using covalent imprinting methods. After polymerization they

hydrolyzed the sugar moiety and used the polymer for selective binding. For covalent molecular imprinting, selectivity of imprinted polymer increases with increasing amount of cross-linker (Wulff *et al.,* 1977). Moreover, the requirements of covalent imprinting are different from those of non-covalent imprinting, particularly with respect to ratios of functional monomer, cross-linker, and template. However, since the choice of reversible covalent interactions and the number of potential templates are substantially limited, reversible covalent interactions with polymerizable monomers are fewer in number and often require an acid hydrolysis procedure to cleave the covalent bonds between the template and the functional monomer (Marthe and Vasquez, 2003).

2.1.4.1.2 Non-covalent approach

Non-covalent approach is frequently used to prepare molecular imprinted polymers. During the non-covalent approach, the spatial binding sites are formed by the self-organisation between the template and monomer, followed by a cross-linking co-polymerization (Svenson *et al.,* 2004).The imprint molecules can interact through non-covalent interactions like ionic, hydrophobic and hydrogen bonding (Ekberg and Mosbach, 1989). The non-covalent imprinting approach seems to hold more potential for the future of molecular imprinting due to the vast number of compounds, including biological compounds, which are capable of non-covalent interactions with functional monomers (Michael *et al.,* 1985). Limits to the non-covalent molecular imprinting are set by the peculiar molecular recognition conditions. The interactions between the monomer and template are stabilized under hydrophobic environments, while polar environments disrupt them easily. Another limit is represented by the need of several distinct points of interactions: some molecules characterized by a single interacting group such as an isolated carboxyl, generally give imprinted polymers with very limited molecular recognition

properties, which have little interest in practical applications. Understanding the basic optimization of non-covalent methods is important for two reasons: the methodology is far easier than covalent methods, and it produces higher affinity binding sites, versus covalent methods. The trends in binding and selectivity in non-covalently imprinted polymers are explained best by incorporating multiple functional monomers for the highest affinity binding sites.

The increased number of binding interactions in the polymer binding site may account for greater strict accuracy of the site, and thus impart greater affinity and selectivity to the site (Sellergren and Kenneth, 1993). An alternative non-covalent or self-assembly approach was introduced by Mosbach and Arshady, (1981). They reported the formation of relatively weak non-covalent interactions like: hydrogen bonding, electrostatic interaction, hydrophobic interaction, Van der Waals forces and dipole-dipole bonds between the template molecule and functional monomers before polymerization, (Figure 2.5).

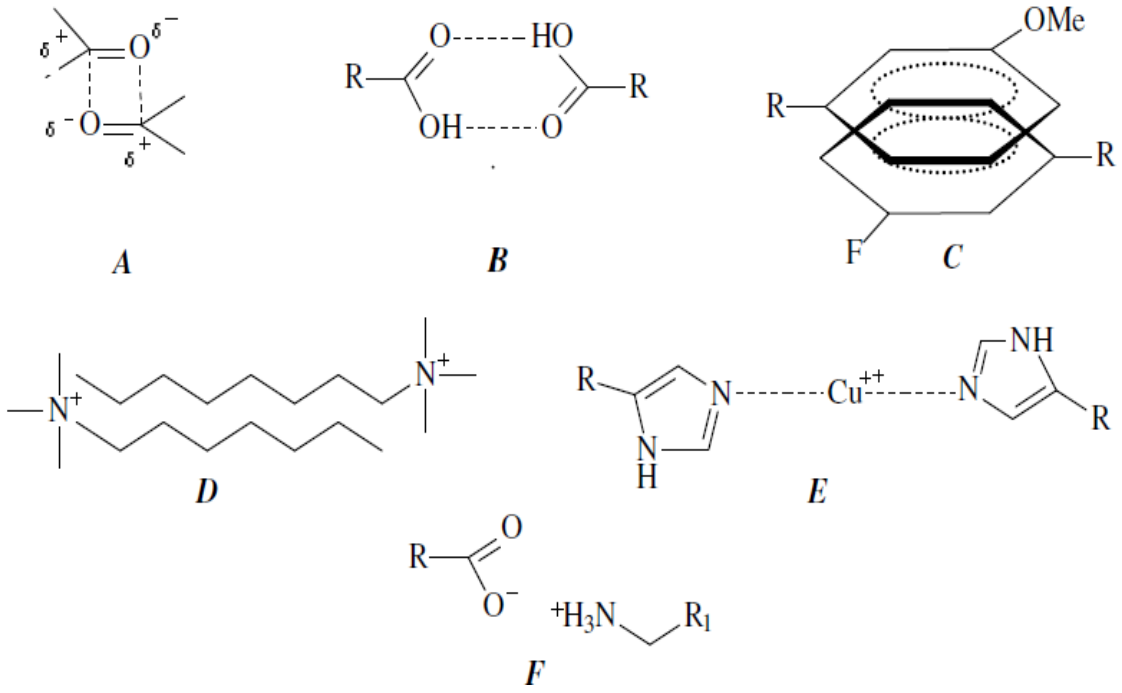

Figure 2.5: Bond types that prevail in non-covalent imprinting. A: electrostatic (dipole-dipole) interaction; B: hydrogen bond interaction; C:π-π stacking; D:Van der waals interaction; E:coordination bond interaction; F:electrostatic ion-ion interaction. Adapted from (Spivak, 2005).

The association and disassociation of the imprint takes place by simple in and out-of-sites flow. Because of its simplicity and exploitable myriads of different monomers able to interact with almost any kind of template, this approach stands as the most recommended for the preparation of MIPs. Heterogeneous or non-selective binding sites are usually formed by this approach as a result of excess free monomer(s) which randomly get linked to the polymeric matrix; this is possible due to the presence of needed high amount of monomer necessary for the equilibrium displacement during the formation of the template-monomer complex. Sellergren and Andersson, (1990) and Whitcombe *et al.* (1995) introduced a midpoint approach which is known as the semi-covalent approach. Here the template is covalently bound to a functional monomer, but the rebinding is based on non-covalent interactions.

Despite the observed disadvantages of the non-covalent approach, it is still the most popularly used, simply because the synthesis is easily carried out and the template removal is done through simple solvent extraction. It is also more versatile and the imprinting step is quite analogous to the identification pattern observed in nature. However there is an obvious disadvantage of multiple binding site interactions but it is usually surmounted by allowing a crowd of interaction points to flow concurrently:

2.1.4.2 Molecular Recognition by Imprinted Polymers.

Molecular recognition ability is dependent on factors, such as shape, functional complementarities and contributions from the surrounding environment. Though all non-covalent interactions impact the molecular recognition between a target molecule and the host polymer; the type of recognition site formed during imprinting, the nature of the template, monomers and the polymerization reaction itself determine the quality and performance of the product polymer. The recognition integrity of the MIP comes from the induced molecular memory, which is

authenticated by the ability of the recognition sites to selectively recognize the imprinted species. Hydrogen bond influence is most often experienced during a molecular recognition interaction in molecularly imprinted polymers. By this, acrylic acid and methacrylic acid have dominated as the adopted functional monomers since carboxyl group functions as a hydrogen bond donor and acceptor at the same time (Mahony *et al.,* 2005). These non-covalent interactions are easily reversed, usually by a wash in aqueous solution of an acid, base, or methanol, thus facilitating the removal of the template molecule from the network after polymerization. In addition to the better versatility of this more general approach, it allows fast and reversible binding of the template.

2.1.4.2.1 Parameters that affect molecular recognition in imprinted polymers.

The challenge of designing and synthesizing a molecularly imprinted polymer can be a discouraging prospect to the uninitiated because of the sheer number of experimental variables involved, e.g. the nature and levels of template, functional monomer, cross-linker, solvent and initiator, the method of initiation and the duration of polymerization (Anderson *et al.,* 1996). Moreover, optimization of the imprinted products is made more difficult due to the fact that there are many variables to consider, some or all of which can potentially impact upon the chemical, morphological and molecular recognition properties of the imprinted materials. Fortunately, in some instances, it is possible to predict how changing any one of such variables like the crosslink ratio is likely to impact upon these properties (Katz and Davis, 1999).

The synthesis of MIPs requires four basic inputs: a template (T), functional monomer (FM), a cross linking agent (CL) to impart stability and cavity rigidity to the resultant polymer, and a porogen to generate a pore structure within the polymer that aids mass transfer during template rebinding. The typical process for MIP formation is outlined in Figure 2.6. With thousands to

millions of available template binding pockets, MIPs possess the ability to recognize and bind specific target molecules.

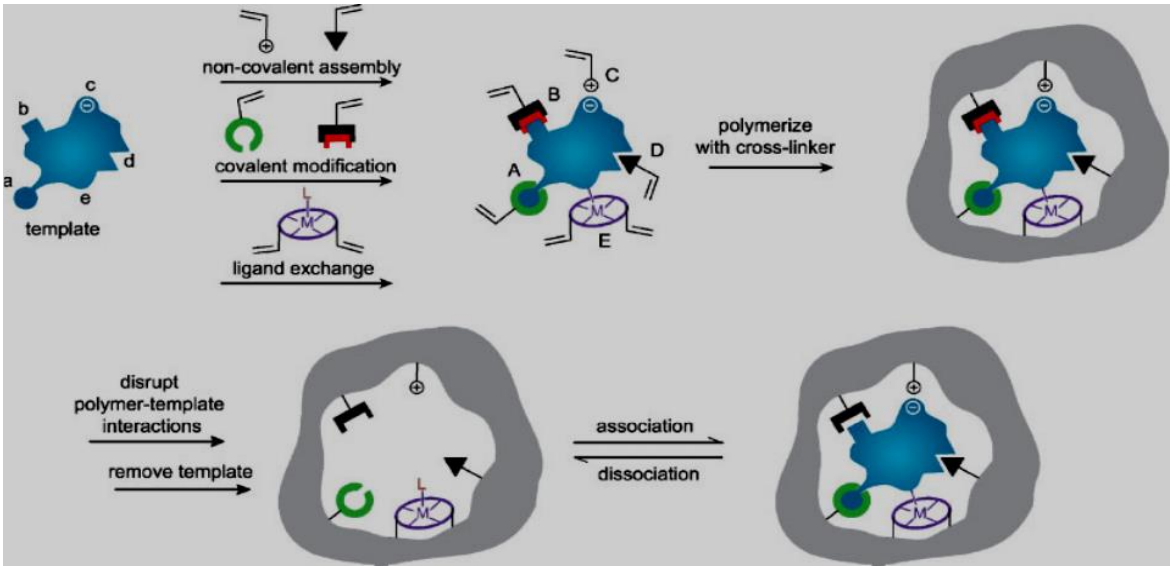

Figure 2.6: Expansively illustrative demonstration of plausible imprinting route: (Alexander *et al.*, 2006)

2.1.5 Fundamental MIP Preparation Methods.

Reversible interactions involving the template and functional monomer(s) can take place via one or combination of van der waals or hydrophobic contacts, electrostatic interactions, covalently linked activated binding species (with preference for non-covalent template-cleavage); ligand species /Co-ordination with a central metal ion and reversible covalent bond(s). Alexander *et al*. (2006) gave a generalized stepwise approach to MIP fabrication irrespective of bond interaction type or route. They reported that a consequent polymerization process yields an insoluble matrix with recognition potential via electrostatic, van der waals or steric interactions with resultant template cavities. The researchers maintained that an "imprint" phenomenon is created where selective template rebinding occurs due to the existence of created template or its analogue cavity (occasioned by the extraction), this is influenced by disruption of the polymer-template

contact. Pictorial representation of this can be seen using the polymerization of a polystyrene based MIP as in Figure 2.7;

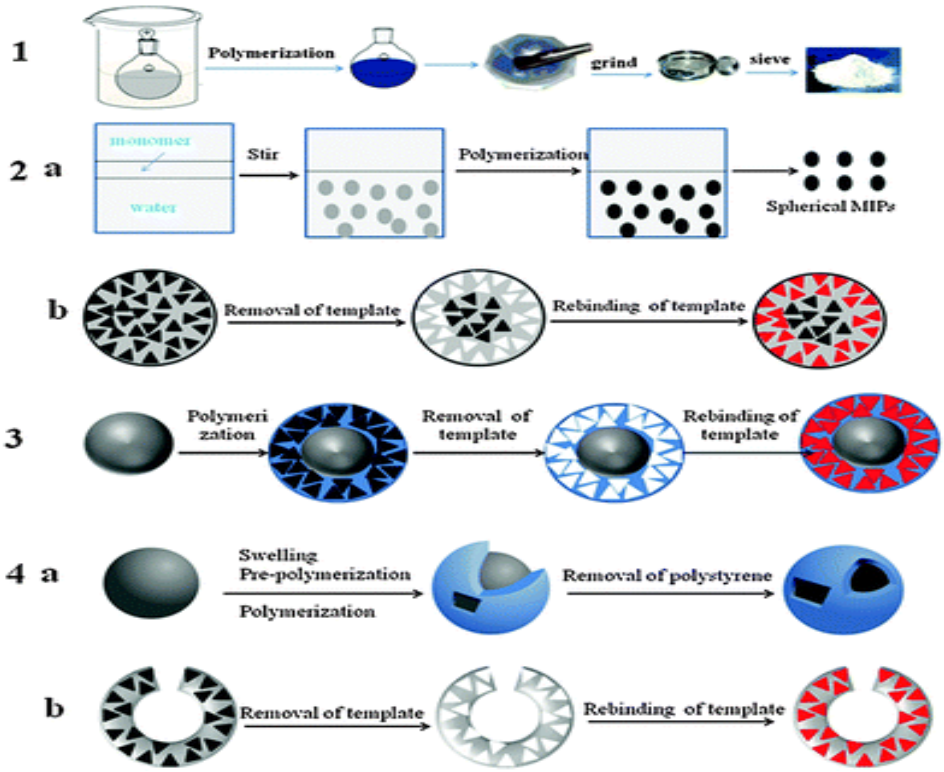

Figure 2.7: Typical sequence for the preparartion of an MIP based on a polystyrene matrix. (Chen, Xu and Li. 2011).

Basically, five different approaches exist for the preparation of MIPs. They are: covalent (pre-organized approach), non-covalent (self-assembly approach), semi-covalent, electrostatic/ionic and metal center coordination.

Before the start of the bulk polymerization process, there is the need to make quick and reproducible confirmation on the feasibility of the proposed molecular imprinting process being targeted. This saves material, time and provides a guide to the expected study outcome. One of the most technoeconomic routes to achieving this is the use of quartz crystal micro balance technology.

2.1.6 Quartz crystal micro balance (QCM) technique for proof-of-concept experiment.

The QCM is a sensor with acoustic potential which is prompted by its piezoelectric crystal property. The QCM sensor measures value changes as small as in Nano gram when less or more mass loadings occur on the surface of the quartz crystal chip. The change is presented as a frequency shift based on the Sauerbrey equation. Any addition or subtraction in mass to the surface of the sensor disc brings about corresponding reduction or addition in frequency value. This phenomenon is applied in studying materials of interest when they are introduced onto the disc. Sauerbrey recognized the underlying feasibility of applying the Q C M's technology, which demonstrates the relatively high sensitivity of piezoelectric devices with respect to changes in mass at disc's electrodes. This is entrenched in his equation expressed as:

$$\Delta f = - Cf \times \Delta m \qquad \text{(eq 1)}$$

Δf - experimental frequency variation, in Hz, Δm – varied mass for each part of area, (g/cm^2),
Cf - the sensitivity factor for the quartz used (At room temperature, a 5MHz supply of energy corresponds to 56.6 Hz μg^{-1} cm^2 of sample).

The above equation depends on a direct sensitivity influence, Cf (a basic attribute of the quartz). The theory accommodates non-calibration of the equipment without errors but only for thin films and uniform rigid samples.

The potential of quartz crystals to exhibit piezoelectric effect was first reported by Curie's research group in 1880 (Nomura and Okuhara, 1982). Rayleigh followed up the research with a report of the effect of a change in inertia of the quartz crystal which leads to shifts in corresponding resonant frequency (Kanazawa and Gordon, 1985). Sauerbrey, (1959),

became the first person to apply the QCM technique for mass sensing after he reported, the linear relationship between change in frequency (Δf) in response to change in mass

The quartz crystal disc has metal electrodes deposited on each side. On one side the electrode is around the perimeter of the crystal (Figure 2.8) leaving most of the surface exposed for experimental work.

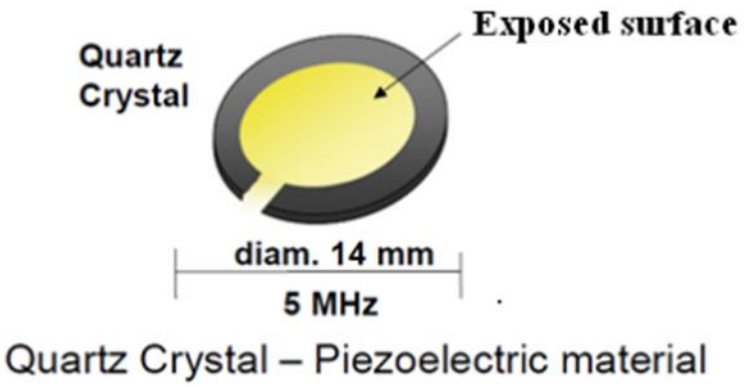

Figure 2.8: Aquartz crystal disc showing the top side with electrode deposited on perimeter. Adapted from QCM manual of Bioloin Scientific, Linthicum MD.

When any material is introduced on the surface of the disc, an external driving circuit generates a pulse of current which sets the crystal into free vibration in the shear mode. This causes an acoustic wave that spreads in a perpendicular direction to the surface of the disc in an in-plane oscillating shear mode (Marx, 2003), (Figure 2.9). The quartz crystal disc serves as both the sensing element and the transducer.The QCM works on the principle of an acoustic sensor feedback.

For an accurate determination of mass of experimental sample, using the Sauerbrey equation, three basic conditions are required. These conditions are:

1. The adsorbed mass must not be greater than 2% of the mass of the crystal.
2. There must be an even spread of sample on the surface of the disc.

3. The applied sample layer must be compact and rigid enough to exhibit elasticity behaviour during experimental period.

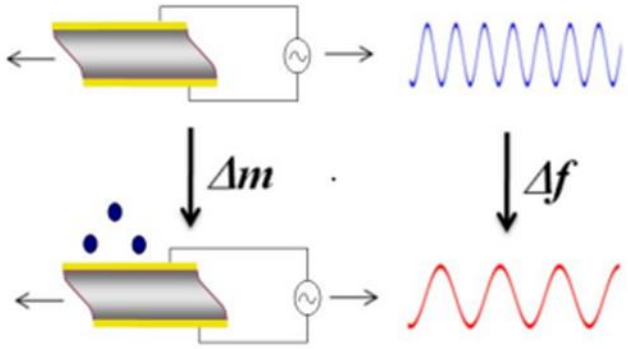

Figure 2.9: Changing of resultant resonant frequency on addition of a mass on to the Surface of the sensor. https://www.nanoscience.com/techniques/quartz-crystal-microbalance/. Accessed 3.19 pm 9/21/2019.

On deposition of sample onto the exposed metal surface of the disc, the vibrational frequency is lowered due to increase in mass (weight difference), this allows the measurement of depositions on the surface in real time situation.

2.1.6.1 Preparation of the quartz disc surface by chemical derivatization

Derivatization is generally the first step in preparing a solid surface for deposition of the polymer sample. This is to make the surface chemically suitable to accept and hold the polymer sample and ensure a strong adsorption. The treatment targets the provision of adequate amount of chemically reactive sites per unit area to ensure attachment of the desired density of sample per unit area. A typical silica surface has 5-6 innate hydroxyl groups per nm^2 (Parfitt, 1981; Mukherjeeroy *et al.*, 1995), and the hydroxyl groups readily react with organofunctional silanes to give a maximum of about three functional groups per nm^2 organofunctional silanes (Mukherjeeroy, *et al*., 1995),. Examples of the groups that are introduced to the silica surface are

amino-functional silane (introduces amine groups), mercapto-functional silane (introduces thiol groups) and acryloxy-functional silane (introduces acryloxy groups).

As presented in Figure 2.10, in derivatization of the silica surface with amino-functional silane; these groups react with corresponding available functional groups. Ideal cases are the reaction of all available methoxy groups with the surface but in real life situation just a few of them do take part in the reaction. Be it as it may, where only one methoxy group reacts, the silane molecule becomes firmly secured.

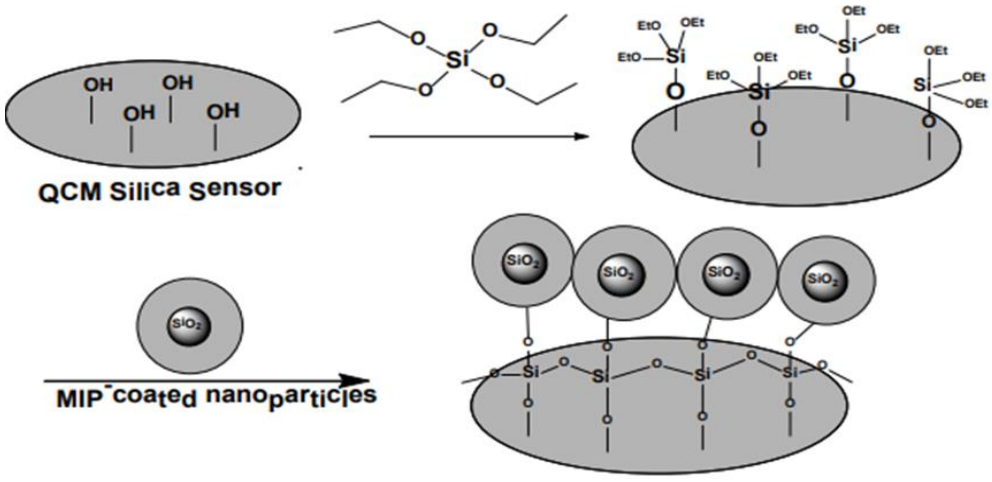

Figure 2.10: Schematic diagram of formation of MIP/NIP-coated nanopoarticles mounted on Sensor disc.

2.1.7 Biodegradable polymers approach for environmental safety and sustainability.

Apart from the culture of recycling plastics, alternative route being pursued in the sustainable and safe use of polymer materials, is the manufacturing method of using biodegradable plastics and polymers in the production of utility items. Conventional non-biodegradable plastics dominated the scene for up to one hundred and twenty (120) years before the biodegradable ones came into industrial recognition, (ASTM D6400-12, 2012). The biodegradable items present

products that are environmentally friendly due to their ability to degrade or break down to non-toxic materials at their end-of-use period. They are also degraded to soil enrichers/fertilizers/manure as the case maybe and this may be viewed as a sort of commutative recycling of the products. Most of the biodegradable materials are natural but can also be tailored to man-made semi-natural products by incorporation of certain chemical components. Research into biodegradable plastics and what can be done to restrict plastic usage to a sustainable level has been ongoing. This is to help realize the full potential of plastics in public health and human society without compromising the quality of life of present and future generations .One early entrant into the competitive disposition of choices is Polylactic acid based bio polymer

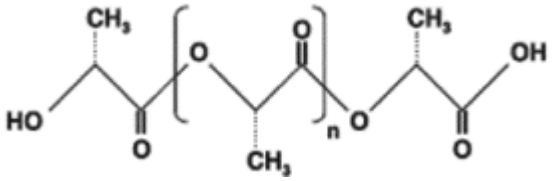

Figure 2.11: biopolymer Polylactic acid

This material is produced by the reactions of the prepolymer lactic acid as displayed in Figure 2.12.

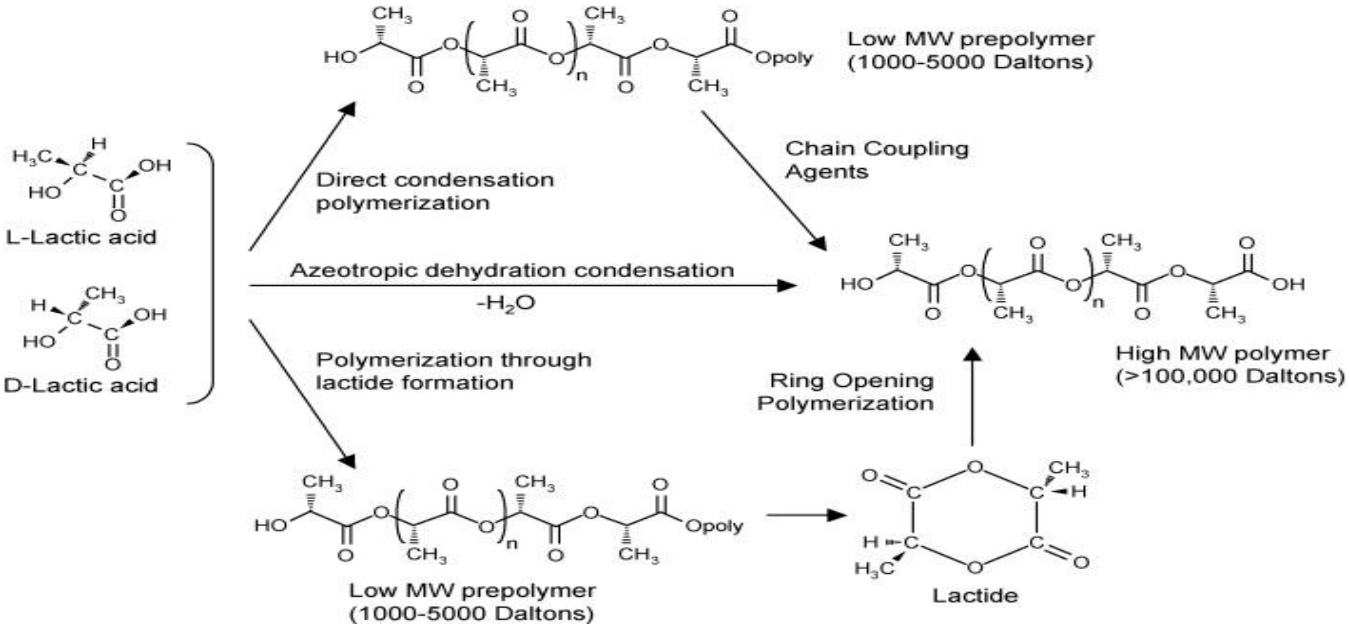

Figure 2.12: .A general approach for manufacturing bio polymer polylacticacid (Lim, Auras & Rubino, 2008)

2.1.8 Selection of Choice Monomer/Polymer, (Chitosan).

Most MIPs are fabricated from entirely synthetic inputs and are therefore presented as the synthetic counterparts to biological receptors and are robust, insoluble materials exhibiting high stability in most media, they generally lack the natural homogeneity of active sites associated with biological receptors. The population of binding sites generated in MIPs typically presents a highly heterogeneous profile because of the influence of the equilibria that govern the T-FM complex formation and the stability and dynamic nature of the growing polymer chains. With the above stated prevailing situation, choice of suitable material for the preparation of the filter material for the sequestration of the tobacco toxicants, favours material with zero or near-zero toxicity both to humans and the environment and recyclability potential.

Effective sustainability without endangering existing resource is of very pivotal importance. These guided the selection of the bio-polymer, chitosan as a techno-economical and sustainable matrix/functional monomer for the MIP fabrication.

2.1.8.1 Chitosan, source, extraction and utility.

Chitosan the deacetylated derivative of chitin with diverse number of N-acetyl groups, (Zvezdova, 2010); is a white to pale-red solid powder, insoluble in water but soluble in inorganic acids. It is naturally extracted from the mucorales, particularly from the mucor, absidia, and rhizopus species. Few researchers have reported the presence of chitosan in basidiomycetes, lentinula edodes and pleurotus sajor-caju. (Gavhane *et al.*, 2013). Other very common sources of chitosan are the demineralized, de-proteinated and acetylated exo- protective parts of aquatic animals (Figure 2.13). Chitosan has been obtained via chemical route from fishery wastes (Kumari *et al.,* 2015), specifically from the scales of fish (Kumari and Rath, 2014) and its

application (Sumathi, Vignesh and Madhusudhanan, 2017). Varun *et al.*, (2017) extracted chitin and chitosan and chitooligosaccharides from crab shell.

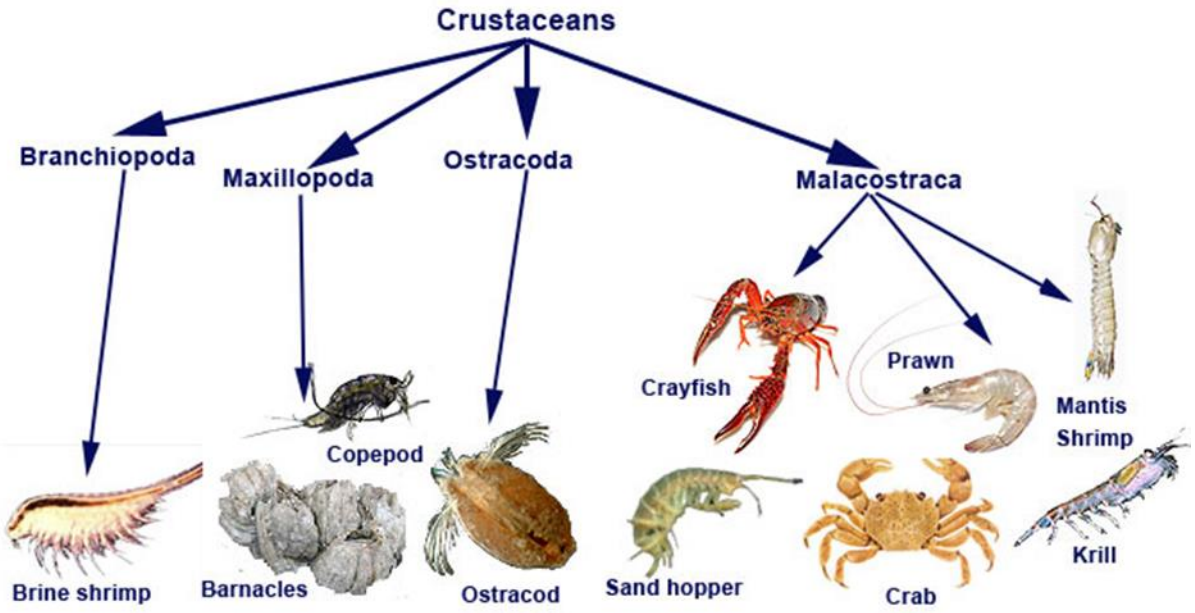

Figure 2.13: Aquatic sources of Chitin and extractable Chitosan (Sukumar, 2016).

Knorr, (1984) reported that a typical crustacean shell being made up of 20-30% chitin alongside other materials. chitin and chitosan are naturally abundant and renewable polymers with excellent properties like biodegradability, biocompatibility, non-toxic and adsorptive (Hudson and Smith, 1998). Chitin and chitosan can undergo many reactions like cellulose, such as, etherification, esterification and crosslinking (Hon, 1996), but those of chitosan are more diversified than that of cellulose. This potential is as a result of the presence of $–NH_2$ functionality inherent in chitosan (Dutta *et al*., 2004). Major influence in the reactions involving chitosan is directed by the molecular weight (Zhou *et al.*, 2003) and degree of deacetylation (proportion of deacetylated units).

2.1.8.2 Chitin

Chitin, is a bio-copolymer of disaccharide N-acetyl-D-glucosamine units linked with β-1,4 covalent glycosidic bonds, where N-acetyl-D-glucosamine units predominate the polymeric chain. It is a fibre-forming polymer by the association of adjacent chains through hydrogen bonds between the N–H and the C=O groups. This material gives a protective attribute to lower eukaryotes just like cellulose in plants. It is widespread in insect peritrophic matrix, crustacean cuticles (exosqueleton), eggshells of nematodes, cyst wall of protozoa fungi, fungal cell walls and structural membrane, particularly of basidiomycetes, ascomycetes, and phycomycetes, mycelium, stalk and spores (Duarte *et al.*,2001). Figure 2.14 presents representatives of the available sources of chitin within our environment.

Figure 2.14: Common natural sources of Chitin. Adapted from Rachel Rosenzweig. experiment.com/u/gnVFg.

It is the next most abundant biopolymer available in the ecology, after cellulose and differ from cellulose because of peculiar pendant functional groups on the sugar moiety.

Sugar-N-C=O ➢ hydrogen bond formed with hydrogen on adjacent sugar group
| |
H CH_3

The presence of the functional groups (N-C=O and NH_2) and their reactivity, gives chitin its peculiar characteristic properties which differentiate it from other polysaccharides as shown in figure 2.15. The figure also shows the slight differences between cellulose, chitin and chitosan. Figure 2.16 points out the existence of the same linkage position that is found with the two materials which is the 1,4-beta linkage. It is obtained from extracting the exoskeletons of crustaceans, insects, mollusks and the cell wall of fungal microorganisms, (Muzzarelli, 1977). The fungal chitin was first extracted in 1811 and given the name fungine while the insect based chitin was extracted in 1823.

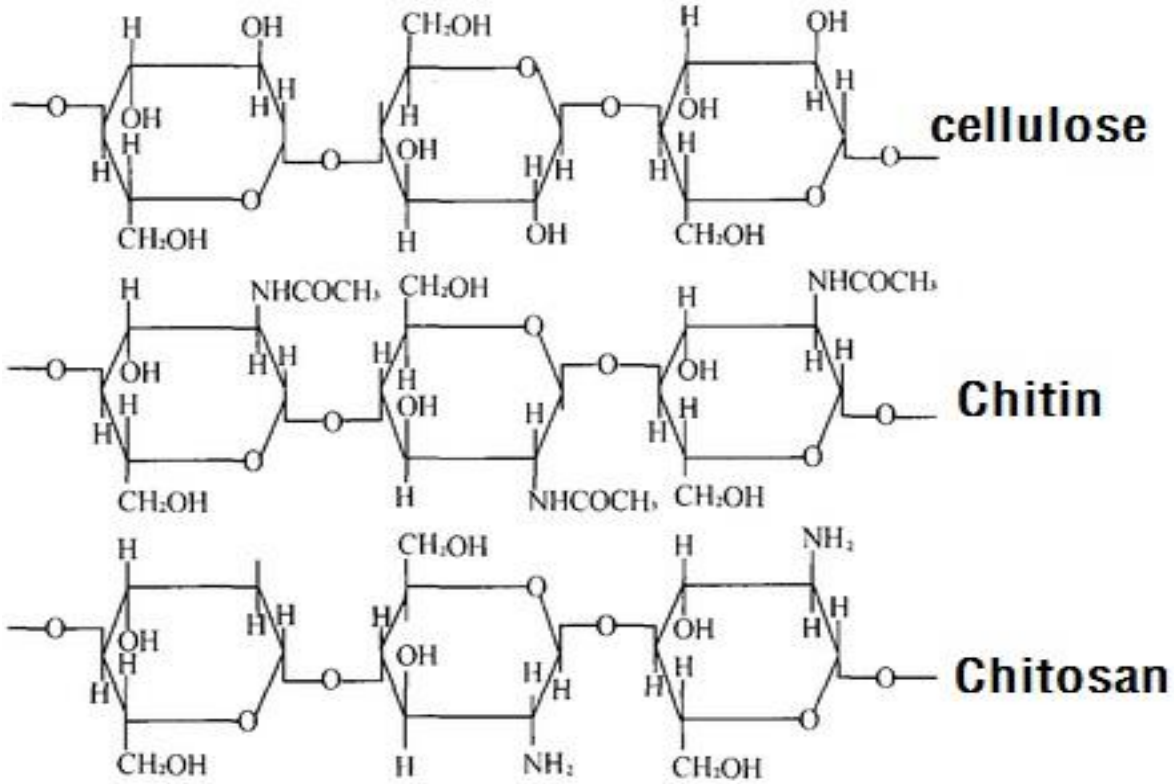

Figure 2.15: Structural comparism between Chitin, Chitosan and Cellulose. Adapted from (Wu et al.,2017)

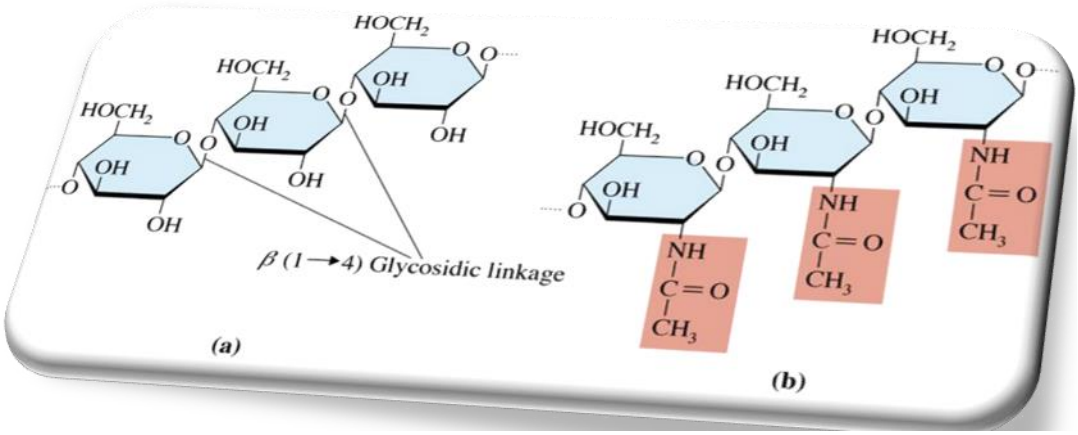

Figure 2.16: Intra-molecular β (1-4) glycosidic bonds of (a) Cellulose and (b) Chitin.Adapted from Houghton Mifflin. 2017 SlidePlayer.com Inc

2.1.8.3 Conversion of Chitin to Chitosan

Chitosan is chemically defined as a copolymer of á-(1,4) glucosamine $(C_6H_{11}O_4N)_n$, having different number of N-acetyl groups (Zvezdova, 2010). It comes as a white to light red solid powder, insoluble in water but soluble in organic acids. Chitin can be isolated from crustacean shells by chemical or biological or combination of the two processes, as reported by Acosta *et al*., (1995) and Zvezdova, (2010). A general scheme is presented in Figure 2.17 and involves the following steps:

A. Demineralization: It involves acid treatment (most commonly with HCl) which removes inorganic matters (particularly calcium carbonate).
B. Deproteinization: It includes the extraction of protein matter in alkaline medium (most commonly with NaOH)
C. Decolourization: It involves bleaching of the product by chemical reagents to achieve colourless product.

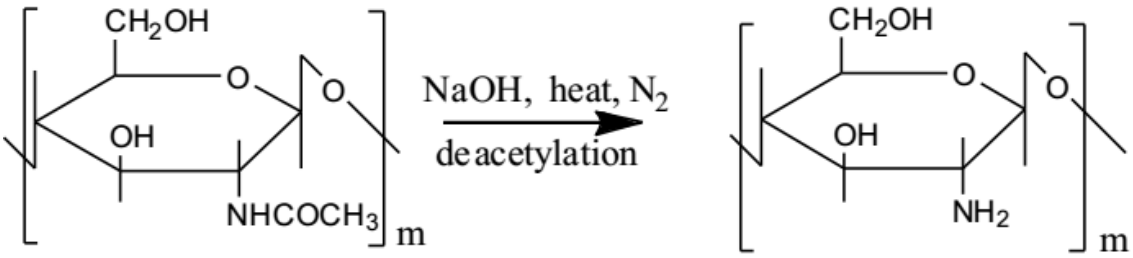

Figure 2.17. The conversion of chitin into chitosan by thermal alkali treatment.

2.1.8.4 Chemical method of extraction of Chitin and Chitosan.

The chemical method of extracting chitin and chitosan may be routed via two modifications as depicted in Figure 2.18:

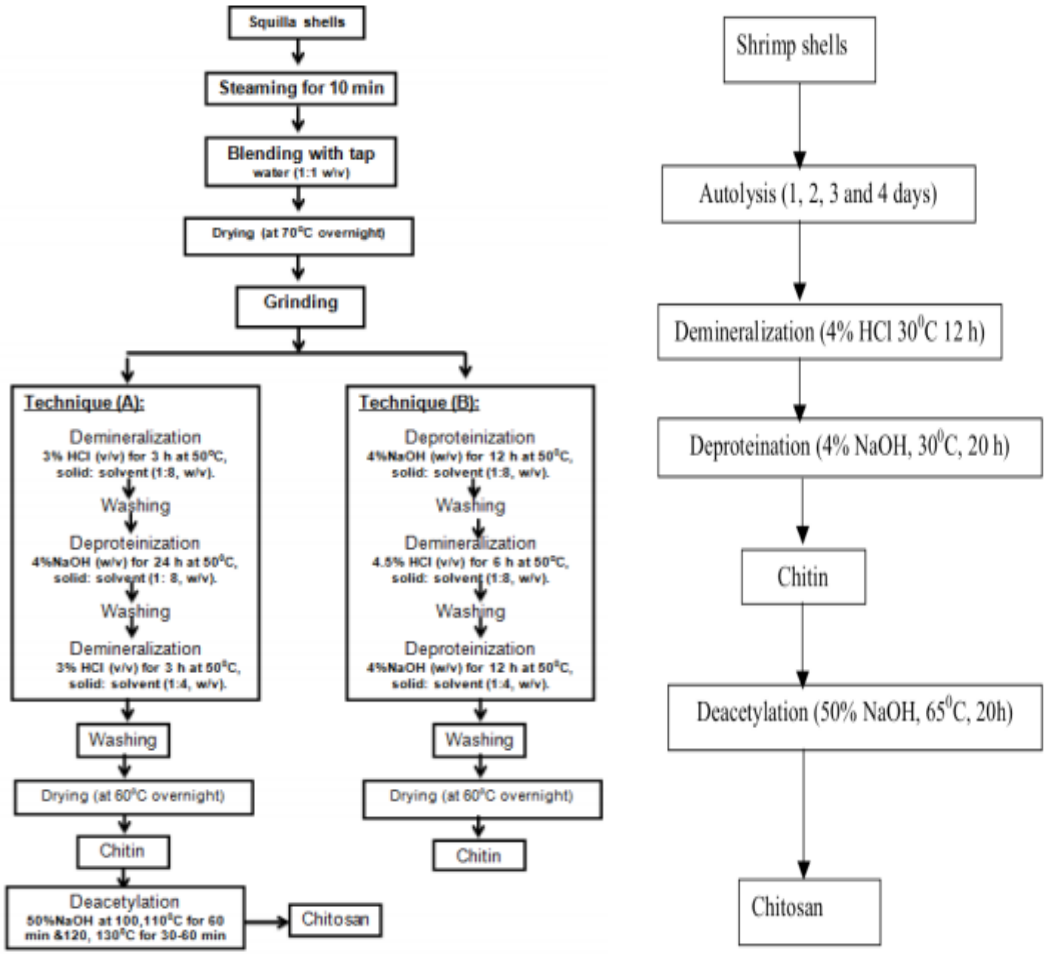

Figure 2.18 Three parallel chemical route extraction techniquesA and B Route extraction technique C. (Nguyen 2009) for Chitin and Chitosan production. Adapted from (Abouzeed et al., 2015).

Depending on circumstances, either a more acidic treatment (route A) or more alkali treatment (route B) or partial autolysis (route C), may be followed (Figure 2.18). Factors that determine the choice are: nature of the raw material, desired degree of purity of final product, target degree of deacetylation and target end-use. The viscosity of product chitosan increased after partial autolysis was applied as an extra treatment of the raw material (Nguyen, 2009). Abouzeed *et al.*, (2015), observed that a single day autolysis of fresh shrimp waste material gave the highest chitin and chitosan viscosity value of 3590 centipoise whereas a close 3580 centipoise value was obtained from frozen shrimp material only after two days of autolysis. The non autolyzed samples for both fresh and frozen gave 2300 and 2700 centipoise respectively. It is expected as usual that the other properties like molecular weight and solubility of the affected samples will equally be affected but that was not the observed case because the later mentioned properties were not affected by the autolysis. Other properties like turbidity and degree of deacetylation were not also affected by the partial autolysis.

Maslova *et al*., (2001 and 2003), developed a modified patented approach for the extraction of chitin from crustaceans via an electrochemical process method. The peculiar advantage of this process is that its processing unit is compact and transportable to any desired source of raw material, (Maslova, *et al.*, 1996). Other chemical process techniques so far developed are the one patented by Varum and Smidsrod (1994).

2.1.8.5 Chemical properties of chitosan

Unlike other naturally occurring polysaccharides chitosan naturally, is highly basic in nature and when neutral forms gel. Consequently, it exhibits several functional properties such as: polyoxysalt formation, film formation, metal ion chelation and optical structural potential (Majeti, 2000 and Hench, 1998). The biopolymer has chemical species with biomedical

potentials.These species are: presence of a linear polyamine, reactive amino groups (-NH_2), reactive hydroxyl groups (-OH) and possessing chelating ability for many transitional metal ions (Dutta *et al*., 2004). This deacetylated copolymer consisting of β-(1–4)-2-acetamido-D-glucose and β-(1–4)-2-amino-D-glucose units with degree of deacetylation usually exceeding 60%. Its importance also resides with its antimicrobial properties and its cationicity. Besides the various chemical properties, chitosan shows diverse biological properties which are also very advantageous to its utility potential (Venter *et al.*, 2006; Younes and Rinaudo, 2015).

A comparative extraction of chitin and conversion to chitosan by biological (enzyme) and typical chemical process is shown by the representations in Figure 2.19:

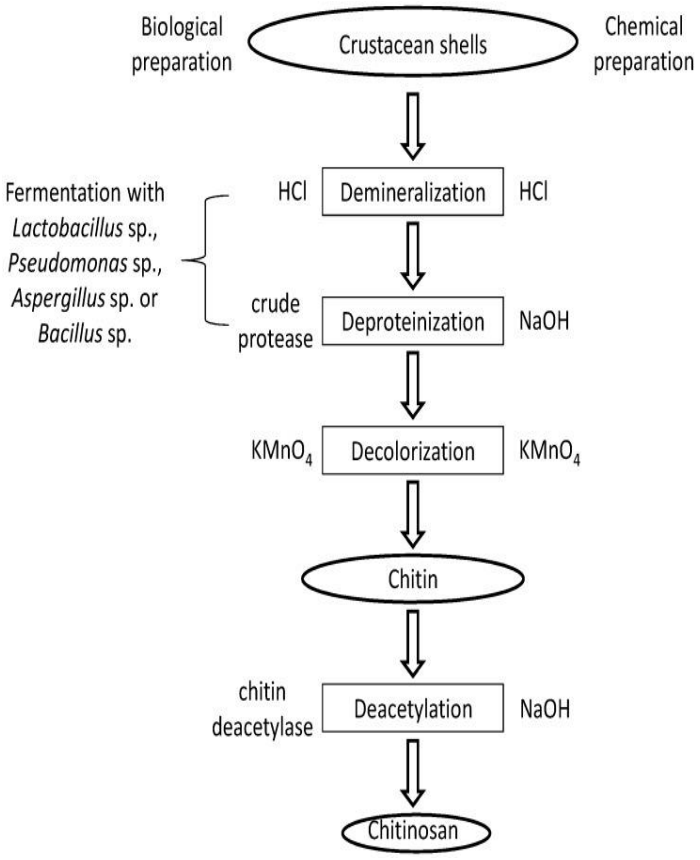

Figure 2.19: comparative extraction of Chitin and conversion to chitosan by biological (enzyme) and typical chemical process

2.1.8.6 Proximate/Composition characteristics

The chemical compositions of extracted chitin, is influenced by the extraction materials, method and sequence and can result in decreased ash and protein contents of extracted chitin. The residual contents of the individual components is influenced by the size of the sample being treated, the smaller the particle size the more exposed the surface with consequently more effective leaching out of the protein and other byproducts with resultant decreased value of ash and protein contents. The moisture content of chitosan is also affected by particle size. A direct relationship between these two properties was confirmed by Mahdy *et al.,* (2013), who observed that 20 mesh sized chitosans had moisture contents of between 11.87–13.12%, that of 40 mesh had between 5.69– 11.40%, while the 60 mesh sized ones had the least values of between 2.60–9.43% respectively. The observed phenomenon is explained according to Bough *et al.,* (1978), as the ability of larger particle sized samples to retain more moisture, accounting for the relative difference in value. Because all Crustacean exoskeletons possess varied amounts of calcium carbonate, and depending on the source and treatment (i.e. extraction process), the residual amount of Calcium carbonate contained in processed Chitin samples differ or are nonexistent (Abdou *et al*., 2008). But when the source of the raw material is fungal, the issue of calcium carbonate as a contaminant in extracted chitin products does not arise as can be observed from Table 2.1.

Table 2.1: .Proximate composition of some Chitin and Chitosan products from Shrimp sources.

Component	Extraction Reagent & concentration	Residual Quantity in Product (%)	Authors	Remark
Moisture	HCl and NaOH	45.65 ± 42.78	Mahdy et. al., (2013)	
	lactic acid bacteria	77.26	Farramae C. Francisco, Rhoda Mae C. Simora, Sharon N. Nuñal.(2015).	
	fish proteases-HCl	3.78 ± 0.31	Assaaˆd Sila et. al., (2013)	
Protein		32.77 ± 4.58	Mahdy et. al., (2013)	
		7.39	Farramae C. Francisco, Rhoda Mae C. Simora and Sharon N. Nuñal. (2015).	
	fish proteases-HCl	7.41 ± 0.52	Assaaˆd Sila et. al., (2013).	
Residual Calcium carbonate			Mahdy et. al., (2013)	
Ash		32.46 ± 2.08	Mahdy et. al., (2013)	
		7.49	Farramae C. Francisco, Rhoda Mae C. Simora, Sharon N. Nuñal. (2015).	
	fish proteases-HCl	0.22 ± 0.01	Assaaˆd Sila *et. al.,* (2013)	

2.1.8.7 Utility Potentials of chitosan and applications

Hudson and Smith (1998) have reported the inherent potentials of Chitosan and Chitin due to their natural composition. Comparatively, the reaction of chitosan is more resourceful than cellulose and this is due to the presence of -NH_2 groups (Dutta *et al.*, 2004). Like cellulose, chitin and chitosan undergo reactions like etherification, esterification and crosslinking (Hon, 1996) and dimerization. The main parameters that affect the characteristics of chitosan are its molecular weight (Zhou *et al.,* 2003) and degree of deacetylation (representing the proportion of deacetylated units) (Shanta *et al.*, 2016).

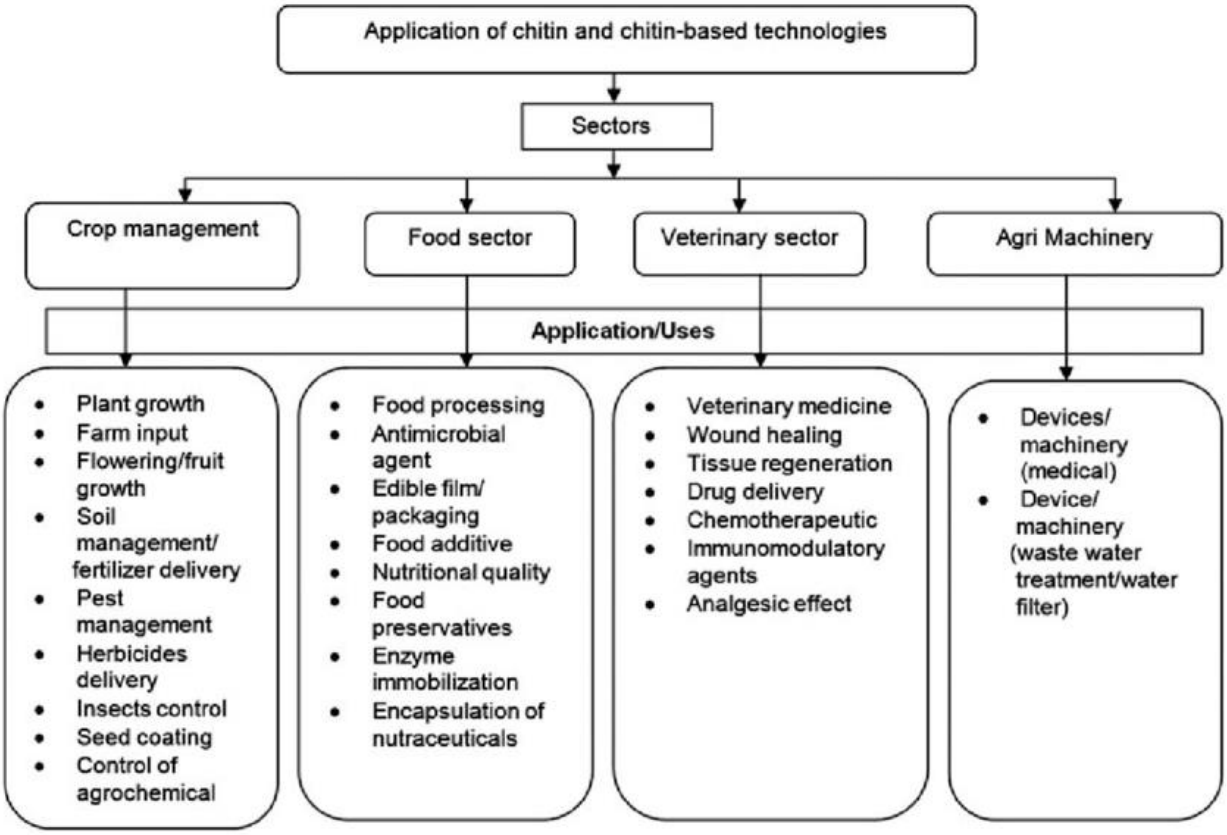

Figure 2.20: A typical impact areas of chitin and its derivatives**.** Adapted from Sastry, *et al*., (2015).

Figure 2.20 presents the application utilities of chitin and chitosan aside being a raw material for man-made yarns, absorbable sutures and wound dressing materials. Chitin and chitosan fibers are also used in waste water treatment (Sridhari *et al*., 2000). Chitosan is being used in the making of shampoos, hair colorants, styling lotions, hair sprays and hair tonics (Rinaudo, 2006). Chitin and chitosan are found as components in creams (a moisturizer), nail enamel foundation, eye shadow and lipstick cleansing materials and bathing agents. They are used in toothpaste, mouthwashes and chewing gum manufacturing. Chitin is also used as dental filler (Rinaudo, 2006). Chitosan acts as chelating agent and heavy metals trapper (Khor and Lim, 2003). Chitosan N-benzyl sulphonate derivatives are used as sorbents for the removal of metal ions in acidic medium and

are effective in removing arsenic from contaminated drinking water as well as to remove petroleum products from waste water (Saha and Sarkar, 2013). Chitosan has been used to remove the color from dye house effluent Weltroswki *et al.* (1996). Due to its non-toxicity it is used in the food industry as flavouring and colouring agent, shelf life extender as well as dietary fibre booster in baked food (Jianglian and Shaoying, 2013).

Chitosan is also employed in tissue engineering; this is the development and manipulation of laboratory-grown cells, tissues or organs that replaces or supports the function of defective or injured parts of the body (Khor and Lim, 2003; Vankatesam and Kim, 2010).

Chitosan has been found to be very useful in the repair of articular cartilage. Microporous chitosan/calcium phosphate composite scaffolds have been synthesized and characterized for tissue engineering. The report presents that chitosan provides the scaffold form while calcium phosphates encourages osteoblast attachement and strengthens the scaffold (Zhang and Zhang 2001; Elzein *et al.,* 2002).

Chitosan shows good effect on wound dressing and healing, while Chitin is utilized as a coating on regular biomedical materials. Recent finding has shown that standard silk and catgut sutures coated with regenerated chitin or chitosan show wound healing activities slightly lower than the chitin fibre (Murakami *et al., 2010*).

Chitin and chitosan are inexpensive and non-hazardous. They can be used for the preparation of dosage forms in commercial drugs (Andrady and Xu, 1997) such as spread dry chitosan acetate and ethyl cellulose are employed as new compression coats for 5-aminosalicylic acid (ASA) tablets (Nunthanid *et al.,* 2009).

Chitin/chitosan controlled delivery systems are in development stages. It is being used for a wide variety of reagents in several environments. (Surini *et al.,* 2003). The treatment of human disorders by the introduction of a genetic material into particular target cells of a patient where the production of the encoded protein occurs (Gene therapy), is being made safe and economical by the use of Chitosan (Corsi *et al.,* 2003).

Chitosan has been found to have growth-reticence effect on tumor cells (Carreno-Gomez and Duncan 1997). Although *in vivo* studies of targeted chitosan nanoparticles are currently limited, results from *in vitro* studies have demonstrated their promise for applications in cancer treatment and diagnosis (Hang, 2010).

Gavhane *et al*., (2013) reported wide biomedical applications of chitin and chitosan. Chitosan's relative high viscousity and low solubility at pH 7.0 exerts limitations in application in such areas, (Kim and Dewapriya, 2014). Nonetheless, chitosan's antimicrobial potential, in the form of film has shown great application promise for food preservation. The antimicrobial activity limits or prevents microbial growth by extending the impact interval period and reducing the growth rate or decreasing live counts of microorganisms (Han, 2000).

In order to correct the observed compromise in the properties of chitosan, various treatments have been used involving both chemical and physical dispositions. Some of these treatments are by the incorporation of reactive modifiers like cross linkers, grafting agents as well as using treatment conditions like ultrasonic, microwaving and irradiation energy systems during desired reaction periods.

2.1.8.8 Approaches in the modification of Chitosan.

In a bid to prevent the inherent shortcomings found with the use of chitosan and to ensure more robust and versatile applications, a number of approaches are employed in the modification of native chitosan. Over the last decades, the modifications of chitosan have been reported.

The presence of certain functionalities like $–NH_2$ and –OH groups in the chitosan molecules provides the basis for interaction with other polymers and biological molecules. Most commonly used methods for the modification of chitosan are blending, graft co-polymerization and curing. These approaches can be explained as:

2.1.8.8.1 Physical modification

Physical modification is the easiest way for modification of polymers. Physical modification is carried out by blending, or physically mixing of at least two polymers to create a new material with different physical properties. Polymer blending is the attractive route to achieve physical modification. It is designed to generate materials with optimized chemical, structural, mechanical, morphological, and biological properties and is a very economical technique for the modification of polymers. An additional advantage of blending is that materials with a wide range of properties can be obtained by altering the composition of the starting materials and the resulting blend polymer may be tailored to meet requirements for specific applications. At thermodynamic equilibrium, mechanical and thermal properties of blends are used to determine their miscibility and compatibility.

When hydrocolloids are blended with chitosan for film production, their inherent potentials are enhanced, (Vergas *et al.*, 2009; Park, Marsh and Rhim, 2002; and Xu *et al.*, 2005). Chitosan/pectin laminated films from blend of chitosan and pectin were produced and it was

found that the interaction was at the cationic group functionality of chitosan and the anionic sets of pectin. Xu *et al.* (2005) also reported an observed reduction in rates of water vapour transmission (WVTRs) when chitosan is blended with thermally gelatinized corn starches.

The mechanical and physical properties of other biofilms have been shown to be improved with blending with chitosan, more specifically with natural protein materials like casein, soy protein, gelatin e t c. chitosan–gelatin blend films have been shown to be homogeneous as a mix and this is due to formed electrostatic interactions between the NH_4 functional component of chitosan and the -COOH functional component of gelatin.

Park *et al.,* (2001) prepared new functional films (chitosan and polyvinyl alcohol) in different acid solutions such as citric acid, acetic acid, lactic acid, malic acid, by blending technique. The chitosan and poly vinyl alcohol (PVOH) improves the mechanical and barrier properties of the chitosan/PVOH blending films. The acid solvent used for preparing these blends promotes molecular interactions between the component polymers. This interaction allows for the development of properties which are intermediate between the component polymers (physical blending) and chitosan/PVOH blend, which is widely used in food applications (Park *et al.,* 2001).

Chitosan membranes blended with PVOH have been reported to show good mechanical properties for medical products as well as for controlled drug delivery. Uragami *et al.,* (1983) reported for the first time PVOH/chitosan membrane as cross linking agent for the active transport of halogen ions through this membrane. Recently Chouwatat et al., (2011) synthesized hydrophobic chitosan by mechanical mixing of aqueous chitosan with sodium dioctyl sulfosuccinate i.e. using solution mixing method. The hydrophobic chitosan was broadly

employed for the preparation of poly lactic acid (PLA)/chitosan blend. The PLA/chitosan blend was prepared by the solution blend method (Uragami *et al*., 1983).

2.1.8.8.2 Chemical modification

From Figure 2.21, the reactive functional groups found in chitosan are the primary hydroxyl group (at the C-3), the secondary hydroxyl group(C-6) and the amino/acetamido group(C-2).

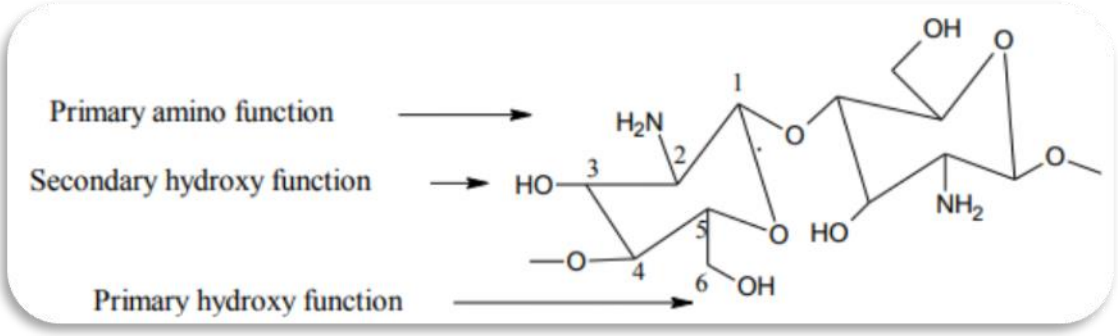

Figure 2.21: Functionality of a Chitosan molecule. Adapted from Rajasree & Rahate (2013)

For whatever modifications that may be carried out on Chitosan, one or both of the functionalities are involved. With some modifications, particularly where the target functionality is the Hydroxyl group, it is very necessary to protect the amino group on the Chitosan before carrying out the modification(s). This is primarily because the amino group is much more highly reactive than the hydroxyl group; therefore any applied interaction to the chitosan molecule is first received by the amino group. Phthalic anhydride is preferably employed as the protecting agent; an alternative to it is Di-tert-butyl dicarbonate (BOC). A number of approaches have been employed in the modification of chitosan based on intrinsic bond and functional group interactions. Functional groups like carboxylic acid and hydroxyl groups have been used to increase hydrogen bonding and to facilitate the formation of chemical bonds. Chitosan undergoes the same reactions as does amines, and this involves N-acylation and Schiff base formation

(Dutta, Dutta and Tripathi, 2004). The former is primarily carried out by the introduction of acid chlorides or anhydrides. This in turn presents amido group to the chitosan nitrogen. The intermediate forms a sort of radical which engages in consequent inclusion of adjacent chains. The most common chemical modification tools currently adopted are: irradiation, plasma induction, photochemical pinging and enzymatic grafting. Specific chemical modification templates applied are: xanthation, Schiff's base formation, sulphonation, nitration, acylation, alkylation, hydroxylation, graft copolymerization and phosphorylation. All of the efforts at modifying chitosan are to expand the versatile application areas which primarily require it being made soluble in various media and pH environments. These modifications are done in such a way that they do not alter the natural and original identity of the chitosan particularly at backbone positions. Recorded modifications s are: sulfated chitosan material which is water-soluble, anionic, and has antiviral(Nishimura *et al*., 1998), antimicrobial, anticoagulant (Preeyanat *et al.*, 2002) as well as osteogenic(Drozd *et al.*, 2001) action.

Ronghua, (2004) and Kai *et al*. (2011), reported the low cytotoxicity of sulfated chitosan derivatives and this makes them a welcome group of materials to be used in areas where toxicity is a major consideration. Two methods of preparing sulfated chitosan were demonstrated by Yuquan and Eugene (2009) and Zhou *et al*. (2009).

Quarternized chitosan, were prepared by Thanou *et al*.(2000); Luo, *et al.* (2010); Liu, *et al*. (2004) etc.

Acylated chitosan, was prepared by Inmaculada, Ruth and Angeles, 2010; Ming-chun LI *et al.*, 2005; Min and Shigehiro, 1995. While N-alkyl chitosan preparation was reported by Fang, Wen and Kang, 2002; Tamara. *et al*., 2008; Elena. *et al*., 2011 and Chun and Kyu, 1998.

Kurita (2006) reported the preparation of N-carboxymethylated chitosan via the formation of Schiff base from the free amino functional group of the native chitosan when reacted with appropriate keto or aldehyde. Other reports on the carboxy alkyl chitosan derivatives are those of Aiping *et al*. (2007); Muzzarelli, 1988; Thanou *et al*., 2001 and Chen and Tan 2006.

Thiolated chitosan's preparation was presented by Norio and Shin, 1998. This type of modification is usually carried out to enhance the muco-adhesive property of chitosan.

Chitosan has been phosphorylated as reported by Norio and Shin 1998. This attribute promotes osteoconduction where chitosan-based implants are used vis-à-vis the attachment to the calcium ions of the phosphate groups which initiates the development of the required calcium phosphate stratum. Foreseen and Kurita (2006), studied the chemical modification techniques for a wide range application in metal cation adsorption, medicine, water treatment, agriculture, separation, and food. Some other barrier applications involving chitosan have been reported, Ham-Pichavant *et al.* (2005) reported application of chitosan singly and in blend with sodium alginate as a fat barrier material, Kjellgren *et al.* (2006) and Despond *et al.* (2005) employed chitosan alone and chitosan-carnauba wax blend as gas barrier material.

2.1.8.9 Application of chitosan in molecularly imprinted polymer architecture/networks.

The application of chitosan and its derivatives in molecularly imprinted polymer matrixes have started gaining a lot of the attention from scientists in recent time. The ability of chitosan to be employed in the fabrication of moleculary imprinted matrixes is primarily due to its ability to dimerize.

2.1.8.9.1 Dimerization

Dimerization is the ability of a compound to have two equally similar fragments in the same compound. Theoretically, only a single amino group (at a time), of the chitosan (chitin dimer) takes part in the template binding; the other available one gets involved in crosslinking reactions. The chitosan polymer which has component make-up of numerous dimers of chitin presents a robust chain network for reactivities. The unit dimer possesses two nitrogen atoms that have sets of free electrons. These amino groups present in the chitosan, in an acidic environment gets protonated, and acquire an overall positive charge ($-NH_3^+$) which carry out ionic interaction between a template material and the host polymer matrix. This is the basis for most of the observed activities of chitin (limited reactivity) and chitosan (enhanced reactivity). For certain types of interactions involving chitosan and guest molecules like metal ions, which results into complex formation, ion exchange, adsorption and chelation, mechanisms are highly implicated but the specific one depends on the factors such as medium of interaction, pH, type of ions and chemical architecture of the matrix (chitosan). This potential allows chitin and chitosan to undertake very robust chemical interactions in imprinting technology and many other chemical interactions like copolymerization, adsorptions and selective target guest displacement/replacement activities.

2.1.9 Template Polymerization

It is known that the volume of polymers produced worldwide is greater than the volume of steel produced. In the last decades, polymers have had applications not just as industrial bulk materials but also in high technological fields such as nanotechnology, optics and biomaterials (Bailey *et al.*, 1964). Due to high demand prompted by pressured requirements for extremely good polymer materials, an increasing possibility to design *"intelligent polymers" i.e.* specialty polymers has

been the critical drive within the industry. These polymers are formed via the process of chain inter-linking of their monomer units via chemical reactions to yield the desired long chain products. These long chain characteristics make polymers different from other chemical entities and give them special and unique properties.

The term “Template”, also known as matrix or replica polymerization is x-rayed as a method of synthesizing polymers in which certain reactions are performed between a template and a growing chain of monomer(s) to produce a specific structured product Figure 2.22, (Stefan, 1997). These coordinated interactions impact on the structure characteristics of the polymerized product and influence the overall kinetics of the process. The type of reaction, sequence and rate is largely dependent on the catalyzing moieties. Ferguson and Eboatu (1989) illustrated the impact of templating in polymerization reactions using “Fenton” catalyst in a redox-initiated polymerization of acrylic acid. In the absence of template material (polyvinylpyrrolidone), a high polymerization conversion of about 80% was achieved at two distinct temperatures of 26^{o}C (room temperature) and elevated temperature of 74C. When the template material was introduced, the percentage conversion was reduced and polymerization time increased. Their finding sends a cautionary message with respect to selectivity and use of template materials in polymerization reactions. It also paves the way for the ability of scientists to prepare polymers with tailored end-use utility based on the characteristic interactions between the monomers, the templates, cross linkers and initiators. Their finding substantiated the impact of template materials in the chemical cocktail encountered during polymerization. This usually occurs with one phase systems in which the monomer, template, and the product are soluble in the same solvent (Banford, 1979) and is referred to as homo polymerization. For systems that differ in this conformation, copolymerization is said to be the overriding phenomenon.

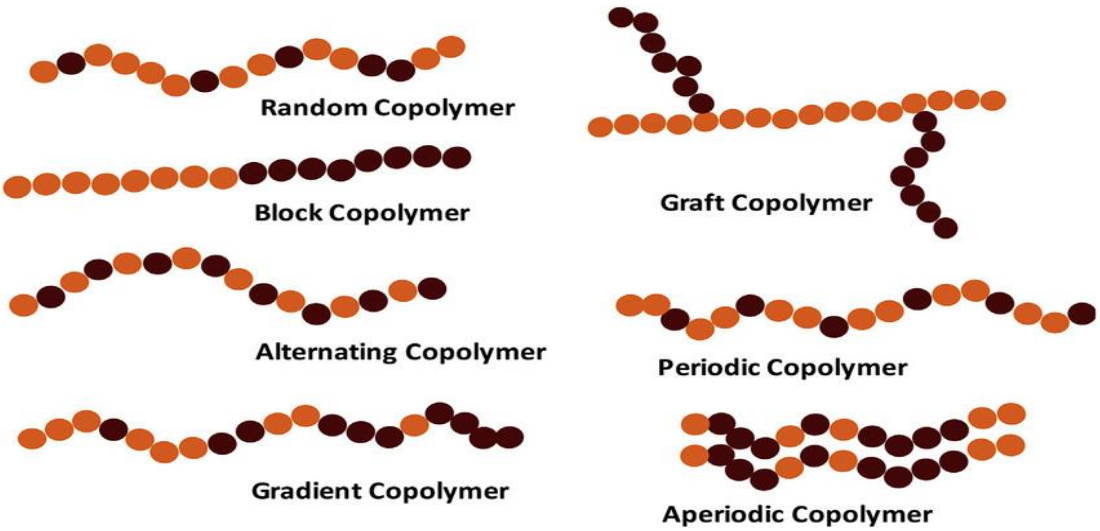

Figure 2.22: Copolymers, showing different family types.

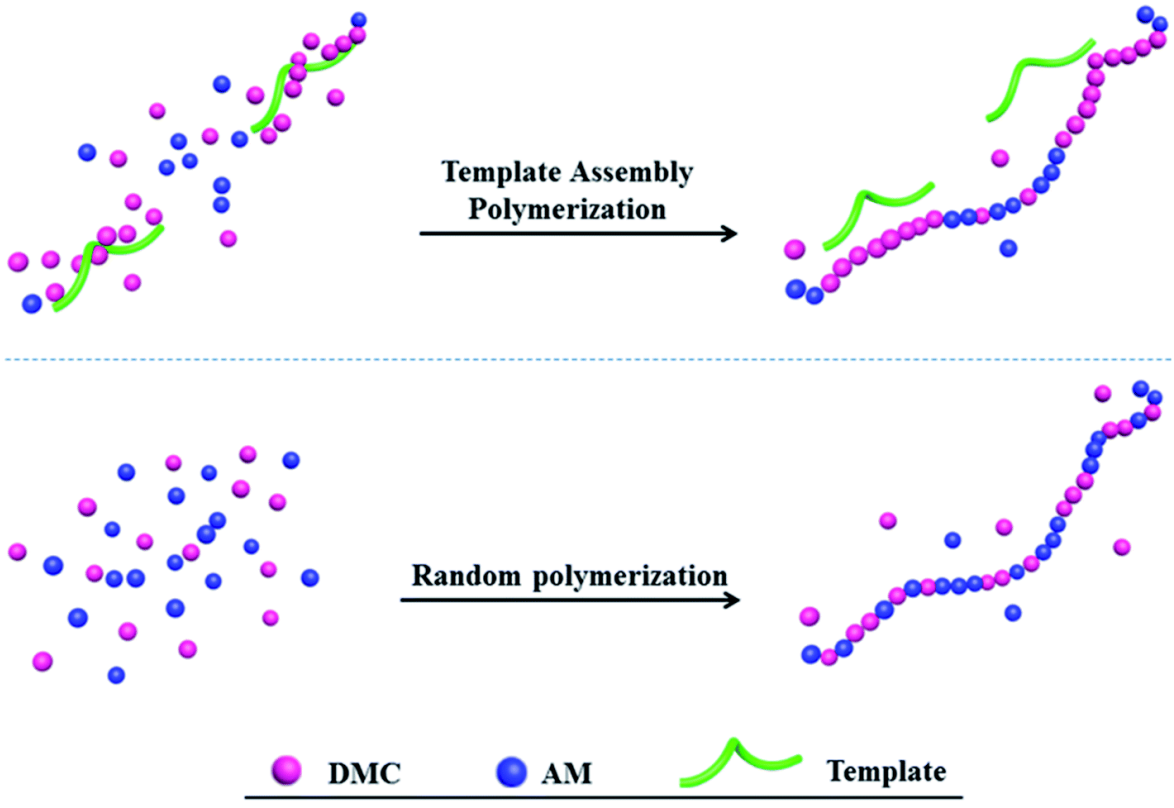

Figure 2.23: Specificity of arrangement for random copolymerization and template copolymerization.(Liu *et. al.*, 2017).

In homo polymerization, addition may lead to either iso or syndio tactic placement, while in copolymerization further ambiguity is introduced by the possibility of reaction between a given

propagating chain and any monomer species present; similar conditions also apply to conventional condensation copolymerization (Watson *et al.,* 1987).

Recently, polymerization of monomer molecules has been studied in the crystalline state, as mono- and multi layers either, in solution, in the liquid-crystalline state, and or on templates. The templates are usually linear polymer molecules having groups which interact with monomer molecules; ideally, to produce a predetermined linear array of the latter (Tan, 1989).

Template polymerization is also remotely related to the field of polymer catalysis. The overbearing need in template polymerization is actualized by the polymerization of monomer units attached to the template in a predetermined manner and thus the synthesis of polymers or copolymers with definite structures complementary to those of the template (Stefan, 2002).

The growth of living organisms is related to very complex processes of polymerization. Low molecular weight substrates, such as sugars, amino acids, fats, and water in animals and carbon dioxide in plants are precursors of polymers (polypeptides, poly nucleic acids, polysaccharides, etc.). They are developed in tissues and can undergo replication. In many biological reactions such as DNA/RNA replication or polypeptide production, low molecular weight substrates and polymeric products are present as precursors in the reaction medium together with the template compounds. A robust array of examples exists within the report by Kullmann (1987). Comparison between natural biological processes and template polymerization of simple synthetic polymers were reported.

During the basic step of peptide formation, two or more reacting components are pre-bonded by the enzyme molecule. A simple model of such reaction is presented in Figure 2.24.

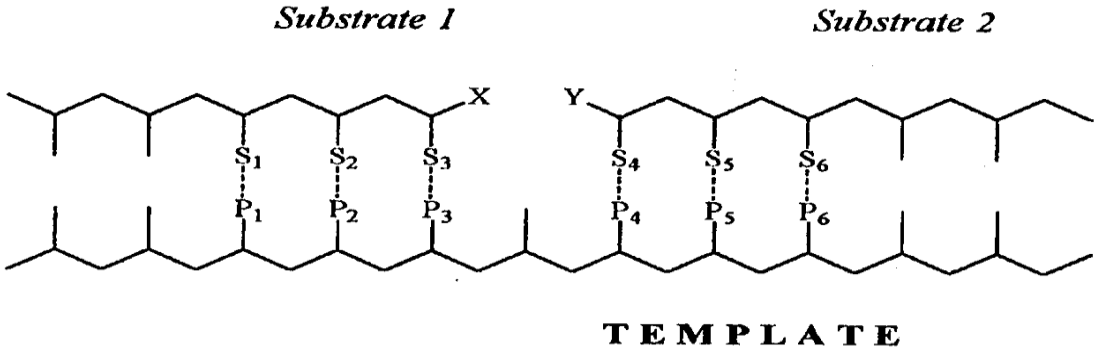

Figure 2.29: Simplified model of enzymatic polypeptide synthesis. X and Y are reacting groups and S1.... P1, S2 ... .P2, etc. alate-substrate. By the selective sorption, the substrate 1 is connected with a specific part of the template (possessing specific sequence of interacting groups P1, P2, P3). The second substrate is absorbed by another part (with sequence of interacting groups P4, P5, P6). As a consequence of the selective sorption, the reacting groups X and Y are brought closer together and reaction between X and Y is promoted (Stefan, 1997).

This simple mechanism clarifies the abnormal selectivity and high efficiency of exemplified template reactions. The specific character of the enzyme's activity towards a particular substrate becomes obvious. The effect of macromolecular template on the rate of reaction and most especially its selectivity clearly shows that this type of reaction is a catalyzed reaction. The template plays the role of a polymeric catalyst (Bamford, 1979). Furthermore, template polymerization has been projected as processes in which polymerization takes place in organized systems (Elias, 1977). Many factors influence such sequential organization of monomer units during polymerization. Example is polymerization activity in solid state which proceeds with molecules of monomer surrounded by molecules already organized in a crystal lattice form. This influences a specific type of polymerization occurring on the surface of solids.

Numerous monomers with long hydrocarbon chains can form mono layers at the gas-water interface and then oriented on the surface of water. Polymerization of systems having such an organization leads to the preparation of polymers with peculiar morphology and properties. This method of polymer synthesis predominates in ultra-thin films of different forms. For instance,

this method is used to produce drugs containing polymeric microspheres. Polymerization in the presence of clays and other minerals is believed to have catalyzed the polymerization of amino-acid derivatives in early life developments/formations. The strength of the bond inherent within this activity strongly bind proteins and resist separation or departiclation without destruction of integral polymer compound. Polymerization in liquid crystalline state is also an example of polymerization in an organized system (Tan and Challa, 1989).

It is very imperative to study template systems in order to make comparison between the template process and products of the reaction with conventional polymerization carried out under the same conditions. It is typical to replace template by a low molecular non-polymerizable analogue. The influences of the template on the process and the product are usually called "template effect" or "chain effect" (Tan, 1989), and these template effects can be expressed as:

I. Kinetic effect - usually an improvement of the rate of reaction and change in kinetic equation.

II. Molecular effect - influence on the molecular weight and molecular weight distribution. In an ideal case, the degree of polymerization of daughter polymer is the same as the degree of polymerization of the template used and this can be called a replication.

III. Effect on tacticity - the daughter polymer can have the structure complementary to the structure of the template used. In the case of template copolymerization, the template effect deals with the sequence distribution of units. This effect is very important in biological synthesis, for instance in the DNA replication.

The template processes can be realized as template poly-condensation, poly-addition, ring-opening polymerization, and ionic or radical polymerization (Inaki and Takemoto, 1987).

Template polymerization allows the growing of monomer radicals in an environment that contains a choice template to produce a macromolecule i.e. a low molecular weight monomer being converted to a polymer with the inclusion of the extractable influencing template by chain polymerization. Such mode of propagation can be achieved through the instigation of cooperative interactions between the growing chain and the template chain, and this usually leads to the formation of an inter-polymer complex. In general, a well chosen template is able to affect the rate of polymerization as well as molecular weight and microstructure of the daughter-polymer. The obtained rate enhancements are usually a function of how slow the termination step is since radicals are less mobile due to their association with influencing template (Tan and Challa, 1987).

The concept of template polymerization was first described by Ballard and Bamford in 1956, with the ring opening polymerization of the N-Carboxyanhydride of D,L-phenylalanine on a polysarcosine template (Ballard and Bamford, 1956). Since then many other systems involving either addition, ring-opening or condensation polymerization have been studied in which one or more template effects were identified, leading to a substantial number of review papers in recent years.

The primary objective in template polymerization was the synthesis of polymer with accurate predetermined structure as occurs in nature with self-replication of DNA and biosynthesis of proteins. The template polymerization of urea and formaldehyde along with poly (acrylic acid) in water led to a complex which cannot be obtained in any other way due to the instability of urea-formed polymer in water (Papisov *et al*., 1984). The general conviction is that by template

growth of a radical, more complete and ordered complexes may be prepared (Kabanov *et al.*, 1973). This is demonstrated with the spontaneous polymerization of 4-vinylpyridine alongside isotactic poly (acrylic acid), leading to crystalline polyelectrolyte complexes. Similar results were reported (Tsuchida and Osada, 1974) during the polymerization of p-styrene sulfonic acid alongside ionene templates. Complexes produced in the polymerization of methacrylic acid (MAA) in the presence of similar ioenes could be spun into fibres (Tsuchida and Osada, 1975). On the same vein, semi and fully interpenetrating polymer networks (IPNs) produced by polymerization of acrylic acid with a crosslinking agent in the presence of linear or crosslinked poly (ethylene oxide) could be used as membranes and their permeability could be changed by varying the pH or ionic strength (Nishi and Kotaka, 1985). Photoinitiated polymerization of acrylic acid in the presence of a surface of poly (dimethydiallyammonium chloride) was used by Ratzsch (Ratzsch, 1985). However, it appeared difficult to actually prove the growth of a radical along the template, through the variation of polymerization rate with template to monomer ratio pointed towards a template process.

2.1.9.1 General Mechanism of Template Polymerization.

Template polymerization follows two general mechanisms; the zip mechanism or type I mechanism and the "pick-up" mechanism or type II mechanism (Tan and Challa, 1981). In the type I mechanism, monomers are joined to the template by interactions such as electrostatic or hydrogen bonding. Polymerization of the monomer takes place along the template. In the pick-up mechanism, monomers are connected with an active oligomer created in free solution complexed to the "template", this allows propagation around the template by the addition of monomer. These two mechanisms are quite different and consequently their kinetics, molecular weight distribution, influence of reaction parameters on the process, etc., differ in both cases. For the same reasons, the template reactions differ, irrespective of the polymerization process

mechanisms adopted (Polowinski, 1994). The diagram in Figure 2.25 shows the two fundamental mechanisms:

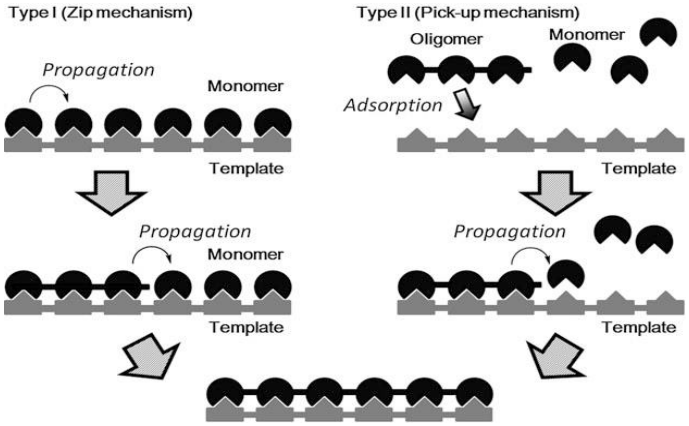

Figure 2.25: Schematic representation of the mechanism of template polymerization (Mitsuru and Hiroharu, 2014).

In the course of achieving a polymerized product, either of the two major routes is usually followed. These routes are; a) the polycondensation and b) chain propagation routes.

2.1.9.2 Template Polycondensation

Template polycondensation or generally, template step poly-reaction, is the most similar to natural synthesis of polypeptides or polynucleotides which occurs in living organisms. Using simple models as macromolecular templates, a superior understanding of the specificity of natural processes of biopolymer synthesis is achievable (Yamazaki and Higashi, 1981).

Because template polycondensation has not been very well studied, the overall general mechanism is difficult to model. The conventional polycondensation is of two primary types and they are the hetero and homo polycondensations (Polowinski, 1984). In the heteropolycondensation, two different monomers take part in the reaction (e.g., dicarboxylic acid and diamine). In the case of homopolycondensation, one type of monomer molecule is present in the reacting system (e.g., amino acid). The results published (Higashi *et al.,* 1980) with respect to template heteropolycondensation indicates that monomer (dicarboxylic acid) is integrated into

the structure of the matrix (N-phosphonium salt of poly-4-vinyl pyridine) while the second monomer (diamine) reacts with the activated molecules of the first monomer. The mechanism can be represented as shown in the figure 2.26.

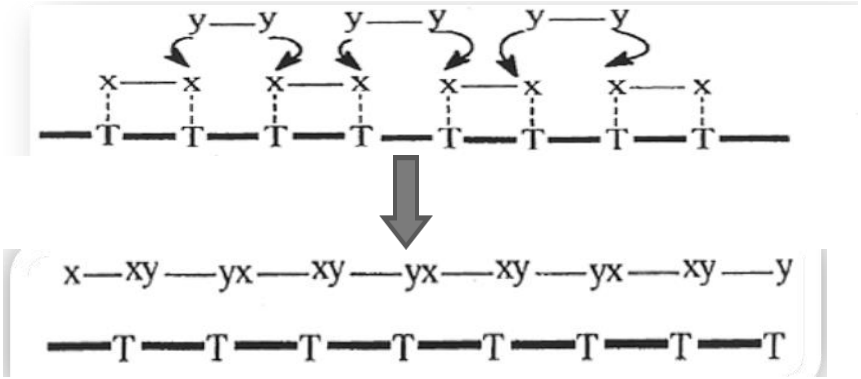

Figure 2.26: Template heteropolycondensation (Stefan, 1979).

In this case, one monomer with groups x (e.g., COOH) can be adsorbed on the template -T-T-. The second monomer with groups 'y' (e.g., amine) reacts, forming a daughter polymer having groups 'xy' and the template is available for further reaction.

2.1.9.3 Chain Template Polymerization

Most papers published in the field of template polymerization dealt with systems in which both template and monomer are dissolved in a proper solvent, and initiation occurs according to the chain mechanism (Simha *et al.,* 1963). Generally, for chain processes at least three rudimentary stages of initiation, propagation and termination play out.

In the case of template processes, this mechanism must be completed by conditions accounting for interaction between template, monomer, and polymer. Intermolecular forces lead to adsorption of the monomer on the template or, if interaction between monomer and template is too weak, oligoradicals form complexes with the template. Taking into account these differences in interaction, template polymerization can be divided into two types of Type 1 and Type 2 (Ogata *et al.,* 1980). In Type I, monomer is pre-adsorbed by, or complexed with, template

macromolecules. Initiation, propagation and perhaps mostly termination take place on the template. The mechanism can be represented by the scheme given in Figure 2.27.

On the template unit, -T-, monomer, M, having double bond is adsorbed. Radical, R•, initiates propagation process which proceeds along the template, and eventually a complex of the template and the daughter polymer, consisting M-units, is created. In extreme cases of template polymerization proceeding according to mechanism I, the monomer units are attached to the template by covalent bonding (Aminabhavi and Munk, 1979). The substrate can be referred to as a multi-monomer, the product after template polymerization as ladder-type polymer. Chain template polymerization of multi-monomer is best understood as being similar to that in Figure 2.27, as is presented in Figure 2.28. The only difference is that hydrogen bonding in Figure 2.27 is replaced by covalent bonding between T and M in Figure2.28 in both the substrate and the product.

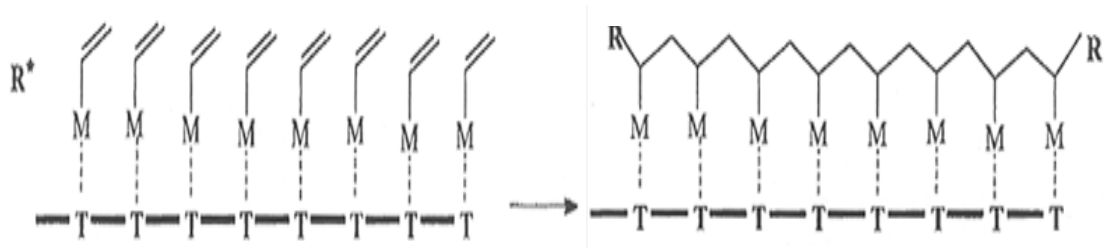

Figure. 2.27: Chain template polymerization of Type I.

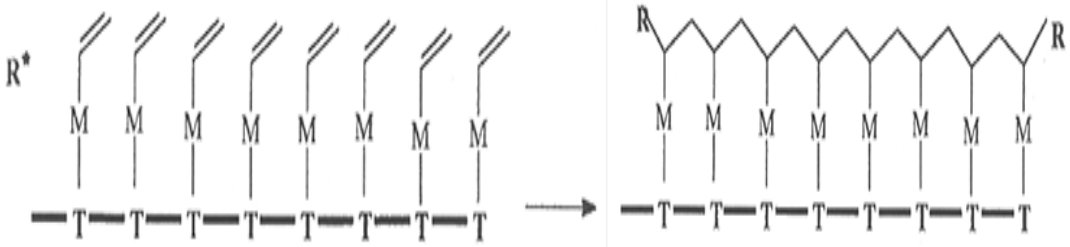

Figure 2.28: Chain polymerization of multimonomer

2.1.9.4 Template Copolymerization

In template copolymerization, the interaction between co-monomers and the template could pre-arrange monomer units in a sequence defining distribution in the macromolecular product.

As seen in the case of template homopolymerization, template copolymerization can be accomplished according to different types of reactions: stepwise (template polycondensation), copolyaddition, radical or ionic polymerization, ring-opening copolymerization, etc. Limited publications are available in literature on template copolycondensation despite the process being a very important one in defining the mechanisms of the processes similar to natural synthesis of biopolymers. Meanwhile the general mechanism of this reaction may be considered using examples of template step homopolymerization.

Investigation of radical template copolymerization has been slightly more extensive. Three fundamental types of interactions exist for this process: covalent bonding, strong intermolecular forces, and weak interactions between template and oligomers which may exceed the critical length. However, these interactions can vary when two different types of co-monomers are used. An example of this is when one monomer is reactively docile with the template. This creates a complex classification of the template copolymerization systems when compared with homopolymerization (Polowinski, 1994).

2.1.9.5 Models of Templated Polymerizations

2.1.9.5.1 Polyacids as Templates

One of the earliest cases of template polymerization was the spontaneous polymerization of 4-vinyl pyridine in the presence of polyacids. Vinyl pyridine can polymerize without adding initiator in the presence of low molecular weight acids and polyacids such as poly(acrylic acid), poly(methacrylic acid), poly(vinyl phosphonic acid) or poly(styrene sulfonic acid). Polyacids

support much higher initial rates of polymerization and lead to different kinetic equations. The chain reaction mechanism includes anion addition to activated double bonds of quaternary salt molecules of 4-vinylpyridine, then propagation in the activated center, and termination of the growing center by protonization.

2.1.9.5.2 Polyimines and Polyamines as Templates

As published by Bamford and Shiiki (Bamford and Shiiki, 1968), polyethyleneimine have been employed as template for polymerization of acrylic acid. The polyethylene imine formed water insoluble complex with polyacrylic acid. Polymerization was done using potassium persulphate as an initiator followed by titration using turbimetry and bromometry. At lower temperatures during the polymerization, precipitation was observed to take place while at higher temperatures, degradation of the complex occurred and the precipitate rapidly disappeared. Polymerization rate was optimized where the template concentration is lower than the monomer concentration. The authors concluded that the obtained result was probably due to template effect, the heterogeneity of the system and a change in the initiation due to the presence of a redox system (polyimine-persulphate). However, no graft or block copolymers were found in the reaction products which seems to implicate the 'template effect'. Other works are those of Cerrai *et al.*, (1994) where the polymerization of sodium acrylate on polyallylamine hydrochloride template was reported. In aqueous solution, sodium acrylate molecules are adsorbed onto a template with ammonium cationic pendant groups. The complex was polymerized in water using AIBN or $K_2S_2O_8$ as initiators.

Some researchers Blumstein *et al.* (1974) reported the use of polybase ionenes like poly (hexamino-1-hexane) and poly (hexamino-1-decane) were used as templates. The formation of complexes involved two steps. In the first step, the ionene bromide was converted to ionene

hydroxide by replacing the Br^- ions with OH^- ions. In the second step, the equivalent quantities of acid and ionene were mixed together. Polymerizations were carried out mostly in water-isopropanol solution. Polymerization of p-styrenesulfonic acid onto various ionenes was studied as a function of the charge density of the template (Blumstein *et al.*, 1974); it showed a linear dependence of rate on charge density. The use of poly ethylene oxide (PEO) and poly vinyl pyrrolidone (PVP), as templates was reported by Smith *et al.*, (1959). These templates were used alongside either acrylic acid AA, (Ferguson and Shah, 1968; Bailey *et al.*, 1964) or methacrylic acids. These monomers are the most usually used due to the fact that they form strong, water insoluble complexes. It was found that the rate of AA polymerization in water, initiated by potassium persulphate is strongly dependent on the concentration of PVP used as a template. The maximum point of this relationship corresponds to equimolar ratio of AA to PVP units. Equimolar complex composition was confirmed by gravimetric experiments. It was shown that 'template effect' strongly depends on the complex formation. When AA was polymerized in the presence of PVP, but at pH=4.5 (when system was homogeneous), no increase in polymerization rate occurred. Also, no acceleration was observed when PVP was replaced by methyl pyrrolidone. The presence of polymeric, interacting compound was found essential for acceleration to take place. It was found that the mechanism of polymerization is the same as in the presence of homopolymer (PVP). However, the rate of polymerization decreases rapidly when vinyl pyrrolidone concentration in copolymer decreases. The concentration of vinyl pyrrolidone residues was kept equimolar to the concentration of acrylic acid. It was stressed that structure of template and, in the case of copolymeric template, sequence distribution of units play an important role in template effect. Polymerization of methacrylic acid, MA, in aqueous solutions, in the presence of PVP, was investigated by Shavit and Cohen, (1977). Fractions of

PVP of varying molecular weights were used as templates. The rate of polymerization increased with the increase in molecular weight of PVP. The change in tacticity of daughter polymer was observed as well as the change in kinetics in comparison with blank polymerization carried out under the same conditions but in the absence of PVP.

2.2 Theoritical Framework

2.2.1 Molecularly Imprinted Polymers and impact of individual inputs.

Molecular imprinting is an easy and effective method to prepare polymeric separation media having specific molecular recognition towards the template molecule. In this method, the molecule is admixed with an appropriate host monomer and a large amount of cross-linking agent and solvent. Possible assembly from the template molecule and the host monomer can be achieved through non-covalent molecular interactions (Kempe and Mosbach, 1995), and this assembly is polymerized and cross-linked to result in molecular imprinted separation media. The molecule, for which selectivity is desired, called template or target molecule, is allowed to prearrange prior to polymerization in presence of monomer(s) with different functional groups that can interact with the template. After polymerization the target molecules are removed, leaving well-defined three dimensional cavities with spatially oriented functional groups in the highly cross-linked polymer network.

Molecular imprinting technique was first demonstrated in the late 1940s by Dickey (Dickey, 1949) and it primarily involves:

a) Pre-arrangement of the print molecule (template) and the functional monomers at low temperature so that complementary intermolecular interactions among functional groups can develop,

b) Polymerization of the monomers under conditions that cause minimal disturbance to the print molecule-monomer interactions, and

c) Extraction of the print molecules from the polymers, which leaves behind "receptor sites" that are complementary to the templates or print molecules in terms of size, shape, and functional group orientations. This technique has been used for the preparation of selective recognition sites for a wide variety of molecules (Mosbasch and Ranstrom, 1996).

Covalent and non-covalent interactions can be employed in pre-polymerization pre-arrangement between template and functional monomer. Covalent bonds are adequately strong but non-covalent interactions require use of functional monomer which forms stable self-assembled complexes. Molecular imprinting is recognized as a powerful technique to synthesize polymer-type artificial receptors. In this technique, functional monomers and cross-linkers are polymerized in presence of a template molecule, which is followed by the template removal from the resultant polymer network to leave a template fitted cavity. The functional monomers used are expected to be laid out in the cavity as complementary to the chemical functionality of the template molecule. This is because the functional monomers are bound with the template molecule during the polymerization. The selection of appropriate functional monomers and the determination of their stoichiometry applied are most important in the design of a molecularly imprinted system for given target molecules. To date, one of the most successful molecular imprinting protocols employed is bulk polymerization to obtain glassy polymer blocks which are used as powder after being crushed, ground, and sieved (Toshifumi *et al.,* 1999).

Molecular imprinting seemed like an ideal platform for the synthesis of transition metal catalysts located within the interior of an imprinted active site. The imprinting process consists of the

copolymerization of organic or inorganic templates into highly cross-linked organic polymers. Most of the MIP efforts have been directed to analytical applications, these techniques have in recent times been applied to problems in synthesis and catalysis (Whitcombe *et al.*, 2000).

In the course of a typical template polymerization process, a number of inputs are brought into bond breaking and formation interactions. Outcomes of such interactions depend on several factors but generally the common inputs that are utilized are:

2.2.1.1 Templates

The template is of central importance and it directs the organization of functional groups pendent to the functional monomers in all molecular imprinting processes. In terms of compatibility with free radical polymerization, templates should ideally be chemically inert under the polymerization conditions, thus alternative imprinting strategies may have to be sought if the template can participate in radical reactions or is for any other reason unstable under the polymerization conditions (Sellergren, 1997). The imprinting of small organic molecules like pharmaceuticals, pesticides, amino acids and peptides, nucleotide bases, steroids, and sugars is now well established and considered almost routine. Optically active templates have been used in most cases during optimization. In these cases, the accuracy of the structure of the imprint could be measured by its ability for racemic separation, which was tested either in a batch procedure or by using the polymeric materials as chromatographic supports. One of the many attractive features of the molecular imprinting method is that it can be applied to a diverse range of analytes. However, not all templates are directly amenable to molecular imprinting processes (Yilmaz, 1999). Most routine imprinted polymers were made using small organic molecules as template. Specially adapted protocols have been proposed for large organic compounds such as proteins; imprinting of such large structure is still a challenge. The primary reason is the fact that

such templates are less rigid and thus do not facilitate creation of well-defined binding cavities during the imprinting process (Anderson, 1999). Mashira *et al.,* (1980), observed from their investigations that the polymerization of bis(p-nitrophenyl) 2- (thymine- 1-ylmethyl) succinate or p-xylenediamine in pyridine-CH_2Cl_2 or DMF was accelerated by the presence of 9- (vinyl benzy1) adenine polymer or copolymer with styrene as templates and concluded that the reaction rate is accelerated in the presence of the template. Lohmeyer *et al*., (1980) studied the polymerization of methacrylic acid in the presence of isotactic monomers (methylmethacrylate) as a possible template at 45^{O}C and 100^{O}C polymerization rate and the radical lifetimes were identical with those of the corresponding blank. Methylacylate on DNA from either X or TX bacteriophase by a special competition test preferentially transcripted directedly by the DNA species used as the template for the synthesis of polymers. Polinnaya *et al*., (1981) studied the template-guided polymerization of decanucleotide and reported on the properties of DNA duplexes with repetitions. They showed that the template-directed polymerization of decanucleotide, induced by water solution carbodimide, yields a number of 40-100 membered polymers with natural 3', 5'-phosphodiester bonds. Reza *et al.,* (1981) investigated the polymerization of methyl methacrylate with varying ratios of $(CH_2{:}CHCONH_2)_2Z$, where Z = CH p-C H or 3,5-CH COOH, in the presence of the templates of Rhodanile blue and safranine 0, and found that the polymers showed relative selectivity toward the templates. Adem *et al*. (2011) studied the Template-Directed Synthesis of Silica Nanotubes for explosive detection; they synthesized fluorescent silica nanotubes using a biomineralization process through self-assembled peptidic nanostructures, and also designed and synthesized an amyloid-like peptide self-assembling into nanofibers to be used as a template for silica nanotube formation. The amine groups on the peptide nanofibrous system were used for nucleation of silica nanostructures.

Silica nanotubes were used to prepare highly porous surfaces, and they were doped with a fluorescent dye by physical adsorption for explosive sensing. Adem *et al.*,(2011) also studied fluorescence quenching based explosive sensing performance of dye doped peptide nanofiber (ALP) templated high aspect ratio silica nanotubes. TEM results of ALP nanofibre showed that the diameter of the ALP nanofibre was about 15 - 20nm and the length was in micrometer range. The silica mineralization was achieved using tetraethyl orthosilicate (TEOS) as a precursor. Nitrogen and carbon signal was not observed in the SEM image. The FSNT sensor surface was characterized with AFM and the result indicated that individual nanotubes as well as thicker structures formed by aggregation of nanotubes. In order to test selectivity and sensitivity of FSNT sensor, vapour phase fluorescence quenching experiments were performed with TNT, DNT, toluene, and xylene. A rationally designed peptide nanostructure was used as a template for silica nanotube preparation. The ALP template also catalyzed silica mineralization by the amine groups. To provide explosive sensing property to the silica nanotubes, they were doped with afluorescent dye. The fluorescent nanotube coated surfaces revealed fast fluorescence quenching against DNT and TNT due to its porous structure. The high selectivity of the FSNT sensor fornitro-explosives was demonstrated by testing the sensor with other control aromatic compounds. The ALP templated high aspect ratio silica nanotubes present a promising platform with their high surface area for sensing and catalysis applications.

2.2.1.2 Functional Monomer

The careful choice of functional monomer is the most important factor to provide complementary interactions with the template and substrates. For covalent molecular imprinting, the effects of changing template to functional monomer ratio are not necessary because the template dictates the number of functional monomers that can be covalently attached;

furthermore, the functional monomers are attached in a stoichiometric manner. For non-covalent imprinting, the optimal template to monomer ratio is achieved empirically by evaluating several polymers made with different formulations with increasing template (Kim and Spivak, 2003). There is an increase in the number of final binding sites in the imprinted polymer, resulting in an increased binding or selectivity per gram of polymer. From the general mechanism of formation of molecularly imprinted binding sites, functional monomers are responsible for binding interactions in the imprinted binding sites. Non covalent molecular imprinting protocols are normally used in excess relative to the number of moles of template to favour the formation of template functional monomer assemblies (Ramstrom *et al.,* 1993). It is very important to match the functionality of the template with the functionality of the functional monomer in a complementary fashion (H-bond donor with H-bond acceptor) in order to maximize complex formation and thus the imprinting effect. High retention and resolution were observed in imprinted polymers with two co-monomers than a single monomer, which indicated an increase in the affinity of the imprinted polymer by the co-operative effect of the binding sites in both monomers. However, it is important to note that the reactivity ratios of the monomers should be verified to ascertain the feasibility of co-polymerization (Yu *et al.,* 2006).The most critical point in the molecular imprinting concept is, (especially when the functional monomers are bound to a template by non-covalent bonding), whether functional monomers form a steady complex with a template molecule. Therefore, the selection of appropriate functional monomers and the determination of their stoichiometry applied are most important in the design of a molecular imprinted system for specific target molecules. Examples of commonly used functional monomers in molecular imprinting are; acrylic acid, methylmethacrylate, p-vinylbenzoic acid, iraconic acid, 4-vinlypyridine, 2-vinylpyridine, styrene, acrylamide, methacrylamide etc.

Bunermann *et al*., (1981)'s reported the synthesis and properties of acrylamide- substituted base-pair specific dyes. The authors demonstrated that acrylamide and other small acrylamide derivatives can be used as binding blocks for the synthesis of polymeric links between base-pair specific monomers. This was possible because the binding affinity of DNA-specific ligands was improved by their di- and oligo-merization. They used AT-specific malachite green and GC-specific phenyl neutral red as primary precursors for the synthesis of base-pair specific monomers and synthesized a set of monomers with structural differences. Smid *et al.* (1983) studied the effect of poly (2-vinylpyridine) as a template for the radical polymerization of methacrylic acid and determined the reaction rate using calorimetry and dilatometry techniques. Alberda *et al.* (1984) carried out an investigation on template polymerization system of methacrylic acid or poly (N-vinylpyrrolidinone) using tert-Butcyclohexyl peroxydicarbonate as initiator and reported that the activation energy of the template polymerization and the blank polymerization reactions were identical but their pre-exponential factors were slightly different. Al-Alawi, (1991) carried out a research on the Complexes prepared by template polymerization and the effect of molecular weight of PVP on the crystallinity of complexes was studied. He prepared macromolecular complexes using two methods; the mixing method and the polymerization method. In the mixing method, aqueous solution of PAA was mixed with an aqueous solution of PVP, without initiator. Each experiment was repeated with PVPs of different molecular weights (complexes I). Complexes III were prepared by mixing an aqueous solution of it-PAA with PVP as described for complexes I. In the polymerization method, acrylic acid was polymerized in the presence of PVP (template polymer) and potassium persulphate initiator. Each experiment was repeated using PVPs of different molecular weights (complexes II). Moisture regain (MR) measurements were carried out and from findings; two types of complexes

were prepared. Complex I was prepared by mixing an aqueous solution of atacticpoly (acrylic acid) with poly (vinylpyrrolidone) of different molecular weights in an aqueous medium. Complex II was prepared by template polymerization of acrylic acid in the presence of PVPs of different molecular weights in an aqueous medium. Result from FT-IR studies showed that the two types of complexes were composed of PAA and PVP. The effect of molecular weight as shown from differential scanning calorimetery (DSC) measurements showed that Tg values for PAA varied from 110 to 120^{O}C. It was found that the Tgs for the PVPs were independent of molecular weight and the results showed that the Tgs for PVPs for different molecular weights were between 90 and 100^{O}C, and that was in agreement with the results reported by Faucher (Faucher *et al.,* 1966). Moisture regain (MR) was carried out to detect the effect of molecular weight of PVP on the crystallinity of the molecules in the complexes. The results showed that the MR for the complexes increased as the molecular weight of PVP increased. Though different results were obtained for the complexes prepared by polymerization of acrylic acid in the presence of PVP (complexes II), the MR decreased as the molecular weight of PVP increased. This could be due to the number of gaps between the particles and could be related to the degree of crystallinity of the complexes. Vladimir *et al.*, studied the Self-assembly of DNA–polymer complexes using template polymerization (Vladimir *et al*., 1998). Their report showed that template polymerization facilitates condensation of DNA into particles that are <150 nm in diameter and that inclusion of a poly (ethylene glycol)-containing monomer prevents aggregation of these particles. For step polymerization reactions, the cationic monomer used is bis (2-aminoethyl)-1,3-propanediamine (AEPD). For Template polymerization with AEPD monomers, all reactions were performed in 1 mM EDTA, 20 mM HEPES. Template polymerization with acrylic monomers was studied by mixing CDiA and DNA in 1 mM EDTA, 50 mM HEPES, pH

7.4 at various ratios. The buffer was degassed under vacuum and saturated with nitrogen gas for 20 min at room temperature. After the thermal radical polymerization initiator 2, 2, 4-azobis (2-amidino-propane) (AAP) was added and the mixture was incubated. Particle sizing and z-potential measurements was done by using a Zeta Plus photon correlation spectrometer, electron microscopy and transfections were also carried out.

2.2.1.3 Cross-linkers

The selectivity is greatly influenced by the kind and amount of cross-linking agent used in the synthesis of the imprinted polymer. In an imprinted polymer, the cross-linker fulfills three major functions:

a) The cross-linker is important in controlling the morphology of the polymer matrix, whether it is gel-type, macro porous or a micro gel powder.
b) It serves to stabilize the imprinted binding sites.
c) It imparts mechanical stability to the polymer matrix (Kempe and Mosbach, 1995).

From a polymerization point of view, high crosslink ratios are generally preferred in order to access permanently porous (macro porous) materials and be able to generate materials with adequate mechanical stability. So the amount of cross-linker should be high enough to maintain the stability of the recognition sites. These may be because the high degree of cross-linking enables the micro cavities to maintain three-dimensional structure complementary in both shape and chemical functionality to that of the template after its removal. Thus the functional groups are held in an optimal configuration for rebinding the template, allowing the receptor to `recognize' the original substrate (Mosbach, 1997). Polymers with crosslink ratios in excess of 80% are often being used. But recent results suggest that a moderate degree of cross-linking (40-50%) is only required for the development of imprinted system with enhanced selectivity and

specificity. Quite a number of cross-linkers compatible with molecular imprinting are known and a few of which are capable of simultaneously complexing with the template and thus acting as functional monomers. Examples of common agents used for cross-linking are;

N,N'-1,4-phenylenediacrylamide, N,N'-methylenediacrylamide, ethyleneglycol dimethlacrylate, 3, 5-bis (acryloylamido) benzoic acid, divinylbenzene, N,O'-bisacryloyl-phenylalaninol, 1,3-diisopropynylbenzene etc.

2.2.1.4 Porogenic solvents

Porogenic solvents play an important role in the formation of porous structure of imprinted polymers, which are known as macro porous polymers. It is known that the nature and level of porogenic solvents determines the strength of non-covalent interactions and influences polymer morphology which obviously directly affects the performance of imprinted polymers (Yu and Mosbach, 2004). The template molecule, initiator, monomer and cross-linker have to be soluble in the porogenic solvents. The porogenic solvents should produce large pores, in order to assure good flow-through the pores of the resulting polymer. Also the porogenic solvents should be relatively less polar, in order to reduce the interferences during complex formation between the imprint molecule and the monomer, as the latter is very important to obtain molecular imprinted polymers with high selectivity (Yu and Mosbach, 2004).

Porogenic solvents with low solubility phase separate early and tend to form larger pores and materials with lower surface areas. Conversely, porogenic solvents with higher solubility phase separate later in the polymerization. This provides materials with small pore size distributions and high surface area. More specifically, use of a thermodynamically good solvent leads to polymers with well-developed pore structures and high specific surface areas. Use of a thermodynamically poor solvent leads to polymers with poorly developed pore structures and

low specific surface areas. However, the binding and selectivity in imprinted polymers does not appear to dependent on a particular porosity (Yu *et al.,* 1997).

Although the results of molecular recognition weaken with increasing polarity of the solvents, it is important to stress that in some cases, sufficiently strong template-monomer interactions have been observed in rather polar solvents. Increasing the volume of porogenic solvents increases the pore volume. Besides its dual roles as a solvent and as a pore forming agent, the solvent in a non-covalent imprinting polymerization must also be judiciously chosen such that it simultaneously maximizes the likelihood of template-functional monomer complex formation. Normally, this implies that a polar, non-protic solvent like toluene are preferred, as such solvent stabilize hydrogen bonds. If hydrophobic forces are being used to drive the Complexation, then water could be the solvent of choice (Masque *et al.*, 2001).

2.2.1.5 Initiators

Many chemical initiators with different chemical properties can be used as free radical source in free radical polymerization. Normally, they are used at low levels compared to the monomer; 1 wt. %, or 1 mol. % with respect to the total number of moles of polymerisable double bonds. The rate and mode of decomposition of an initiator to radicals can be triggered and controlled in a number of ways, including heat, light and by chemical or electrochemical means depending on its chemical nature. For example the azo initiator, azo-bis-iso-butyronitrile (AIBN) can be conveniently decomposed by photolysis or thermolysis to give stabilized, carbon-centered radicals capable of initiating the growth of a number of vinyl monomers (Mosbach and Haupt, 2006). A careful choice of initiator for particular polymerization process has to be made in order not to hinder the optimal polymerization result desired because a complexation reaction between

the template material and the initiator may change the target end-material (Ferguson and Eboatu, 1989); their report was confirmed by spectroscopic evidences.

2.14 Polymerization Process Method and Conditions

A generalized method of preparing templated polymer products can be described using the schematic Figure 2.29.

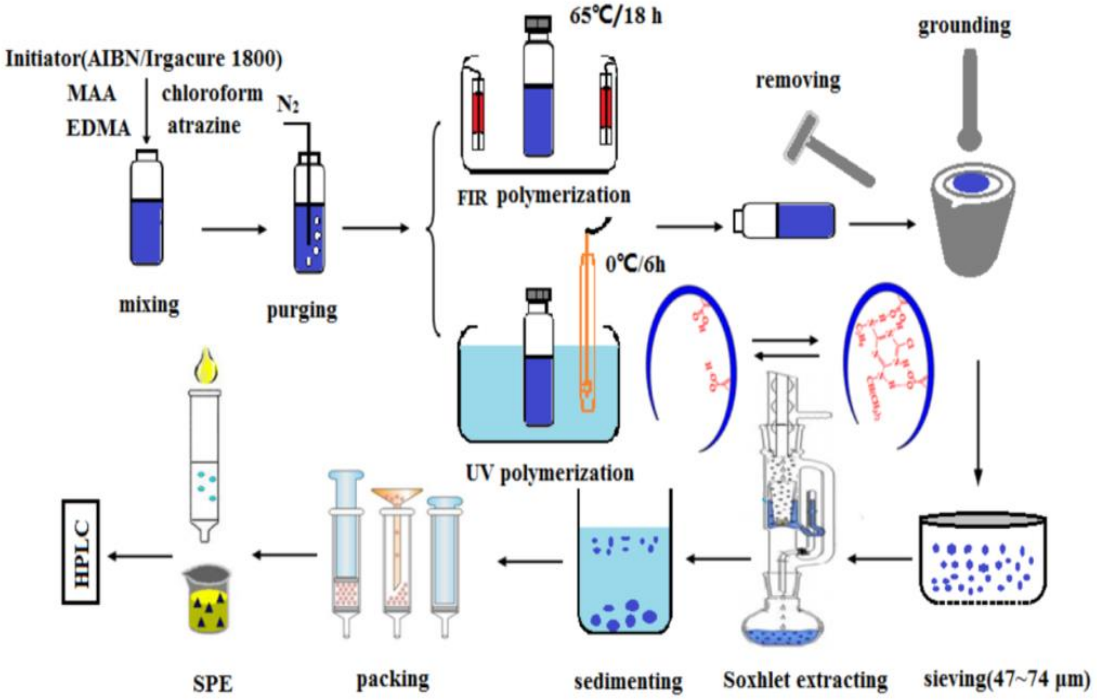

Figure 2.29: Process steps in the preparation of molecularly imprinted polymers Adapted from Chen *et al., 2014.*

The effect of parameters like pressure can be linked to temperature effects, emphasizing that temperature control is the most important factor which influences other parameters. In selecting the best conditions for preparing materials suited to a particular application, some compromises may have to be made between performance and the desired property. It should be noted that the polymerization reaction is a very complex process which could be affected by many physical factors. To produce high-performance molecularly imprinted polymers, all factors should be thoroughly considered and controlled appropriately (Elena *et al.,* 2009).

Sato *et al*., (1979)'s study on the radical polymerization of maleic acid initiated by potassium persulfate in the presence of poly (vinylpyrrolidone) (PVP) in aqueous solution showed that, as the temperature of the reaction increases, the formation of the polymer complex was accelerated, concentration of initiator and monomer, and molecular weight of PVP used were also impacted. They also reported the effect of the structure of a component polymer chain on the inter-polymer complexes. It was found that the effective ionic sites for complexation are changed significantly by the pH change of the solution.

Lohmeyer *et al*. (1980), did a study on the temperature effect on template polymerization of methacrylic acid in the presence of isotactic monomers (methy1methacrylate) (it-PMMA) in DMF and other solvents and found that in DMF at-10^{O}C, the distinct kinetic template effect was detected in the polymerization.

Template polymerization to fabricate hydrogen-bonded poly (acrylic acid)/poly(vinylpyrrolidone) hollow microcapsules with a pH-mediated swelling-de-swelling property was carried out by Zhiquang *et al*. (2007). Hydrogen-bonded hollow microcapsules with a lightly cross-linked shell structure were fabricated by Polymerization of acrylic acid in a solution containing surface-modified silica particles and poly-(vinylpyrrolidone) and a subsequent core removal with HF. Cross-linker was further added to produce a highly cross-linked shell structure with better stability against changes in pH. Wang *et al*. (1999) did a study on binding florescent sensor by template polymerization by the preparation of a fluorescent sensor for D-fructose. They described the development of polymeric sensors with response to the binding event with a significant fluorescence intensity change without the use of an external quencher. They designed and synthesized an anthracene-boronic acid conjugate with a methacrylate moiety attached to it to allow for its incorporation into imprinted polymers. The

fluorescence intensity of the anthracene moiety of the functional monomer increased with the formation of an ester with a cis diol. The template-directed polymerization was carried out using D-fructose as the imprint (template) molecule. D-Fructose was chosen as the test compound because it was known to bind strongly with the boronic acid moiety. The D-fructose boronic acid complex was preformed so as to maximize the complementary interactions at the binding sites.

Reiko and Hiroaki's (2002) report on the synthesis of polymers by template polymerization and the effects of solvent and polymerization temperature, demonstrated the synthesis of a novel template monomer with multiple methacryloyl groups with α-cyclodextrin by the acetylation of primary hydroxyl groups and the esterification of secondary hydroxyl groups with methacrylic acid anhydride. When the monomer concentration was lower than $4.12x10^{-3}$M, radical initiated polymerization was limited in the molecule of the template monomer with any initiator. R,R-azodiisobutyronitrile(AIBN), which is one of the common free radical initiator was used, the degree of polymerization (DP) of the methacryloyl group in the template monomers was polydispersed.

2.2.2 Characterization of molecular imprinted polymers

Analytical characterization of the molecular mechanisms occurring in the pre-polymerization solution will govern the resulting binding site distribution and the recognition properties of the imprinted polymer matrix. In the non-covalent approach, the stability of the template-functional monomer complex formed in the pre-polymerization mixture will govern the resulting binding site distribution and the distribution properties of the imprinted polymer matrix. Close analysis of the pre-polymerization solution can provide fundamental insights to the various interactions occurring during imprinting. Consequently, spectroscopic studies of the pre-polymerization mixture provide prevalent information on the imprinting process. Sincere organization of

functional groups at the binding sites is required during rebinding, the spectral studies before and after rebinding can also put light into rebinding (Nicholls *et al.,* 2001).

2.2.2.1 Proton Nuclear Magnetic Resonance (^{1}H NMR) spectroscopy.

Proton NMR titration experiments facilitate observation of hydrogen bond formation between bases and carboxylic acid through hydrogen bonding. These studies have been introduced in molecular imprinting for investigating the extent of complex formation in pre-polymerization solutions; thus evaluating the shift of a proton signal due to participation in hydrogen bond was used as the selection criterion for complex formation between the functional monomer and templates (Shea and Sasaki, 1991).

2.2.2.2 Fourier Transformed InfraRed (FT-IR) spectra

In addition to ^{1}H NMR, FT-IR spectra provide the fundamental analytical basis for rationalizing the mechanism of recognition during the imprinting process probing the governing interactions for selective binding site formation at the molecular level. The interaction between the functional monomer and template during pre-polymerization complex formation and the template incorporation into the imprinted polymer during rebinding can be confirmed by the characteristic FT-IR absorption analysis (Wulff *et al.,* 1987).

2.2.2.3 Scanning electron microscopy (SEM)

SEM can be used in a variety of distinct ways to probe imprinted polymers on a variety of length scales. Scanning electron microscopy is the most widely used technique to study the shape, size, morphology and porosity of polymers (Gregg and Sing, 1982).

2.2.2.4 Pore analysis (pore size distribution).

It is possible to probe the morphology of imprinted polymers in the same way as one is able to do with most porous solids. Depending on the method of analysis, useful information may be

acquired on the specific pore volumes, pore sizes, pore size distributions and specific surface area of materials. Pore size, pore volume and surface area analyses are usually performed by nitrogen adsorption. The surface area was determined using the BET model, the t-plot using Harkin-Jura average thickness equation and the pore volume and pore size distribution using the BJH model (Tomoi *et al.,* 1987). During the process of adsorption of gas, condensation ultimately takes place resulting to the existence of liquid condensate. This condensate fills up the available pores spaces by capillary action (capillary condensation) and this displays a hysteresis fingerprinting phenomenon. Based on an earlier model theory for correlating the relationship between pore condensation pressure of an adsorbed gas and the available pore diameter by Kelvin (Gregg and Sing, 1995; and Ruthven, 1984), Barret, Joyner and Halenda presented a method for calculating the particle size distribution (PSD) in materials for materials that exhibits hysteresis (Barrett, Joyner and Halenda, 1951). The shapes of the hysteresis as observed from the resulting isotherms are always controlled by the branching points of the forward adsorption pathway and the backward desorption pathway (Figure 2.30).

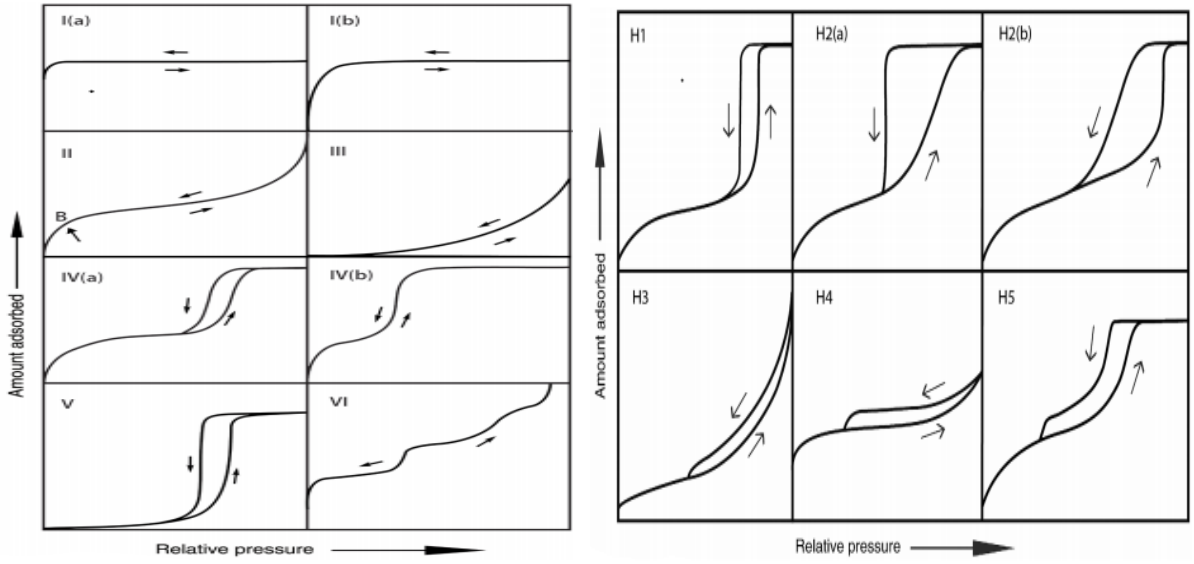

Figure 2.30: IUPAC classified standards sorption Isotherms(I-VI) and Hysteresis loops(H1-H5).

2.2.3 Applications of molecularly imprinted polymers.

Molecular imprinting technique has become a well-known means for the preparation of bio-mimetic recognition matrices. The resultant materials have good binding affinity, stability and selectivity towards the target molecule, and thus have been widely applied in separation science, recognition of proteins, bio-sensing, catalysis and drug delivery (Liu and Wulff, 2008).

2.2.3.1 substitutes for biological antibodies and receptors.

Molecular imprinted polymers can more properly be characterized as a 'rational design' approach allowing research and application problems to be solved. Using simple molecular building blocks, material chemists can now produce tailored synthetic materials of much improved stabilities, able to replace or complement natural receptors. The problem of the recognition provided by single imprinted polymer is relatively weak and can be solved using an array of different molecular imprinted polymers simultaneously. The combination of imprinted arrays with appropriate chemo metrics would considerably simplify the analysis of more difficult samples. Molecular imprinted polymer has been found useful in the field of agriculture. With significant advantages in easy preparation, low cost, predictable specific recognition and high stability, the synthesized molecularly imprinted polymers have the capability of specific adsorption and recognition of the template molecule. Several herbicides such as phenoxy acetic acid, 2, 4- dichloro phenoxy acetic acid and 2, 4, 5-trichloro phenoxy acetic acid could be successfully imprinted on polymeric systems with optimum rebinding (Annamma, 2008).

2.2.3.2 solid phase extraction materials.

Molecular imprinting is an emerging technique for the design of polymeric materials possessing selective affinity towards target analytes. The method involves complexation in the solution of a target compound with appropriate functional monomers. Molecularly imprinted polymers offer

distinct advantages compared to natural receptors: ease in preparation, low cost, tolerance to extreme chemical and thermal conditions, long shelf life, and enhanced versatility in experimental design. Separation and solid phase extraction are the major application areas for the imprinted polymers. Molecularly imprinted polymers provide tailor-made media that can solve complex separation problems and improve the generic selectivity of the conventional chromatographic media by increasing the separation of the target analytes. To achieve increased selectivity, higher extraction yields and analyte purification in solid phase extraction, several methods were investigated for the production of molecular imprinted polymers for flavonoids (Anderson, 2002).

2.2.3.3 Binding assay materials.

It was first demonstrated by Mosbach, who in 1984 developed molecularly imprinted polymers based assay for the bronchodilator theophylline and the tranquilizer diazepam, due to the potential of molecularly imprinted polymers to bind a target molecule selectively, they could conceivably be employed in immunoassay type binding assays in place of antibodies (Vlatakis *et al.,* 1993*).* The assay yielded a cross reactivity profile very similar to that of the natural monoclonal antibodies.

2.2.3.4 artificial catalysts.

Molecular imprinting based on non-covalent interactions can also be used to produce catalytic polymers. Polymers that mimic the properties of amino acid esters have been prepared from imidazole monomers (Leonhardt and Mosbach, 1987). Recently, other approaches have been explored to improve enzyme mimicking polymers (Robinson and Mosbach, 1989). Example is the preparation of antibodies by imprinting the transition state analogue, p-nitrophenyl methyl phosphonate against a phosphonic ester for alkaline ester hydrolysis (Robinson and Mosbach,

1989). This enhanced the rate of ester hydrolysis immensely. Molecular imprinting presents an ideal platform for the synthesis of transition metal catalysts located within the interior of a polymer-imprinted active site. This has hightened the potential to develop new specific catalysts for target chemical reactions at reduced activation energy conditions.

2.2.3.5 polymeric sensors.

The ability to develop chemical sensors with high selectivity characteristics of biological enzymes or antibodies, while the robustness to operate in harsh environments such as in high temperature and in organic solvents is a long term aim in sensor research (Andrea *et al.,* 2001). Molecular imprinted polymers are having the advantage that the recognition sites are tailor made, and at the same time incorporated into a solid polymeric support. Taking into account the very high specificity that can be obtained as well as the chemical and physical stability of imprinted polymers; there have been a number of attempts to construct chemical sensors based on these materials as the recognition elements (Dicker *et al.,* 2001). The challenge currently facing those wishing to exploit the recognition properties of molecular imprinted polymers in such devices is, to develop a transducing mechanism to translate the binding event into a measurable signal. Several molecular imprinted polymers based sensing systems have been proposed including sensors utilizing field effect devices, conductometric measurements, amperometric measurements (Levi *et al.,* 1997), and fluorescence measurements (Piletsky *et al.,* 2005).

2.2.3.6 stationery phase materials in Chromatography.

Thin Layer Chromatography is one type of characterization method employed in the MIP standardization. Depending on the target and complexity, simple systems can be employed or where specialty separations are required for example with chiral or enantiomers are involved,

specialized adsorbents as found in chiral TLC plates, are used. For the Chiral type, finely ground imprinted polymer, mixed with binders has been investigated for use in chiral TLC (Nilsson *et al.,* 1994). The inherent advantages of TLC, such as multiple parallel samples and simplicity, are still attractive. If new preparative methods for imprinted polymers successfully address the problem of binding site heterogeneity, chiral TLC with imprinted polymers may prove useful when large numbers of samples have to be semi quantitatively screened. Other chromatographic methods are the High Performance Liquid Chromatography (HPLC) and the Gas Chromatography in tandem with Mass Spectroscopy (GCMS). They all work based on the general principle of relative adsorption of eluents on solid supports.

2.2.3.7 Chiral recognition materials.

Polymers prepared by molecular imprinting utilizing non-covalent interactions exhibit enantioselectivity and substrate selectivity for their original print molecules. Ping *et al.,* (2009) reported that under at optimized conditions, such as with an optimized MIP's inputs preparation composition, pH of mobile phase, and separation voltage, enantiomers can be separated. The first and the most important application of molecular imprinted polymers are in the enantioseparation of racemic mixtures of chiral compounds. This also provides a convenient method for quantitative assessment of the quality of imprints produced by a particular recipe or strategy. Most work has concentrated on the resolution of chiral compounds. Specialized interactions between imprinting molecules and molecular imprinted polymers are caused by both the complementary functional groups and the suited structures of molecular imprinted polymers (Karsten, Haupt and Mosbach. 2000). There is an increasing demand, especially in the agricultural chemicals and pharmaceutical industries, for better and more efficient means to prepare, purify, and analyze chiral compounds. This demand is driven sometimes markedly by

different biological activities of the enantiomers of a given compound and increasing regulations regarding optically active molecules (Vincent *et al.,* 1999).

2.2.4 Summary on template polymerization

Template polymerization as a technique for the preparation of specialty products is gaining huge attention and vigorous expansion from activities of scientists globally. Expectation is that this technique will eventually dominate synthesis processes because of the desire by scientist to produce target specific products with less side or by-product outputs. The technique also aids in raw material conservation during synthesis.

MIPs with acidic monomers entrap enormous quantities of nicotine from tobacco environment while the neutral or alkaline monomer types have more preference for the TSNAs. In the selection of cross linkers, it has been established that hydrophobic cross linkers are more TSNA sensitive and responsive than towards Nicotine.

Reports are available on the feasibility of using Chitosan as a functional monomer in the synthesis of MIP (Saifuddin and Yasumira, 2010). A feasible and reproducible amount to be used during synthesis can be sieved from the works of these researches to be an average of 3.5g of Chitosan in a 0.9: 1 ratio with Methacrylic acid as co polymer material. The first part of this research has the proof-of-concept, report (Ofoegbu *et al*., 2018), showing the feasibility of the concept and confirmation of this quantity of Chitosan as input in the course of the MIP synthesis. An environmentally friendly and recyclable product in the form of a molecularly imprinted polymer fabricated from biodegradable input materials for filter materials consequently presents the choice selection. This product and its technology have been extensively employed in separation science, catalysis, recognition of proteins, drug delivery as well as in biosensing (Piletsky and Turner, 2002).

2.3 An Emperical Framework

2.3.1 Applications of QCM and MIPs in Problem Areas.

Dickert and Hayden, (2002) gave pioneering report on the use of QCM based MIP study. Their work presented a fast and selective recognition tool for yeast cells recognition via the surface-imprinted technique, (Dickert and Hayden, 2002). Seifner *et al*., (2009), used an MIP coated QCM sensor with affinity and selectivity in recognition for erythrocytes in blood samples. 1-vinyl-2-pyrrolidone was employed as the functional monomer while N,N′-methylene-bis(acrylamide) served as the cross linking agent. The template was an erythrocyte sample and UV served as the source of energy. Tai *et al.*, (2005) reported the first study of MIP-based QCM sensors for successful recognition of dengue virus. They also fabricated an MIP-QCM platform for detecting an antigen that protects from anthrax infection. This method also was found useful in identification of other microorganisms like flaviviruses and dengue viruses (Tai *et al*., 2010). Staphylococcal enterotoxin B (SEB) was detected in samples by Liu et al., (2012), using an MIP coated QCM sensor. From their report, detection limit was around 6.1 ng•mL−1 while Selectivity efficiency was done using a cocktail containing bovine serum albumin (BSA) , staphylococcal enterotoxin C1 (SEC1), ovalbumin (OVA) and staphylococcal enterotoxin A (SEA). On another vain, effect of reactancts was studied using the QCM technique as demonstrated by Phan *et al.,* (2014). They examined the implication from varying the cross linker amount in MIP fabrication. They also considered the monomer ratio as it affects response time and sensitivity. Other parameters examined are effect of different mechanism of polymer preparation as well as solvent systems.

2.3.1.1 Applications of QCM and MIPs in environments containing nicotine and TSNA analogues.

Studies involving the use of Nicotine as template on an MIP-QCM system have been recorded. In one of such studies, Alenus and coworkers used L-Nicotine in an aqeous medium and then with biological sample as a real-life situation (Alenus *et al.,* 2012). They carried out detection of L-Nicotine in human saliva using an MIP prepared by bulk polymerization (Alenus *et al*., 2013). Their results showed that MIPs gave a sequestration ratio of 4:1 of L-nicotine when compared with the NIPs(in water) and 2:1(in PBS at pH 9).Presence of L-Nicotine was detected in samples of patients after they chewed nicotine gums and using smokeless tobacco. Croux *et al.,* (2012) prepared an MIP-based QCM sensor with a four-channeled system. Methacrylic acid was the functional monomer, EGDM as cross linker, L-Nicotine was templated within the matrix. Mirmohseni *et al.,* (2008) worked with phenylalanine as the template and used the polymer on a QCM chip. The limit of detection for this system was 45 mgL^{-1} and it showed sensitivity and selectivity in the presence of the target amino acid phenylalanine in a linear response pathway.

The combination of MIPs with quartz crystal microbalances (QCM) gives a straightforward and sensitive device, which can measure frequency based on weight-amount of analyte present in the target environment. Alenus et al., (2013), prepared and used bulk polymerized L-nicotine MIPs to demonstrate the feasibility of L-nicotine detection in biological samples (saliva and urine). The researchers initially spiked saliva and urine samples with L-nicotine and after dilution in demineralized water and 0.1percent phosphate-buffered saline solution measured the presence of the analyte as proof-of-concept. They further analyzed saliva samples that were collected during mastication of either nicotine tablets with different concentrations or smokeless tobacco. The MIPs-QCM selectively and specifically identified between these samples: proving the

effectiveness of the concept with saliva, which mediates the oral uptake of nicotine as an alternative to the consumption of cigarettes.

Li et al., 2015, reported the grafting of MIP on to silica gel and using it as binary filter substance to filter TSNAs from mainstream tobacco smoke. The adsorption rates of between 15.32 percent and 41.33percent were obtained. With nicotinamide as template, the filter additive selectively filtered N-nitrosoanabasine, N-nitrosonornicotine, N-nitrosoanatabine, and 4-(methylnitrosamino)-1-(3-pyridine)-1-butanone from the stream. Four milligrams of the filter additive per cigarette was effective for the filtration. In the case of other harmful substances like polycyclic aromatic hydrocarbons (PAHs), Xie et al., (2013) prepared a pyrene (PYR) imprinted polymer as a part of improved filter for the determination of the PAH content of mainstream cigarette smoke. The MIP gave a binding capacity (Qmax) of 18.33 mg/g for pyrene. Once the cellulose acetate-filter was substituted with the pyrene-templated imprinted polymer-filter, a 63.6 percent reduction in the PAHs content in the mainstream smoke was achieved. Other reports Ho, Lin, Liu and Chen, (2010) presented similar results.

By applying the a CORESTA (CRM 75) recommended Method (Intorp, Purkis & Wagstaff, 2012) for identifying and quantifying the presence and amount of tobacco smoke stream toxicants like the tobacco-specific nitrosamines (TSNAs), Nnitrosonornicotine (NNN), N-nitrosoanabasine (NAB), Nnitrosoanatabine (NAT) and 4-(N-nitrosomethylamino)-1-(3-pyridyl)-1-butanone (NNK); imprinted polymers were prepared using various functional and cross-linking monomers, templates, porogens and thermal treatments; tested by adapting them as solid phase extraction (SPE) materials. The SPE systems were subsequently optimized (Zander, et al., 1998). Exceptional selectivity for nicotine in the search for a rapid cleanup step for nicotine and some of

its oxidation products in chewing gum formulations was possible using these MIPs. This activity produced phases that showed significantly higher recoveries of the analytes (three out of four analytes were quantitatively) as against the use of a C18 reversed-phase column or the non-imprinted polymer counterpart (only nicotine was recovered). Sensitivity and recovery result was reported by Mullett, Lai and Sellergren, (1999), who prepared and used molecularly imprinted solid phase extraction with differential pulsed elution (MISPE-DPE) to determine the nicotine and myosmine content of tobacco. They reported that over 95% of the sequestered myosmine and only 43% of the sequestered nicotine were desorbed and eluted by a '20 µl pulse of methanol'; while a '20 µl pulse of 1% trifluoroacetic acid in water' desorbed and eluted the residual quantity of sequestered nicotine. Consequently MISPE-DPE method provides innate selectivity for nicotine within a smaller examination phase of 3min at detection limit of 1.8µg ml^{-1} and a linear dynamic range of up to 1000 µgml^{-1} and at a cheaper cost when compared to liquid chromatographic methods. These analytical outcomes are better than previously obtained results from several other nicotine–MIP-based procedures.

2.3.2 Methacrylic acid based molecularly imprinted polymer matrixes.

The use of Methacrylic acid as functional polymer in preparing nicotine specific binding MIP was demonstrated by Liu, Liu and Wang, (2003). With nicotine as template, they prepared an MIP having Methacrylic acid (MAA), ethylene glycol dimethacrylate (EDMA) as cross linker and chloroform as the porogen. Interaction between the nicotine and the functional monomer was shown by UV spectroscopic analysis to be by electrostatic interaction via hydrogen bonding and ionic interaction. The result from the SPE-adapted removal of nicotine was found to be better than that of the commercial filters. Xie et al., (2018) employed similar reagents in preparing an MIP solid-phase extraction (MISPE) coupled with gas chromatography-mass spectrometry. This

was used to sequester and recover nicotine from nicotine in the zero-level refill liquids of electronic cigarettes. The MIP matrix was synthesized on the surface of vinyl-SiO_2 nano spheres. High adsorption capacity (247.0 μmol g^{-1}), imprinting factor of 4.40, selectivity coefficients higher than 2.9; good linearity in the range of 2.00–40.00 μg mL^{-1}; limit of detection (LOD, S/N = 3) of 0.50 μg mL^{-1}, limit of quantification (LOQ, S/N = 10) was 1.66 μg mL^{-1} and average recoveries of between 76.2% to 83.9% with relative standard deviations lower than 6.4% (n = 6) were obtained.

Krupadam, Venkatesh and Piletsky, (2013) prepared MIPs for detecting nicotine and related carcinogenic substances in using itaconic acid-ethylene glycol dimethacrylate copolymer. They demonstrated that MIPs may be fabricated to exhibit selective sequestration ability in biological systems. The formation of nano cavities with size 24±5 nm the polymers presented high selectivity for nicotine comparable to those of natural molecules like acetylcholine esterase (AChE). One striking feature of the polymers was their pH sensitivity. Effective pH range of 6.8-8.2 was required for optimal sequestration and this falls within the natural nicotine receptors favoured pH 7.6 for optimal binding.

2.3.3 Chitosan based molecularly imprinted polymer matrixes.

Attempt has been made by some researchers to review works done in this area but there is the need to update on this information data base. Molecular Imprinted recognition technology activities have been courting the versatility of chitosan-based matrixes as new category of materials with potentials for man-made receptor mimics for application in very many areas of need. Researchers (Aburto, Mendez-Orozco and Borgne. 2004; Espinosa-García *et al.,* 2007; Yu, Deng and Yu., 2008; Guo, *et al.,* 2004 and 2005), carried out preparations using chitosan

matrixes for imprinting purposes targeted at applications in different arrears. Table 2.2, shows some of the activities in this regard.

Table 2.2: Examples of Chitosan of different degree of deacetylation as matrixes in target utility areas Yu, Deng and Yu. (2008).

Matrix	CS Characteristics	Crosslinker	Template	Application
Cs hydrogels	DD 94%,30 kDa	Glu	DBT	Fuel desulfurization
Cs hydrogel	DD 90%, 78 kDa	Genipin	O-xylene	Waste water treatment
CS	Non data	ECH, GLU	PFOS	Waste water treatment
Cs	DD 90%, 521 ml/g	ECH	Hemoglobin	Protein binding
Cs, binary xilosanes	DD 98% $6*10^4$g/mol	ECH, form	BSA	Protein binding
CS , nylon membranes	DD 98%, $1*10^5$g/mol	GPTMS	PEG	Protein binding
CS, acrylamide	DD 90%, 92,47,29 kDa	MBA	BSA	Protein binding
CS, acrylamide	DD 90%, 504 kDa	MBA	Hb	Protein binding
Cs TiO2	DD 90%	ECH	Ni, Cu	Metal Recovery and photodegradation
Cs fungi mycelium	DD 90%	ECH	Ni	Metal recovery
Cs, fungi mycelium, TiO2	DD 90%	ECH	Ni	Metal Recovery and photodegradation
CS resin	DD 90%	ECH	Ni	Metal recovery
Cs silica gel	DD 98%, $8*10^5$g/mol	GPTMS	PEG, sucrose	Metal recovery
Cs , fungi mycelium, TiO2	CS 90%	ECH	Ni	Organic compound degradation and metal recovery
Cs silica gel	DD 98%, $6*10^4$	GPTMS	Cd	Cd recovery
CS, acid metacrilic	DD 90%, 521ml/mg	ECH	quercetin	Flavonoids recovery
Cs	DD 92%	GPTMS	L-Phe	Quiral resolution

ECH: epichlorohydrin GLU: Glutaraldehyde GPTSM γ-glycidoxypropyltrimethoxysilane; MBA: metilenbisacrilamida; Form: Formaldehyde DBT: Diben PFOS: Perfluorooctane sulfonate. BSA: bovine serum albumin. L-Phe : L-phenylalanin. PEG: Polyethylene glycol.

Fu *et al*. (2007), in their work studied the effect of chitosan's Molecular weight on the rebinding properties of prepared imprinted chitosan based matrixes. They employed chitosan samples with molecular weights of 92, 47 and 29 kDa and reported having best rebinding activities with sample having molecular weight of 47 kDa. In biomedical applications, non-linear optics, electronics and catalysts production, the high affinity of chitosan's cationic property for metal ions has been explored in the preparation of utility products. Huang, Yuan, and Yang (2004), reported a chitosan mediated, UV-light induced reduction and stabilization of metal ions to give a chitosan-metal ion nano material. The feasibility is as a result of the presence of the free amino group functionality of chitosan. The glucosamine component of chitosan when it dimerizes, has accounted for the ability of chitosan to reduce the metal ions "in situ" in the absence of any other reducing agents to give the templated chitosan-metal nano material. Huang, Yuan and Yang (2004), prepared gold nanoparticles in acidic media in the presence of chitosan at 55^{o}C while, Twu *et al*. (2008), using chitosan with a KDa of 1240, DD=87%, as the only reducing and capping agent, prepared silver nanoparticles from an alkali medium at high temperature. They proposed that electron supply is as a result of the low molecular weight of the chitosan which made it possible to obtain an electron rich environment based on characteristics of the free amino functional group and high DD. Murugadoss and Chattopadhyay, (2008), also prepared a chitosan-silver nano composite. The experiment was conducted in an alkali environment and elevated temperature using a high Molecular weight chitosan (DD=75 %,). From characterization, the authors implicated the hydroxyl group component of the chitosan in addition to the free amino functional group as being responsible for the metal ion reduction of the silver compound. The ability of the metal (Ag) nano particle to be adsorbed topically on the chitosan based on their interaction with the amino functionality, aided in particle size control

because it limited the particle aggregation tendency. In acidic medium, Chitosan also mediates in the prepararti on of nano particles. Several authors, Wei *et al.,* (2007); Wu *et al*., (2008); Yang *et al.,* (2007), and others have employed chitosan samples of varied DD and Mw in acidic environment with levels of successes achieved. The authors proposed that the free amino groups are attached to metal ions of the nanoparticles exerting control over particle size while the reduction primarily occurs because of oxidation of hydroxyl functional groups. On the other hand, the molecular weight of chitosan is believed to also play a role in the metal reduction process particularly in an alkaline environment. Other researchers (Chen *et al.,* 2007), employed an alternative energy input in chitosan-nano particle preparation. This was done in a very low pH environment using radiation energy. Here, the dimerization (depolymerization), of chitosan appears to be the driving factor as a result of the radiation energy. chitosan's influence on morphology based on molecular weight was demonstrated by Wu *et al.*, (2007) when spherical gold nanoparticles were prepared by using chitosan of 50kDa molecular weight. They observed that apart from the spherical shaped samples, nano plates of sub-micro-size were also produced. This proved that the Mw influences the morphology, and this was supported by the findings of Yang, *et al*., (2007) who used chitosan of Mw 5000 Da to prepare gold 2D nanoparticle chains.

The dimerization ability of chitosan gives it an added advantage over so many other biopolymer materials and enhances its potential utility status within diversified niches and sectors. The current application of chitosan in nano and molecular imprinting, complemented with its compatibility with very many monomer and polymer materials will immensely avail the scientific community the much desired corridor of exploiting and establishing in-roads to formerly delicate and difficult utility productions particularly in the medical, pharmaceutical and

food sectors where caution has always been applied in selecting bio-friendly and benign raw material inputs.

In all of these the need for a more biological and environmentally degradable MIP fabrication becomes very apt at a time like these so as to establish a system that has a natural product base-matrix with a co-polymerizable potential with the established methacrylic acid monomer. The fabrication of an MIP with the specific biological pH of the humane system particularly that of the saliva (which has direct contact with the tobacco smoke) in order to attain an optimal efficiency in sequestration becomes vital. The need to also confirm the efficacy of the MIP even as a thin film and biosensor for rapid and on-the-field detection of nicotine and other carcinogens from tobacco products demands the use of the QCM as a proof-of-concept experiment.

In a bid to solve the tobacco health problem, manufacturers designed the filter; different materials like hemp, cloth, straw etc. had been used in the manufacturing of these filters but with different degrees of performance failure and environmental impacts as evidenced from available literatures. Recorded success stories are with the synthetic rayon, cellulose acetate fibre and the natural charcoal filter materials. Globally, more than 95% of filters are cellulose acetate based, the rest are either rayon or paper. However, these two materials come with inherent shortcomings The filters despite the level of recorded success are a source of pollution and health concern to the society. More than 2.1 billion pounds of these items are indiscriminately dumped by smokers worldwide annually and this has created a global litter issue. Chemical leachates from discarded filters are established deadly biohazards to the aquatic animals (Register 2001), an LC_{50} has been established for discarded one or two used filter(s) for every litre of water in contact with it. In a move towards creating safer alternative, the charcoal filter seamed the answer but research has

shown no convincing advantageous impact from the consumption of charcoal-filtered cigarette in comparism with non-charcoal filtered cigarette. Current literature (Coggins and Gaworski,2008), suggests that smoke filtration performance from standalone charcoal filter approaches are not likely efficient enough to reduce smoking-implicated diseases. With these, research are presently cantered around the production of smokeless cigarette (e-cigarettes) with an overrated success. The filter technology makes use of either the fibrous nature of the material (cellulose acetate, rayon, paper, hemp etc.) or the particulate and cavity properties of the material (charcoal, titanium dioxide, carbon particles etc.), in the filtration and entrapment of the degraded products from tobacco. No work is currently targeted at exploiting these inherent filtration potentials of materials vis-à-vis the cavity and possible intercalated nature of materials to prepare an efficient alternative filter material. The issue of biodegradability and recyclability have also not been potentially explored. Consequently this research is focused on filling this gap by exploiting the use of chitosan and geranic acid as natural material inputs, in the fabrication of an efficient filter material for degraded tobacco products such as cigarette and cigar.

CHAPTER THREE

MATERIALS AND METHODS

3.1 Equipment

3.1.1. Equipment for product synthesis.

Falcun tubes (2ml)

Quartz crystal QCM Chips from Bioloin Scientific, Linthicum MD. Sweden.

Chip holder.

High-Intensity, Long-Wave UV Lamp; 8-ft lead, 220 VAC/50 Hz. Cole-Parmer, USA.

BIOTEC-FISCHER SCO-Water Bath, WBD11; with Thermostatic microprocessor controller.

Heidolph 036130000 Reax Top Vortex Mixer, with variable speed control range 150 to 2500rpm.

Laboratory/kitchen Microwave unit.

Sonicator(Branson 2510 model sonnicator)

Reaction vessel (glass)

Nitrogen generator/supply unit.

Dried Air generator/supply unit

Rotary evaporator (equipped with an efficient vacuum pump 0.5-1Hp)

Simple distillation unit (with accessories)

Complimentary glassware (measuring cylinders, beakers and others)

Freeze Dryer (VirTis Benchtop Freeze Dryer Model BT4KZL-105).

Temperature regulated Water baths (Grant Y14 Circulating Water Bath and Grant OLS 200 Shaking Water Bath)

Vortex machine (Heidolph 036130000 Reax Top Vortex Mixer, Variable Speed Control Range: 150 to 2500rpm, 115V).

Rotary mixer (FINEPCR ROTATOR AG From Bio-Active Co. LtD, Thailand, with serial no: AG-09080908).

Circular shaker

Centrifuge (Avanti J-25, centrifuge; JHY 96 H51. Beckman Coulter).

Ependorf tubes (1ml, 2ml, 5ml, 15ml and 50ml)

3.1.2 Analytical Instruments.

a. Quartz Crystal Microbalance (QCM) (Isogen Life Science Attana A100® C-Fast System: Attana A100 Biosensor with integrated automated sample handling, temperature control, integrated degasser, Attester software, computer, telephone and e-mail support. Flow rate 1-150 µl/min, Sample volume 100-235 µl, Molecular weight detection ≥ 1KDa, Temperature control 4-40°C ± 0.1°C; Sample capacity 192 samples).
b. Fourier Transformed Infra-Red Spectrophotometer (CARY 630 FTIR spectrometer by Agilent Technologies).
c. Bibby Stuart Scientific melting point SMP1 machine.
d. High Performance Liquid Chromatography (HPLC) (Waters Alliance 2690 HPLC System with Micromass LCT Mass Spectrometer. SN:J99SM4210M, Model 2690 with Photodiode Array Detector. Operated at 115 VOLTS with a quaternary pump).

e. Scanning Electron Microscope (SEM) (Leo 1550 Gemini instrument furnished with a field emission electron gun in the high vacuum mode).

f. Ultra Violet-Visible Spectrophotometer (UV-VIS) (PharmaSpec Uv-1700 spectrophotometer from SHIMADZU).

g. Proton Nuclear Magnetic Resonance Spectroscope (Fourier Transformed NMR Spectrometer of 500MHz, manufactured by Unity Inova, Varian Germany).

h. Transmission Electron Microscope (TEM) (JEOL, JEM-2010 Electron Microscope. Courtesy Prince of Songkla University, HatYahi, Songkla Thailand).

i. Simultaneous Thermal Analyzer (STA) (Simultaneous Thermal Analyzer, STA8000, Perkin Elmer, USA).

j. Dynamic light scattering, Zeta Particle size analyzer (Malvern instrument's zeta analyzer. Serial num. MAL 1033461. Installed at Prince of Songhkla University, HatYai Thailand).

k. Laser Particle size Analyzer (Coulter TM LS230 laser granulometer with Optical model: garnet.rf780d PIDS).

l. Surface Area, Pore Size and Pore Volume Analysis using BET Method. (Quantachrome Instrument, with NovaWin, NOVA Quantachrome Instruments, version 11.03. data analysis software).

m. Swelling Capacity study.

3.2. Reagents and Standards

3.2.1 Reagents

Chitosan was procured from SIGMA-ALDRICH Ltd. Dorset, England.

Nicotine from Fluka Chemicals Ltd. Dorset, South East England, England.

Triethylamine (TEA) was obtained in its analar grade from MERCK Ltd.

Methacrylic acid (MAA), 1,4-Bis (acryloyl) piperazine (BAP), Ammonium persulphate, Toluene, Acetone, Tetrahydrofuran (THF), Hydrogen Peroxide, Sulphuric Acid, were all of analar grade and procured from SIGMA-ALDRICH Ltd. Poole England.

Phenylalanine amide, 3-PhenylPiridine, Geranic acid, Acetic acid procure in their analar grade from Sigma-Aldrich Ltd England.

Methanol, Ethyl acetate, Chloroform, Ethanol and Acetone were of analar grade and procured from Merck KGaA, Darmstadt, Germany.

Sodium phosphate monobasic monohydrate and Ammonium chloride were all of analar grade and procured from SIGMA-ALDRICH Ltd. Sodium phosphate dibasic anhydrous, Sodium Hydroxide pellets and Methanol were all bought from Merck, Darmstadt, Germany. Sodium phosphate dibasic heptahydrate and Sodium chloride were sourced from Thermo Fisher Scientific Ltd for the preparation of Phosphate Buffer Saline pH 7.4

3.2.2 Preparation of Standard stock solutions.

3.2.2.1 Functional monomers

Chitosan

A 500ml, 2% solution of Acetic acid was first prepared by introducing 10ml of analar grade concentrated Acetic acid into 490ml of double distilled water, with shaking for proper mixing. Into this solvent, 15g of low molecular weight (190,000-310,000Da) Chitosan was added. With vigorous stirring, the Chitosan was completely dissolved in the solvent to give a moderately viscous solution with a glassy appearance. Required volumes were taken from this stock solution for all the synthesis.

Methylacrylic acid

The reagent is simply redistilled under vacuum to remove all impurities and the reagent was well capped and kept in the refrigerator untill when needed.

3.2.3.2 Template materials.

Nicotine

A 15 ml, 10mM stock solution of Nicotine (FW 162.2g/mol), was prepared by introducing 24.3µl of analar grade liquid Nicotine into the glass reagent bottle containing 10ml of phosphate buffer (pH 7.4). The mixture was agitated for 3min before adding extra buffer solution to make up the required 15ml.

2-Pyridinemethanol

For the same concentration and volume as Nicotine, 16.34µl of 2-Pyridinemethanol (FW 109.13g/mol), was introduced into the same phosphate buffer solvent and made up to 15ml as was done with the Nicotine.

3.2.3.3 Cross linkers

1,4 Bis (acryloyl)piperazine

The stock solution was prepared by dissolving 0.1165g of the solid in 50ml of phosphate buffer saline (PBS) of pH 7.4. The molecular weight of BAP was 194.23g/mol. This gave a concentration of 0.012M solution to be used for the synthesis of the polymer samples.

Geranic acid

The same as above but with a molecular weight of 168.24g/mol, 104.04µl of the acid was completely mixed into 40ml of phosphate buffer and made up to 50ml.

3.2.3.4 Initiator

0.24g of Ammonium persulphate was dissolved in 20ml of double distilled water and used fresh without keeping. This gave a 0.36mol/L concentrate. The molar mass of Ammonium persulphate was 228.18g/mol.

3.3 Process Methods.

3.3.1 Determination of Functional Monomer-Template reacting Ratio.

Using Fourier Transformed NMR Spectrometer of 500MHz, manufactured by Unity Inova, Varian Germany; the proton (^1H) shift experiment was carried out.

1H NMR	500 MHz, METHANOL-d4 & CCl_4-d4
H'NMR	fids
Solvent	METHANOL-d4
Temperature (degree C)	30^0C; 40^0C and 60^0C
Acquisition Time (sec)	6.9999
Frequency (MHz)	499.7021
Nucleus 1H Number of Transients	16

The most suitable reacting ratio and condition(s) between the functional monomer and template materials was determined via the Proton NMR titration. This required keeping the amount of template fixed while that of functional monomer varied. The resulting chemical shift was studied to select the reacting ratio that generated optimal chemical shift for particular functional group on the monomer and in this case, the amide functionality. This occurred at the point(s) of interaction between the two reactancts during polymerization. The result of the study guided the choice of the functional

monomer-template stochiometry used in the course of preparing the MIP samples for the study.

The samples were prepared by dissolution of Chitosan in 2% acetic acid-d_4(deuterated water), then adding CD_3OD. This solution was taken in different volume ratios of 1 and 4 and mixed with the template materials (Nicotine, Phenylalanine amide and Nicotine-Phenylalanine amide blend) of fixed volume ratio of 1. The reactants were then introduced into an NMR centrifuge bottle which was inserted into the NMR reactor.

3.3.2 Proof-oF-Concept Experiment (Based on QCM Technique).

This is about the fabrication of a preliminary, proof-of-concept chitosan based MIP product with a multi-template system capable of entrapping more than one pollutant material in a given single contact exposure. Copolymerization involving Chitosan and methyl acrylic acid as cofunctional monomer is adopted. The template materials are Nicotine and its structural analogue 3-Phenylpyridine. BAP served as the cross linker.

3.3.2.1 Quartz crystal microbalance instrumentation

A quartz crystal microbalance from ATTANA Ltd, installed in the bioorganic laboratory of Linnaeus University Kalmar, Sweden was used (plate 2). The sensing element of this instrument is an AT-cut piezoelectric quartz disc with a diameter of 14 mm, a thickness of 0.3 mm, and a resonant frequency of 5MHz. The ultra-pure deionized water used throughout the experiments was obtained from a MILLI-Q purification system, sensor discs were obtained from Q-sense, Biolin Scientific, Linthicum Heights, MD. The peristaltic pump drew solvents and solutions (that had been sonicated to eliminate bubbles), through the flow cells at a rate of 88 µL/min. All experiments conducted in flow cells were run at $25^{O}C$.

3.3.2.2 Residual frequency measurement (Extracting template from the MIP)

Extraction of the template molecule from the MIP was conducted in the flow cells of the QCM, each of which contained a sensor disc bearing adhered, MIP. First, DI water was pumped through the flow cells until a stable baseline value of vibrational frequency was established. Then PBS of pH 7.4 was pumped through the cells to change the pH and effect extraction of template from the MIP. After this, DI water was again pumped through the cells and the difference in vibrational frequency before and after the extraction with PBS solution was noted. This difference was termed residual frequency.

3.3.2.3 Evaluation of Selectivity of MIP

Selectivity and sensitivity of MIP/NIP nanoparticles mounted on sensor discs for Nicotine and TSNA analogues in preference to similar compound (Caffeine) was carried out with the QCM. Sensor discs of the NIP and MIP-coated nanoparticles were placed into the flow cells of the QCM. Baselines were established with flowing solvent of PBS. Then individual solutions of the template materials in PBS but of five different concentrations (5mM, 2mM, 1mM, 0.5mM, 0.2mM and 0.1mM) in the same solvent (PBS), were introduced to the flow cells and changes in frequency were monitored in real time with the QCM. After the signals had leveled off, the solvent (PBS) was re-introduced to the flow cells and the residual frequency was measured for each cell.

3.3.2.4 Cleaning of chip surface.

The first step carried out was the cleaning of the quartz crystal chip surface and this was done by combining an adapted method by Liu, *et al.,* (2012) where SiO_2-coated crystals

were washed in piranha solution (70% H_2SO_4 and 30% H_2O_2) by gentle swirling of the chips in the solution for 120secs. A liberal amount of double distilled or ultrapure water was then used in rinsing the chips before being neutralized in a 0.1M NaOH solution using a sonicator for 20mins

The chips were dried in a stream of Nitrogen gas. The chips are then sonicated first in Acetone followed by Tetrahydrofuran and finally Toluene; each for 20mins. It was dried using Nitrogen gas and kept in Falcun tubes for the next stage of silanization.

3.3.2.5 Functionalization of chip's surface (silylnization)

Salinization was carried out on the cleaned surface of the chips by immersing the chips in a solution containing 7.2uL of 3-(Trimethoxysilyl) propylmethacrylate (silane), 0.72uL of Triethylamine (TEA) and 360uL of Toluene; for not less than 24hrs, wrapped with Aluminum foil paper and kept in a cupboard.

At the end of the contact period, the chips were rock-washed for 30mins each in Toluene, THF and Acetone sequentially and allowed to dry in a stream of Nitrogen gas.

3.3.2.6. Preparation of the MIP and NIP sample

Molecular imprinted polymers as well as the non-imprinted polymer matrices were prepared using a blend ratio of 1.6:12:55:1:1.26 for solvent, functional monomer cross linker, template and initiator respectively. For the experimental investigation of best mass density of Chitosan for the MIP architecture, varied quantities of Chitosan were tested while all other inputs were kept constant, Table 3.1.

The blend was vortexed (plate 3a) for 30secs before a 0.5uL volume was introduced onto the surface of the functionalized crystal chip.

Table 3.1: MIP blend formulation adopted. 0.04 mole = 1g of Chitosan in 10ml 2% Acetic acid solution.

Materials	Quantities				
	Sample 1	Sample 2	Sample 3	Sample 4	Sample 5
Chitosan (mmol/l)	0.12	0.08	0.04	0.02	0.16
Methacrylic Acid (uL)	8.5	8.5	8.5	8.5	8.5
BAP (mg)	1	1	1	1	1
Template (uL)	7	7	7	7	7
Ammonium persulphate (mg)	0.0001	0.0001	0.0001	0.0001	0.0001

The initial respective frequencies of uncoated chips were determined using the QCM machine. After formulation, the samples were coated on the activated resonators and polymerized at 60^{o}C for 2hrs; in a temperature regulated water-circulating bath and duplicate samples were made using UV irradiation to obtain a surface induced free radical polymerization. The MIP was prepared with the template materials Nicotine (MIP Product A), 3-phenylpiridine (MIP Product B) and a 50:50 combination of both templates (MIP Product C); while the NIP was prepared without templates.

3.4 Generic bulk polymerization Method

(a) Addition of the template material to the mixture of functional monomers and cross-linker preceeded the prearranged association of template with functional monomers (by sonication and vortexing).

(b) Resultant pre association of functional monomer/cross linker/ template cluster was subjected to polymerization conditions (water bath heating and Microwave radiation).This resulted into structurally-specific cavity formation within the polymer network.

(c) Template removal (solvent washing) to obtain and validate template specific cavities.

Template materials, Chitosan, MAA, Ammonium persulphate were dissolved in porogen solvent (2% Acetic acid solution). The mixture was sonicated for 2min then purged with nitrogen and placed in the microwave oven set for 2min, 4min, 6min, 8min, 10min, 12min, 14min, 16min, 18min and 20min (varied time intervals). For the conventional heating, temperature regulated water bath set at 70^{O}C was used for bulk polymerization. The resulted MIPs were washed with different solvent regimes aided by sonication until no template material was detected in the rinse solution. Non-imprinted polymers (NIPs) for control experiments were obtained following the same procedure described above but without template material.

3.5 Specific Process

The blend formulation Table 3.2 was employed for the synthesis of the MIPs. Using the method reported by Kumbar, Soppimath and Aminabhahavi, (2012) with slight modification, the MAA was introduced into the reaction container containing the solution of Chitosan, then vortexed for 5mins for proper mixing. This served as material [A]. The cross linker(s) was introduced into [A] and vortexed for another 10mins [B] at the end of which the template material was added and the vortexing continued for an additional 5mins. Three families of singular templates and their blends were prepared for the entire work, the ones with the individual template materials and the one with a 50:50 blend ratio of both template materials. The template materials are Nicotine and its TSNA analogue 2-Pyridinemethanol. The Initiator was added finally and the blend vortexed for 3min. This was the prepolymerized sample material[C].Table 3.2 presents the formulation used.

Table 3.2: Blend formulation for Bulk polymerization for preparation of NIP and MIP samples.

Materials	Amount per sub group				
	a	B	c	d	e
Chitosan	20ml (0.12mmol/l)	20ml (0.12mmol/l)	20ml (0.12mmol/l)	20ml (0.12mmol/l)	20ml (0.12mmol/l)
Methacrylic acid	1.2ml	1.2ml	1.2ml	1.2ml	1.2ml
Cross linker	2ml	3ml	4ml	5ml	6ml
Template	238.2µl	238.2µl	238.2µl	238.2µl	238.2µl
Initiator	2.4ml	2.4ml	2.4ml	2.4ml	2.4ml

The formulation was used with the two crosslinker materials, Geranic acid, and 1,4Bis (acryloyl) piperazine (BAP). This guided the understanding on the effect of using natural and synthetic cross linkers as represented by the first and the last ones respectively.

The reaction conditions follow two primary path ways:

1. Heating with constant agitation in a water bath for 12Hrs at temperatures of, $60^{O}C$.
2. Microwaving at a power rating of 750W for the earlier stated time intervals.

   The employed systems are:

   M –Microwave assisted

   P - Water bath heated at $60^{O}C$ for 12hrs

   1 – BAP-Nicotine blend

   3 – BAP-Phenylalanine amide blend

   5 – BAP-Nicotine-Phenylalanine amide blend

   6 – Geranic acid-Nicotine blend

   8 – Geranic acid-Phenylalanine amide blend

   10 – Geranic acid-Nicotine-Phenylalanine amide blend

Each of the system was divided into five groups based on the amount of cross linker, a, b, c, d, e, while the f is for the Non-imprinted samples with varied amounts of the cross linker in mls, within the range: a= 2, b=3, c=4, d=5, e=6 and f=5.

At the end of the polymerization reaction, the products were washed with 2% acetic acid solution, rinsed with double distilled water and dried under vacuum. Samples at this stage were taken for FTIR and SEM analysis for pre-wash evaluation. The products were then washed with Methanol and rinsed with double distilled water before being dried under vacuum. The washing with Acetic acid was to remove any unpolymerized Chitosan while the washing with Methanol removed the template material and residual Acetic acid. The dried polymers, were then ground to particle sizes less than 25µm by passing them through a sieve of 25µm pore size. The same treatment was employed for the NIP sample. The polymer products were then taken for analysis again with FTIR, SEM, UV-VIS and Melting point ascertion. The pH of the samples was also noted. The thermal profiles of the samples were determined using a Simultaneous Thermal Analyzer. Rebinding studies were carried out using High Performance Liquid Chromatography (HPLC). Other analyses were, Pore size distribution (BET) and surface area analysis and Size and Zeta potential of the particles analysis (Photon Correlation Spectroscopy).

3.6 Product Characterization

3.6.1 Functional group activity and Degradation

FTIR spectroscopy was done to determine the monomer template interaction as well as the functional group activity and degradation owing to influence on hydrolysis cleavage to extract template molecule.

Fourier Transformed Infra-Red spectroscopy (FTIR), allows the possibility of mining qualitative evidence with respect to the arrangement of the NIP or MIP synthesized. Considering the cocktail of chemical fluxes within the prepared matrix as a result of interactions between the additives, it becomes very necessary to use this analytical tool to characterize samples based on the functional groups present or absent and the inter-plays that occur during the polymerization, template elution and or rebinding. It particularly gives clear insight into the bond type that exists such as the non-covalent hydrogen bonding or other weak bonding phenomenon. From an interpretation of the bonding type, plausible mechanism of the interaction between template and matrix is understood and consequently directs the scope of specific interactions and preferences for the monomer-cross linker interaction, monomer-template relationship and all these help in the prediction of the rebinding ability of the complex matrix, (Shunli et al., 2013). Functional groups' presence or absence have been identified, (Ding *et al.,* 2011) and used by researchers to draw conclusions on the effective elution of template, (Sanagi *et al.,* 2013). Shunli *et al.,* (2013), reported strong bands at 3441.76 cm^{-1} corresponding to the OH stretching vibration, bands at 3441.76 cm^{-1}, 1732.5 cm^{-1} and 1259.65 cm^{-1} of carboxyl functionality as well as absorbance at 1638.63 cm^{-1} consigned to stretching of C–C bond. This may be used to differenciate between NIP and MIP samples which can be authenticated even in the presence or absence of the template material, (Wang, *et. al.,* 2006).

3.6.2 UV-VIS Spectroscopy.

UV-VIS spectroscopy provides information on the presence and specific amount of template material with respect to the MIP matrix. This is achieved by noting the

absorbance from the NIP and MIP or in some comparative study, differences in absorbance values. This technique also gives insight into the binding capacities of matrix and template. Reports have presented cases where it was used to characterize substances like benzotriazole, (Dong, Tong and Li, 2003) tetracycline, (Vendamme, *et al.*, 2009) b-estradiol, estradiol benzoate, ethynyl estradiol e.t.c, (Golker, *et al.*, 2013), as well as the extent of the binding that is feasible.

3.6.3 Particle shape and Morphology.

TEM and SEM analysis were carried out to study particle shape, morphology and orientation between the polymer materials. The analysis provided information about the topographical, morphological, compositional and crystalline natures of the products. The images presented samples at a molecular level, thereby creating the possibility of structure and texture identification. The FESEM (plate 5), was used to investigate the surface morphology of synthesized polymer matrix, which influences the chemical, binding and thermal capacities of analyte-matrix system. This has a direct relationship with binding specificity within the polymer matrix (Rosengren, Karlsson and Nicholls, 2013 and Sauerbrey, 1959). This then necessitated the study and characterization of synthesized NIPs and MIPs using SEM. light microscopy verifies the fundamental physical reliability of matrix's globules while SEM confirms the image macrospores, (Janshoff, Galla and Steinem, 2000). The TEM (plate 6), showed how the aggregate units are distinctly resolved and analyzed as individual units. Results from the TEM analysis gave the cavity dimensions.

3.6.4 Determination of Particle size:

The size and zeta potential of the particles were determined by Zeta Nano particle sizer, and confirmed with Laser particle analyzer. The particle size of the MIP samples as relates to their hydrodynamic tendencies, Polydispersity Index (PDI) and the Zeta potential were carried out using Malvern ZetaNanosizer particle characterization instrument. Malvern Instruments Ltd.United Kingdom; located at Prince of Songhkla University, HatYai, Songhkla, Thailand.

The measurement of the particle size by the instrument is done primarily by Differential Light Scattering technique. The spherical diameter of the sample which moves at the same diffusion speed as the particle of polymer is taken as the size of the sample of interest. The instrument uses well known theories to interpret the size based on Brownian motion characteristics of MIP sample.

The samples were prepared by introducing 0.15mg/ml of the sample in 15ml plastic containers. They were allowed to stand for 2hrs to induce swelling before being vortexed for 2minutes. The samples were kept to stand overnight then centrifuged at 3000 revolutions per minute (rpm) using a table top centrifuge. 1ml of the supernatant was collected using a pipette and transferred into a plastic cuvette. The cuvette was then inserted into its chamber in the instrument and after setting the parameters ($25^{O}C$ temperature, 1.33 as refractive index of milli Q water and 1.58 as refractive index for Chitosan), the sample was analyzed. The results are as presented Table 4.8.

Laser light scattering reports a sample's particle size distribution with respect to equivalent spherical diameter and may be expressed as a number spread or volume dispersal. Any buildup of particles larger than or within a molecular scale, actually contains various different sizes of particles and a typical gathering contains an uninterrupted range of sizes.

Pore size distribution and surface areas of the polymers were analyzed by Brunauer-Emmett-Teller (BET) method. Relevant information was obtained by ploting the values of pore size versus incremental pore volume and this gave the pore size distribution. The surface areas and total pore volumes of the polymers were thus obtained. IUPAC In 1985 produced a manual on how to Report Physisorption Data for both fluid and Solid Systems (Sing, 1985), in the cause of ascertaining the specific integrities of solid surfaces and pore structures with respect to their surface area and pore size distribution/porosity.The results are presented as graphical Isotherms and Hysteresis loops.

3.6.5. Surface Area, Pore size and Pore volume

Materials that allow the permeation of fluids into their interlatices, invariably posses openings or cavities. In order to define the actual boundries of these cavities, in 1916 Langmuir proposed a model (Langmuir, 1916), with which to calculate the surface areas of such cavities. The model is based on the assumsion that the percolated films are not thicker than the size of one molecule. One shortcoming of this model is that it is best suited for material sizes within the micropore range only. Consequently, Brunauer, Emmet and Teller derived another model that was presented in 1938 which explains the interaction of the fluids within a multilayer surface environment (Eddaoudi, 2005). The BET theory accounts for surface areas within the meso- and macropore ranges and has remained the accepted starndard method for the analysis of surface areas of materials with exceptions to only ultrmicroporous pores. The BET theory is based on three basic assumsions which are:

1. All layers of adsorped gas molecules are comparable.
2. All the surfaces of interaction are homogeneous (usually not true in real life cases).
3. Resultant parallel forces among adsorbed multilayer gas molecules are ignored.

3.6.6 Determination of Thermal Profile of Samples

The thermal profile was done with the aid of a Simultaneous Thermal Analyzer (STA), STA8000,Perkin Elmer, USA accessed at the scientific equipment center of the Prince of Songkla University HatYai Songkhla Thailand (plate 10). The technique used is based on Thermogravimetry-Differential Thermal Analysis. The test condition involved the use of Nitrogen as the purge gas at a gas flow rate of 20cc/min. Samples were heated from 25^{O}C to 60^{O}C at 10.00^{O}C/min. The choice of using the simultaneous thermal analyzer is because of its inherent application advantages over TGA or DSC individually. The equipment simultaneously carries out Thermogravimetry (TGA) and Differential Scanning Calorimetry (DSC), of samples.

3.6.7 Determination of Swelling Characteristics of Samples.

Swelling measurements were carried out using 20 milligrams of each MIP and NIP. They were introduced into plastic disposable cuvettes and ensuring that they maintained a leveled height across the entire surface of the MIP in the cuvettes. The initial height in millimeters of the MIP sample (dry) was taken before the introduction of 3ml of phosphate Buffer Saline at pH of 7.4 (mimicking the pH of saliva from a healthy individual, which usually wets cigarette butts during smoking by some smokers). The set-up was allowed for a contact period of 24h. The heights of the swollen MIPs were taken at the end of the set time and with the difference in height, the swelling factor of the samples was calculated.

The crystallinity of Chitosan is determined using X ray diffraction analysis. Here, characteristic peaks at $2\theta = 9.28$ and $20.18°$, in ranges of $2\theta = 9.9 – 10.7$ and $19.8 – 20.7$, are indicative of the crystallinity of the sample. The more dense the inherent crystalline structure, the sharper the peaks.

3.6.8 Rebinding Studies:

High Performance Liquid Chromatography (plate 11), was used to determine the rebinding potential and efficiency of the samples based on the obtained peaks of the characteristic template compounds. UV-VIS was employed in determining the wavelength (max) and the MIPs binding potential of guest template material. With the 2 AU absorbance capacity obtained from the UV-VIS analysis, the analyte took up the whole range of effective critical absorbance. Consequently, a mobile phase that absorbed within only a 1 AU was used. The analyte was left with the remaining 1AU, not minding its visibility status (due to the auto zeroing). A typical example is sighted where, at 205 the absorbance of MeOH was about 1 AU and ACN less than 0.1 or near zero. The analyte peaks showed higher/more prominent absorption with consequent higher area count due to the lower UV cutoff of ACN. The reverse was the case with methanol whose mobile phase absorbed significantly, a higher AU value that presented a non-linear range of response curve with lesser observable absorbance for the same given concentration. The more absorbance the mobile phase exhibited, the less effective was the absorbance range left for the analyte to operate in.

Considering the very close properties of the templates, a gradient profile was created using first, a normal increment from low to high elution strength effect of Methanol in the mixed mobile phase of Buffer and Methanol. This targeted a defined separation of the component template materials that have different stationary phase affinities. The presence of multiple and probable overlaps in peaks observed from the preparative UV-VIS study, encouraged the inclusive adoption of isocratic elution mode. This ensured the effective separation of templates that have the same or closely the same stationary phase affinity.

Four adapted (Murray, 2014) schemes of conditions for the HPLC analysis were employed:

A) Gradient elution i 90/10, pH 7.9 Phosphate Buffer/MeOH

ii 70/30, pH 7.9 Phosphate Buffer/MeOH

iii 50/50 pH 7.9 Phosphate Buffer/MeOH from 0 to 3 minutes;

B) Isocratic elution iii 50/50 pH 7.9 Phosphate Buffer/MeOH from 3 to 6.5 min.

HPLC Conditions for Analysis (adapted)

The initial step was to identify the machine detectable concentrations of the template solutions. The lambda max of the templates as individual entities and blend were determined using UV-VIS spectrophotometer by introducing varied concentrations of the template solutions. From a 10mM stock solution of the different template materials, serial dilutions were made and introduced into the UV-VIS machine. The concentration that gave sharp peak and Lambda max value at 1.0 intensity or closest to 1.0, was chosen (Figure 3.1). Subsequent use of the template solution for rebinding studies was based on this dilution. The respective values were then applied in the conditioning of the HPLC equipment (calibration), for rebinding analysis. The obtained dilutions for the template solutions is shown in Figure 3.1:

The MIP and NIP samples were prepared by first, washing and eluting the unreacted input materials and templates before introducing known concentrations of template materials for sequestration within the cavities of the MIPs and NIPs. From the result of the trials, 0.6g of MIP and NIP samples were weighed and introduced into 15ml ependorf tubes and 3ml of template solutions (at detectable dilute solutions), were introduced. The tube was securely closed and clamped to the circularly rotating mechanical shaker. The shaker was set at a rotational speed of 60rpm (No 4) and inclined at an angle of 60o. The rotational agitation was carried out for 24hrs, at the end of which the content of the tubes were centrifuged at 3000rpm for 10min. The supernatant was collected and 30µl of it injected into the HPLC column.

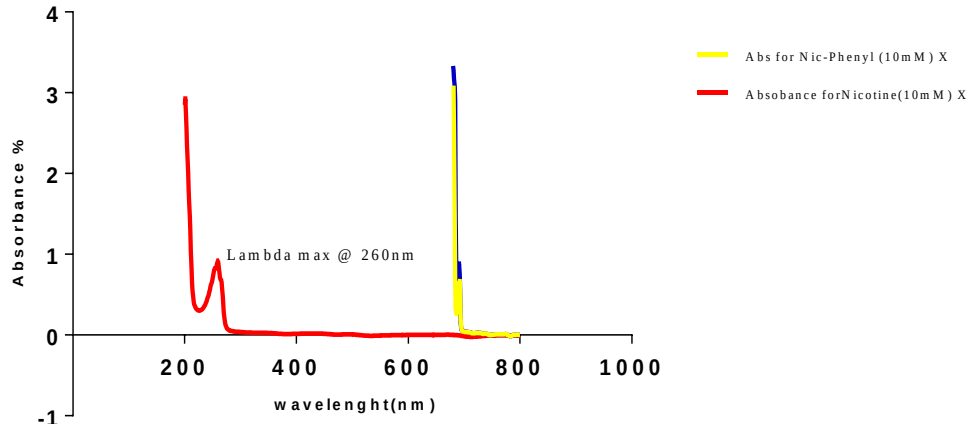

Figure 3.1: UV-VIS was employed in determining the wavelength (max) and the MIPs binding potential of guest template material.
Analyte concentrations: Nicotine in PBS (pH 7.4), 10 mill molar = x25
Phenylalanine amide in PBS (pH 7.4), 10 mill molar = x2
Nicotine-Phenylalanine amide in PBS (pH 7.4), 10 mill molar = x15

Table 3.3: presents the identities of the samples as analyzed by the HPLC-MS equipment and their corresponding polymerization identities and platforms (templates and cross linkers).

Table 3.3**: S**amples IDs And Status Used In HPLC-MS Based Rebinding Studies.

HPLC Sample IDs	MIP Sample IDs (single washing)	MIP Sample IDs (double washing)	Template ID	Cross linker ID
1 to 6	P1S (a-f)	-		
7 and 8	MP1Sd and MP1Sf	-	**Nicotine**	
1R to 6R	-	P1S(a-f)		**BAP**
7R and 8R	-	MP1Sd and MP1Sf		
16 to 21	P3S (a-f)	-		
22	MP3d	-	**Phenylalanine amide**	
16R to 21R	-	P3S(a-f)		
30 to 35	P5S (a-f)	-		
30R to 34R	-	P5S(a-f)	**Nicotine- Phenylalanine amide**	
9 to 14	P6S (a-f)	-		
15	MP6Sd	-	**Nicotine**	**Geranic acid**
9R to 14R	-	P6S(a-f)		
15R	-	MP6Sd		
23 to 28	P8S (a-f)	-	**Phenylalanine amide**	
29	MP8Sd	-		
35 to 40	P10S (a-f)	-		
41	MP10Sd	-	**Nicotine- Phenylalanine amide**	

The Binding Capacity (Q)

(Q) Was calculated according to Equation (1).

$$Q = Co - Ce \times V / m \quad (1)$$

C0 and Ce represent the initial and equilibrium DA concentration (mmol), respectively; V is the volume of the solution in mL; m is the weight of the polymer in g.

The Imprinting Factor

The imprinting factor (IF), which is the result of the relationship between the coefficients of the MIP and the NIP from the equation:

$$KD = (Ci - Cf) \times V \div Cf \times m \quad 1$$

KD = Distribution coefficient

Ci = conc of template solution before adsorption

Cf = conc of template solution after adsorption

V = volume of the solution

m = mass of the polymer,

is obtained by dividing that of the imprinted by that of the non-imprinted

$$IF = KD (MIP) / KD (NIP) \quad 2$$

3.7 Adapted-Real Life Efficiency of Prepared MIPs (representative samples)

The real-life efficiency of the prepared MIP vis-a-vis its ability to trap and retain the TSNAs was evaluated by HPLC analysis of extracts/eluents from adapted machine smoked cigarette samples. Plates 3.1 to 3.5 present the adapted machine smoking regime. Adapting and modifying the method by Ying Liu, Xueliang Liu and Junde Wang (2003), 1g each of MIP samples P1, P3, P6, P8, P10; MP1, MP3, MP6, MP8 and MP10, were in an improvised 1cm diameter tubes that served as cigarette holder. This was fixed into the MISPE column (Plate 3.2). Rolled Malboro

brand of cigarettes each weighing 0.75g (without butts), measuring 5.5cm length (without filter butt) and diameter of 0.8cm, were fixed into the improvised MIP containing cigarette holders. The cigarettes were then smoked by application of suction from the vaccum pump connected to the column. Using SHIMADZU LC-2030 3D HPLC equipment, serial no. L214552, SHIMADZU CORP 00405 with Diode Array Detector(DAD) and column chamber temperature control system; at a pump pressure set at 2030psi, temp., 30OC, flow rate of 1ml/min, injection volume of 20µl; the presence and concentrations of the adsorbed and eluted degraded products from the cigeratte smoking were determined. A 50:50 methanol: PBS pH 7.4 buffer solution was employed as mobile phase using a Kromasil C18 column (250mm, 4.6 mm, 5 mm) as stationary phase. Isocratic elution method was adopted with elution time of 10mins. The procedure was carried out in triplicate and average of the readings taken for comparison.

Plate 3.1: Set-up of the machine aided cigarette smoking experiment.

Plate 3.2: .The MIPs packed in the adapted column before and after the cigarettes are attached.

Plate 3.3:.The Cigarettes attached and ready to be smoked with the aid of the machine.

Plate 3.4: The smoking regime and entrapment of TSNAs by the prepared MIP samples.

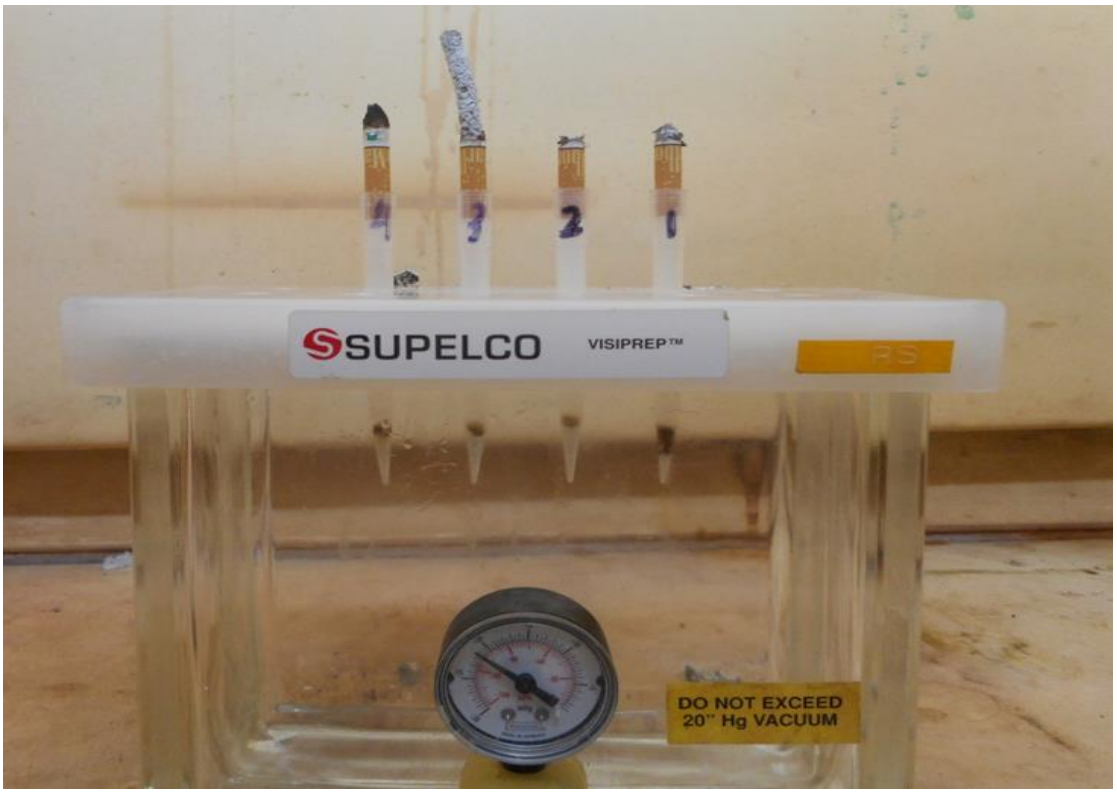

Plate 3.5: Smoked cigarettes from the machine smoked experiment showing the discolouration of the MIP samples in the column due to entrapped cigarette smoke constituents.

3.8 Stripping And Analyses of Sequestered Nicotine and TSNA Analogues After The Machine-Aided Smoking Regime.

Methanol was used to strip the MIPs of the sequestered degraded cigarette smoke constituents using the method by Sahar Taghavi *et al.* (2012), in the detection of the sequestered Nicotine and analogues from the cigarette smoke but with slight modifications. Here, the MIP samples were put in an ependorf tube and 15mls of Methanol was introduced into the tube. The set-up was placed in a vortex stirrer over night to allow the extraction of sequestered components of the cigarette smoke.

Plate 3.6: Rotatory shaker with the secured eluted materials from the MIP SPE.

Then a 50% dilution was made with a Phosphate buffer saline solution pH 7.4 before being filtered through a 0.5 µm PTFE Millipore filter. This served as the stock solution from which desired volume of 20 µl was taken for HPLC studies.

1 ml of the extract was made up to 10mls of sample solution by the addition of a 0.01 M solution of Phosphate Buffer Saline (pH 7.0). 20 µl volume injections were introduced into the HPLC machine and analyzed at wavelengths of 254, 259 and 260 nm for Phenylalanine amide analogues, nicotine and other nicotine analogues as well as analogues of their blends respectively.

CHAPTER FOUR

RESULTS AND DISCUSSION

4.1 Proton Nuclear Magnetic Resonance (^{1}H NMR) spectroscopy result

Analysis, interpretation and discussion.

The ^{1}H NMR spectra for functional group (chitosan-methacryllic acid) against template compounds (nicotine, phenylalanine and blend of nicotine-phenylalanine), are displayed as appendices i to viii. Appendix i is the spectra of blend of chitosan-Methacrylic acid while appendix ii presents the stacked spectra of the representative three template materials using the Advanced Chemistry Development (ACD) Spectrus Processor as influenced by the varied reaction temperatures of 30 ^{o}C, 40 ^{o}C and 60 ^{o}C.

Appendix iii is a representative spectrum of functional polymer-template interaction showing the plausible point of interaction between the template and the functional monomers. The spectrum shows the Chitosan's C2 amine H as the interacting Hydrogen atom on which the substitution and bonding primarily occurs. This is shown on the spectrum (coloured green). This serves as a guide in studing any characteristic chemical shift that may occur during the titration. Initially, a blend of 1:1 chitosan-methacrylic acid (functional monomer): nicotine and phenylalanine amide (templates) were used in carrying out the titration using methanol-d4 at three different temperatures of 30^{o}C, 40^{o}C and 60^{o}C, (appendix iv and vi). Deuteium oxide was substituted for methanol and similar trend was observed. An increase in amount of functional monomer against a constant amount of template was also considered, to investigate possible influence of amount of functional monomer on the effective interaction with the template; for this, a 4:1 blend was studied and the stacked spectra presented as appendices v, vii and viii for nicotine, phenylalanine amide and 50:50 blend of the two respectively. From appendix iii, the C-2 amine hydrogen of the chitosan is shown to be the

interaction site for the methacryllic acid while the peaks at 6.04 ppm and 5.62 ppm are the characteristic chemical shifts. Interaction from the chitosan molecule at this point is expected to influence either an increased or decreased downfield or upfield shift via electron withdrawing functionalities like the Halogens, NO_2, -OCOR or –OH. Here, obsereved influence caused a deshielding effect on the adjacent 1H nuclei with consequent downfield shift relative to an initial position. Tables 4.1 to 4.5 presents the results of the integrated peaks from the H^1NMR titration.

Table 4.1: Chemical Shifts for Templates (ppm)**.**

Numbering and assignments on the Nicotine compound.

NICOTINE (Aromatic Hydrogens)				
A (C-2 Proton)	**B** (C-6 Proton)	**C** (C-4 Proton)	**D** (C-5 Proton)	Remark
8.49	8.43	7.85	7.42	

PHENYLALANINE			
Aromatic Hydrogens	CH	CH_2 (A)	CH_2 (B)
7.31	4.03	3.20	3.00

NICOTINE-PHENYLALANINE							
Nicotine aromatic Hydrogens				**Phenylalanine aromatic Hydrogen**	CH	CH_2	CH_2
A	**B**	**C**	**D**				
8.49	8.43	7.84	7.41	7.29	3.80	3.11	2.90

Table 4.2: Chemical Shifts of titrated Functional monomer vs Templates at 1:1 and 4:1blend ratios at varied temperatures of 30°C, 40°C and 60°C.

Interaction Conditions (blend ratio and temp).	Aromatic Hydrogens of Nicotine				Ar-Hydrogen of Phenylalanine	CH of Phenyl alanine	CH_2 of Phenylalanine A	CH_2 of Phenylalanine B	Remark
	A	B	C	D					
Nicotine									
1:1/30°C	8.68	8.65	8.06	7.61					
1:1/40°C	8.79	8.76	8.17	7.72					
1:1/60°C	9.01	8.98	8.37	7.92					
4:1/30°C	**8.72**	**8.69**	**8.17**	**7.70**					
4:1/40°C	**8.83**	**8.80**	**8.26**	**7.80**					
4:1/60°C	**9.09**	**8.99**	**8.41**	**7.97**					
Phenylalanine									
1:1/30°C					7.36	4.20	3.24	3.15	
1:1/40°C					7.47	4.31	3.35	3.26	
1:1/60°C					7.68	4.54	3.56	3.49	
4:1/30°C					**7.35**	**4.22**	**3.23**	**3.14**	
4:1/40°C					**7.46**	**4.34**	**3.33**	**3.26**	
4:1/60°C					**7.68**	**4.56**	**3.54**	**3.48**	
Nicotine-Phenylalanine									
1:1/30°C	8.68	8.65	8.06	7.61	7.34	4.19	3.22	3.14	
1:1/40°C	8.79	8.76	8.17	7.72	7.46	4.31	3.32	3.26	
1:1/60°C	9.00	8.97	8.36	7.92	7.67	4.52	3.55	3.48	
4:1/30°C	**8.73**	**8.69**	**8.20**	**7.72**	**7.34**	**4.22**	**3.22**	**3.15**	
4:1/40°C	**8.82**	**8.79**	**8.28**	**7.81**	**7.44**	**4.33**	**3.33**	**3.27**	
4:1/60°C	**9.01**	**8.99**	**8.43**	**7.98**	**7.67**	**4.55**	**3.55**	**3.49**	

Table 4.3: Selected Chemical shifts for Nicotine Template.

Interaction condition.	Template	Proton	Initial position	Final position	Shift
1:1/30^{O}C	**Nicotine**	H-2	8.49	8.68	**+0.19**
1:1/40^{O}C				8.79	**+0.30**
1:1/60^{O}C				9.01	**+0.52**
4:1/30^{O}C				8.72	**+0.23**
4:1/40^{O}C				8.83	**+0.34**
4:1/60^{O}C				9.09	**+0.60**
1:1/30^{O}C		H-6	8.43	8.65	**+0.22**
1:1/40^{O}C				8.76	**+0.33**
1:1/60^{O}C				8.98	**+0.55**
4:1/30^{O}C				8.69	**+0.26**
4:1/40^{O}C				8.80	**+0.37**
4:1/60^{O}C				8.99	**+0.56**
1:1/30^{O}C		H-4	7.85	8.06	**+0.21**
1:1/40^{O}C				8.17	**+0.32**
1:1/60^{O}C				8.37	**+0.52**
4:1/30^{O}C				8.17	**+0.32**
4:1/40^{O}C				8.26	**+0.41**
4:1/60^{O}C				8.41	**+0.56**
1:1/30^{O}C		H-5	7.42	7.61	**+0.19**
1:1/40^{O}C				7.72	**+0.30**
1:1/60^{O}C				7.92	**+0.50**
4:1/30^{O}C				7.70	**+0.28**
4:1/40^{O}C				7.80	**+0.38**
4:1/60^{O}C				7.97	**+0.55**

Table 4.4: Selected Chemical shifts for Phenylalanine Template

Interaction condition.	Template	Proton	Initial position	Final position	Shift
1:1/30^{O}C				7.36	**+0.05**
1:1/40^{O}C				7.47	**+0.16**
1:1/60^{O}C				7.68	**+0.37**
4:1/30^{O}C		Aromatic-H	7.31	7.35	**+0.04**
4:1/40^{O}C				7.46	**+0.15**
4:1/60^{O}C				7.68	**+0.37**
1:1/30^{O}C				4.20	**-0.10**
1:1/40^{O}C				4.31	**+0.01**
1:1/60^{O}C				4.54	**+0.24**
4:1/30^{O}C	**Phenylalanine**	CH	4.30	4.22	**-0.08**
4:1/40^{O}C				4.34	**+0.04**
4:1/60^{O}C				4.56	**+0.26**
1:1/30^{O}C				3.24	**+0.04**
1:1/40^{O}C				3.35	**+0.15**
1:1/60^{O}C				3.56	**+0.36**
4:1/30^{O}C		CH_2 (A)	3.20	3.23	**+0.03**
4:1/40^{O}C				3.33	**+0.13**
4:1/60^{O}C				3.54	**+0.34**
1:1/30^{O}C				3.15	**+0.15**
1:1/40^{O}C				3.26	**+0.26**
1:1/60^{O}C				3.49	**+0.49**
4:1/30^{O}C		CH_2 (B)	3.00	3.14	**+0.14**
4:1/40^{O}C				3.26	**+0.26**
4:1/60^{O}C				3.48	**+0.48**

Table 4.5: Selected Chemical shifts for Nicotine-Phenylalanine Template.

Interaction condition.	Template	Proton	Initial position	Final position	Shift
1:1/30^{O}C		H-2		8.68	**+0.19**
1:1/40^{O}C				8.79	**+0.30**
1:1/60^{O}C				9.00	**+0.51**
4:1/30^{O}C			8.49	8.73	**+0.24**
4:1/40^{O}C				8.82	**+0.33**
4:1/60^{O}C				9.01	**+0.52**
1:1/30^{O}C		H-6		8.65	**+0.22**
1:1/40^{O}C				8.76	**+0.33**
1:1/60^{O}C				8.97	**+0.54**
4:1/30^{O}C			8.43	8.69	**+0.26**
4:1/40^{O}C				8.79	**+0.36**
4:1/60^{O}C				8.99	**+0.56**
1:1/30^{O}C		H-4		8.06	**+0.22**
1:1/40^{O}C				8.17	**+0.33**
1:1/60^{O}C				8.36	**+0.52**
4:1/30^{O}C			7.84	8.20	**+0.36**
4:1/40^{O}C				8.28	**+0.44**
4:1/60^{O}C				8.43	**+0.59**
1:1/30^{O}C		H-5		7.61	**+0.20**
1:1/40^{O}C				7.72	**+0.31**
1:1/60^{O}C				7.92	**+0.51**
4:1/30^{O}C			7.41	7.72	**+0.31**
4:1/40^{O}C				7.81	**+0.40**
4:1/60^{O}C				7.98	**+0.57**
1:1/30^{O}C	**Nicotine-**			7.34	**+0.05**
1:1/40^{O}C	**Phenylalanine**			7.46	**+0.17**
1:1/60^{O}C				7.67	**+0.38**
4:1/30^{O}C		Aromatic H	7.29	7.34	**+0.05**
4:1/40^{O}C				7.44	**+0.15**
4:1/60^{O}C				7.67	**+0.38**
1:1/30^{O}C				4.19	**+0.39**
1:1/40^{O}C				4.31	**+0.51**
1:1/60^{O}C			3.80	4.52	**+0.72**
4:1/30^{O}C		CH		4.22	**+0.42**
4:1/40^{O}C				4.33	**+0.53**
4:1/60^{O}C				4.55	**+0.75**
1:1/30^{O}C				3.22	**+0.11**

1:1/40^{O}C			3.32	**+0.21**
1:1/60^{O}C			3.55	**+0.44**
4:1/30^{O}C	CH_2(A)	3.11	3.22	**+0.11**
4:1/40^{O}C			3.33	**+0.22**
4:1/60^{O}C			3.55	**+0.44**
1:1/30^{O}C			3.14	**+0.24**
1:1/40^{O}C			3.26	**+0.36**
1:1/60^{O}C			3.48	**+0.58**
4:1/30^{O}C		2.90	3.15	**+0.25**
4:1/40^{O}C	CH_2(B)		3.27	**+0.37**
4:1/60^{O}C			3.49	**+0.59**

4.1.1 MNOVA result of the ^{1}HNMR

Figures 4.1 to 4.22.are the MNOVA integrated peaks after calibrating the solvent system with D_2O :

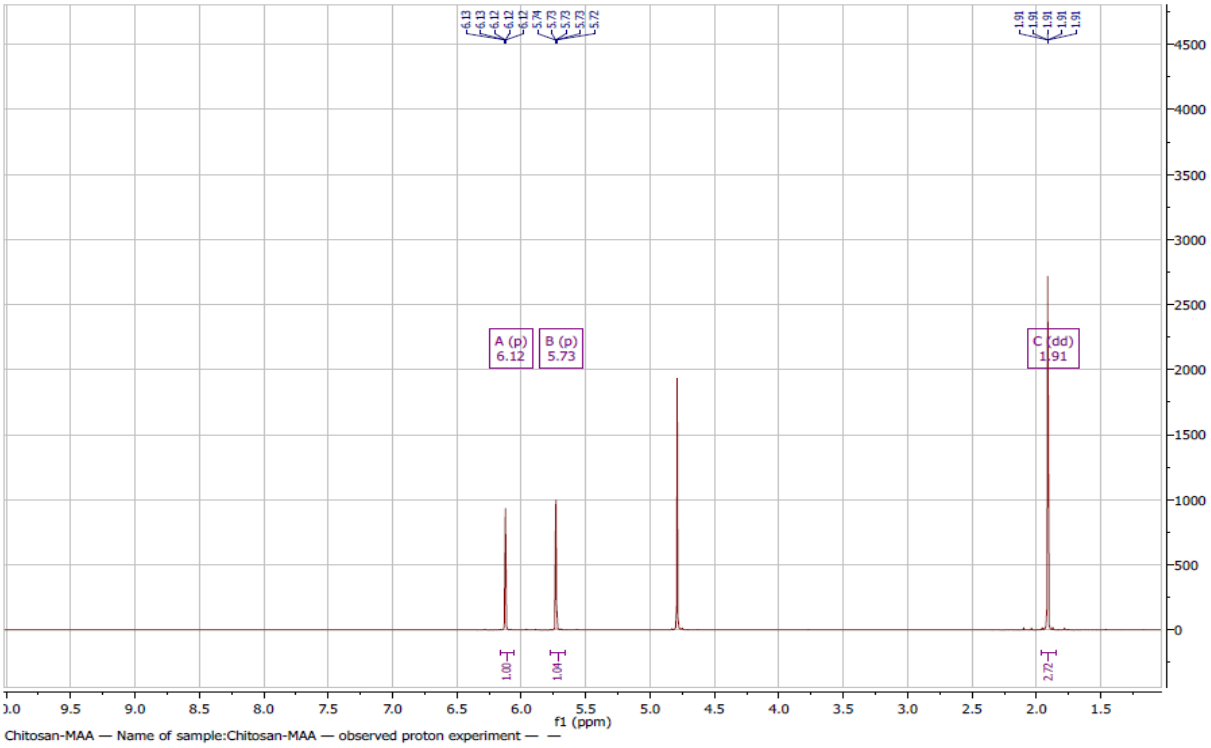

Figure 4.1: MNOVA integrated peacks of Chitosan-MAA H'NMR spectra

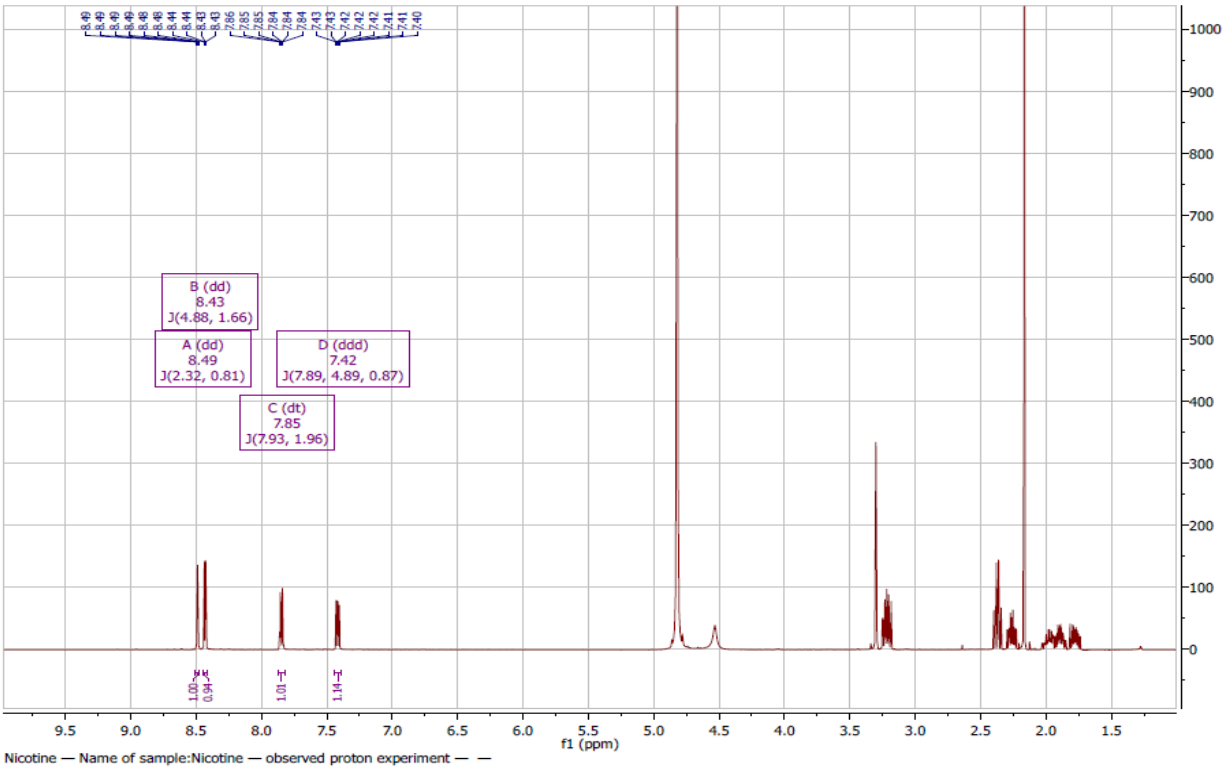

Figure 4.2: MNOVA integrated peacks of Chitosan-MAA-Nicotine H'NMR spectra

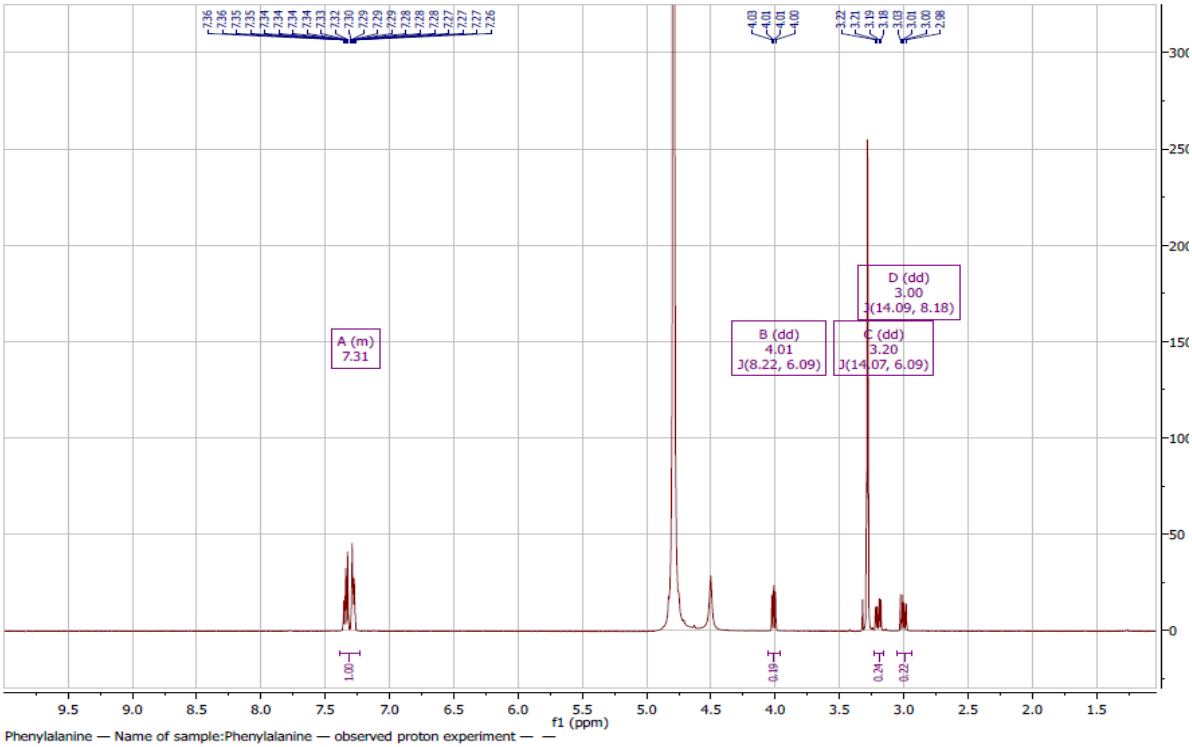

Figure 4.3: MNOVA integrated peacks of Chitosan-MAA-Phenylalanine H'NMR spectra

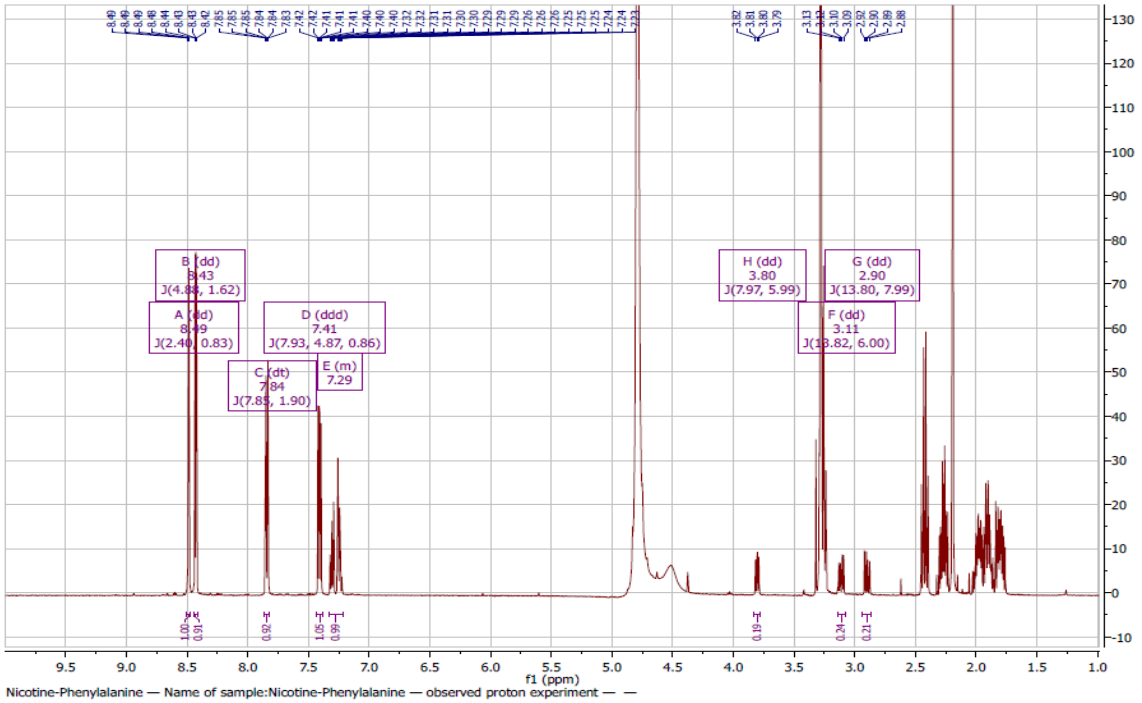

Figure 4.4: MNOVA integrated peacks of Chitosan-MAA-Nicotine-Phenylalanine H'NMR spectra

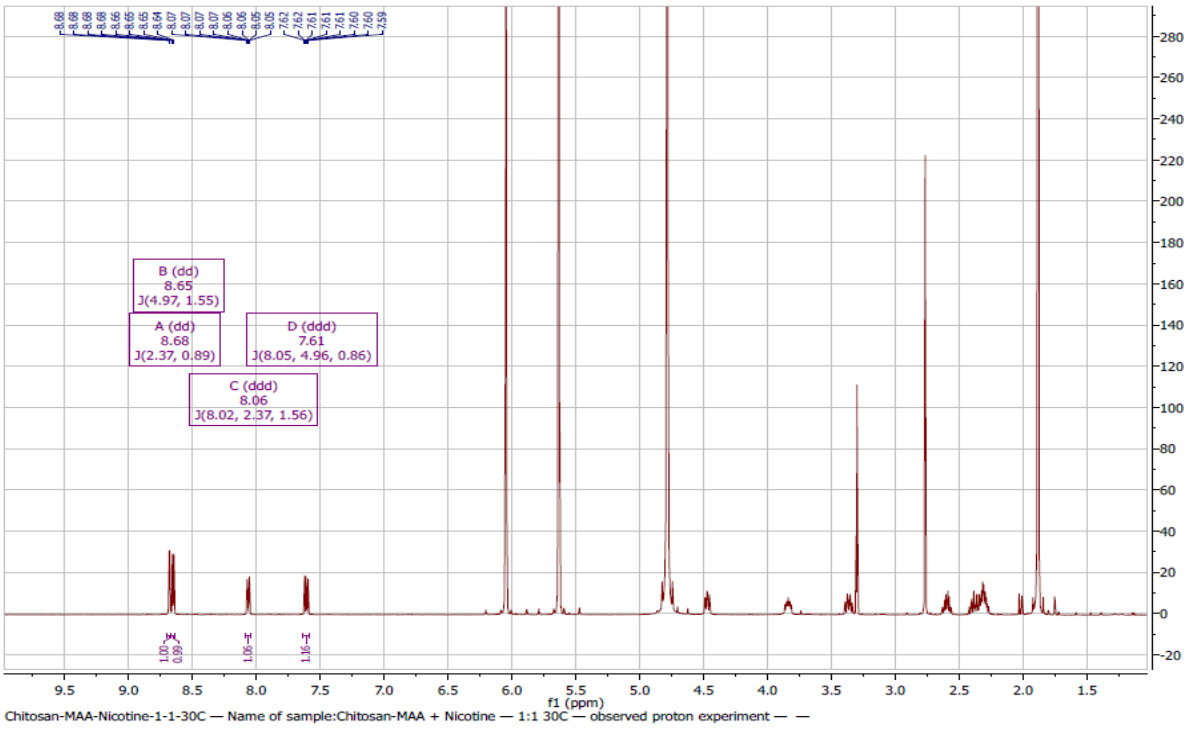

Figure 4.5: MNOVA integrated peacks of Chitosan-MAA-Nicotine 1:1 @ 30^{O}C H'NMR spectra.

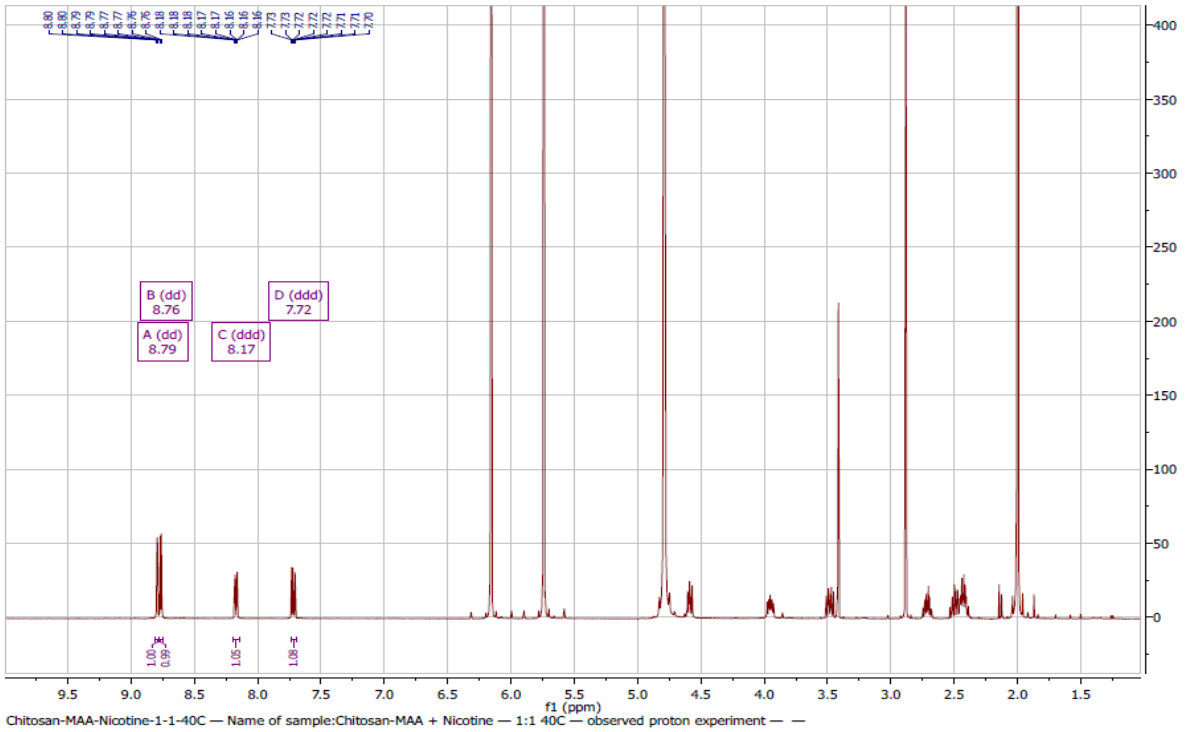

Figure 4.6: MNOVA integrated peacks of Chitosan-MAA-Nicotine 1:1 @ 40^{O}C H'NMR spectra.

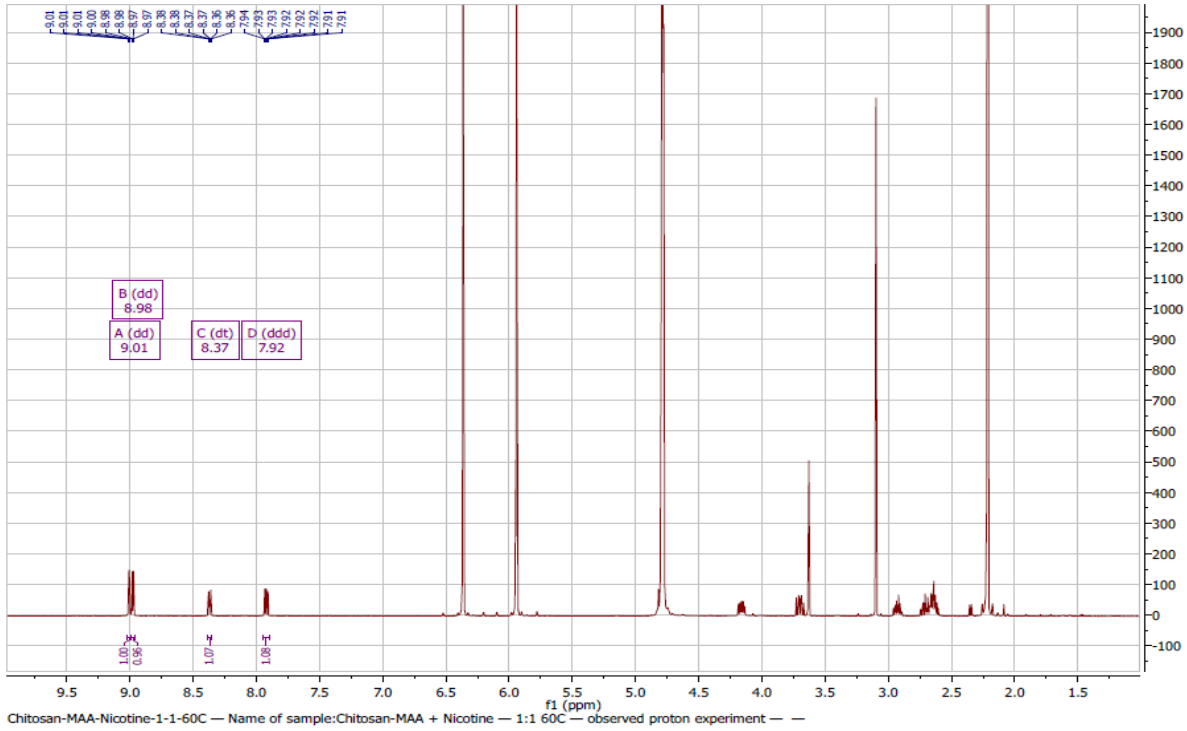

Figure 4.7: MNOVA integrated peacks of Chitosan-MAA-Nicotine 1:1 @ 60^{O}C H'NMR spectra.

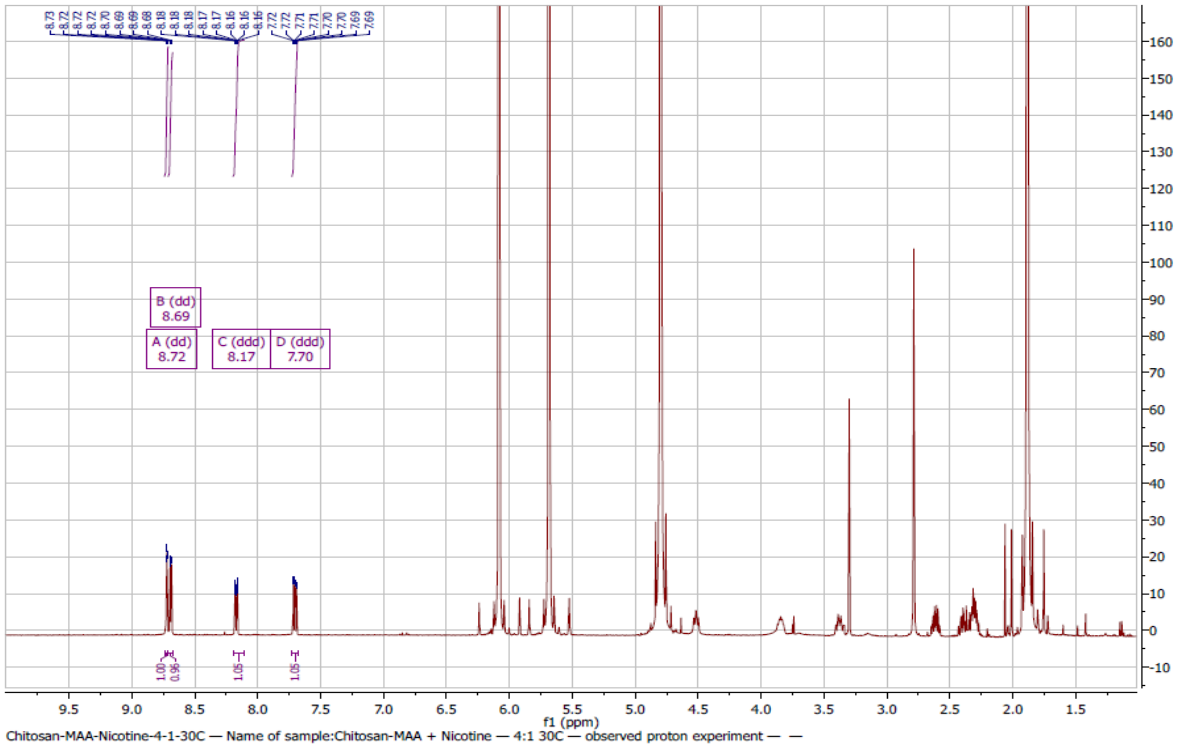

Figure 4.8: MNOVA integrated peacks of Chitosan-MAA-Nicotine 4:1 @ 30^{O}C H'NMR spectra.

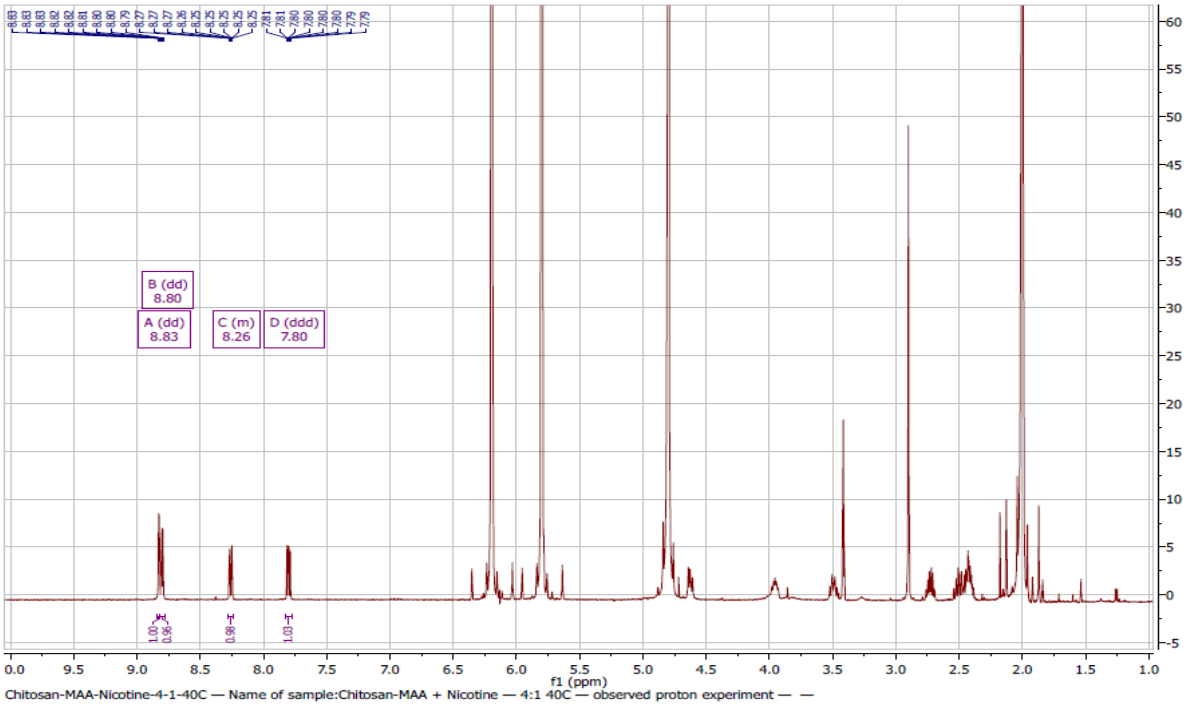

Figure 4.9: MNOVA integrated peacks of Chitosan-MAA-Nicotine 4:1 @ 40^{O}C H'NMR spectra.

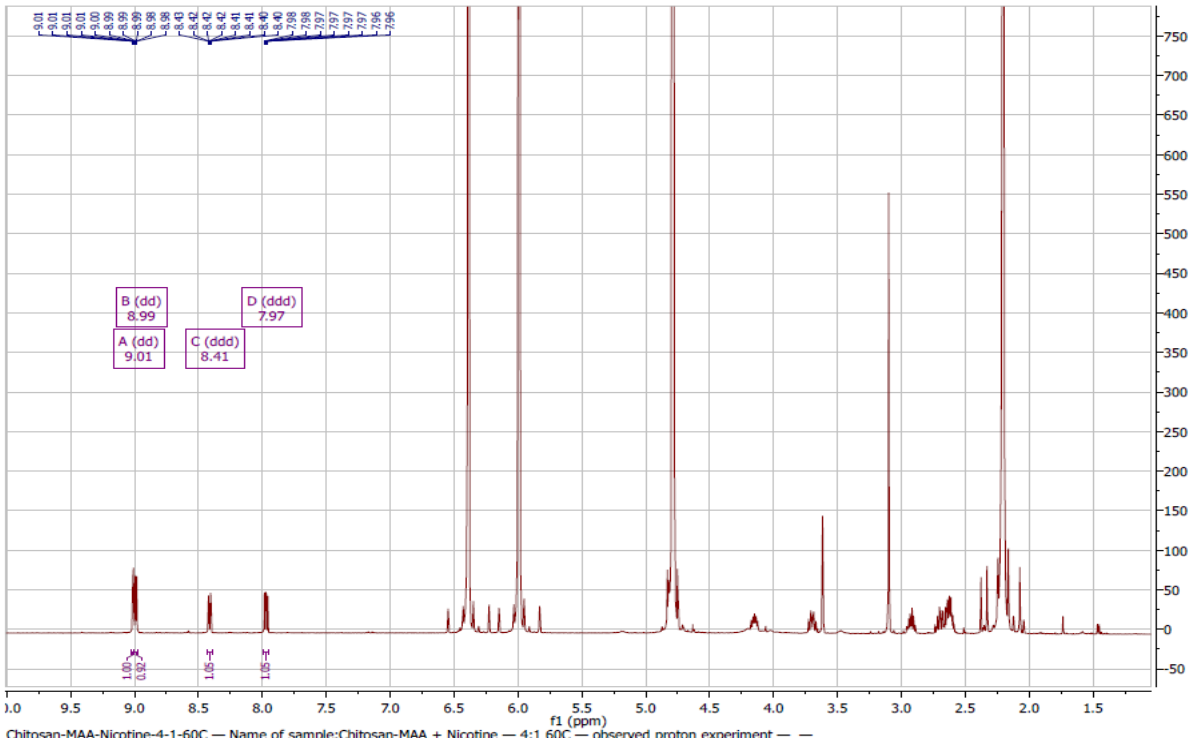

Figure 4.10: MNOVA integrated peacks of Chitosan-MAA-Nicotine 4:1 @ 60^{O}C H'NMR spectra.

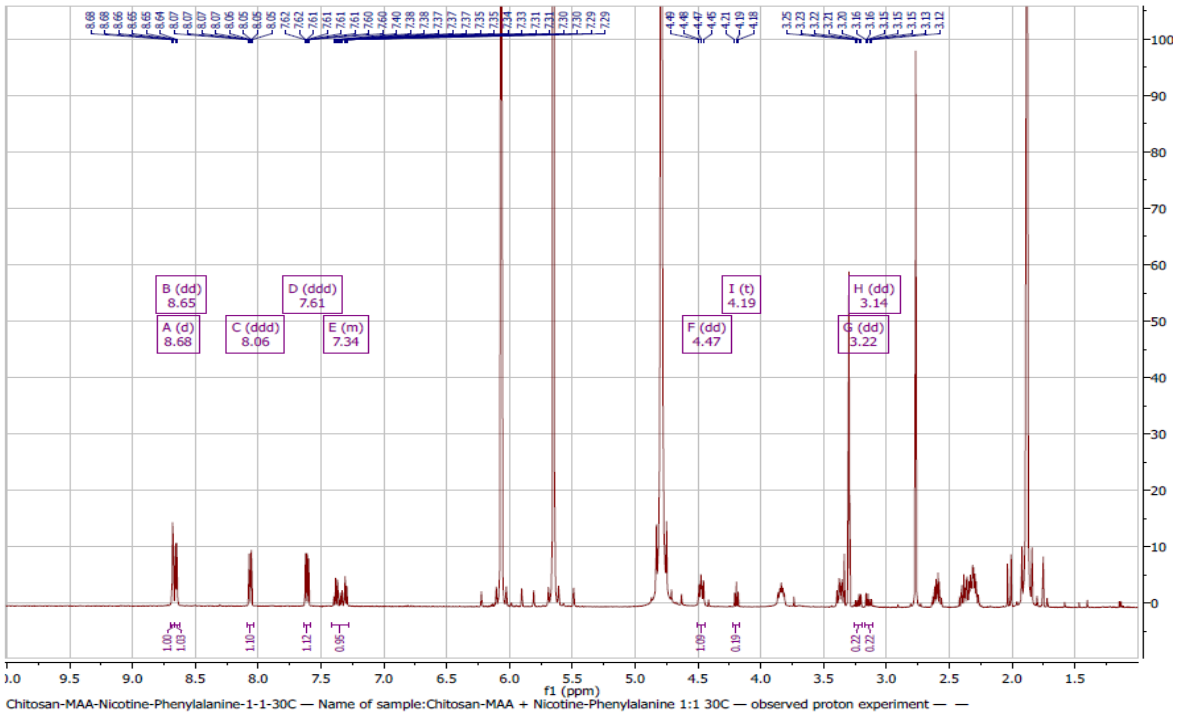

Figure 4.11: MNOVA integrated peacks of Chitosan-MAA-Nicotine-Phenylalanine 1:1 @ 30^{O}C H'NMR spectra.

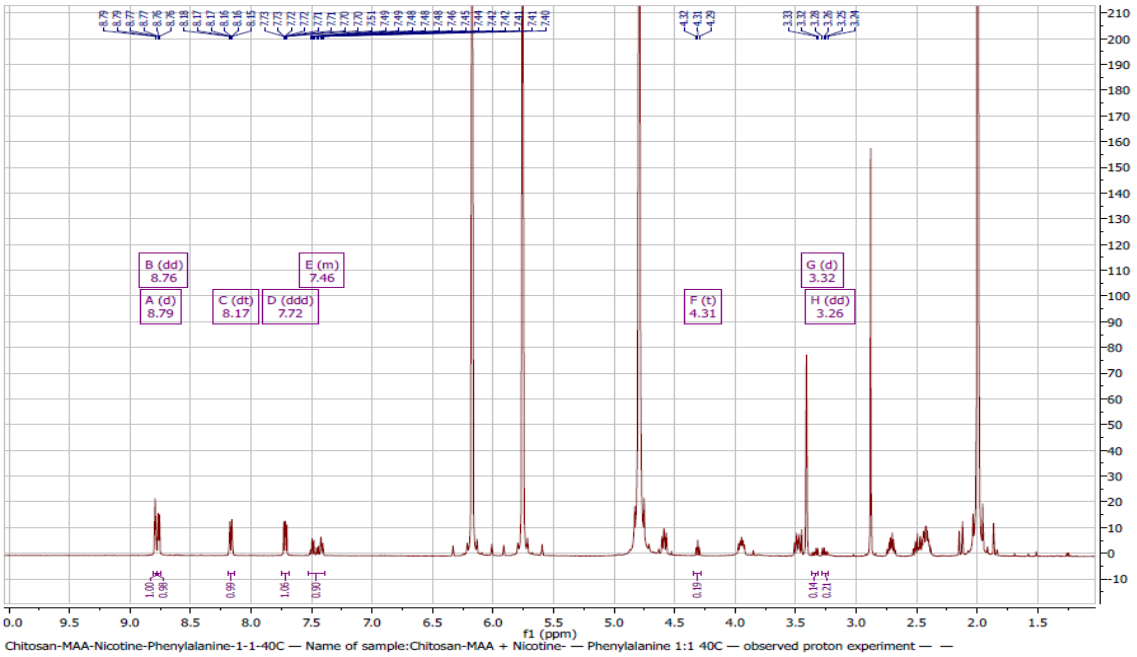

Figure 4.12: MNOVA integrated peacks of Chitosan-MAA-Nicotine-Phenylalanine 1:1 @ 40^{O}C H'NMR spectra.

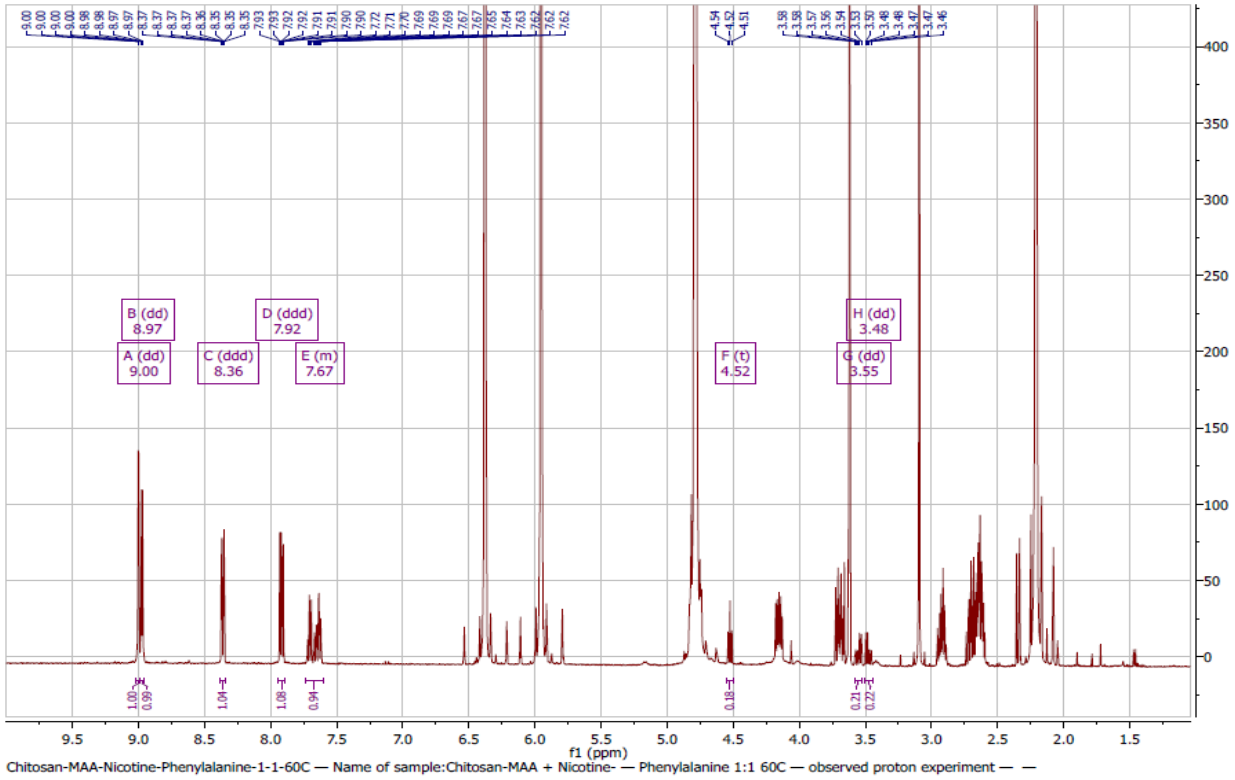

Figure 4.13: MNOVA integrated peacks of Chitosan-MAA-Nicotine-Phenylalanine 1:1 @ 60^{O}C H'NMR spectra.

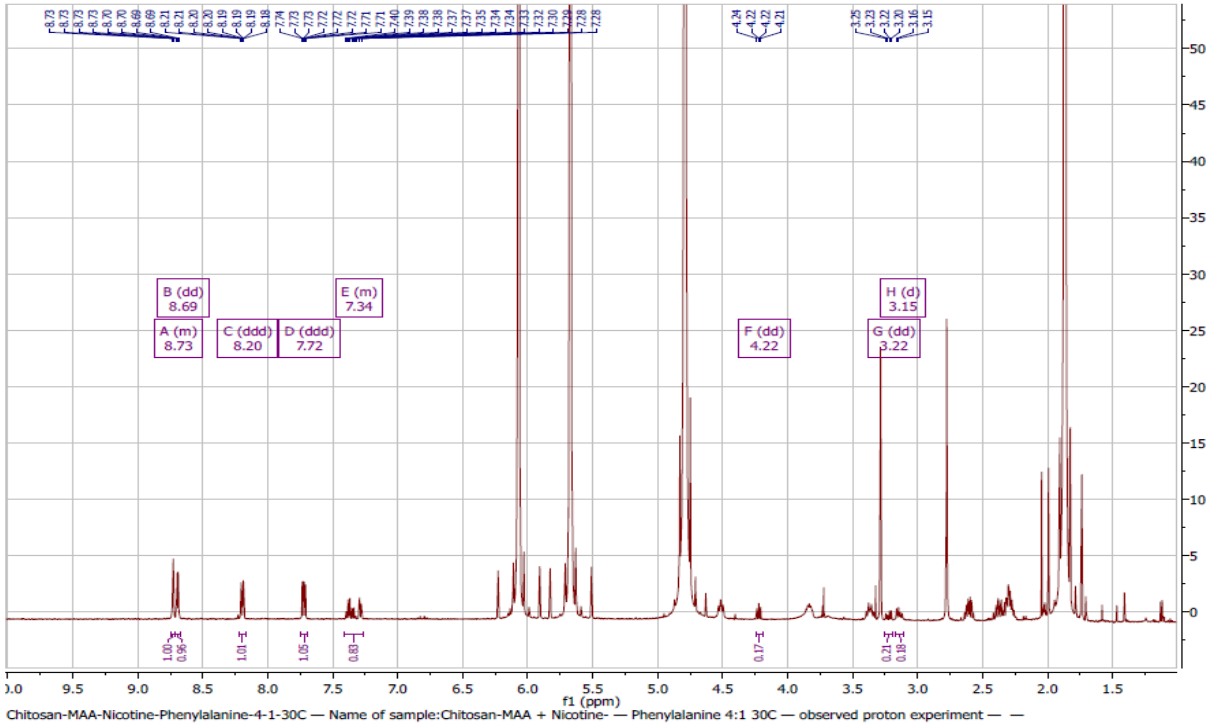

Figure 4.14: MNOVA integrated peacks of Chitosan-MAA-Nicotine-Phenylalanine 4:1 @ 30^{O}C H'NMR spectra.

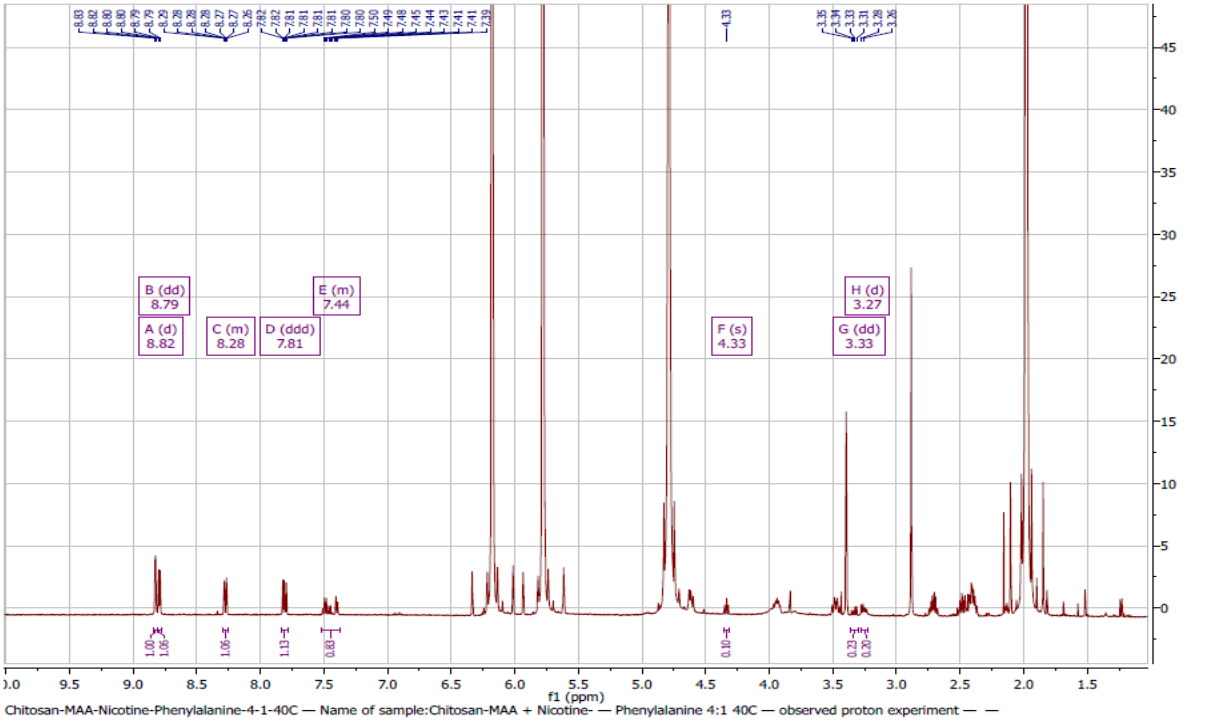

Figure 4.15: MNOVA integrated peacks of Chitosan-MAA-Nicotine-Phenylalanine 4:1 @ 40^{O}C H'NMR spectra.

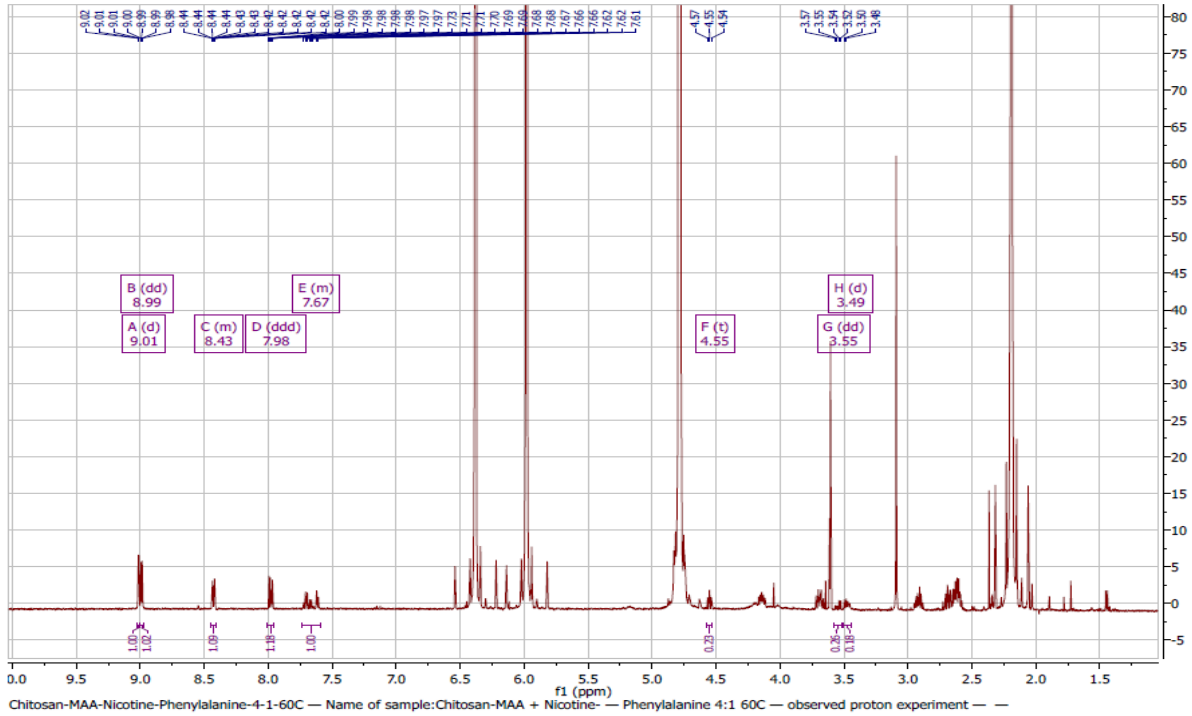

Figure 4.16: MNOVA integrated peacks of Chitosan-MAA-Nicotine-Phenylalanine 4:1 @ 60^{O}C H'NMR spectra.

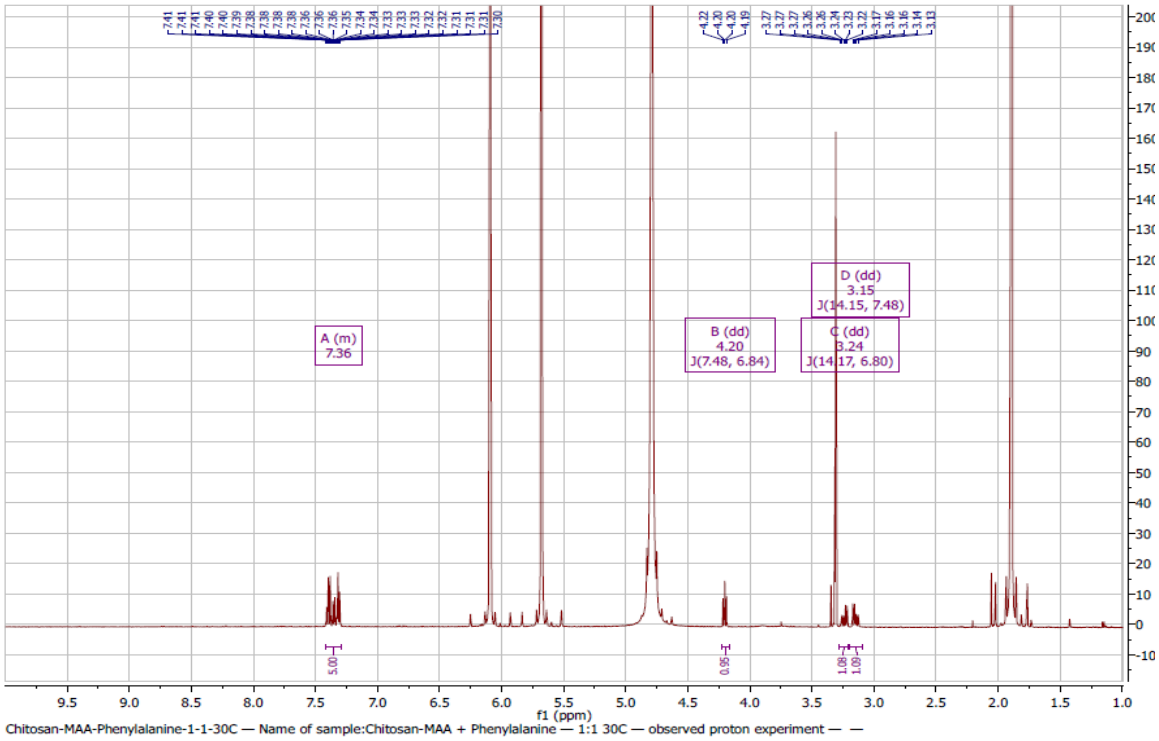

Figure 4.17: MNOVA integrated peacks of Chitosan-MAA-Phenylalanine 1:1 @ 30^{O}C H'NMR spectra.

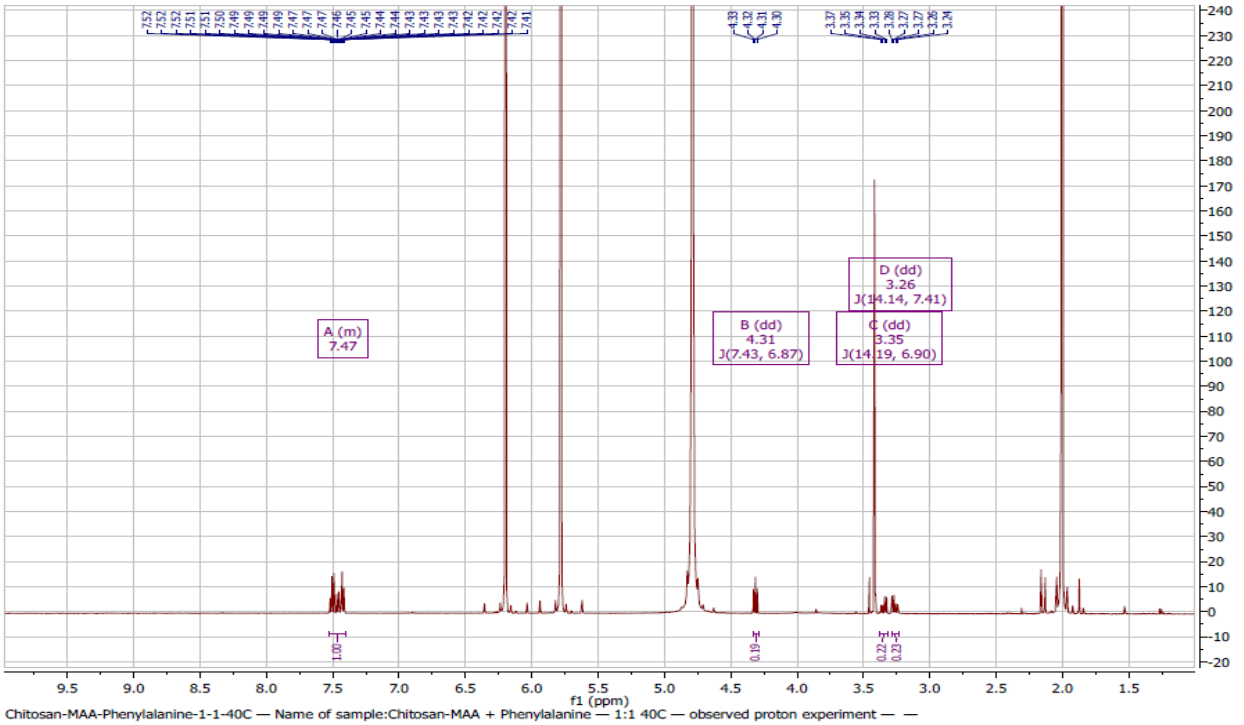

Figure 4.18: MNOVA integrated peacks of Chitosan-MAA-Phenylalanine 1:1 @ 40^{O}C H'NMR spectra.

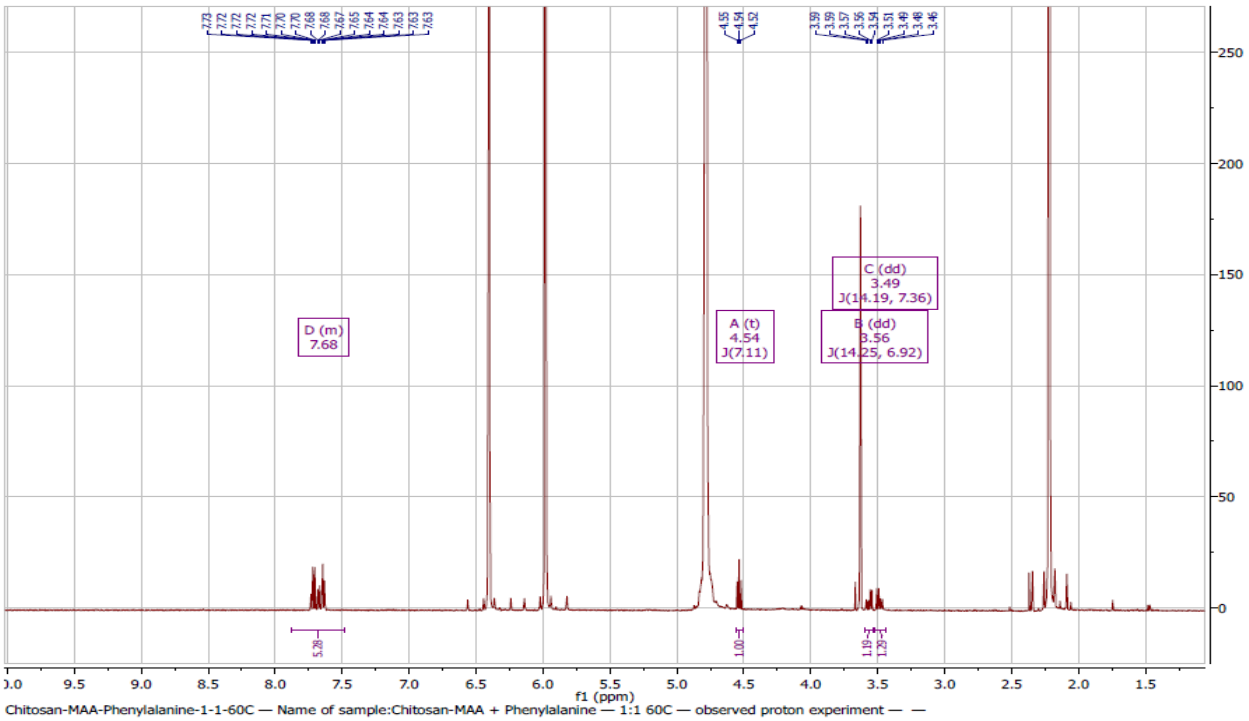

Figure 4.19: MNOVA integrated peacks of Chitosan-MAA-Phenylalanine 1:1 @ 60^{O}C H'NMR spectra.

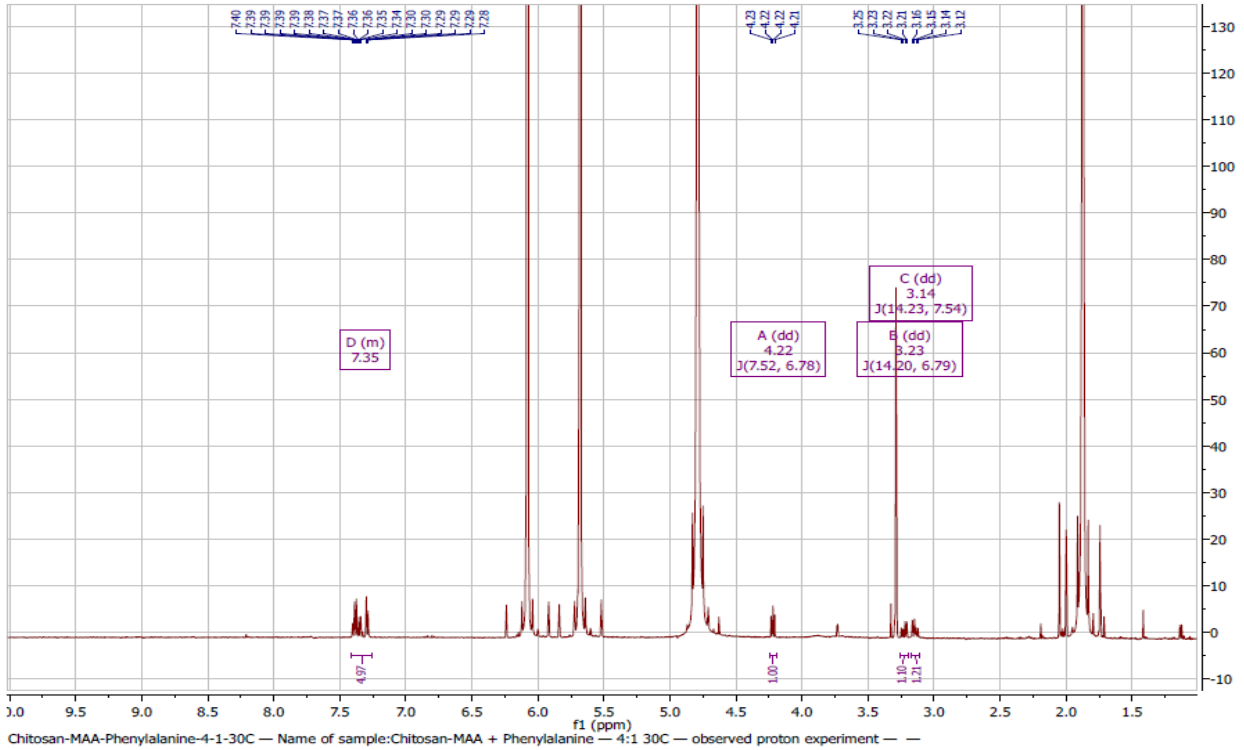

Figure 4.20: MNOVA integrated peacks of Chitosan-MAA-Phenylalanine 4:1 @ 30^{O}C H'NMR spectra.

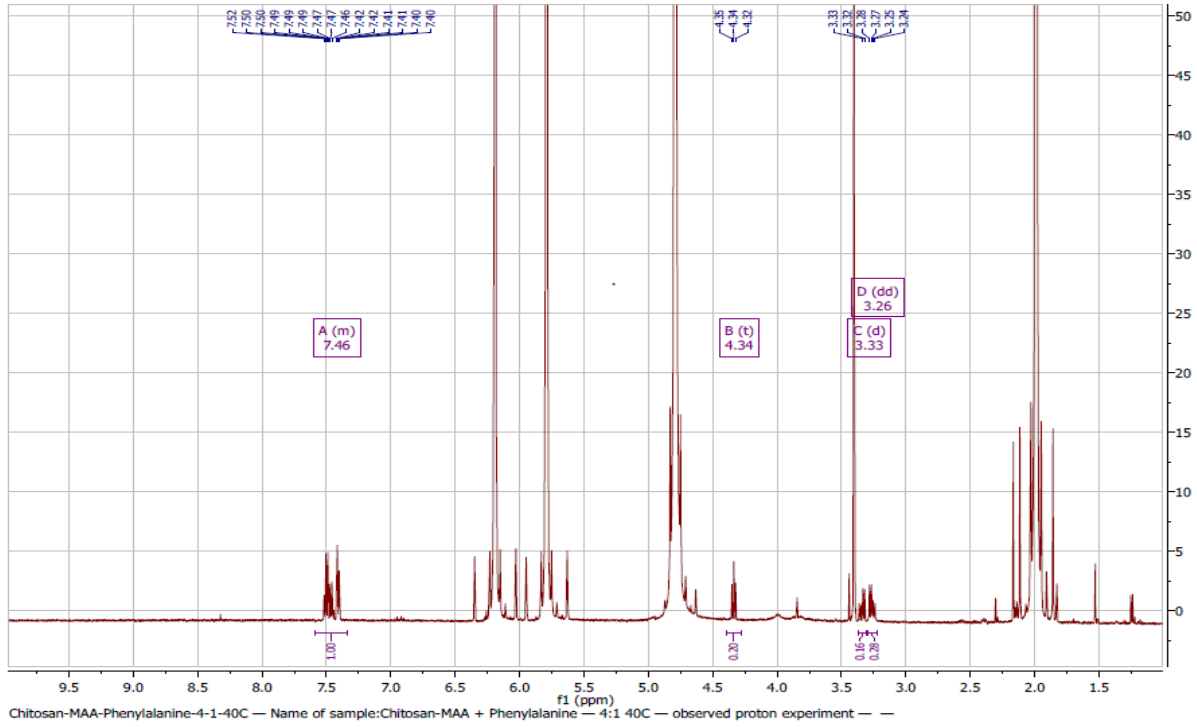

Figure 4.21: MNOVA integrated peacks of Chitosan-MAA-Phenylalanine 4:1 @ 40^{O}C H'NMR spectra.

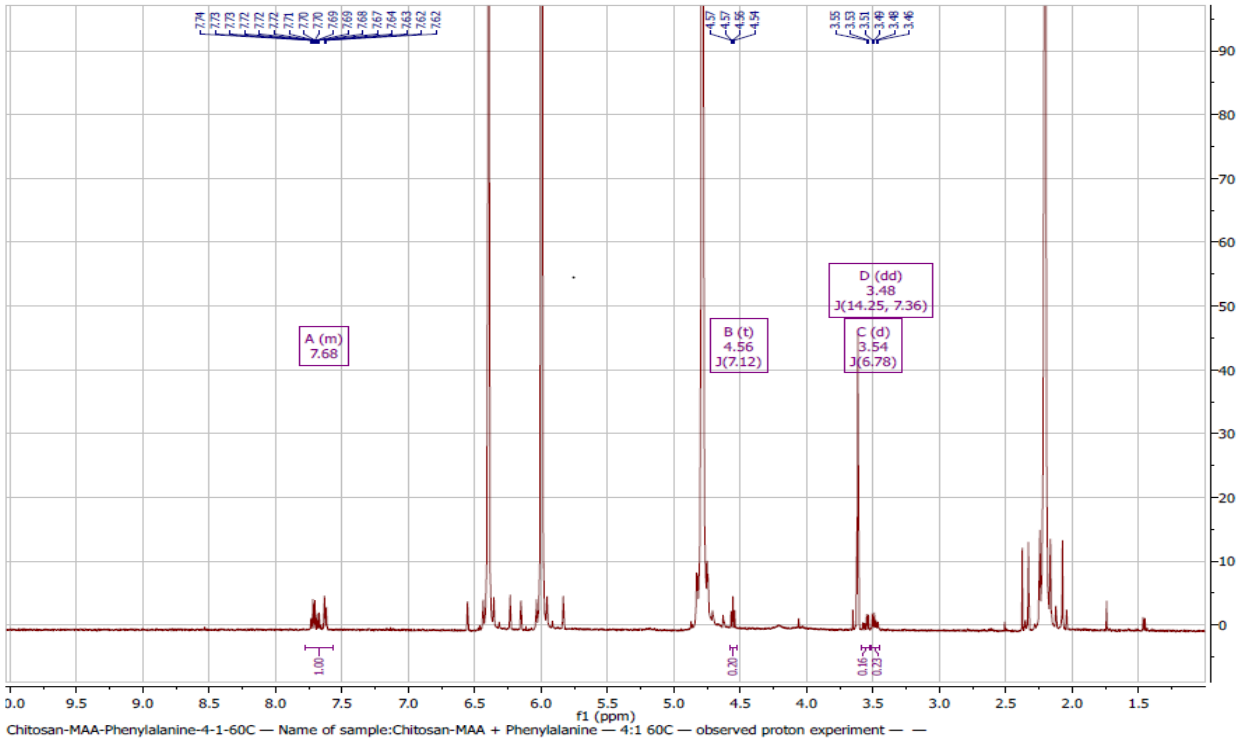

Figure 4.22: MNOVA integrated peacks of Chitosan-MAA-Phenylalanine 4:1 @ 60^{O}C ^{1}H'NMR spectra.

4.1.2 Discussion of the MNOVA integrated ^{1}H NMR titration.

From the results of the MNOVA integration (Figures 4.1 to 4.22), an increase in reaction temperature from 30^{o}C to 60^{o}C, showed progressive downfield shift in resonance of the protons in blends of 1:1 and 4:1 functional monomer: template. This shift is as a result of a deshielding effect on the protons adjacent/close to the nitrogen atoms in the templates. Similarly, the alkyl protons of the Phenylalanine template were affected. This influences the extent of interaction/binding with the amine hydrogen on the chitosan moiety. The single long range coupling constant of H-2 relative to H-4 and the large coupling constant of H-6 relative to H-5 (Whidby, Edwards and Pitner, 1979), in the Nicotine, distinguish the protons from each other when interpreted from the COSY spectrum. The deshielding effect allows a more pronounced and stronger grafting/copolymerization between the chitosan-methacryllic acid and the templates. The observed downfield shieft characterizes the hierarchical structural dimension of

the chitosan-methacryllic acid grafting which is in line with the report from Bundi and Wüthrich (1977).The overall downfield chemical shift occurring with increase in temperature and monomer concentration, created a more robust non covalent interaction and invariably supported the selection of the reaction temperature of 60^{o}C and a 4:1 stoichiometry for the entire Nicotine template experiment, which corroborates the deductions from Fu *et al.* (2015). A deviation is shown by the Phenylalanine template where the aromatic hydrogen of five (5) combined protons, presented the same chemical shift for both the 1:1 and 4:1 stoichiometries i.e. a homotopic proton status while the alkyl protons presented the 1:1 stoichiometry as the most deshielded but the proton adjacent the amine functionality presented the 4:1 stoichiometry as the most deshielded. The observed trend may be attributed to the prochiral planar presentations of the alkyl (CH_2) protons about the amine Nitrogen with consequent regioselective stereochemical influence of the Nitrogen on the protons. From the chemical shift results, the most possible sites of interactions for the templates are N-1, H-2 and H-6 positions for Nicotine while alkyl protons are more plausible for the Phenylalanine. This is because with the homotopic protons of the aromatic moiety, the configuration of the aromatic portion is kept constant. Therefore binding interactions that leads to replacement or changing of the functionality of the protons with different atom is favoured because it creates a chiral and stable center at the carbon atoms (MCAT study discussions, 2017). This is evidenced by the difference in resultant chemical shift between the alkyl protons which shows that they are chemically non equivalent and are diastereotropic protons. Table 4.3 – 4.5 presents the specific proton shifts from the interactions.

By implication, Figure 4.23 may be the possible structures for the functional monomer-template compounds:

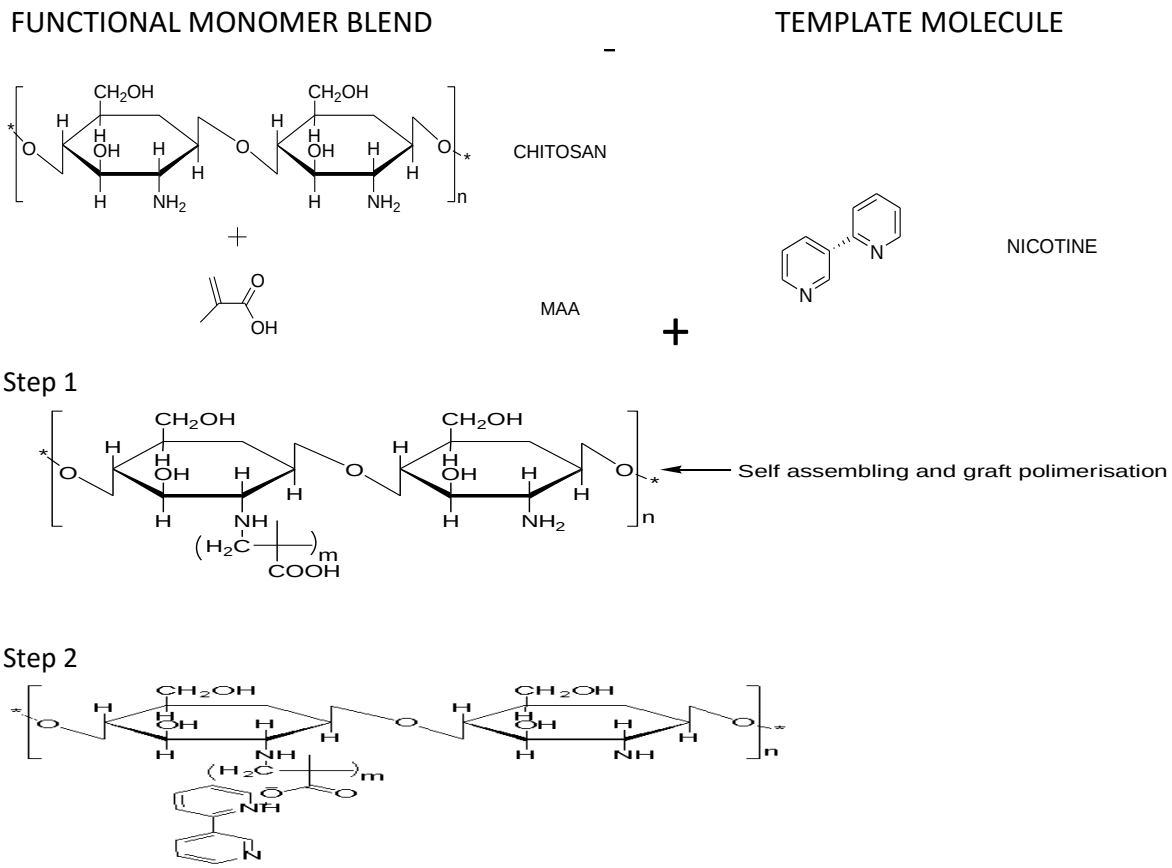

Figure 4.23: Schematic representation of the interacting functional groups and bonding between the functional monomers (Chitosan and Methacrylic acid) & templates (Nicotine, Phenylalanine & their blend).

Polymerization temperature affects the affinity and specificity of molecular imprinted polymers, both of which could be significantly improved by selecting a lower polymerization temperature. The optimum temperature with respect to polymer performance depends on the temperature used in polymer preparation. Thus, polymers synthesized at high temperature will perform better at higher temperature and similarly polymers prepared at low temperature perform better at low temperature. It was found that photo-initiated polymerization resulted in polymers with high degree of cross-linking and specificity (Chen *et al.,* 2014). This is also related to the lower temperature achieved during polymerization. Usually most studies used 60°C as the polymerization temperature. Where complexation is driven by hydrogen bonding, then lower polymerization temperatures are preferred, and under such circumstances, photochemically

active initiators may well be preferred as these can operate efficiently at low temperature. For example, Mosbach *et al* (1993),presented a study on enantioselectivity of L-Ph-NH-Ph imprinted polymers polymerized at 60°C, and 0°C The results showed that better selectivity is obtained at lower temperature versus the identical polymers thermally polymerized at 60°C. The postulate is on the basis of Le Chatelier's principle, which predicts that lower temperatures will drive the pre-polymer complex toward complex formation, thus increasing the number and possibly the quality of the binding sites formed (Mahony *et al.,* 2005).

4.2. Quartz Crystal Microbalance experiment's results (proof-of-concept experiment).

4.2.1 Experimental outputs that guided the parameters used in the QCM experiment.

Preliminary trials of various instrumental conditions and process were carried out in order to obtain best reaction conditions and reactancts' properties for best experimental outputs. These trials are:

4.2.1.1 Chip and monomer concentration selection.

Respective vibrational frequencies were obtained for quartz crystal chips in order to select the best chip and polymer blend with respect to amount of chitosan that will be required for the experiment. A plot of the frequencies over time that is required to equilibrate the adsorption and rebinding experiment was ploted as shown in Figure 4.24.

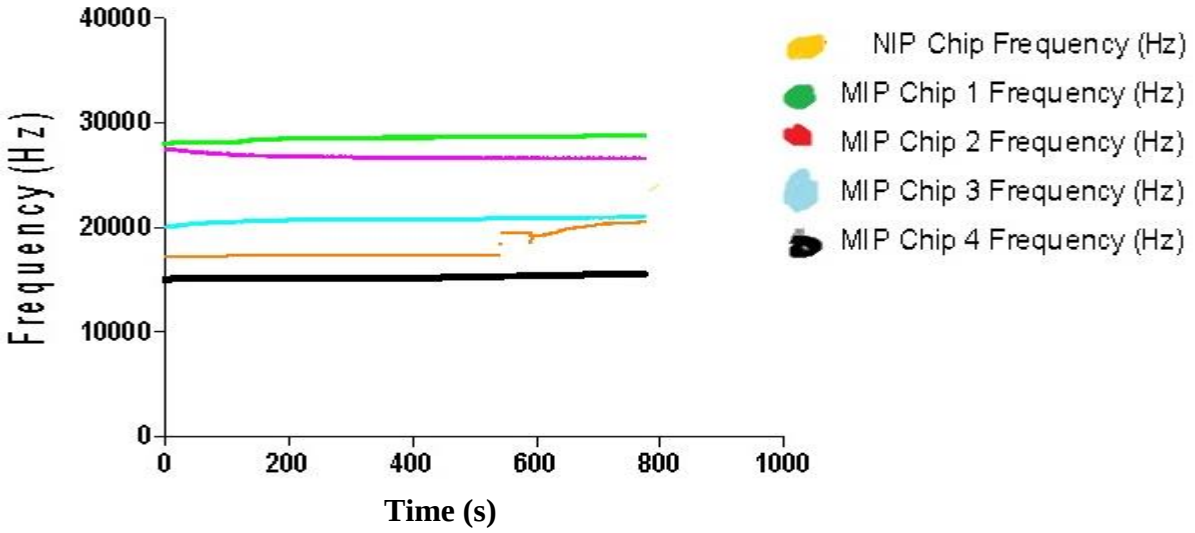

Figure 4.24: Graph of vibrational frequency against time of polymer film coated Chips.

Ignoring the effect of area, Figure 4.24 shows that polymer mass-density increase relates directly to increase in film thickness and inversely to frequency value (Coates, 2000; and Erbahar *et al.*, 2014), and the MIP 1 had higher frequency values than the NIP. Here, the order of magnitude of the frequency follows thus: 1> NIP >3>2> 4. From Figure 4.24, a non-zero residual frequency was obtained considering that, at equilibrium and subsequent injections of rebinding solutions at different concentrations, the difference in frequency (residual frequency) did not give a zero value. This is in agreement with result obtained by (Sha *et al.*, 2014). The implication is that there was a permanent material deposition on the resonators which confirms a successful polymerization which established and template specific cavities. This result guided the selection of chip no 3 with MIP formulation containing 0.04mmol of Chitosan (Table 3.1), because it presented a middle cuase in quantity of Chitosan desired to prevent excess mass deposition. This is also supported by the result from figure 4.25 since the relative frequency values of the MIPs were higher than that of the NIP when chip 3 was used for sensor analysis, which is indicative of the difference in mass-density and the imprinting of the templates in the MIPs.

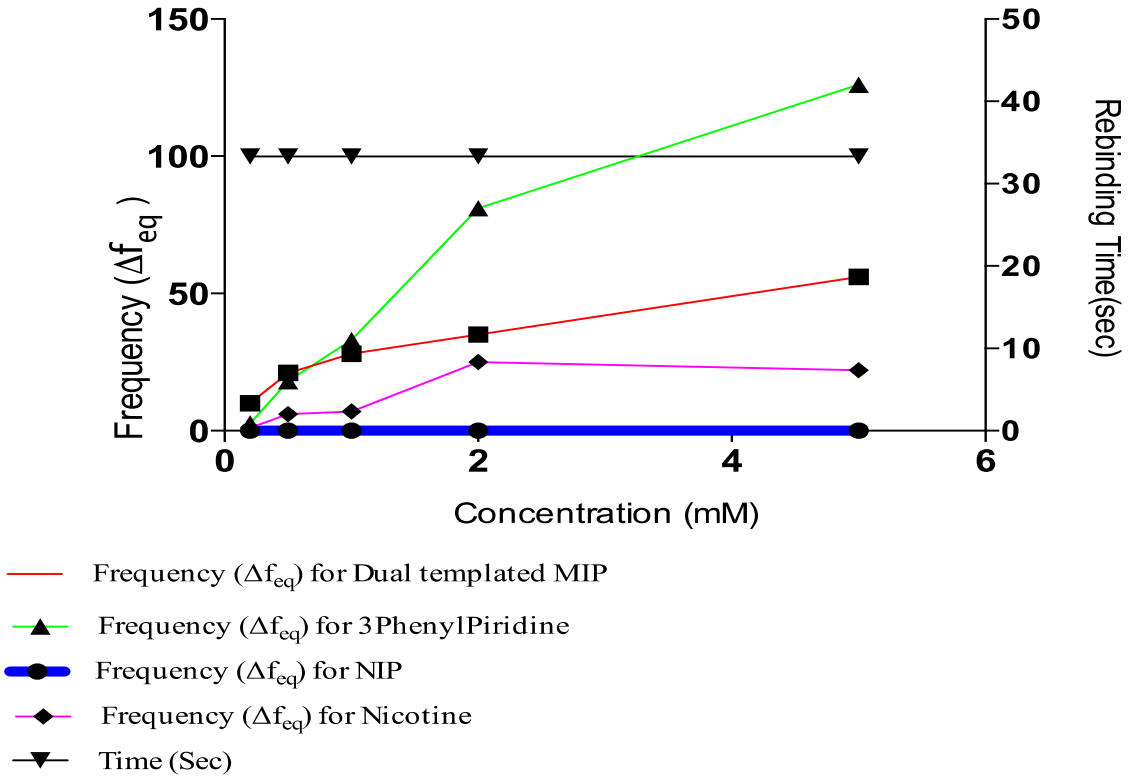

Figure 4.25: Comparative plot of concentration, rebinding time and resonant frequency using chip no 3

4.2.1.2 Most suitable blend formulation.

The residual frequencies for all samples were significantly higher than that of the NIP, which is expected. Interestingly, the frequency value for the blend of template occurred in-between the respective frequencies of individual templates with that of Nicotine being lower than the blend and that of 3-PhenylPiridine positioned above that of the blend. At lower concentrations specifically 0.5mM, the frequencies of both 3-PhenylPiridine and that of the blend template were approximately the same. This implies that at lower concentrations of detections it may be a little bit difficult to specifically identify 3-PhenylPiridine in a mixture of close analogues while that of Nicotine distinctly stands out. Longer rebinding time is also required for detection of 3-PhenylPiridine as shown from the plot (Figure 4.26). All other detections were made within the

time frame of 99sec except for the highest concentration of 3-PhenylPiridine-template sample, which was done at a much higher detection period. Over all, detections of chitosan based Nicotine and its analogue template as well as blend of them can be made using the QCM resonator at micro trace levels despite the hydrophilic character of Chitosan, which prompts its swelling and astronomical increase in mass density during sensing.

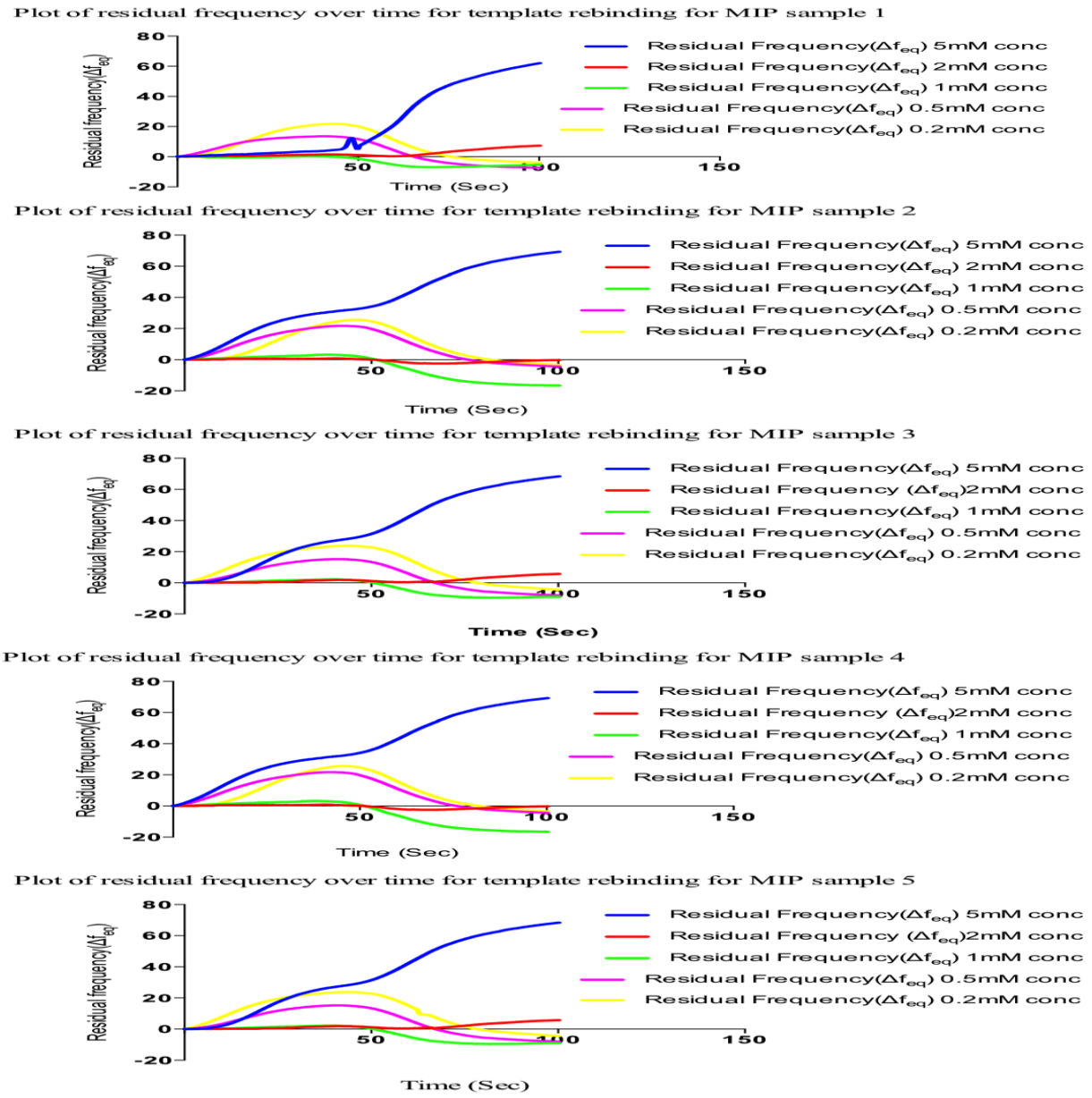

Figure 4.26: Residual frequency rates of MIP thin films coated on QCM resonator.

The results from Figure 4.26, demonstrated the potential of Chitosan MIP thin film as surface sensor material. The best blend formulation appears to be the one containing 0.02g of Chitosan (Table 3.1), and this formulation was used in the synthesis of the dual-template MIP thin film.

4.2.2 Selectivity of sensogram.

The Sensogram study was done using a Phosphate buffer solution (PBS) at a pH of 7.4 and rebinding template solutions of concentrations of 5mM, 2mM, 1mM, 0.5mM, 0.2mM and 0.1mM contained in the PBS carrier solution. Attana 100 QCM machine was used for the flow injection analysis (FIA) at a temperature of $22^{O}C$, flow rate of 25, time scale of 50mins, frequency scale of 100Hz. A frequency offset of 0.0 and injection volume of 100micolitter and 2cycle injections; was operated at for the rebinding study Figure 4.27, shows the Sensogram chart of the rebinding study with three repeat cycles.

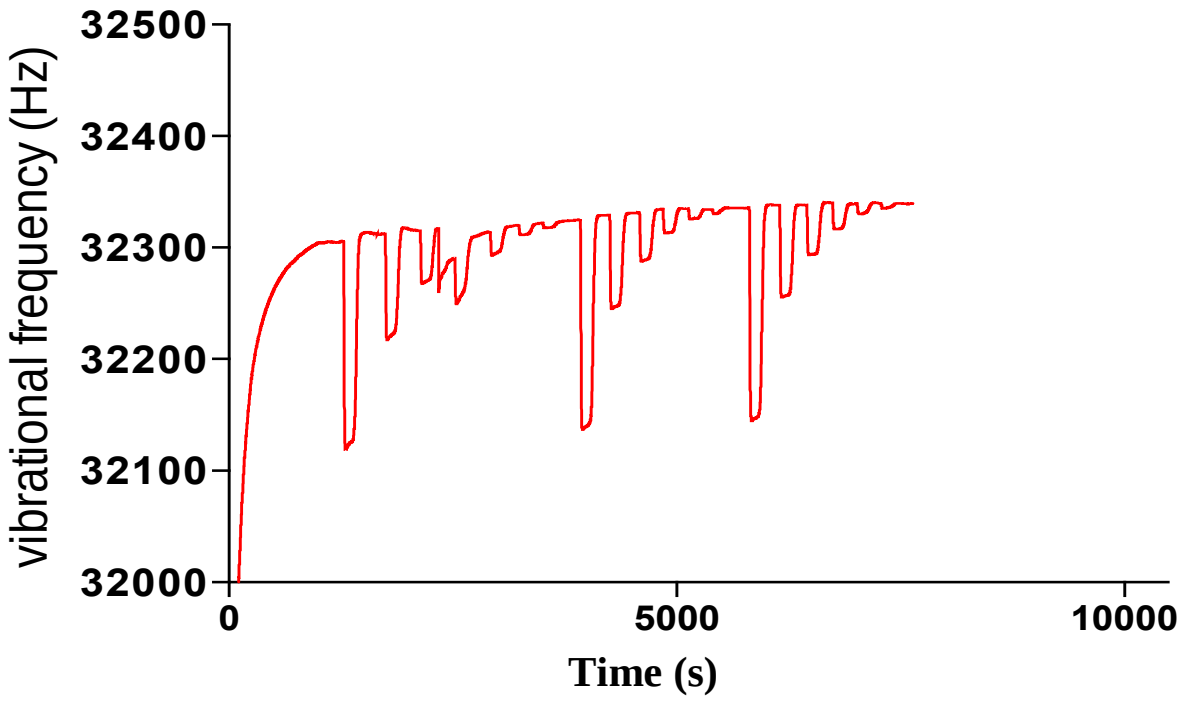

Figure 4.27: Template rebinding Sensogram of synthesized Chitosan-Nicotine-3PhenylPiridine MIP.(3 repeat cycles for 6 different concentrations).

The Sensogram shows the ability of the fabricated MIP thin film to reproducibly bind the template material contained in the carrier medium without significant alterations in repeat cycles. Changes in resonance vibrational frequency (Hz) and dissipation were detected upon injection of the template containing solutions. The changes as presented by the value of the length of the inverted peaks are in direct relationship with the concentrations used. The reproduced partern from the three cycle application, is an indication that the MIP is constituted of rigid and template-sensitive cavities as earlier reported by in the Another insight was evident when the concentration of the carrier medium was altered indicative of the electrostatic influence of a carrier medium on the effective binding of templates by MIP samples (Kanazawa and Cho, 2009). As is shown in figure 4.28, in a 1:10 dilution, the rebinding sensitivity took a reverse sequence, with the highest concentration of 5mM giving the least vibrational frequency value and the least concentration of 0.1mM giving the highest vibrational frequency value.

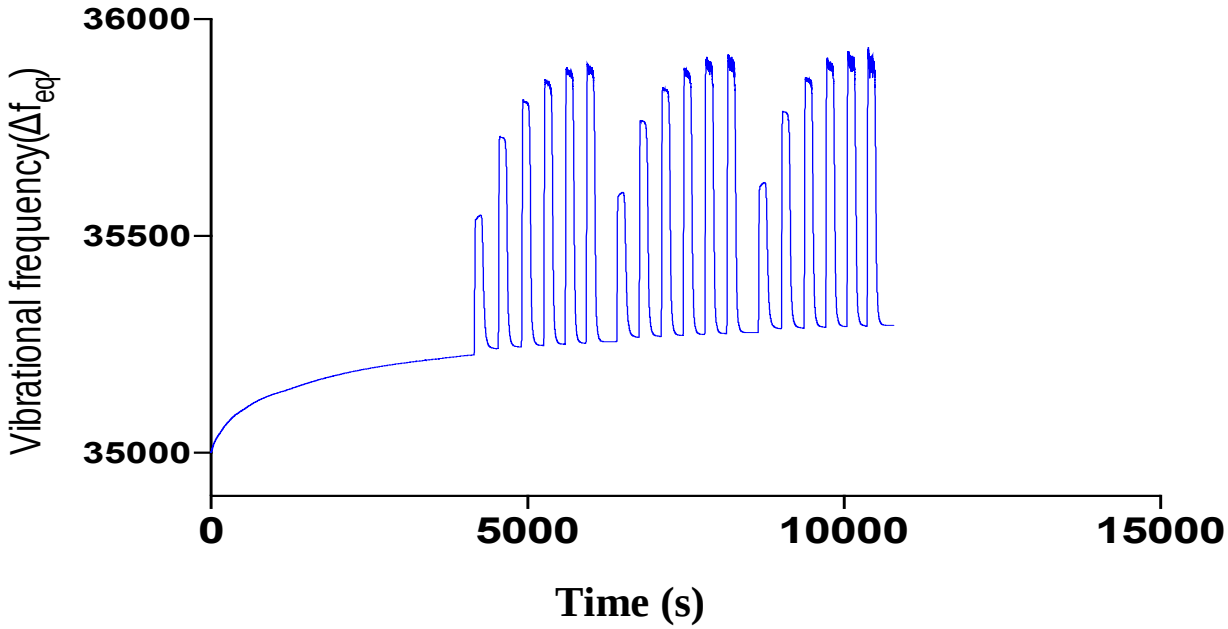

Figure 4.28: Effect of change in conc. of solvent (1:10 dil), on the vibrational frequency of MIP films.

This shows the plausible steric hindrance or electrostatic effect due to ionic concentration, on the effective binding of template molecules within the cavity of the polymer matrix. This is suggestive of the fact that this architecture may possibly be used in a reverse separation process when the concentration of the carrier fluid is altered while keeping the concentration(s) of the templates constant.

The polymer film prepared without the template molecules or the non-imprinted polymer (NIP) figure 4.29 shows that the rebinding by the MIP was actually due to imprinting of the templates, because it failed to rebind significantly with the non-templated material as is shown in the Sensogram figure 4.29.

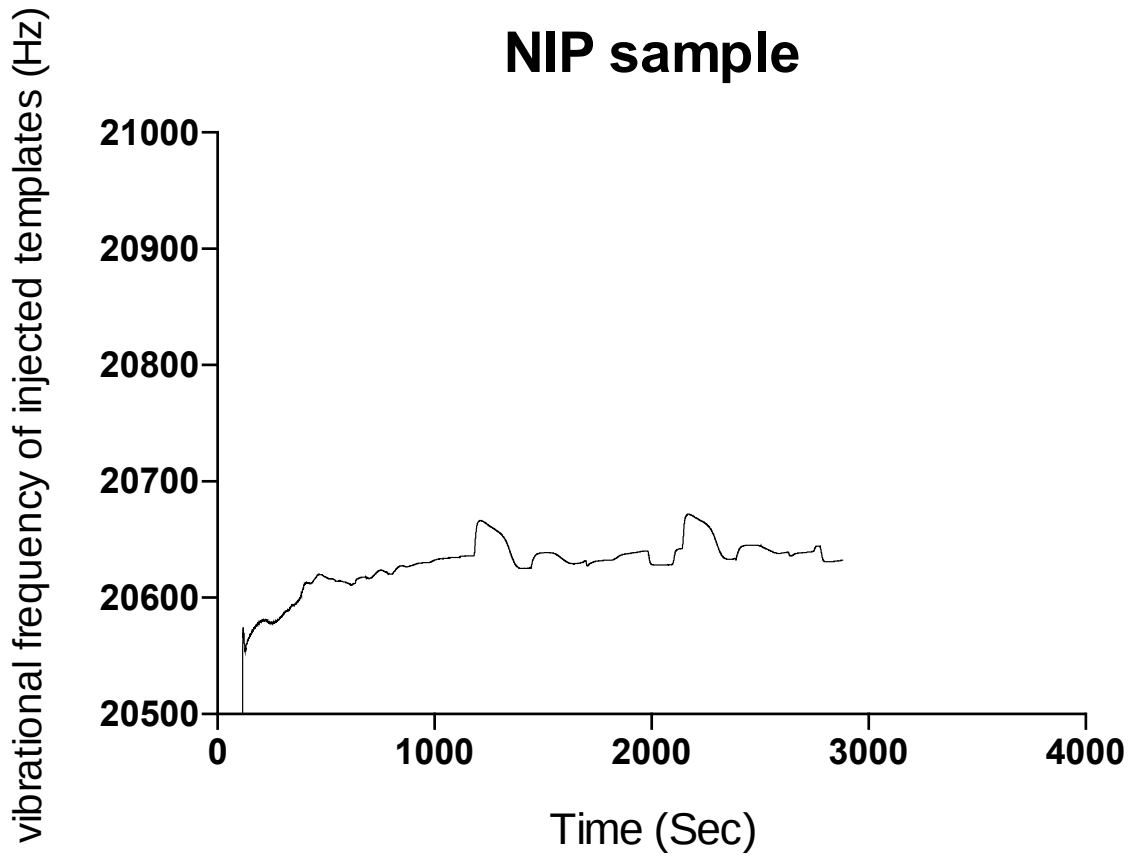

Figure 4.29: Sensogram of non-rebinding activity of NIP sample from the fluid injection analysis.

4.2.3 Preferential Selectivity and Sensitivity of Sensogram

A selectivity and sensitivity study of the MIP was carried out using Nicotine, PhenylPiridine, Caffeine and Phenylalanine amide as template molecules alongside the blend template system. The choice of the compounds is due to their closely related structural and physicochemical properties particularly for Caffeine. Nicotine and PhenylPiridine were used to confirm the relative sensitivity of the MIP material in the presence of only one of the blend components and possible change in preference in the presence of the two but in different concentrations. Their individual molar masses are also closely valued and this tries to rule out the possibility of the effect of size or steric preference. Figure 4.30, shows the selectivity of the MIP for Nicotine less than 3PhenylPiridine, which is less than the blend template sample. This shows the selectivity and sensitivity of the MIP even in the presence of closely related analogues either singly or combined. This sensitivity is further confirmed by the non-binding of the Caffeine and the reverse slight adsorption of the Phenylalanine amide molecule in figure 4.30.

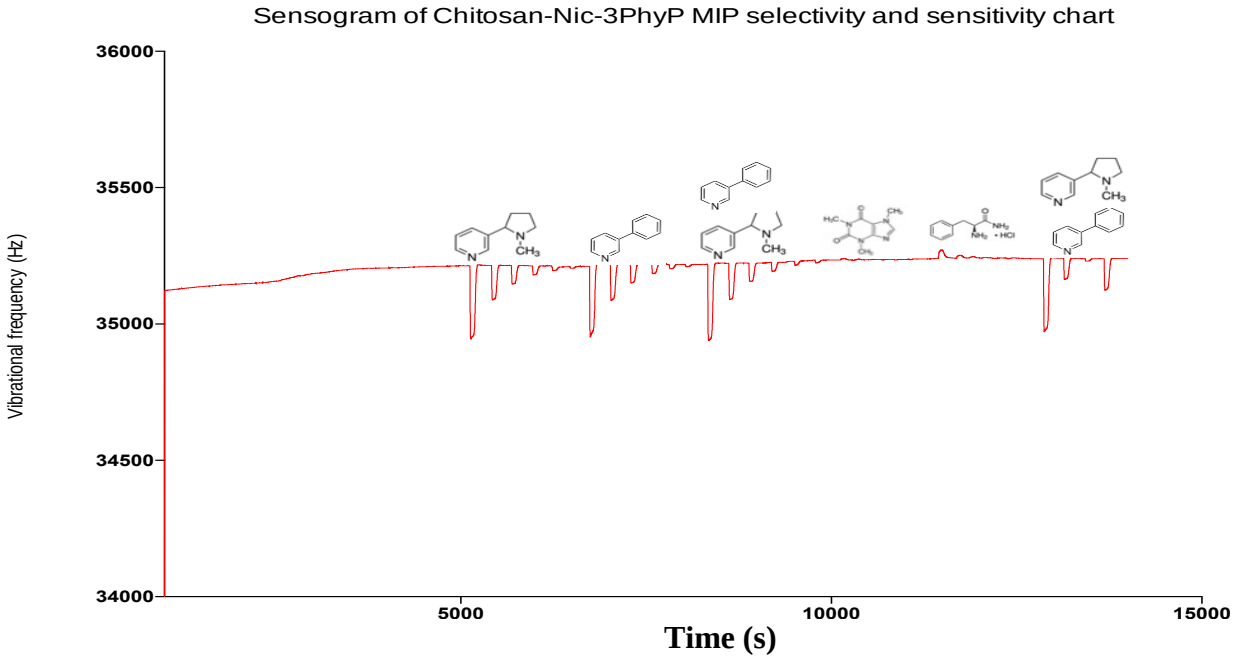

Figure 4.30: Selectivity and sensitivity Sensogram of Nicotine-3PhenylPiridine Chitosan based MIP.

A plot of the residual frequency against concentration of the templates (5Mm - 0.1mM), shows the selectivity and sensitivity potential of the MIP in the presence of the templates, Figure 4.31.The templates employed in the fabrication of the MIPs were identified and selected in the course of the rebinding experiment while the closely related materials, caffeine and phenylalanine amide were not selected and adsorped. This attests to the sensitivity and selectivity of the MIPs and this result concurs with results of similar experiments carried out by other researchers, (Rodahl and Kasemo, 1996; Lu and Xu, 2017; Farrington, Magner and Regan, 2006; Prasad, *et al.*, 2010 ;). It is also evidenced that the fabricated MIPs maintained their sensitivity and selectivity even after coming in contact with templates that were made for (last three structures in Figure 4.30). After the rebinding with caffeine and phenylalanine amide, on introduction of the blend template of Nicotine and 3PhenylPiridine, the Sensogram recorded similar rebinding trend with the initial blend template result (the third set of peaks on the Sensogram).

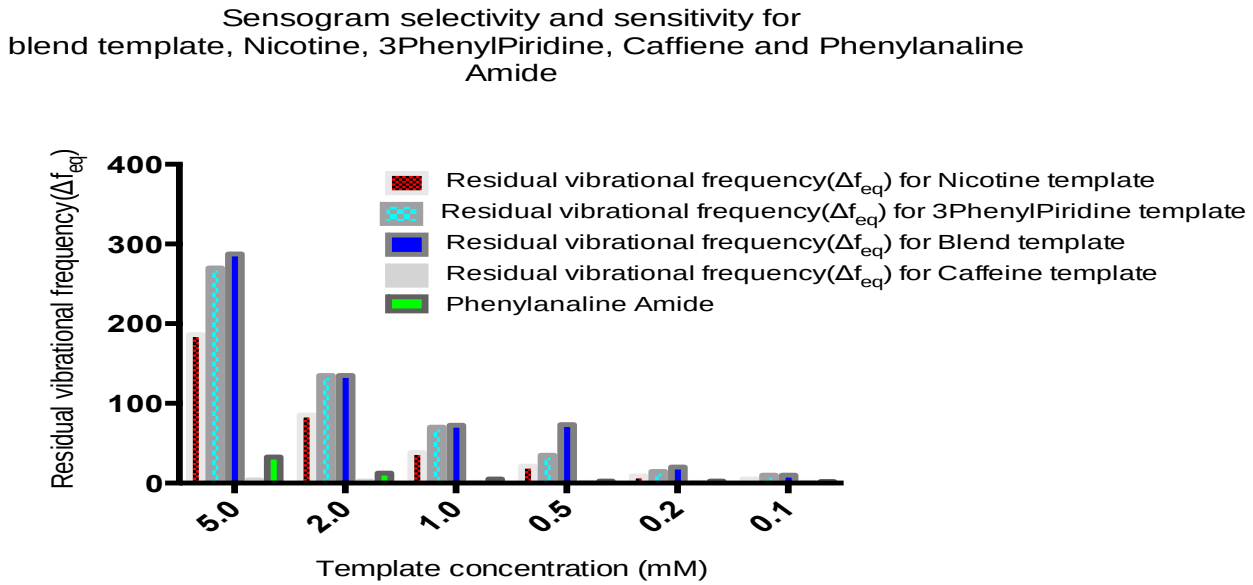

Figure 4.31: Sensitivity and selectivity of Nicotine-3PhenylPiridine Chitosan based MIP.

The plot shows the clear selectivity of the MIP in adsorption of different templates from an environment where different template materials are present. The MIPs adsorped templates in a direct relationship to their concentration, the residual vibrational frequencies increased in response to the templates' concentration. This is in agreement with earlier works by Marx (2003) Further characterization was done to support the above findings and these include temperature dependent changes as well as the earlier mentioned analysis.

4.3 FTIR spectroscopy from QCM experiment

The FTIR spectra of MIP samples show all components of the polymer blend, which may be composed of similar functional groups particularly:- OH, CH_2, CH_3, NH_2. Similar peaks are observed from the spectra of both the NIP and very significantly with the MIPs. But differences are shown from the relative intensities of transmittance as is shown in Figure 4.32.

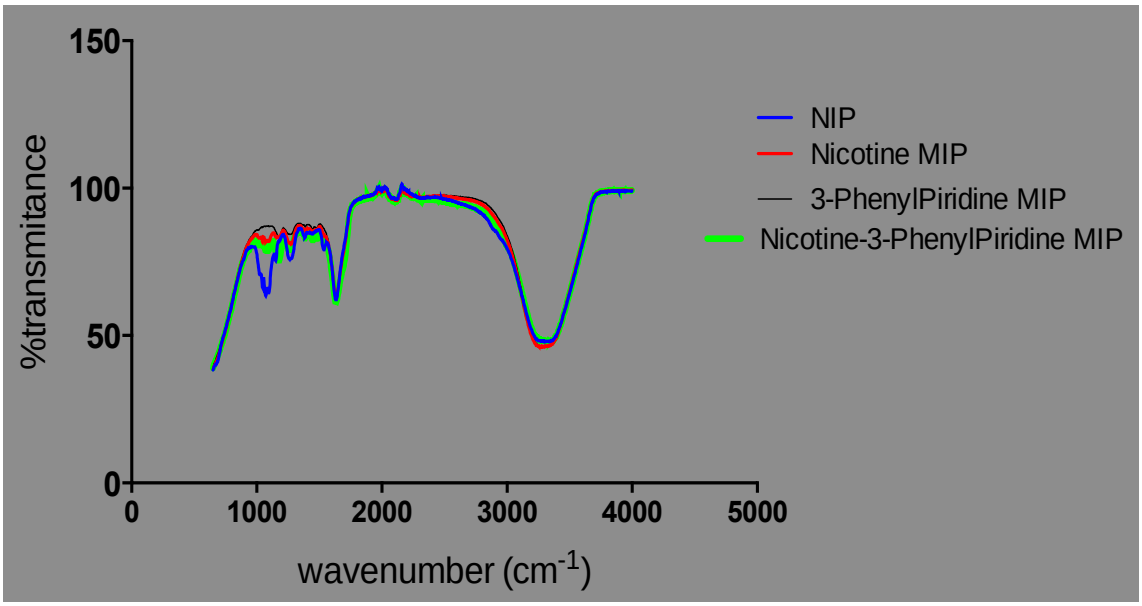

Figure 4.32: plot of transmittances against % intensities for MIPs and NIP

The observed overlaps, disappearances and visibilities occur as a result of the cross-linking and graft/copolymerization processes. The characteristic peak of chitosan, which is within an average of 1555.2 cm^{-1}, is observed in all the samples but with differing percentages of transmittances,

Figure 4.33. These are peaks within 1550s cm^{-1}. The value for sample MIP3 is the least with an average of 83.4 while sample MIP2 has 85.3, sample MIP4 having 91.6 and samples MIP5 and MIP1 with 94.2 and 95.3 respectively. The differences in percent transmittances are indicative of the degree of polymerization that occurred with individual sample components. The lower the value of transmitance, the better the degree of polymerization.

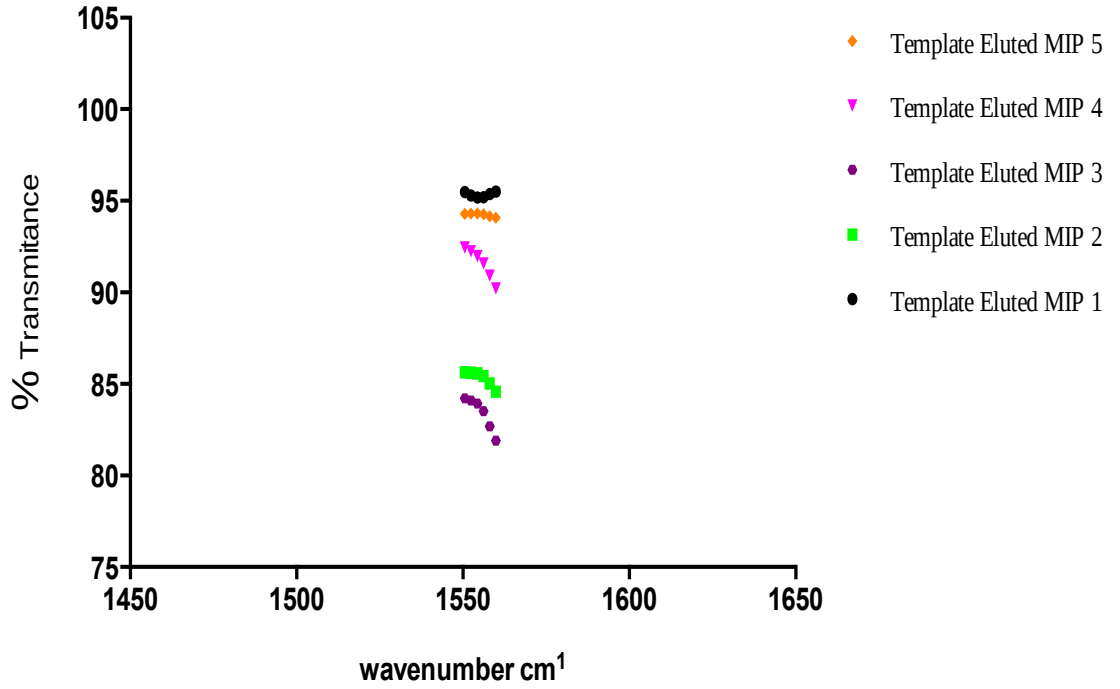

Figure 4.33: Characteristic peak of chitosan (1550 cm^1 range) intensities for eluted samples

This tallies with the quantities of Chitosan added to the individual sample blends except for the observed shift in correlation between samples 3 and adjacent sample 4 which may be interpreted as due to the relative degree of grafting that occurred with sample 3, resulting to a reduced degree in intensity of the characteristic peak of chitosan present. This may be indicative of the blend with optimal grafting and crosslinking in the synthesis of the MIP. A further confirmation is observed with the relative degree of intensities with the characteristic peak of the C-N functionality. The sole presence of characteristic strong and broad band peak ranges from 3200-

3700 cm^{-1}, which are the extension vibration of the N-H functionality and the O-H vibrational stretching of ungrafted or uncross-linked Chitosan molecule. This presents support for the cross-linked grafting of the Chitosan and Methacrylic acid in the presence of 1,4-Bis (Acryloyl) piperazine (BAP) or anyother cross linker. It is observed that there is a shift towards the asymmetric and symmetric $–CH_2$ functionality is evidenced in Figure 4.34, with increased prominence of peaks within the range of 2920s and 2869s (Brugnerotto *et al.*, 2001).

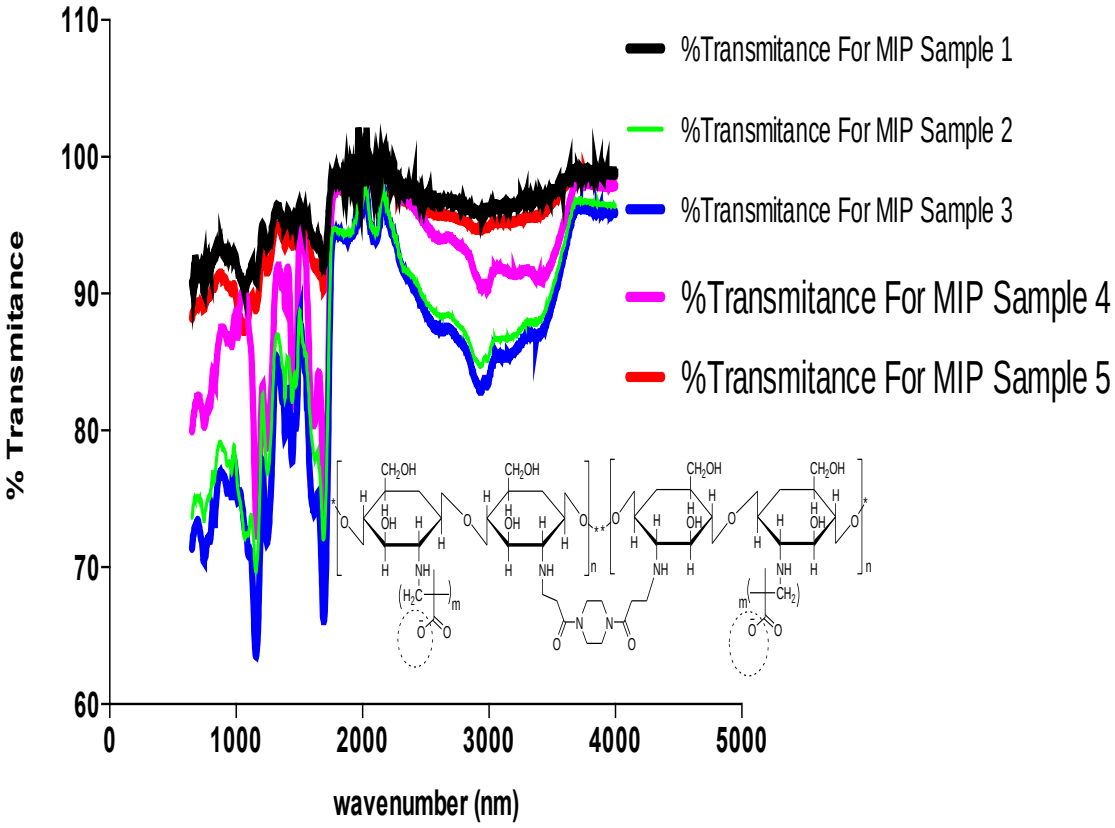

Figure 4.34: Spectra chart of template-eluted MIP samples.

From the FTIR spectra of the template eluted MIP samples (Figure 4.34), the prominent peaks are as shown in Table 4.4 and the representative functional groups are likewise identified.

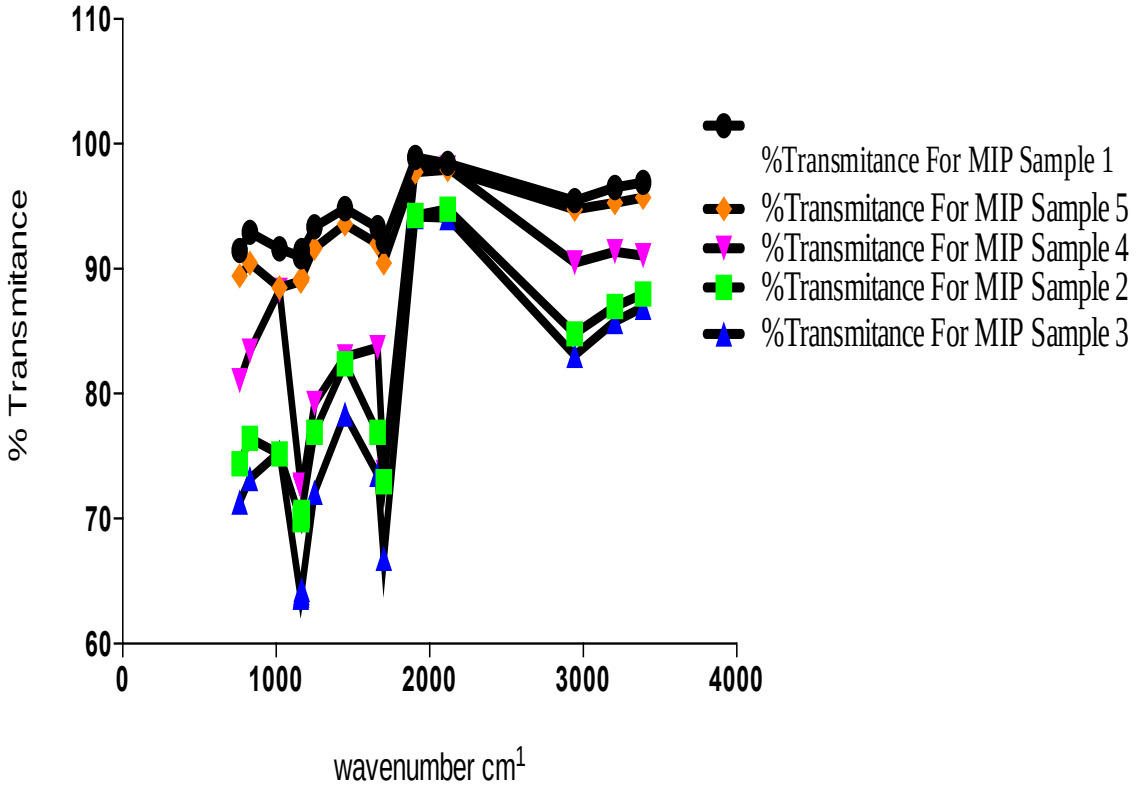

Figure 4.35: Plot of transmittance against wavenumbers of prominent peaks of MIP samples.

The individual plot of % transmittance against the wave number for Chitosan, MAA and BAP, depicts their characteristic assignments as displayed on the graph (Figure 4.35). Overlap in transmittances occurring at wavenumbers, 954.19,1695.94, 1293.39, 1435.03, 2174.9 and 3073.13cm.$^{-1}$ Chitosan's characteristic peak at 3328.51 and MAA's peaks at 2963.23, 2817.87, 2629.64 and 946.74cm^{-1} on cross-linking with BAP (Figures 4.36 and 4.37), gave a cross-linked matrix with distinct peaks at 1110.75(confirmatory secondary alcohol C-O stretch), 1298.98(primary or secondary OH in-plane bending), 1470.43(carboxylate functionality from carboxylic acid of MAA after cross-linking with Chitosan in the presence of BAP), 1649.35(primary amine N-H bend), 2126.45 and 3324.79cm^{-1}(normal polymeric OH stretch and N-H stretch of primary amine) .

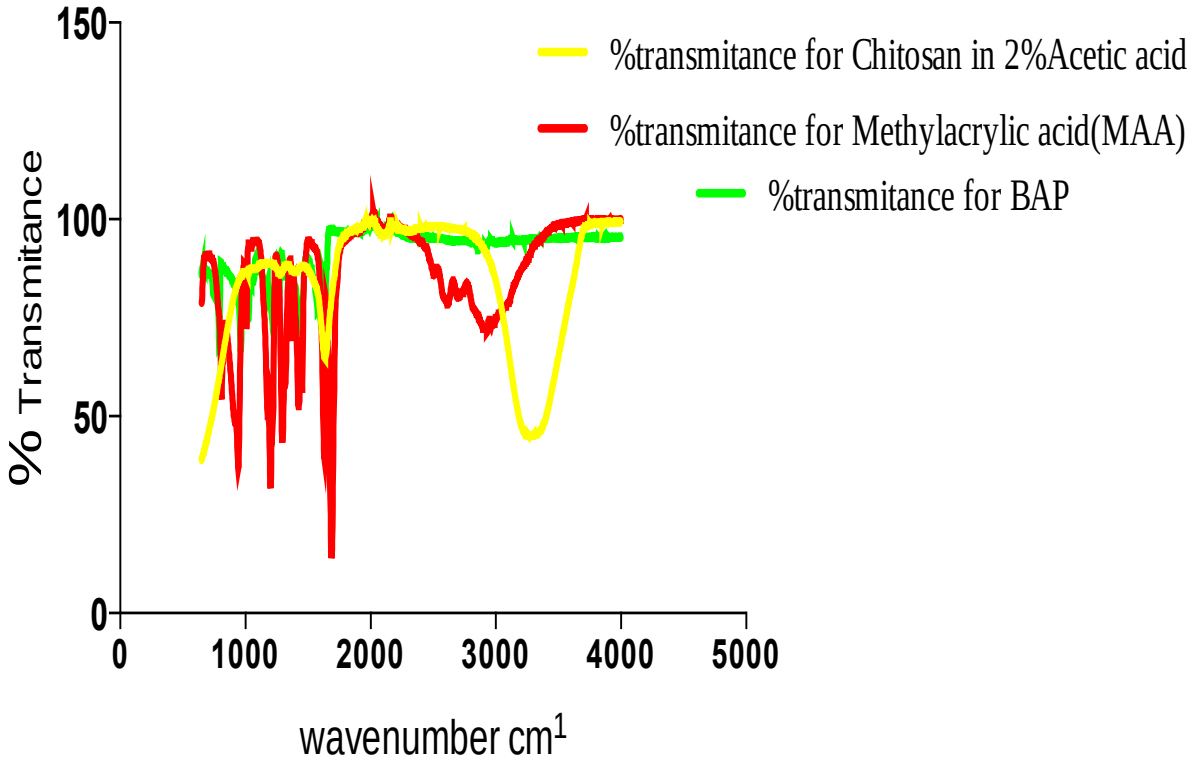

Figure 4.36: An overlay of spectra of Chitosan, MAA and BAP.

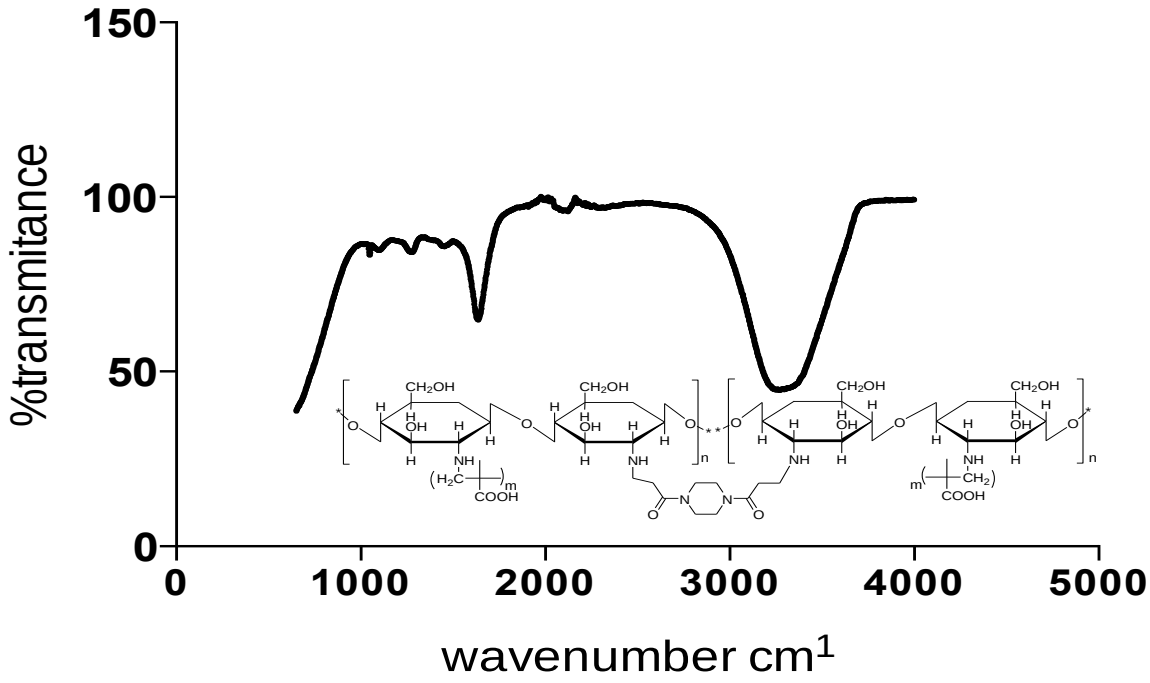

Figure 4.37: Plot of transmittance against wavenumber of Chitosan, MAA and BAP.

Table 4.6: Observed peaks contained in MIP samples and the representative functional groups.

Characteristic Peacks (cm^{-1})	Characteristic Functional Group
762.2410	**N-H** wagging due to shift on the bonding.
829.3330	**N-H** wagging due to shift on the bonding
1023.1500	Medium intensity observed with MIP sample 3 and this is indicative of **C-N** functionality. The strong intensity observed with the rest MIPs is indicative of **N-H** assignment. This relates to the degree of amide group interaction in the Chitosan molecule.
1161.0700	**C-N** Tertiary amine stretching assignments. This supports the crosslinking of the Chitosan and the MAA with the BAP.
1162.9300	
1164.7900	
1166.6600	
1250.5200	**C-N** assignment
1448.0700	α-CH_2 bending assignment occurring as a result of **CH_2** and **CH_3** deformation
1662.3900	**C=O** of Amide bond
1701.5300	
1906.5300	**C=C** asymmetric stretch
2118.9900	**-N=C=O** medium intensity assignment
2944.6000	Multiple peak assignments due to overlap of **C-H** of carboxylic acid, resulting in a broad **O-H** assignment. The observed intensity at range 2690-2840, is complementary C-**O-H** functionality.
3207.3700	

4.4 Ultra violet-visible spectroscopic result from QCM experiment

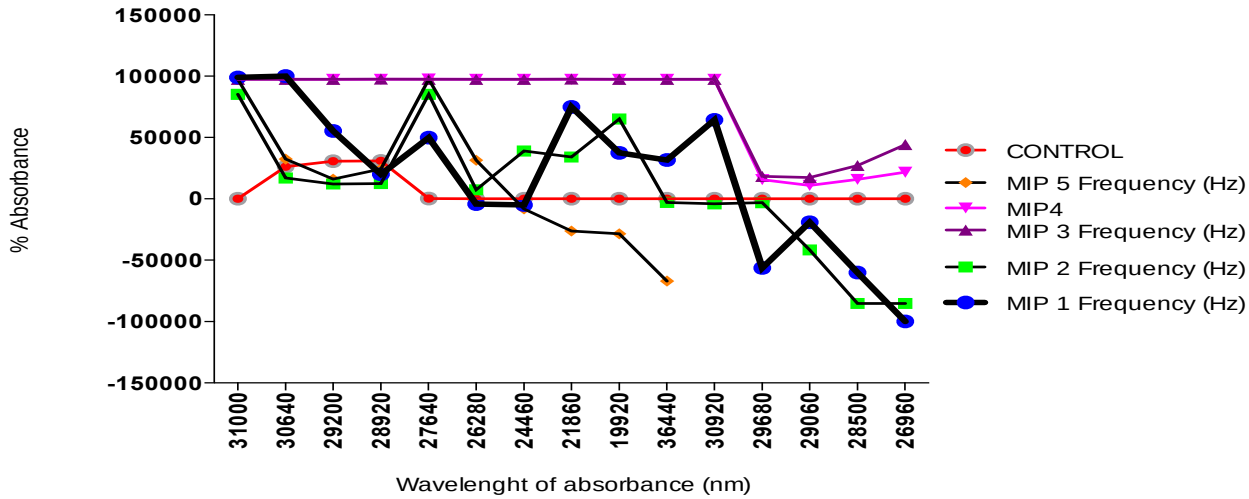

Figure 4.38: UV-VIS graph of wavelength vs % absorbance for MIPs and a control sample (NIP).

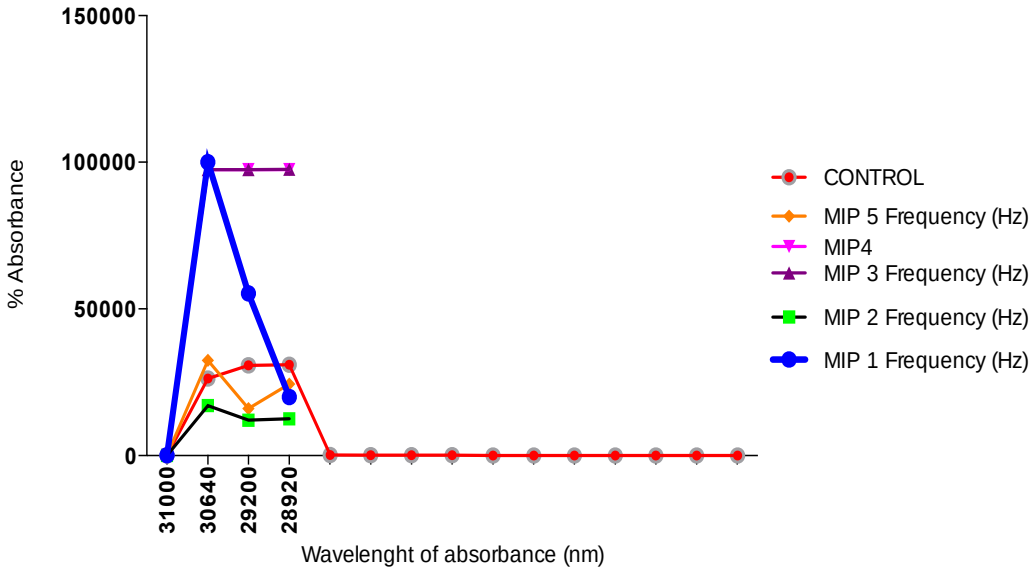

Figure 4.39: Extraction of the wavelength maxima for control and MIP samples.

Plotting the data from the UV-VIS analysis of the rebinding experiments, it was observed that the template materials and other substances were extracted during the soxhlet extraction process (Figure 4.38). Nonetheless, the wavelength maxima obtained from the control sample; show that the templates gave three wavelength maxima at 306nm, 292nm and 289.2nm. Figure 4.39, shows that apart from the NIP, MIP samples all have their lambda max at around 306nm though the percent absorbances differed from sample to sample. Generally, all five samples gave satisfactory rebinding results from the % absorbance values of more than 20 relative to that of the control (NIP). This further supports the results from the QCM analysis of the polymer films.

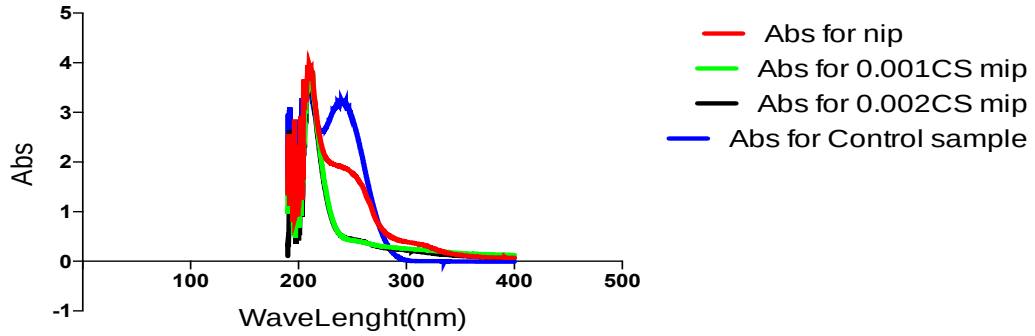

Figure 4.40: UV-VIS rebinding study for the dual template MIP and NIP samples.

The graph, Figure 4.40, shows the relative residual absorbance for the NIP and MIP as against the blend template in Phosphate buffer of pH 7.4. It is observed that due to the blending and interaction with the polymer matrices, the template molecule with initial dual peak absorbance converged to only one significant peak with reduced absorbance maxima. This phenomenon is observed to also occur with the NIP but at a much-reduced level considering the existence of dual peak spectra absorbance as a low positioned 'elbow' within wavelength range of between 250nm and 300nm. The MIP samples show only one prominent peak within wavelength between 200nm and 250nm. The single prominent peak is as a result of the appearance of the templates at an overlapping wavelength and absorbance (max) due to their very closely related electronic π-π^* and n-π^* configurations.

4.5 Temperature Induced changes of polymer films from QCM experiment.

Using a Bibby Stuart Scientific melting point SMP1 apparatus with power capacity of 50W, voltage of 230v and heating rate of 1^{o}C/4.9sec; physicochemical changes were observed with respect to material stability at elevated temperatures, Table 4.7. Samples without templates (NIP) shrank from an average temperature range between 82^{o}C and 98^{o}C. This is due to evaporative instance of water molecule. Samples with only Nicotine showed no visible sign of shrinking but decomposed at temperatures between 100^{o}C and 300^{o}C, for samples with highest content of Chitosan. This implies that the more the amount of Chitosan with effective copolymerization, the more the stable the product. The samples with only 3PhenylPiridine had a higher decomposition temperature but a closely shorter range difference between component blend samples starting from 171^{o}C to 240^{o}C for samples with highest amount of Chitosan. These samples did not shrink but turned translucent before decomposition. This indicates a sustained stability property prior to decomposition, particularly for samples with a phenyl group substituent, aromaticity maybe a

probable cause of this. Samples with the blend templates, exhibited both the shrinking and translucency but in a reversed order of becoming translucent before shrinking, then decomposing. This phenomenon started from a temperature of 140^{o}C up to 220^{o}C. This indicates the effect and evidence of blending between the two templates. This characteristic reflects the observed trend in Figure 4.26, where the MIP with the blend template had resonant frequency in-between the two individual templates, showing a sort of compensational compromise obtained from blending the templates. This response can be used to identify blends of templates in environments with multi template molecules.

Table 4.7: Observed melting and decomposition temperatures of MIPs and NIPs.

Sample ID	Decomposition Temperature Range (°C)	Remarks
Chitosan-BAP Ref. sample	110 – 210	
Chitosan-MAA-BAP Ref. sample	110 – 220	
NIP sample 1	79 - 109	
NIP sample 2	140 - 152	
NIP sample 3	98 - 119	
NIP sample4	94 - 114	Shrinking occurred from 82°C to 90°C
NIP sample 5	105 - 121	Shrinking occurred from 82°C to 98°C
Nicotine-template MIP sample 1	100 - 160	
Nicotine-template MIP sample 2	115 - 165	
Nicotine-template MIP sample 3	115 - 170	
Nicotine-template MIP sample 4	117 - 185	
Nicotine-template MIP sample 5	190 - 300	
3-PhenylPyridine-template sample 1	171 - 210	Became translucent at 110°C
3-PhenylPyridine-template sample 2	172 - 210	Became translucent at 100°C
3-PhenylPyridine-template sample 3	180 - 220	Became translucent at 120°C
3-PhenylPyridine-template sample 4	200 - 290	Became translucent at 120°C
3-PhenylPyridine-template sample 5	170 - 240	Became translucent at 120°C
Nicotine/3-PhenylPyridine template blend sample 1	140 - 200	Became translucent at 100°C and shrank in size.
Nicotine/3-PhenylPyridine template blend sample 2	142 - 220	Became translucent at 10°C and shrank in size
Nicotine/3-PhenylPyridine template blend sample 3	142 - 220	Became translucent at 110°C and shrank in size
Nicotine/3-PhenylPyridine template blend sample 4	168 - 220	Became translucent at 110°C and shrank in size
Nicotine/3-PhenylPyridine template blend sample 5	172 - 220	Became translucent at 110°C and shrank in size

4.6 Elution of template materials

At the end of the polymerization process, the polymer films on the surface of the chips were washed first with 1ml Acetone, then 1ml of Acetonitrile (polymerization solvent for sample 2), Methanol (for sample 4) and finally with 0.01M NaOH for both the MIPs and the NIP samples. This was done in two washing cycles, for 10mins each using the rock-washing equipment. This treatment eluted the template materials from the polymer films. The MIPs and NIP were then kept for testing and analysis using the Attana QCM machine.

Apart from the fact that QCM operates at sensitivity of up to the nano gram level, it has the ability to detect elusive variations within an environment, which may occur as a result of mass-volume-viscosity in a medium. It also detects variations within the rigid material as it affects the viscoelastic properties. More so, the surface free energy parameter is characteristically accounted for by using the technology. Consequent to these and more, QCM presents a very cost effective, fast and efficient tool for a spot confirmation of the feasibility of the synthesis of molecularly imprinted materials. The technique has contributed towards the clarifying of several inherent properties of biological systems. This is achieved by considering studying the direct correlation between change in frequency (Δf) and mass per volume quantity (Δm) (Marx, 2003), by the application of its sensitivity at the sub mono layer level. Despite its draw back (Chuekachang et al., 2013), which violets the Sauerbrey assumption of adsorption occurring at only 'rigid' state of sample, QCM have found application in very many areas in biomaterials (Wu *et al.*, 2015; Duan *et al.*, 2013 and Lee *et al.*, 2012).

The overall chemistry of the preparation of the MIP is as follow:

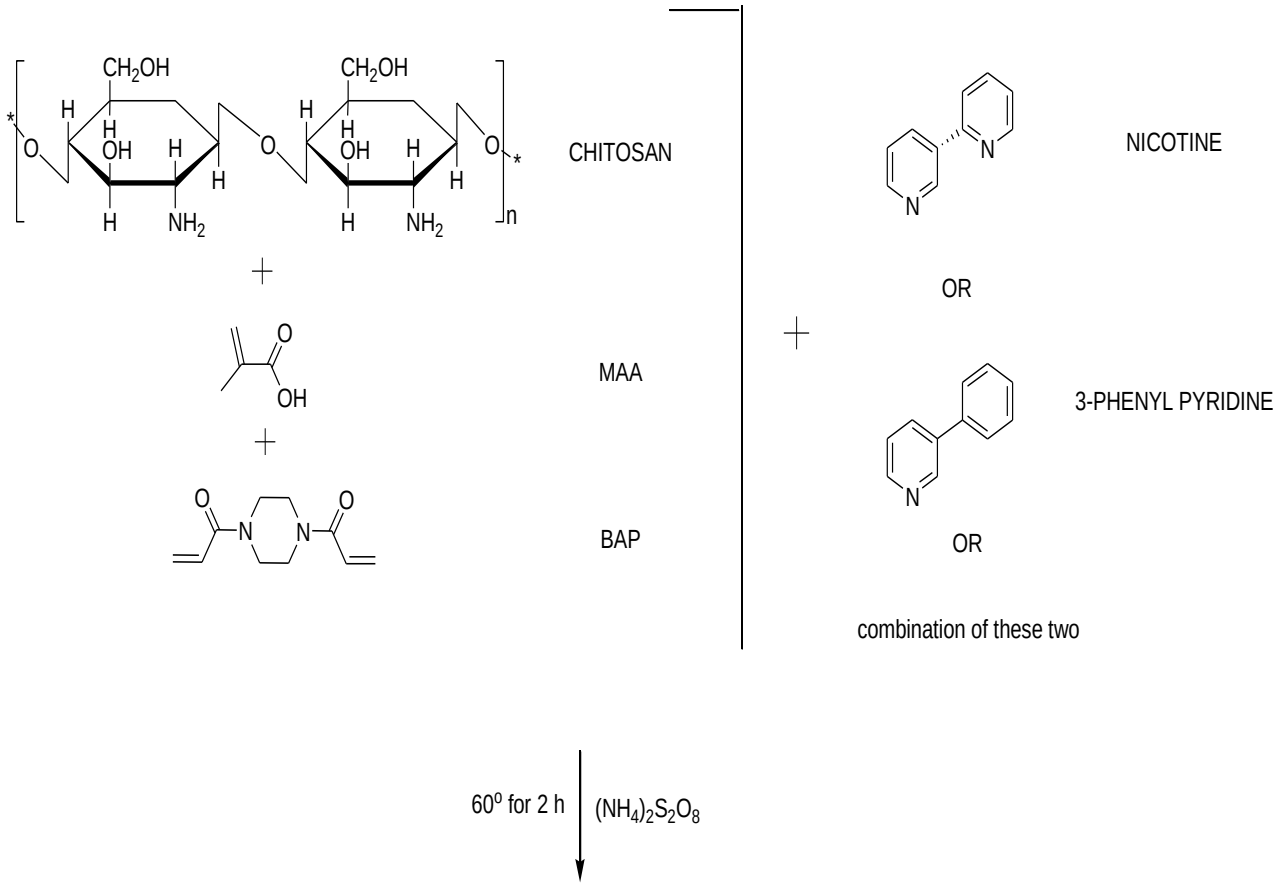

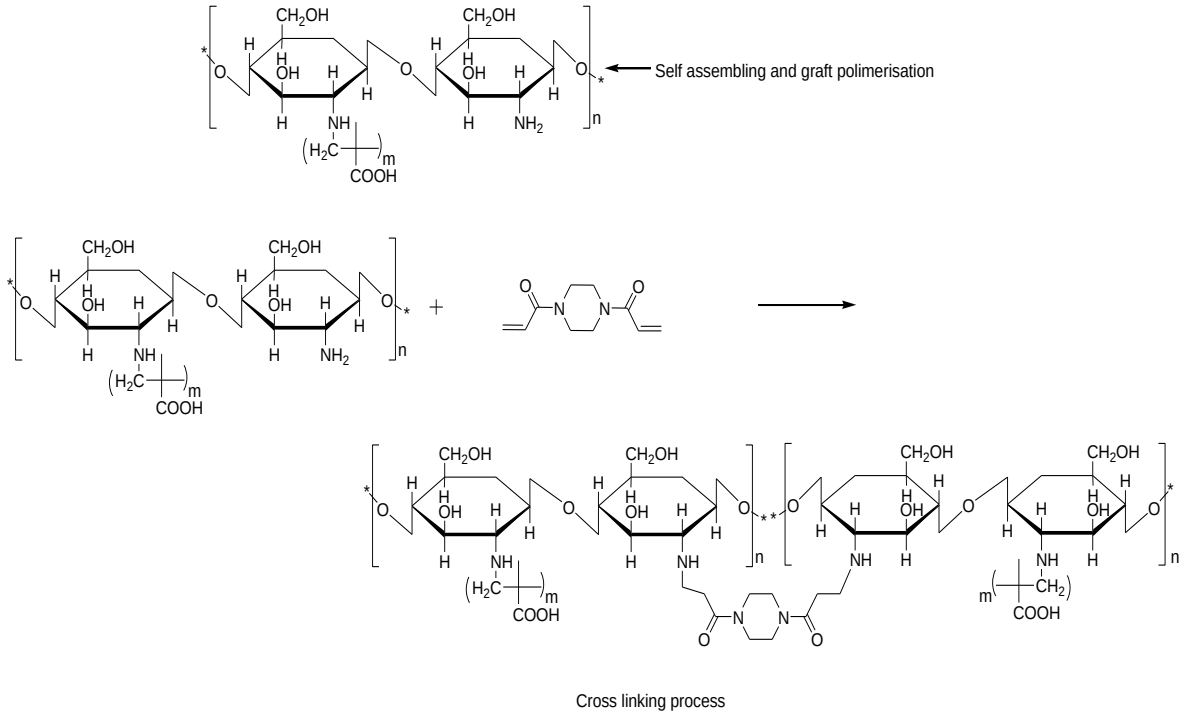

Figure 4.41: Resultant MIP Products A, B and C based on particular Template(s).

MIP Product A (Nicotine Template)

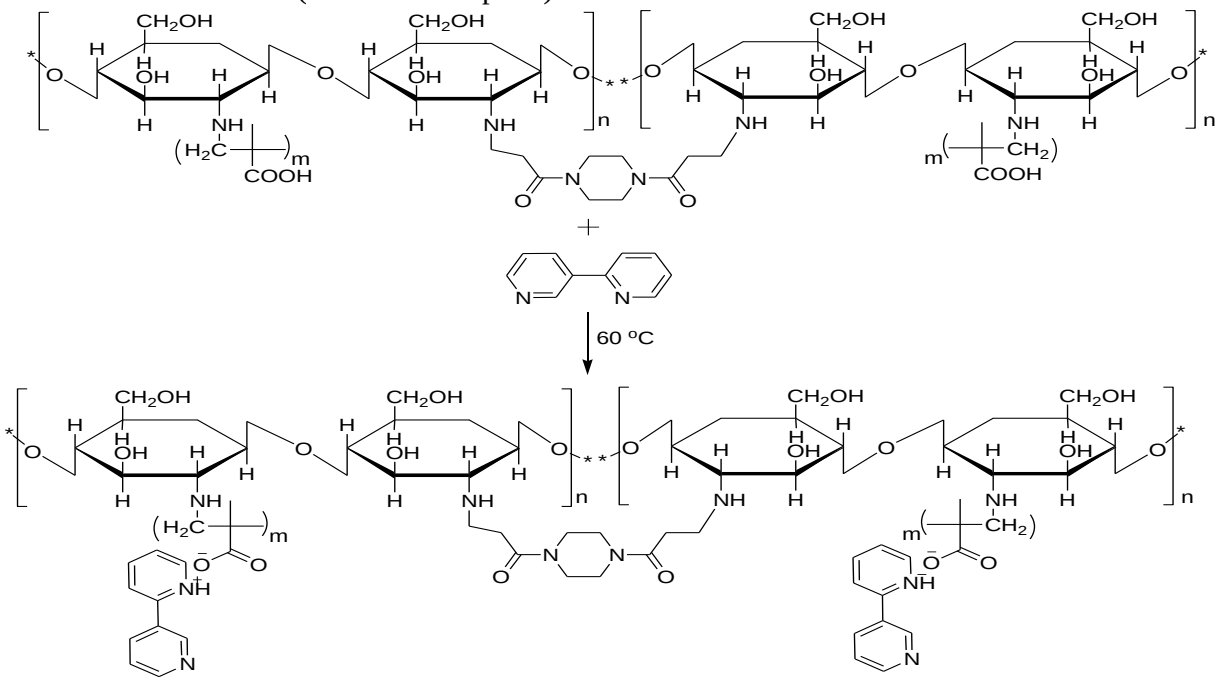

MIP Product B (3-PhenyPyridine Template)

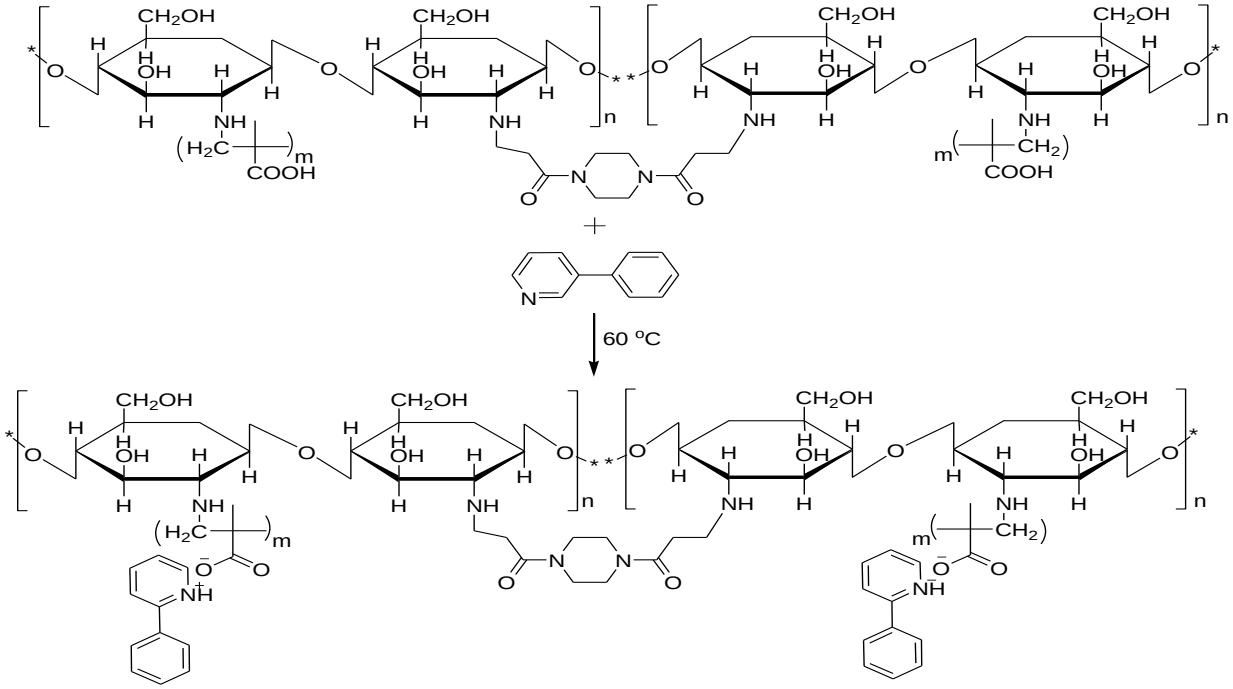

MIP Product C (50:50 Blend of Nicotine and 3-PhenylPyridine)

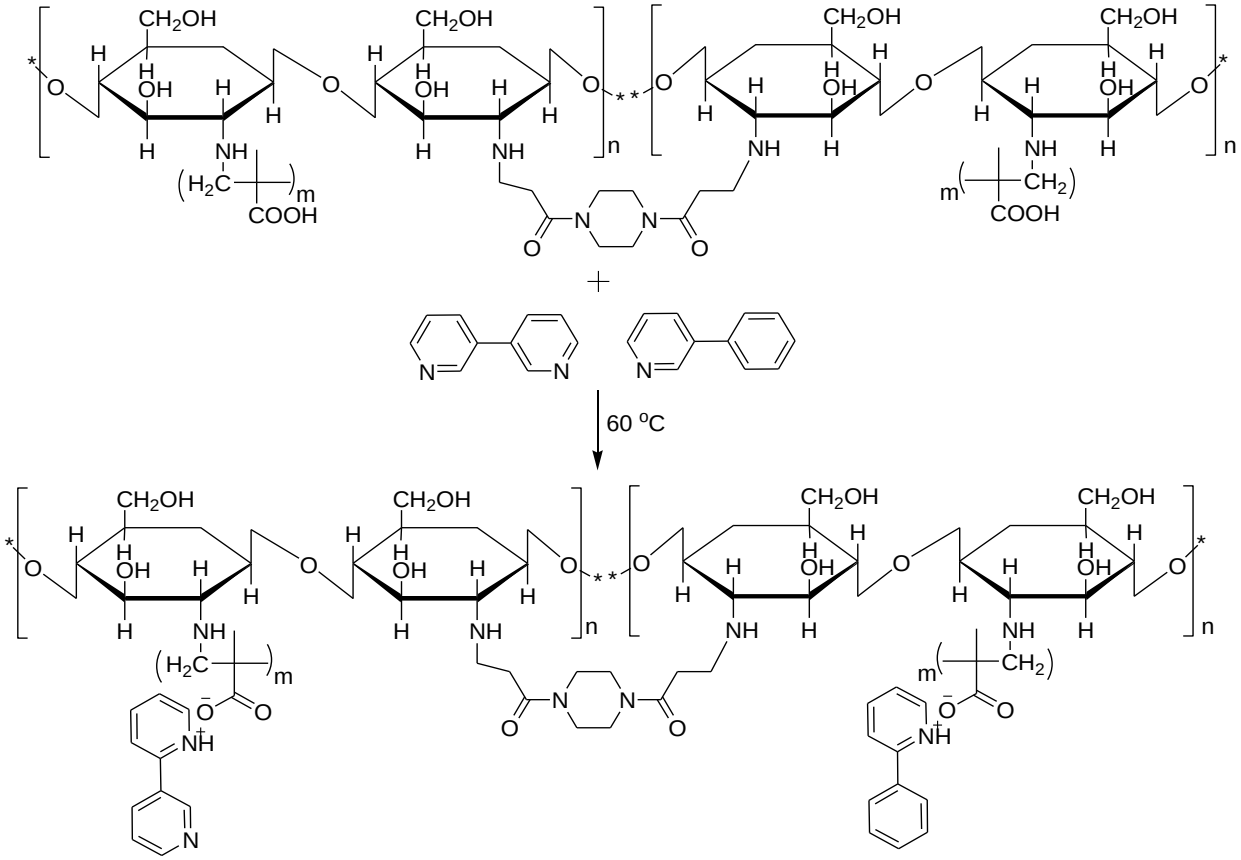

4.7 Conclusion from QCM experiment

Despite the promising and evidenced utilization of Chitosan as additive, in various industries and in different nature and sizes (Goosen, 1997; Knorr, 1991; Drewnowska, et al., 2013; Przekora, Palka and Ginalska, 2014; Ahmed and Aljaeid, 2016; Kamiński and Modrzejewska, 1997), its extensive use in a diversified industrial economy has been faced with inherent challenges due to its hydrophilic nature and limited temperature tolerance.

In molecularly imprinted polymer systems, the material surfers a setback that is associated with the presence of the hydroxyl functionality. This catalyzes its inherent disposition to swell in the presence of water and makes it challenging for thin film surface studies to be carried using it as a matrix. Scientists in a bid to overcome this attribute of Chitosan have adopted approaches like copolymerization and grafting to stiffen and restrict the swelling potential amongst other target goals (Kyzas and Bikiaris, 2015; Jain *et al.,* 2013; Thakur and Thakur, 2014; Mourya and Inamdar, 2008; Alves and Mano, 2008 and Zhang *et al.,* 2015).

Molecularly imprinted fabrications have over the years progressed from uni-template systems with specific single analyte detections (Jing *et al.,* 2011 and 2013; Du *et al.,* 2014), to uni-template systems with selective family analogue detections, (Manzo *et al.,* 2015; Hung and Hwang, 2008 and Nong, *et al.,* 2013); up to recent uni-template systems with ability to select multi-analyte protocols (Madikizela and Chimuka, 2016; Luo *et al.,* 2011 and Ferrer *et al.,* 2000).These systems function well but with obvious limitations that occur as a result of complexity of contact environment, stereo-specificity of available analytes or differences in pH of the environment. Consequently, researchers have recently delved into the feasible modification of matrices with multi-template binding inclusions,

(Dai *et al.*, 2012; Zhang *et al.*, 2015 and Cambridge Enterprise, 2011). It is advantageous to employ multi-templated MIPs within an environment that has group analogues or family species so as to simultaneously adsorp the pollutants. This will reduce the burden of synthesizing numerous matrices for individual selective adsorptions

From the results obtained, a matrix based on Chitosan copolymerized with MAA, was synthesised and a molecularly imprinted polymer material prepared with it using two template materials (Nicotine and its analogue), singly and in simultaneous blend. A feasible deposition volume on resonator was also established taking into consideration, the hydrophilic nature of Chitosan, which characteristically prompts swelling and consequent damping on the surface of a QCM resonator. This has been a challenge in the use of Chitosan thin films in biosensor fabrication. This challenge has been taken care of by this experiment. The QCM analysis established the viscoelastic properties of the polymer thin film as well as the feasibility of having a blend of templates within a singular matrix. These MIPs can be used in environments at temperatures above 60^{O}C but below 250^{O}C as shown from the result of the effect of temperature using the melting point apparatus.

4.8 Results from the bulk polymerization experiment

4.8.1 Fourier Transformed Infra Red (FTIR) spectroscopy results

The presentation in Figure 4.41, agrees with the findings and reports from Peng, (2011) and Yanti *et al.,* (2016). The report by Peng, (2011), buttresses the potential of MAA to ‘dimerize’, and consequently provide additional robust platform for template binding via, van der Waals interactions, H-bond donor, dipole-dipole and H-bond receptor interactions.

For the Prepolymerization, a higher transmittance and or insignificant change in transmittance for the formed complex is due to the incidence of a slight degree of Complexation or the presence of negligible fine size of the particles of the Complexation reaction as well as the counter, strong electrostatic interaction between the $-NH^{3+}$ species.

4.8.1.1 Typical Points Of Interest Across The Interaction Platforms Within The MIPs' Systems:

1) Displacement (oxidation) of the amide (NH_2) functionality of the Chitosan compound, to the N-H radical functionality.
2) The shift in the pendant OH functionality of C-C bonded group.
3) Saturation from alkene functionality to alkane functionality by the methylene group of the Methacrylic acid during Prepolymerization and polymerization reactions.
4) The observable shift/presence of the Carboxylate functionality from the Methacrylic acid.

These interactions are observable within the complex system but can be identified from study of individual interaction environments. The environments of interest may be divided into:

1. Prepolymerization/Polymerization environment between the Chitosan and the Methacrylic acid,
2. Crosslinking reaction environments between the functional monomer/matrix and the cross Linkers: Chitosan-Methacrylic acid (BAP)

   Chitosan-Methacrylic acid (Geranic acid).

3. Interaction environment between the functional monomer-Matrix-Cross linker-Template:
   a. CS-MAA-BAP-Nicotine.
   b. CS-MAA-Geranic acid-Nicotine.

c. CS-MAA-BAP-Phenylalanine

d. CS-MAA-Geranic acid-Phenylalanine

e. CS-MAA-BAP-Nicotine-Phenylalanine

f. CS-MAA-Geranic acid-Nicotine-Phenylalanine.

Considering the observable presences of same functional groups among the individual compounds, overlaps occur, though some of the charts show expected differences. Nonetheless, interactions and their degrees are distinguished by their relative percent transmittances.

FTIR results of prepared samples are interpreted based on the overriding percentage transmittances as well as the presence or abscenec of characteristic functional groups. A reverse/decrease, in transmittance is initiated at the onset of grafting/copolymerization starting from the initiated Prepolymerization stage. The more the degree of grafting/copolymerization between Chitosan and Methacrylic acid, the lower the percent transmittance (Moraes *et al.*, 2008). This relates directly with the amount of unreacted and available amide groups on the chitosan backbone, while higher percent of transmittance as a result of the presence of free NH_2 moieties evidenced by the amide intensities at around 1545 cm^{-1}, while the substitution of the H---H of the amide functionality of the Chitosan and consequent polymerization affecting the C=C double bond stretching and double bond C=O bending on the Methacrylic acid moiety; translates to the decreased intensities of the double bond of C=C double bond stretching (1635 cm^{-1}) alongside the O-H stretching at 2935 cm^{-1}. The O-H bending vibration at 1383 cm^{-1} confirms the presence of carboxylic acid groups as the polymerization gets more intense.

4.8.1.2 Comparative Plots of Prepolymerized and Polymerized samples.

4.8.1.2.1 a) BAP cross linked samples.

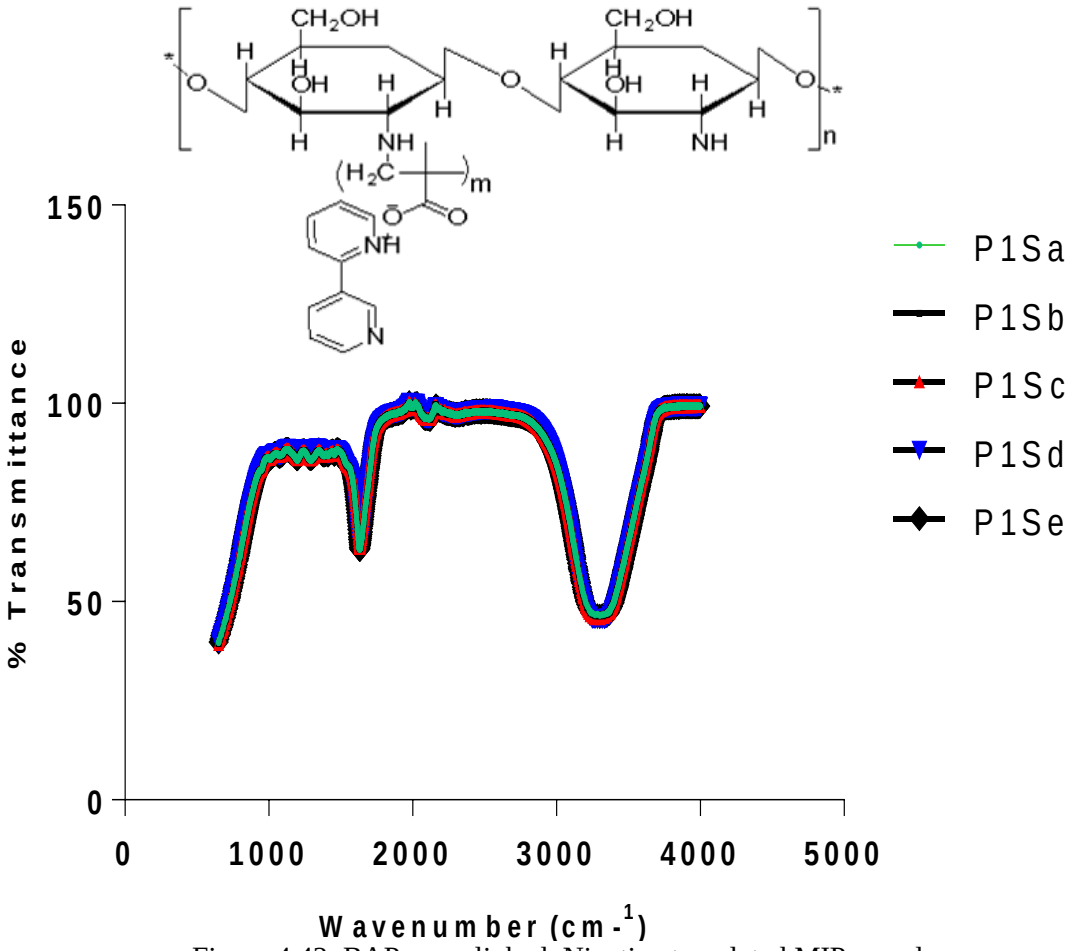

Figure 4.42: BAP cross linked, Nicotine templated MIP samples.

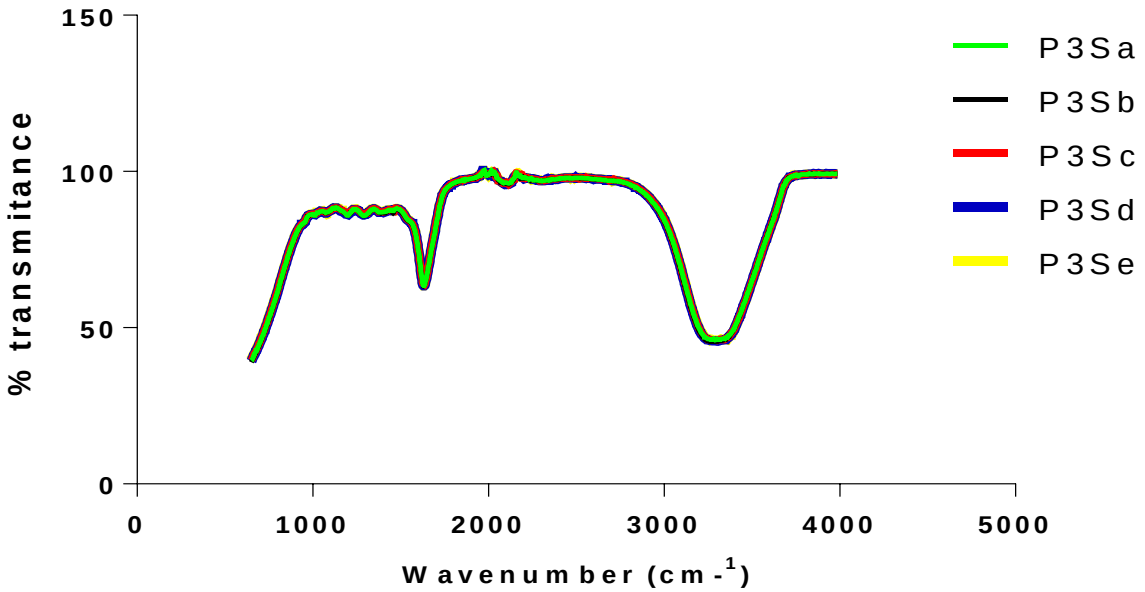

Figure 4.43: Phenylalanine amide templated samples.

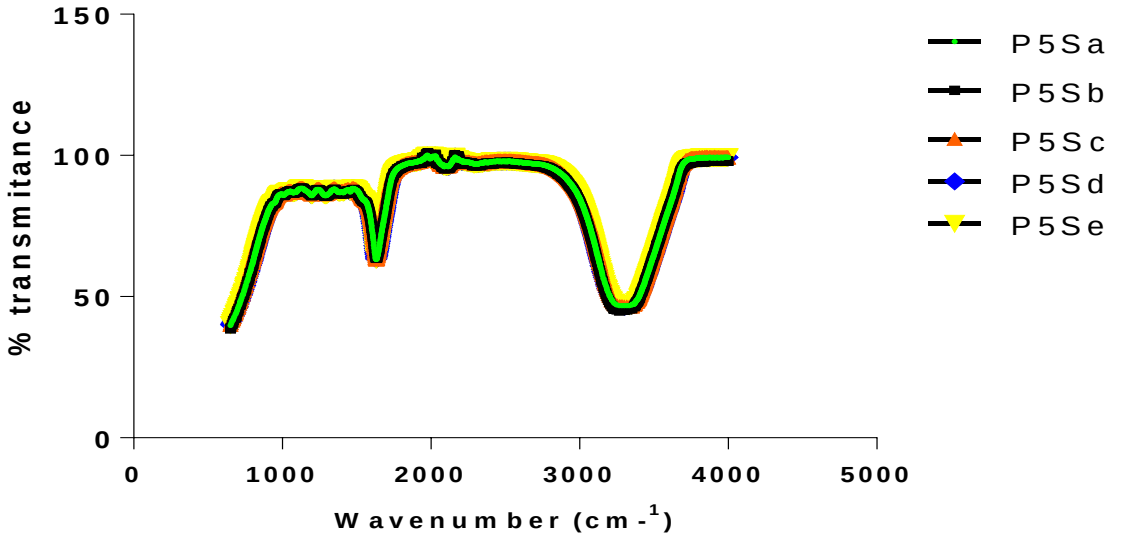

Figure 4.44: **Nicotine-Phenylalanine amide blends templated samples.**

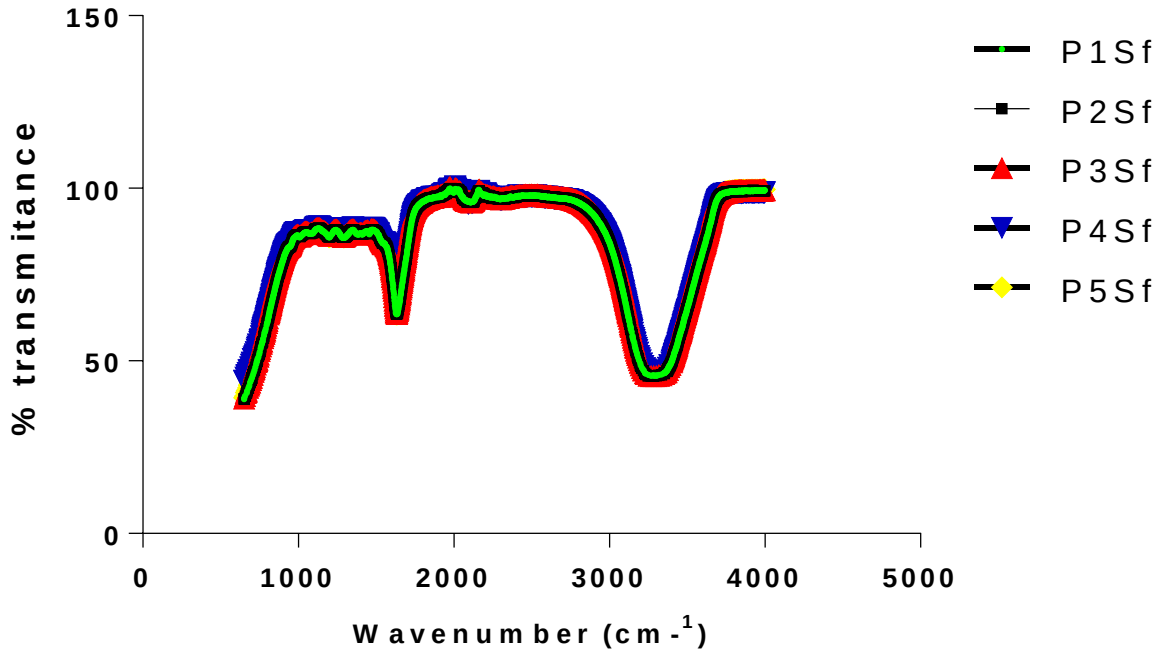

Figure 4.45: Comparative chart of Non templated BAP cross linked samples.

From the charts of the MIPs displayed in Figures 4.42, 4.43 and 4.44, MIP samples P1Se for Nicotine templated, P3Sd for Phenylalanine templated and P5Sd for Nicotine-Phenylalanine templated; present the best sample products while for the non-templated samples, Figure 4.45, the relationship is presented as, P3Sf > P2Sf > P1Sf > P5Sf > P4Sf, substantiating the selection of sample P3Sf as the representative non-templated imprinted sample.

Comparison of the pre- and polymerized MIPs presented as Figures 4.46, 4.47 and 4.48 as plots of the percent transmittance against the wavenumber. Polymerization of the materials occurred effectively based on the lower values of % transmittances of the polymerized products, as reported by Yanti *et al.*, (2016). The reduced percent transmittance is consequent to the presence of a high population of bonds with resultant vibrational energies.

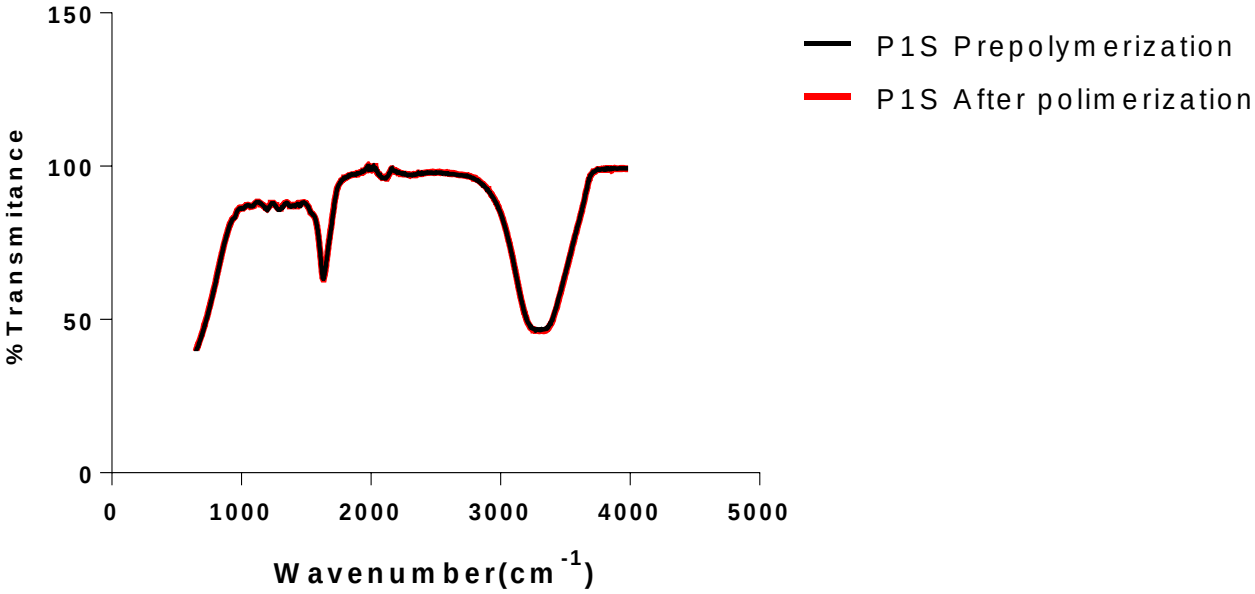

Figure 4.46: plot of pre and after polymerization of BAP crosslinked, Nicotine templated MIP.

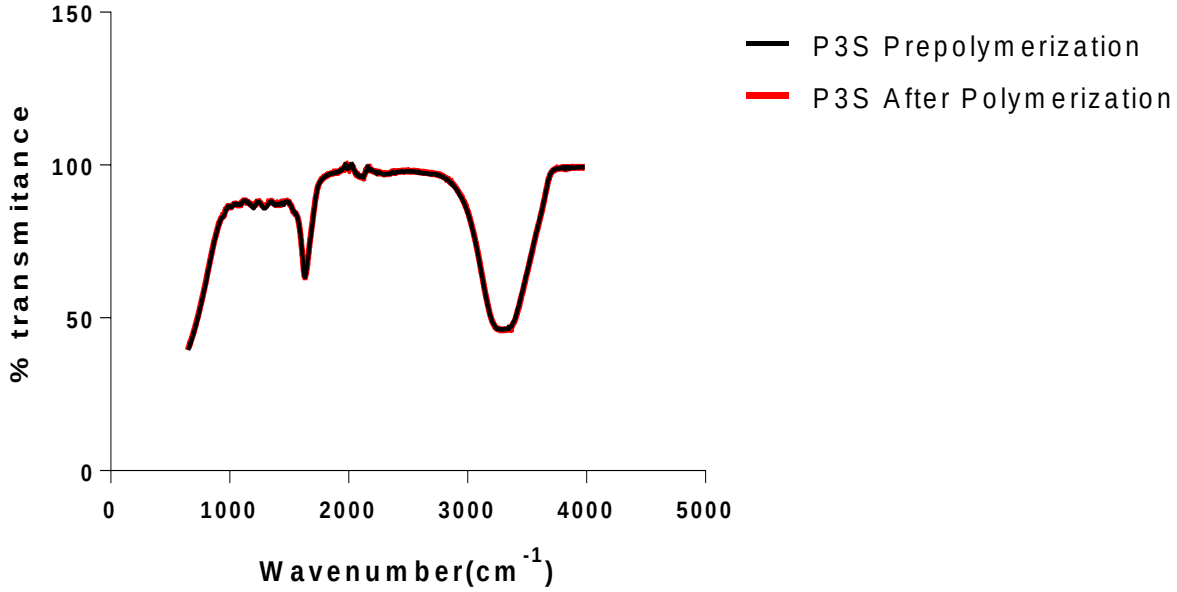

Figure 4.47: plot of pre and after polymerization of BAP crosslinked, Phenylalanine templated MIP.

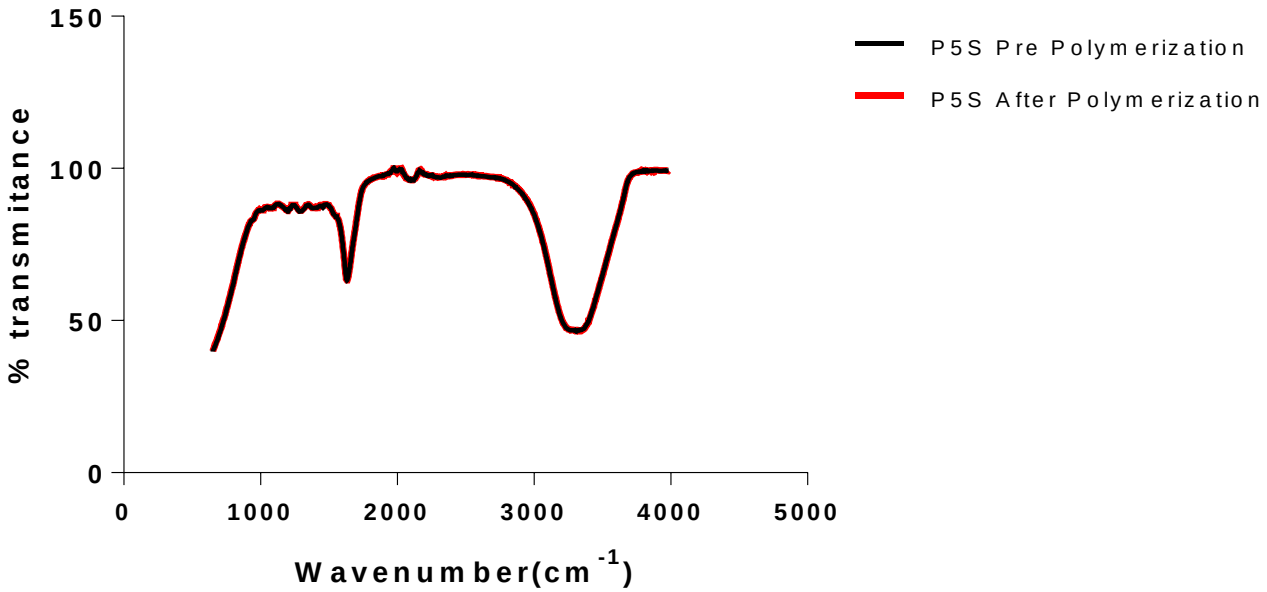

Figure 4.48: plot of pre and after polymerization of BAP crosslinked, Nicotine-Phenylalanine templated MIP.

4.8.1.2.2 b) Geranic acid cross linked MIPs.

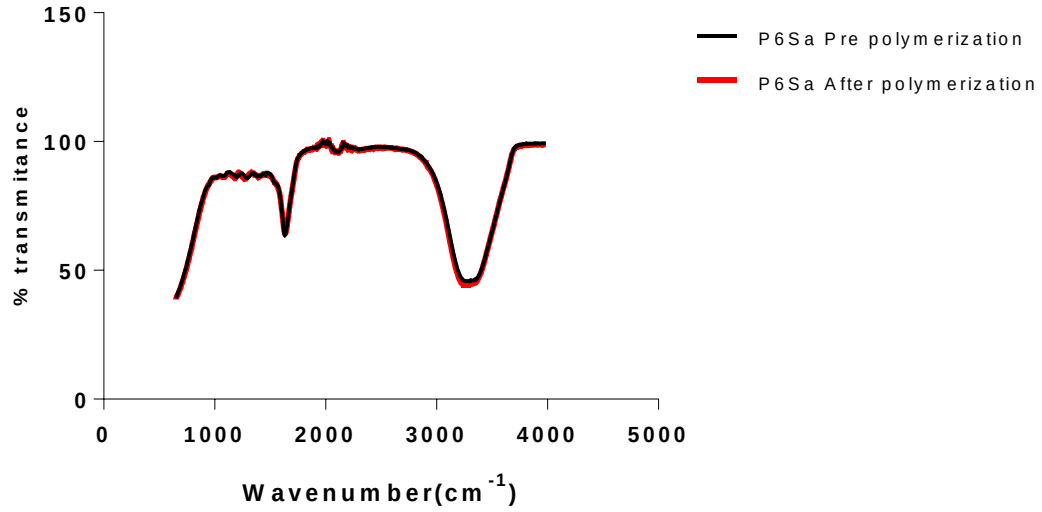

Figure 4.49: plot of pre and polymerized MIP using 2ml of Geranic acid crosslinker and Nicotine template.

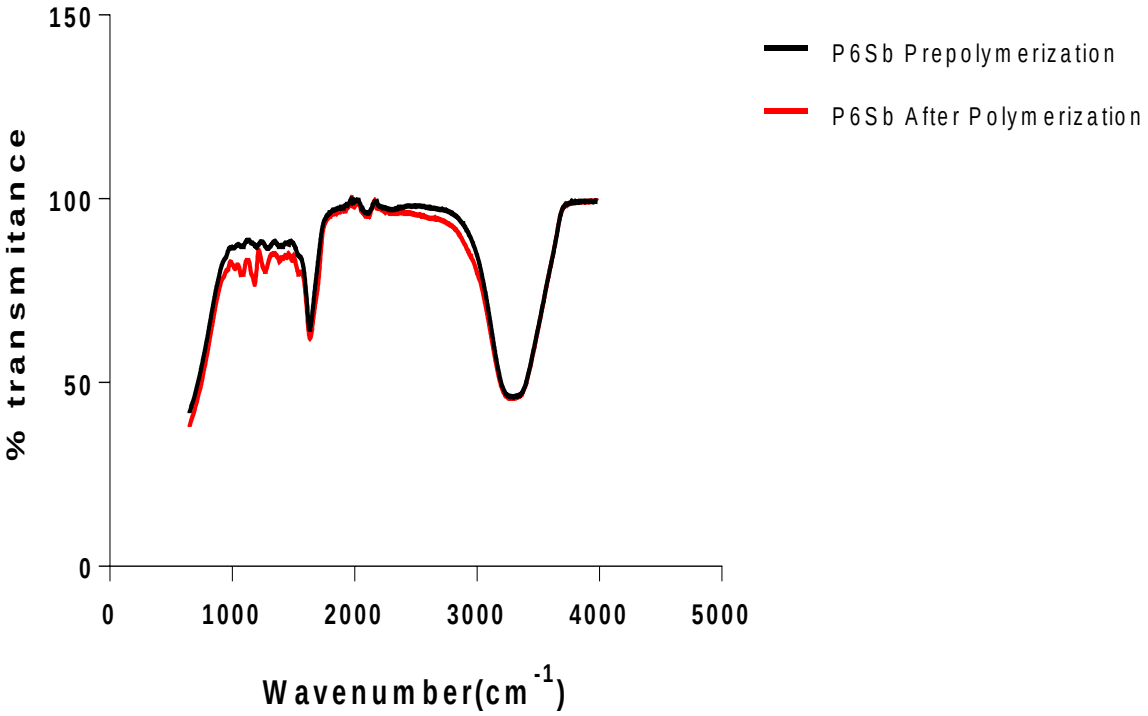

Figure 4.50: plot of pre and polymerized MIP using 3ml of Geranic acid crosslinker and Nicotine template.

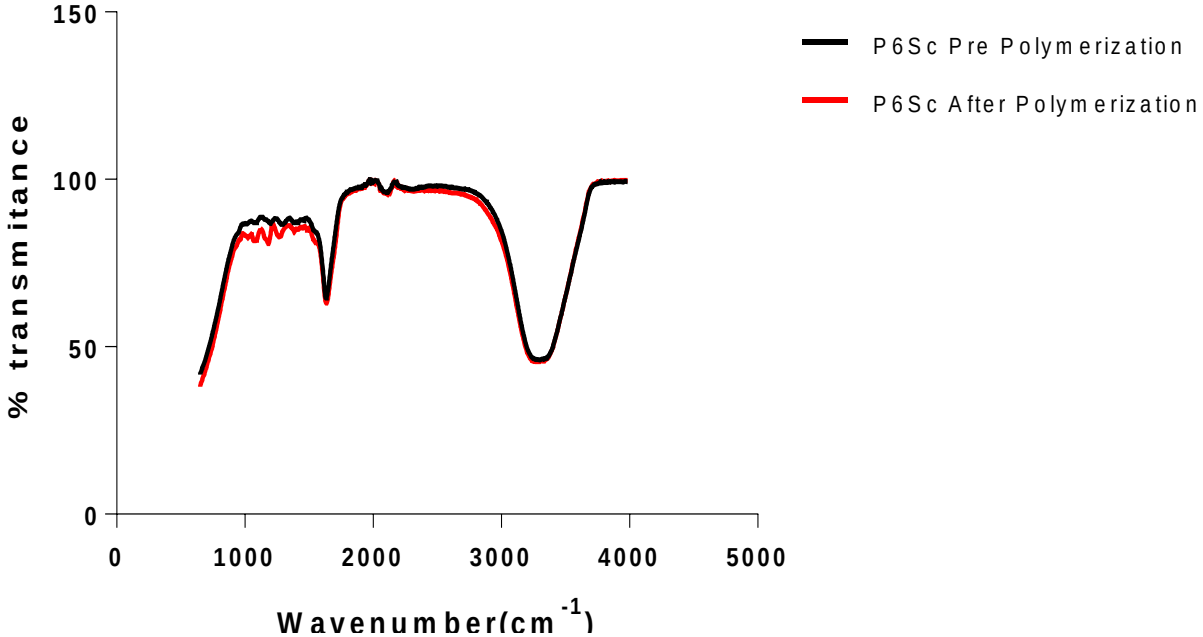

Figure 4.51: plot of pre and polymerized MIP using 4ml of Geranic acid crosslinker and Nicotine template.

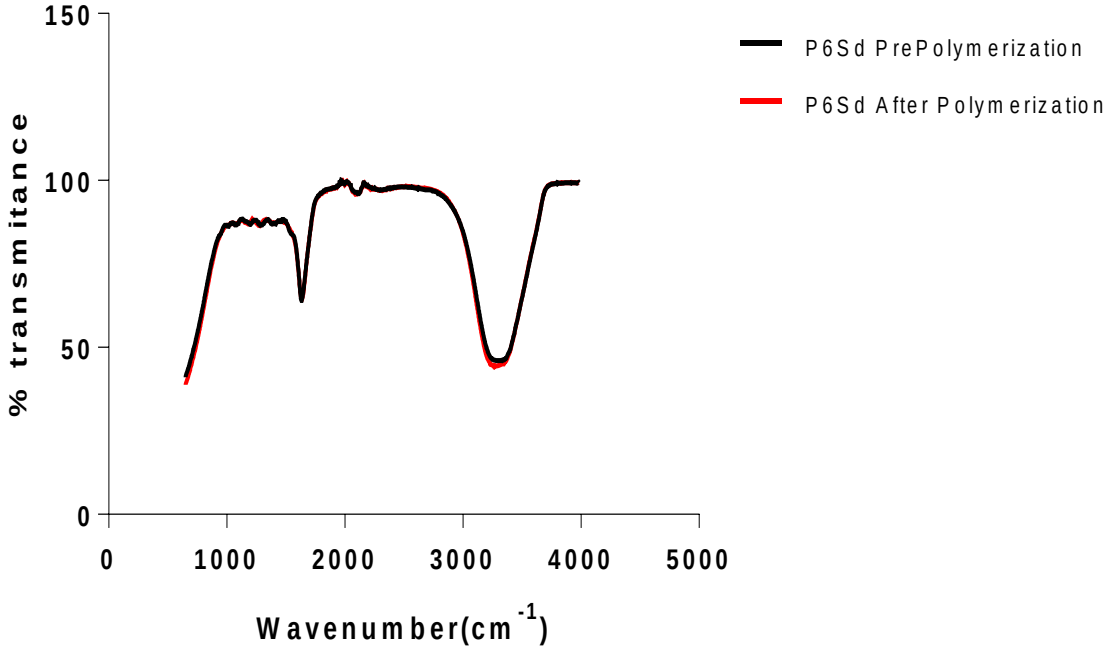

Figure 4.52: plot of pre and polymerized MIP using 5ml of Geranic acid crosslinker and Nicotine template.

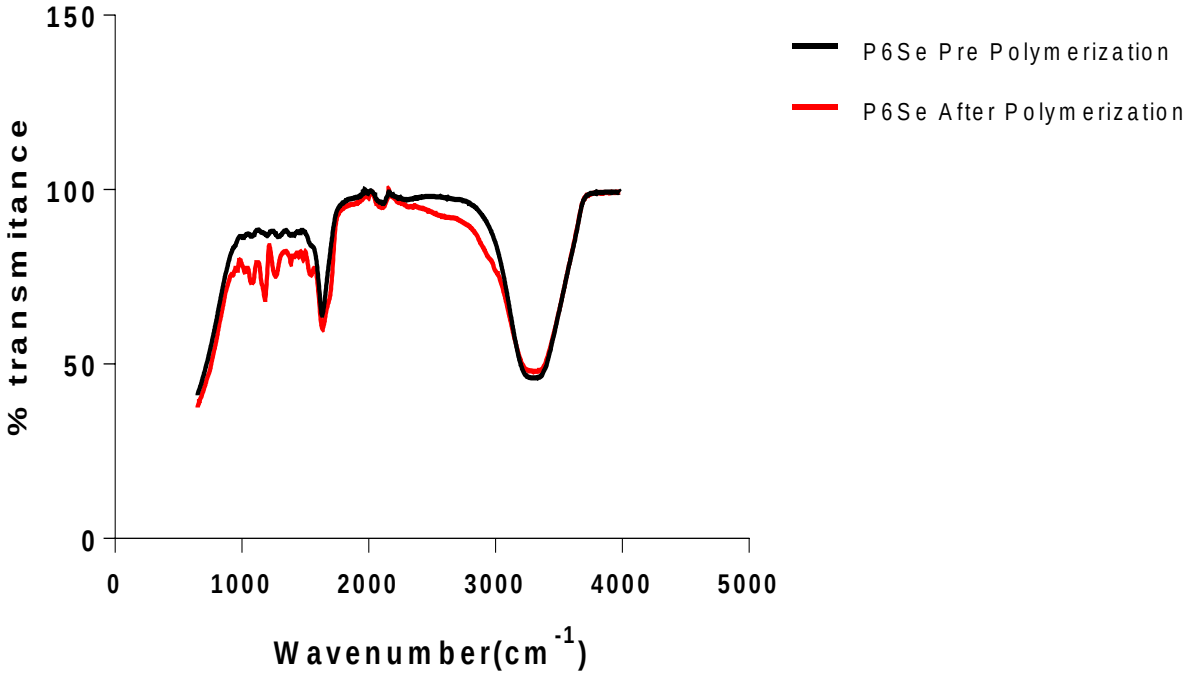

Figure 4.53: plot of pre and polymerized MIP using 6ml of Geranic acid crosslinker and Nicotine template.

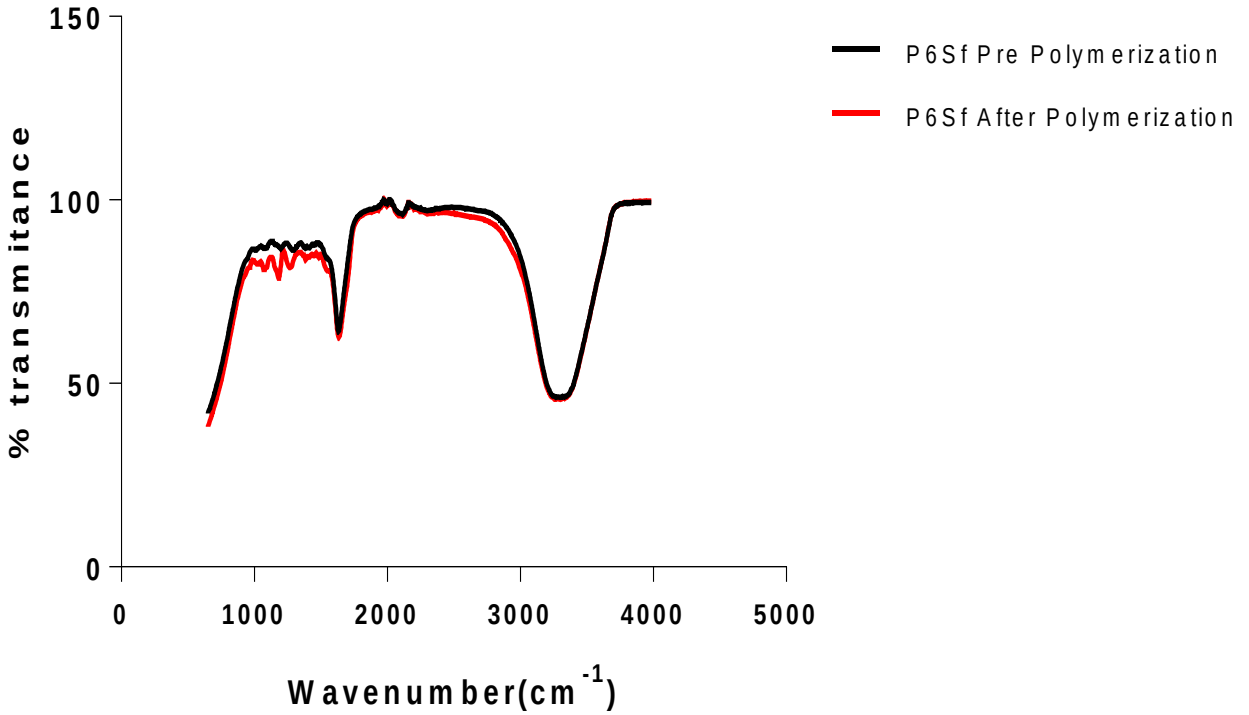

Figure 4.54: plot of pre and polymerized NIP using 5ml of Geranic acid crosslinker without template.

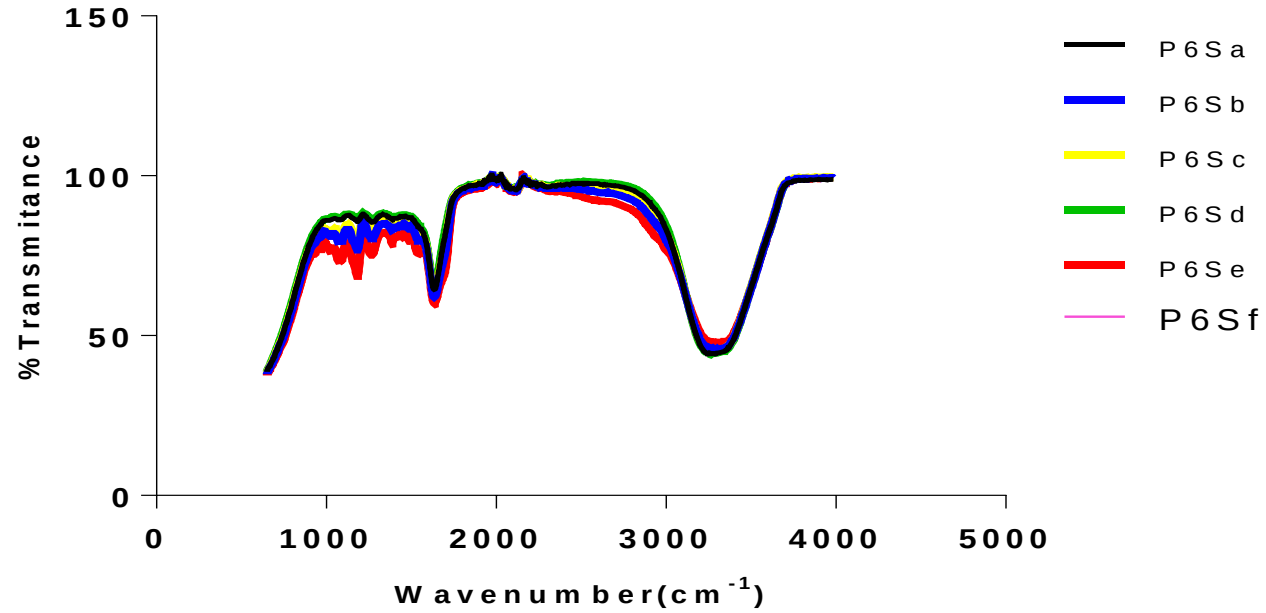

Figure 4.55: Comparative plot of % transmittance against wavenumber for Genaric acid cross linked, Nicotine templated MIPs.

Figures 4.49 - 4.54, show the effective polymerization of the MIPs crosslinked with Geranic acid and containing Nicotine templates as compared with the Prepolymerization samples, while from Figure 4.55, sample P6Se presents the best product of the polymerization. Sample P6Se therefore became the representative MIP sample for this group. Nonetheless, P6Sb and P6Sa may be employed as acceptable formulation blends during the fabrication of MIPs of particular application.

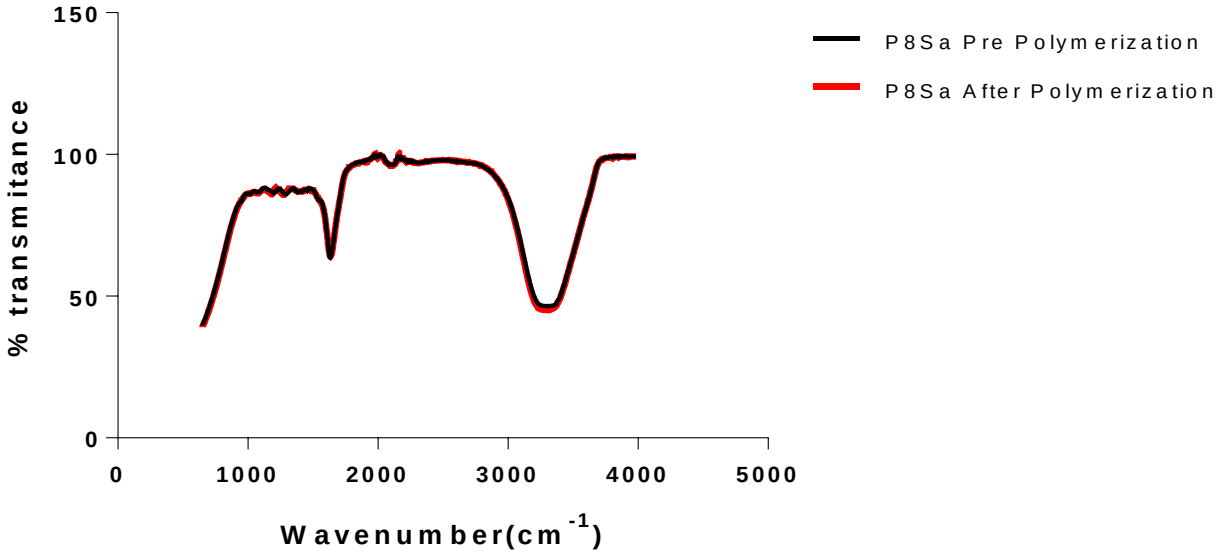

Figure 4.56: plot of pre and polymerized MIP using 2ml of Geranic acid crosslinker and Phenylalanine template.

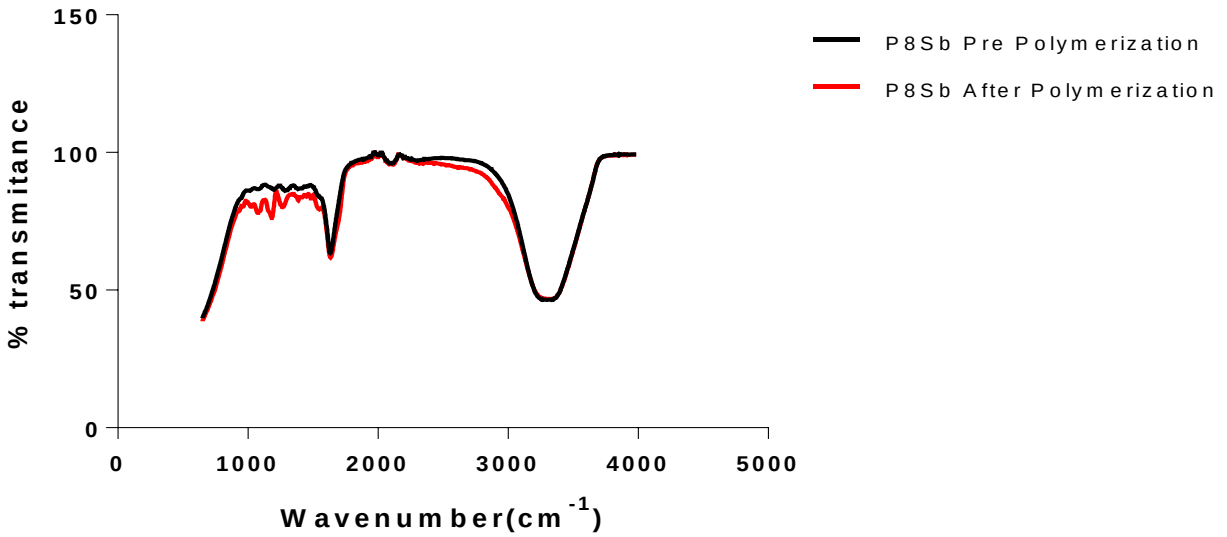

Figure 4.57 : plot of pre and polymerized MIP using 3ml of Geranic acid crosslinker and Phenylalanine template.

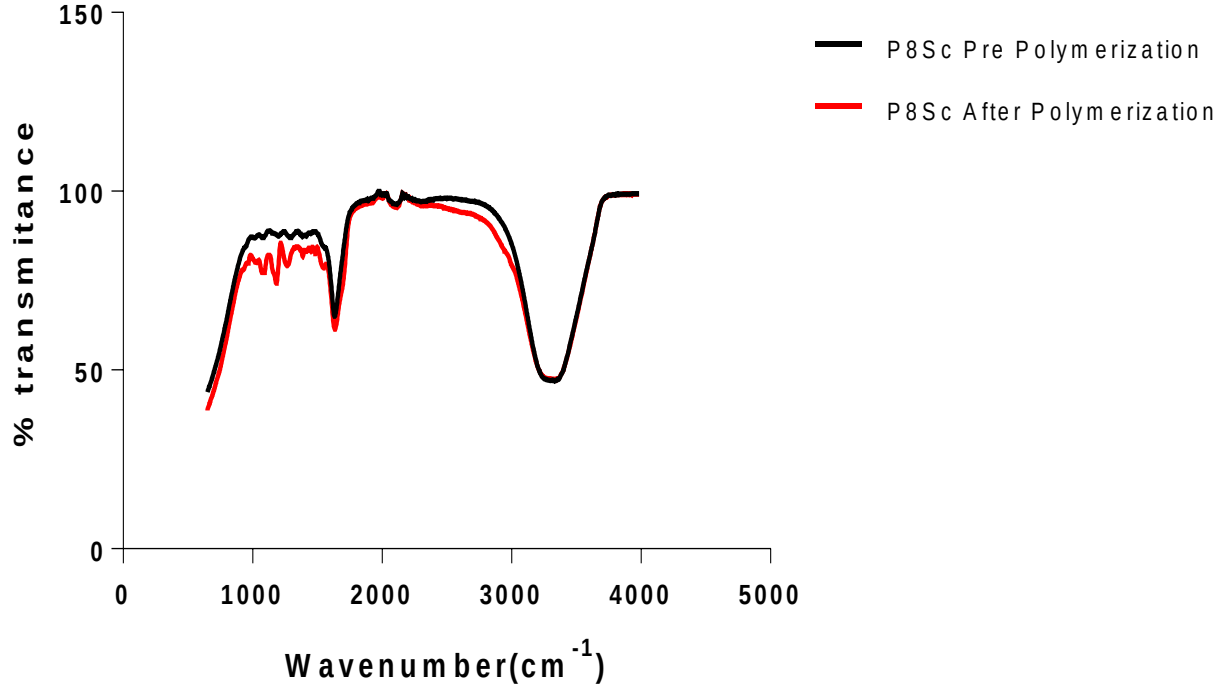

Figure 4.58:plot of pre and polymerized MIP using 4ml of Geranic acid crosslinker and Phenylalanine template.

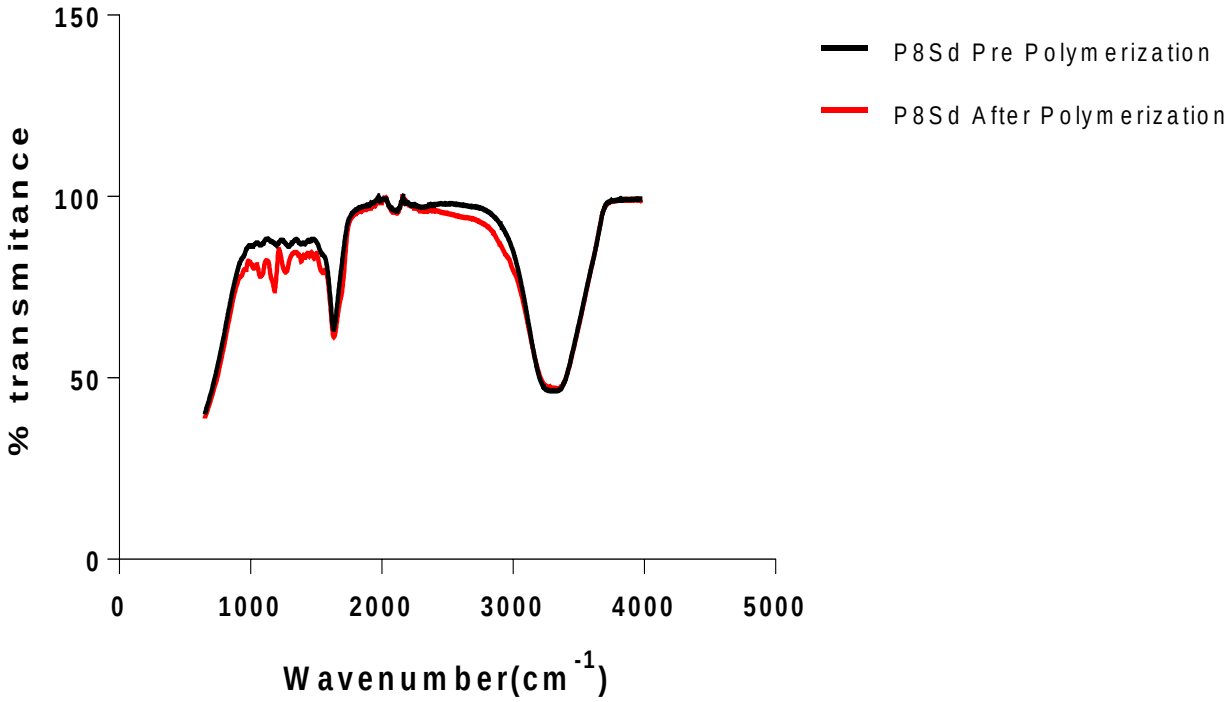

Figure 4.59: plot of pre and polymerized MIP using 5ml of Geranic acid crosslinker and Phenylalanine template.

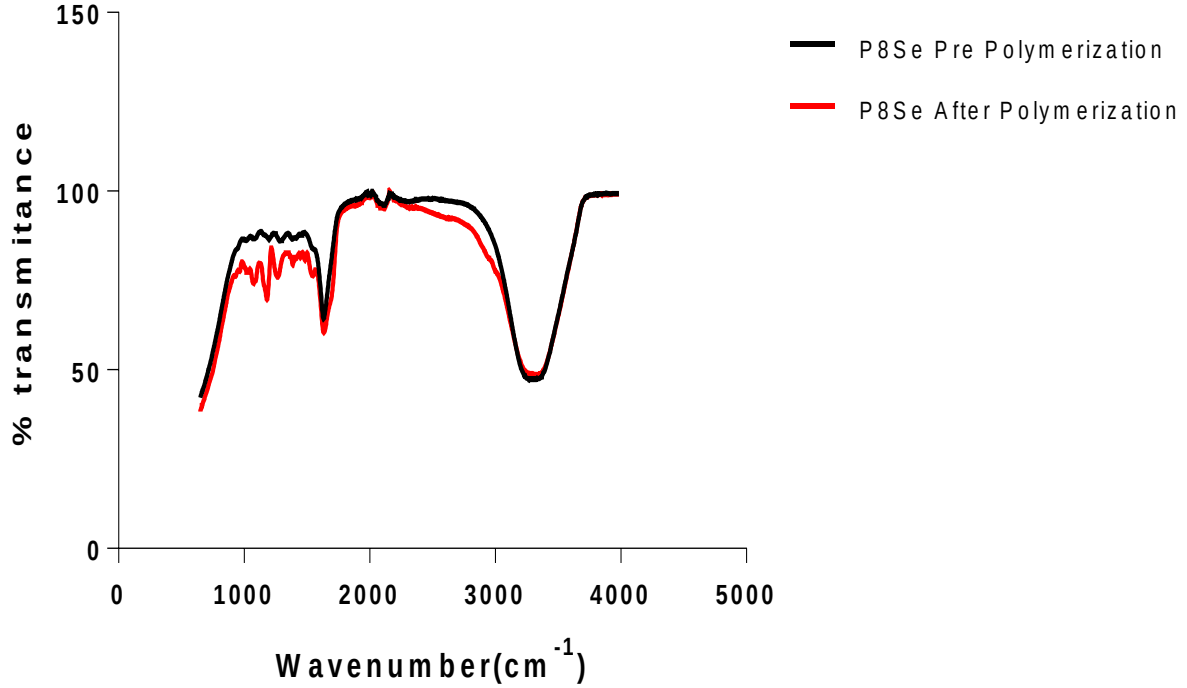

Figure 4.60: plot of pre and polymerized MIP using 6ml of Geranic acid crosslinker and Phenylalanine template.

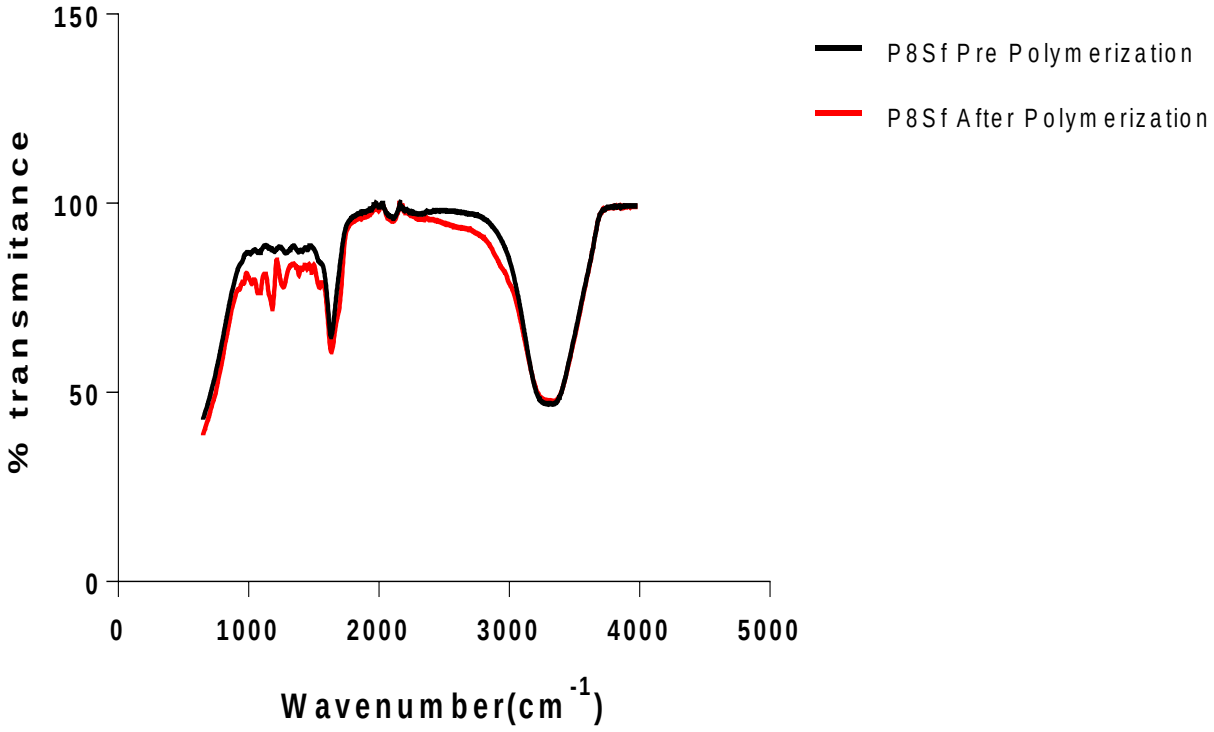

Figure4.61: plot of pre and polymerized NIP using 5ml of Geranic acid crosslinker without template.

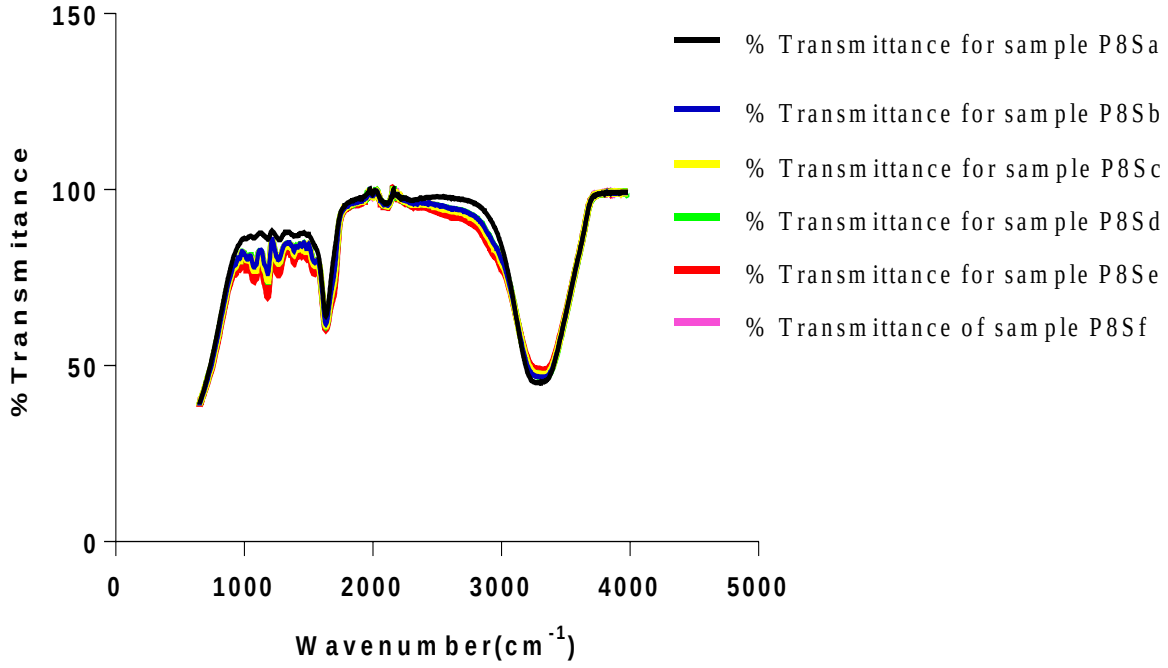

Figure 4.62: Comparative plot of % transmittance against wavenumber for Genaric acid cross linked, Phenylalanine templated MIPs.

Figures 4.56 – 4.61, show the effective polymerization of the MIPs crosslinked with Geranic acid and containing Phenylalanine templates as compared with the Prepolymerization samples, while from Figure 4.62, sample P8Sd presents the best product of the polymerization. Sample P8Se therefore became the representative MIP sample for this group.

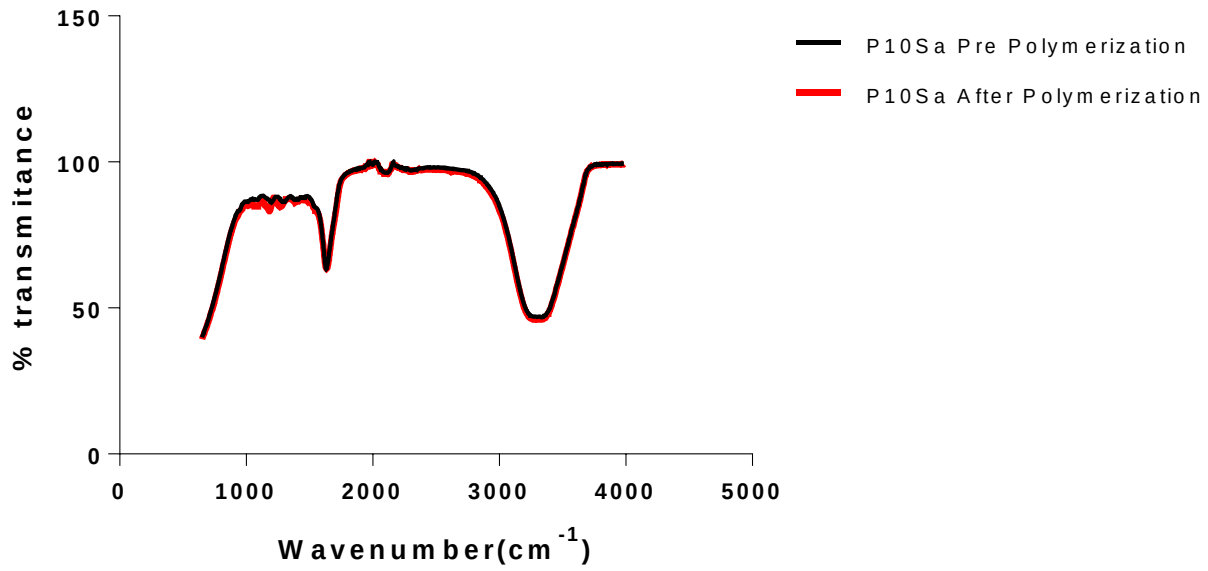

Figure 4.63: plot of pre and polymerized MIP using 2ml of Geranic acid crosslinker and Nicotine-Phenylalanine template.

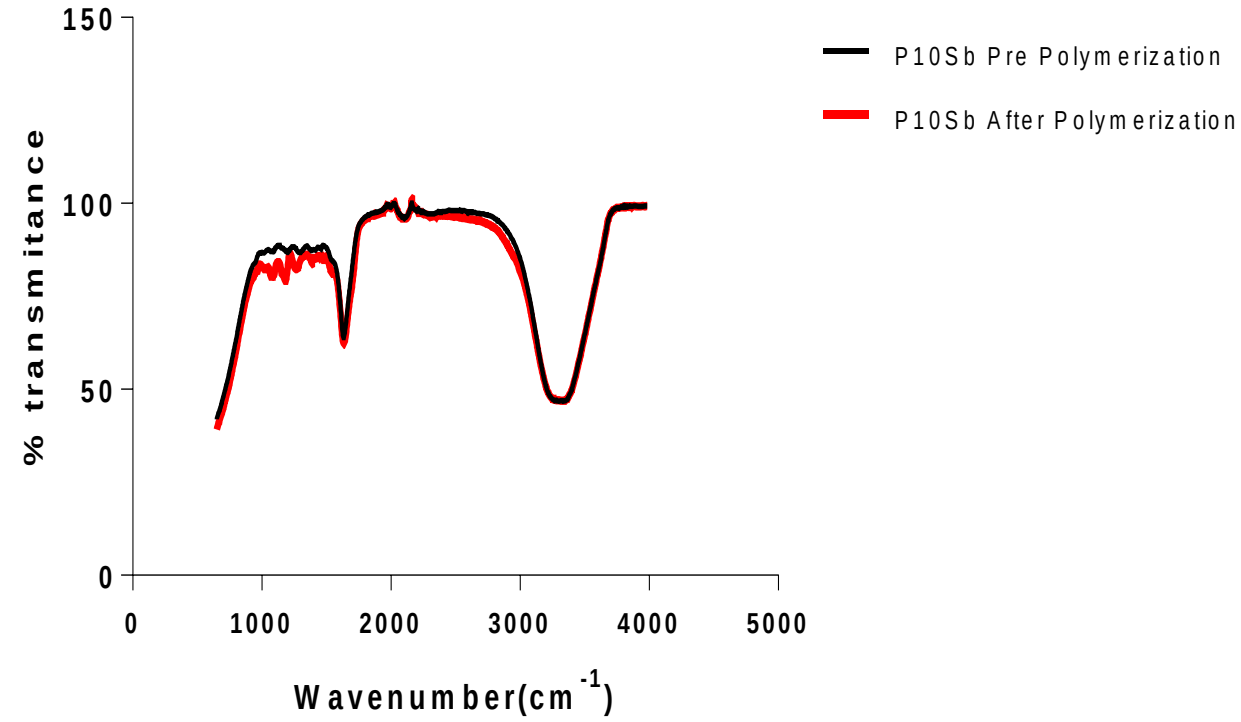

Figure 4.64: plot of pre and polymerized MIP using 3ml of Geranic acid crosslinker and Nicotine-Phenylalanine template.

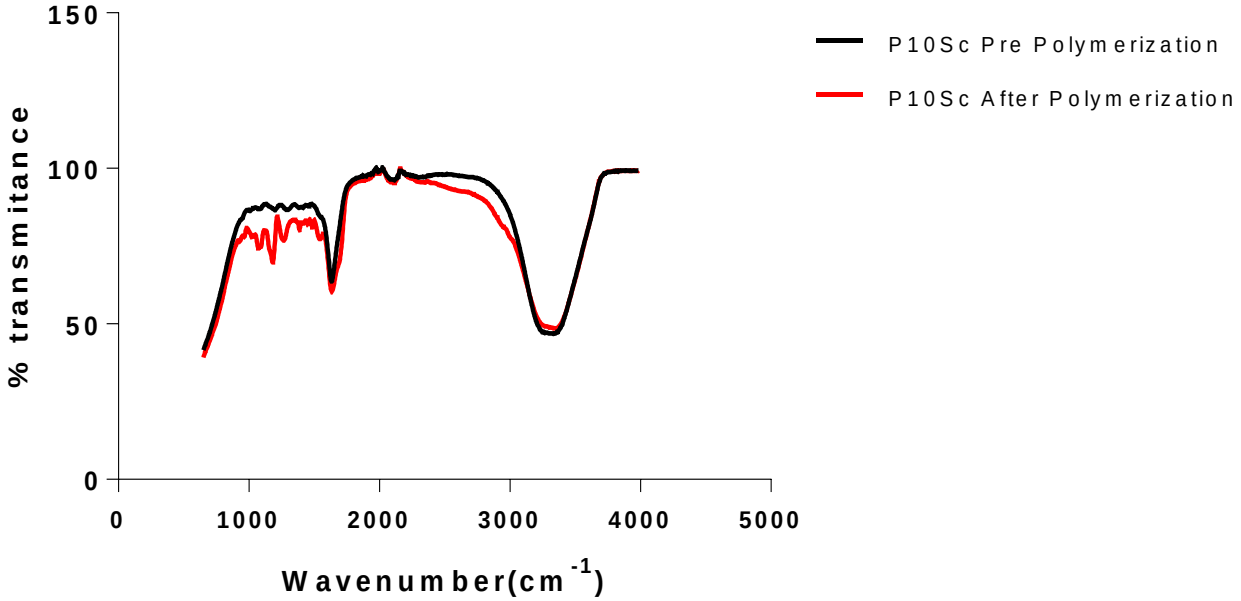

Figure 4.65: plot of pre and polymerized MIP using 4ml of Geranic acid crosslinker and Nicotine-Phenylalanine template.

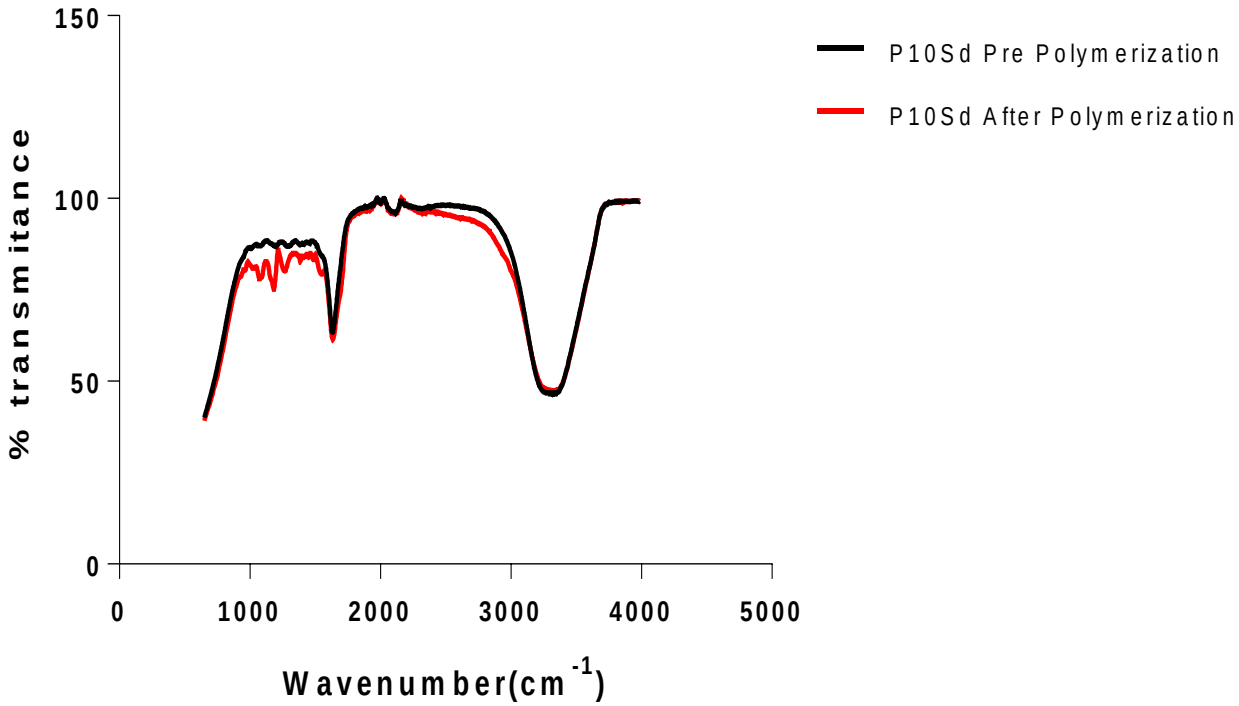

Figure 4.66: plot of pre and polymerized MIP using 5ml of Geranic acid crosslinker and Nicotine-Phenylalanine template.

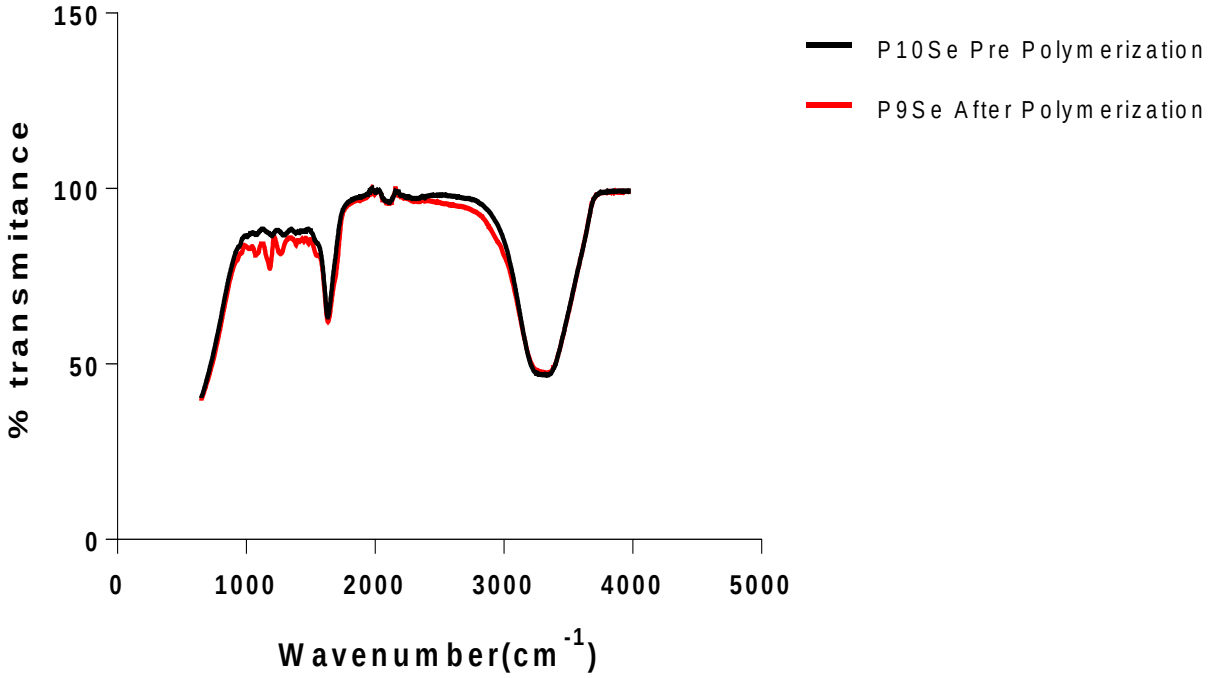

Figure 4.67: plot of pre and polymerized MIP using 6ml of Geranic acid crosslinker and Nicotine-Phenylalanine template.

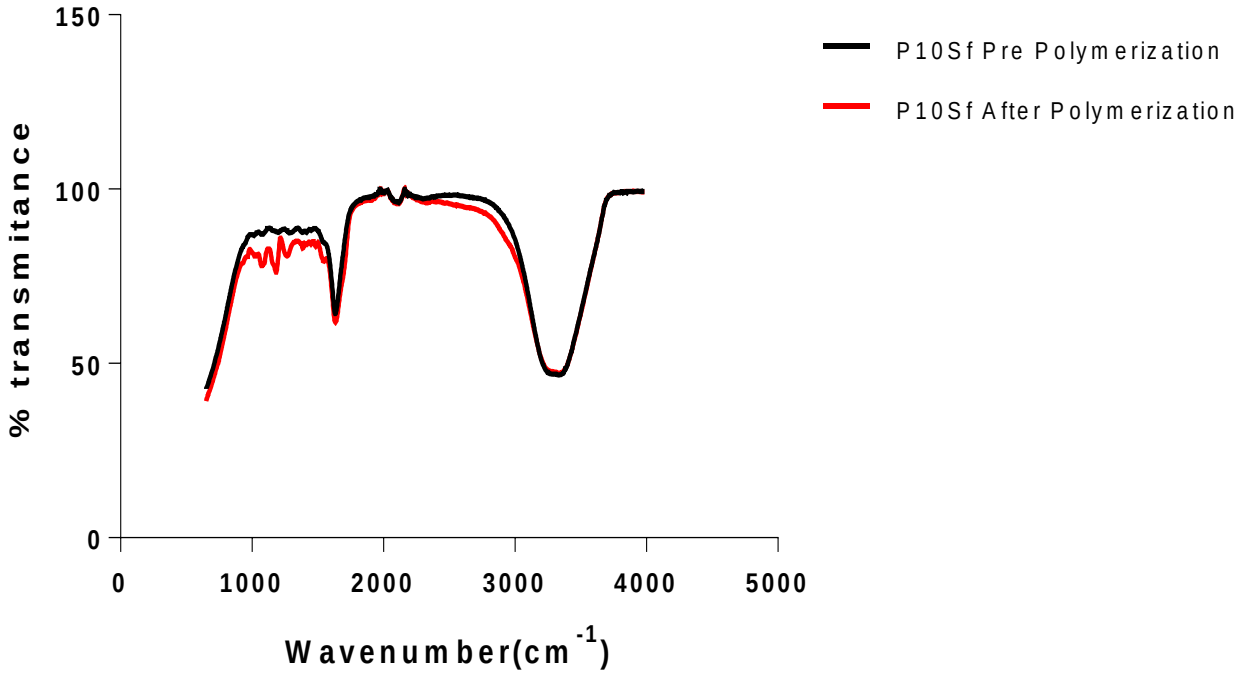

Figure 4.68: plot of pre and polymerized MIP using 5ml of Geranic acid crosslinker without template.

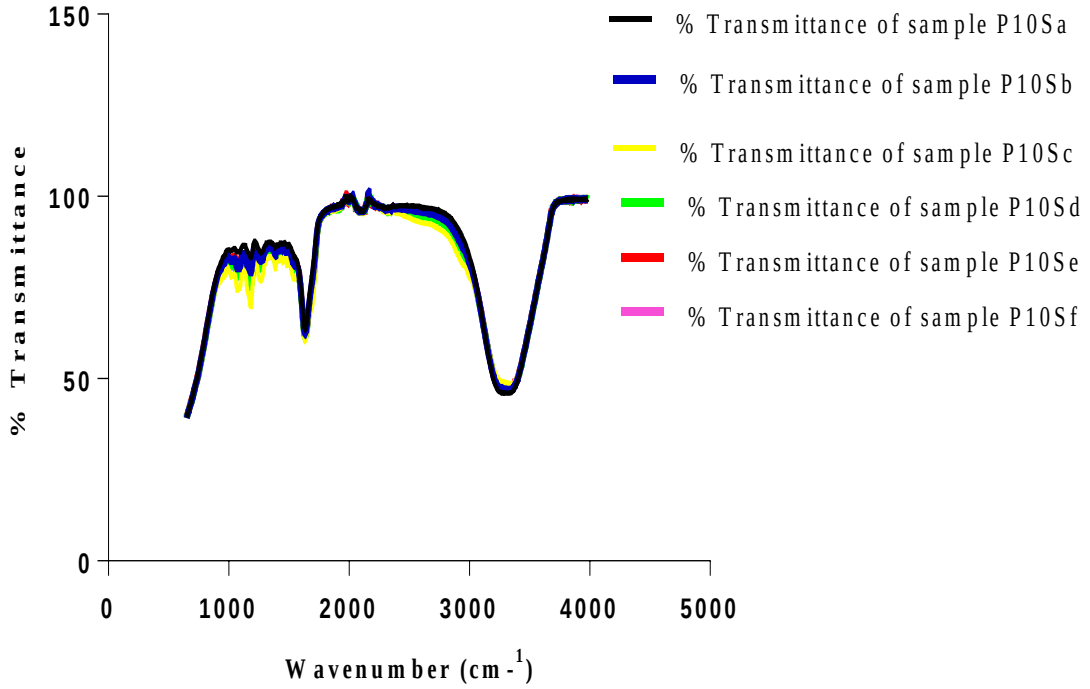

Figure 4.69: Comparative plot of % transmittance against wavenumber for Genaric acid cross linked, Nicotine-Phenylalanine templated MIPs.

Figures 4.63 - 4.68, shows the effective polymerization of the MIPs crosslinked with Geranic acid and containing Nicotine-Phenylalanine templates as compared with the Prepolymerization samples, while from figure 4.69, sample P10Sd presents the best product of the polymerization.

Conclusion

From the plots of Figures 4.55, 4.62 and 4.69, it is evident that samples P6Se for Nicotine templated, P8Sd for Phenylalanine templated and P10Sd for Nicotine-Phenylalanine templated; present the best sample products. While all the non-templated samples gave closely related results and thereby making it acceptable to choose anyone of them as the representative sample material.

4.8.1.3 Plots of FTIR results of selected best samples of BAP cross linked samples against Geranic acid cross linked samples.

4.8.1.3.1 a) Nicotine templated samples.

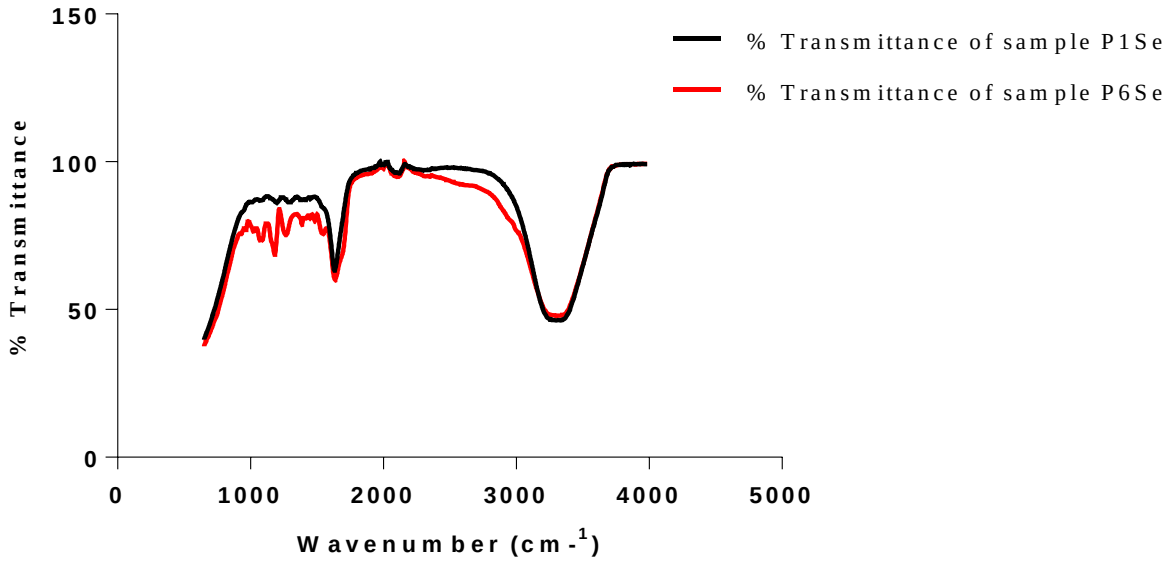

Figure 4.70: Comparative effect of cross linker type on degree of polymerization of MIP. Plot of P1Se against P6Se

4.8.1.3.2 b) Phenylalanine amide templated samples.

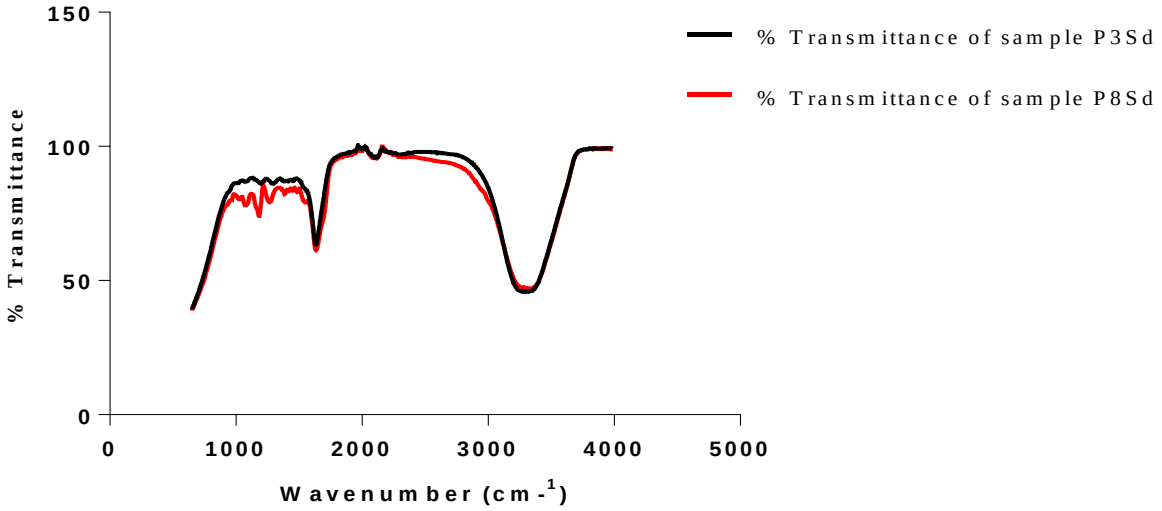

Figure 4.71: Comparative effect of cross linker type on degree of polymerization of MIP. Plot of P3Sd against P8Sd

4.8.1.3.3 c) Nicotine-Phenylalanine amide blends templated samples.

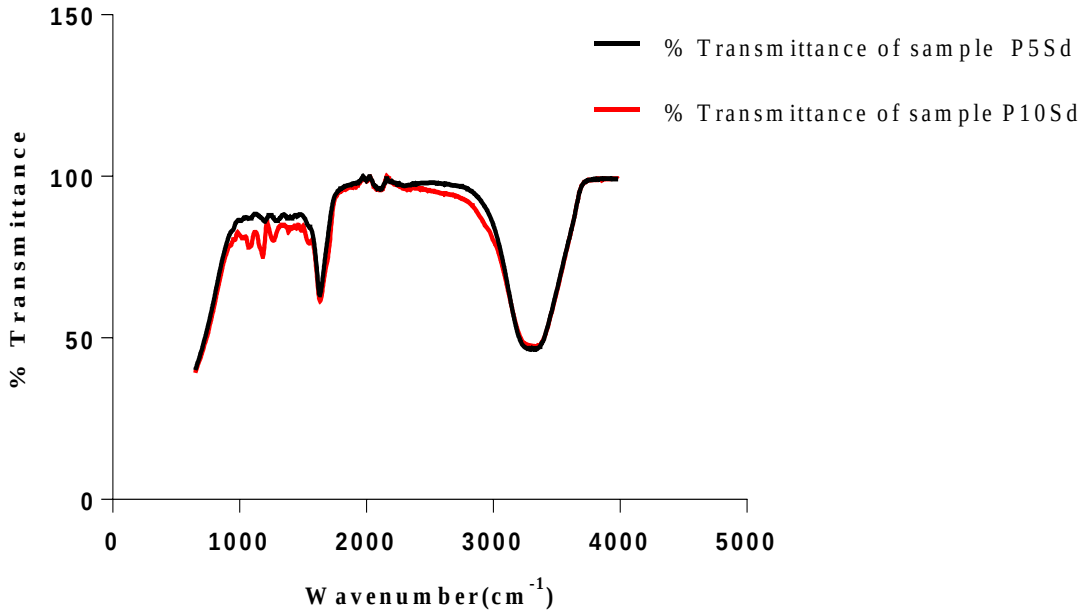

Figure 4.72: Comparative effect of cross linker type on degree of polymerization of MIP. Plot of P5Sd against P10Sd.

From Figures 4.70, 4.71 and 4.72, considering the values of the percent transmittances, MIPs cross linked with Genaric acid present better polymerized products (lower values of percentage

transmitances) than those crosslinked with 1,4 Bisacrylol. Table 4.8 shows the comparison of the prevailing vibrational frequencies in both the BAP and Geranic acid crosslinked MIPs.

Table 4.8: Comparative vibrational frequencies for select assignments in the MIP samples from sample Crosslinked with BAP and Geranic acid and the resultant differences in %Transmittance.

Functional group assignment	**Vibrational frequencies**	**%Transmitance for BAP crosslinked**	**%Transmitance for Geranic acid**	**Difference in %Transmitance**
		P1Se	**P6Se**	
Carboxyllic acid C-H, C-O-H	3306.1	40.19	47.886	+7.696
Medium intensity assignment of N=C=O	2122.7	96.019	95.06	-0.959
Amide C-O	1632.6	63.189	60.659	-2.53
CH_2, CH_3 deformations	1455.5	87.156	81.497	-5.659
Characteristic C-N	1198.3	86.109	74.885	-11.224
		P3Sd	**P8Sd**	
Carboxyllic acid C-H, C-O-H	3306.1	45.657	46.980	+1.323
Medium intensity assignment of N=C=O	2104.1	95.798	95.714	-0.084
Amide C-O	1632.6	63.386	61.468	-1.918
CH_2, CH_3 deformations	1457.4	87.05	84.279	-2.771
Characteristic C-N	1295.2	86.016	82.211	-3.849

Secondary Amine C-N Stretching	1198.3	86.058	78.756	-7.302
		P5Sd	**P10Sd**	
Carboxyllic acid C-H, C-O-H	3304.3	46.461	47.446	+0.836
Medium intensity assignment of N=C=O	2105.5	96.07	99.193	+3.123
Amide C-O	1630.7	63.258	61.803	-1.455
CH_2, CH_3 deformations	1457.4	87.215	84.667	-2.548
Characteristic C-N	1291.5	86.15	82.483	-3.667
Secondary Amine C-N Stretching	1193.3	86.05	77.343	-8.707

From Table 4.8, it is evident that the Nicotine templated MIPs that were crosslinked with BAP, gave better polymerization results with percentage transmittance of 40.19 as against the 47.89 of the Geranic acid crosslinked analogue by a resultant 7.70 % difference in transmittance. Conversely, other assignments showed Geranic acid cross-linked MIPs as having better polymerization output with the C-N assignment having the most prominent percentage difference in transmittance of -11.22, CH_2, CH_3 deformations (-5.66), amide C-O (-2.53) and N=C=O (-0.96). A similar trend occurred with the Phenylalanine templated MIP where C-H and C-O-H of the carboxylic acid (1.32), secondary amine C-N (-7.30), characteristic primary amine C-N (-3.85), CH2, CH3 deformations (-2.77); amide C-O (-1.92) and N=C=O (-0.08). The blend

template likewise trailed except with the N=C=O assignment that showed a positive percentage difference of 3.12.

In as much as the cross-linking reactions lead to the formation of chitosan derivative with superior enhanced adsorption capacity and ruggedity, it slightly decrease the adsorption capacity because some functional groups like the amino or hydroxyl groups take part in the cross-linking and therefore unavailable for adsorption activities (Kyzas and Bikiaris, 2015). The inclusion of the Methacrylic acid which is a form of grafting compensates for this by increasing the number of adsorption sites and consequently the adsorption capacity. Presence of double bonds enhances susceptibility to polymerization reactions and improves the degree of crosslinking which help maintain the structure of the template based cavity irrespective of solvent medium, (Chen, *et al.,* 2016). Close similarity of the geranic acid cross linker in chemical reactivity maybe the reason for it imparting better copolymerization reaction (Xu, *et al.,* 2015) as evidenced from the result of the FTIR spectroscopy. This is advantageous because it prevents the unwanted dominance of either the monomers or the cross linker during polymerization process (Xu, *et al.,* 2015). With the use of Geranic acid, functional groups, such as the COOH and OH, were more dominant and active as evidenced by the percentage transmittance values from the charts of PS6, PS8 and PS10 in relation to those of PS1, PS3 and PS5. This created a more robust imprinting platform for the target templates as noted by the difference in percent transmittances between the pre and post polymer samples for BAP cross linked MIPs/NIPs and for Geranic acid crosslinked MIPs/NIPs.

4.9 Surface Morphology.

The MIP/NIP materials were further characterized based on their morphology using three instrumental tecniques, Field Emission Scanning Electron Microscope (FESEM), Transmission Electron Microscope (TEM) and gas (Nitrogen) sorption measurement using the Brunaruer-Emmet-Teller (BET) method. These analyses substantiated the fundamental physio-structural attributes of the materials which endows on them the observed recognition potential.

4.9.1 Field Emission Scanning Electron Microscopy (FESEM).

4.9.1.1 Field Emission Scanning Electron Micrographs of Samples from Microwave heated, Nicotine Templated BAP cross linked MIP.

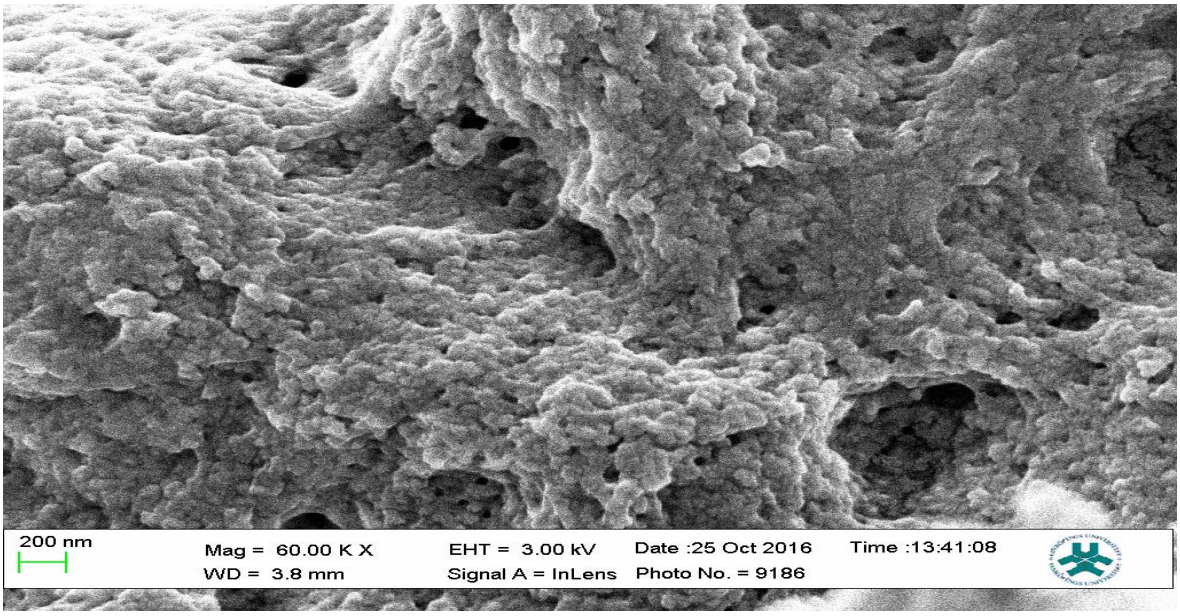

Plate 4.1: MP1Sd

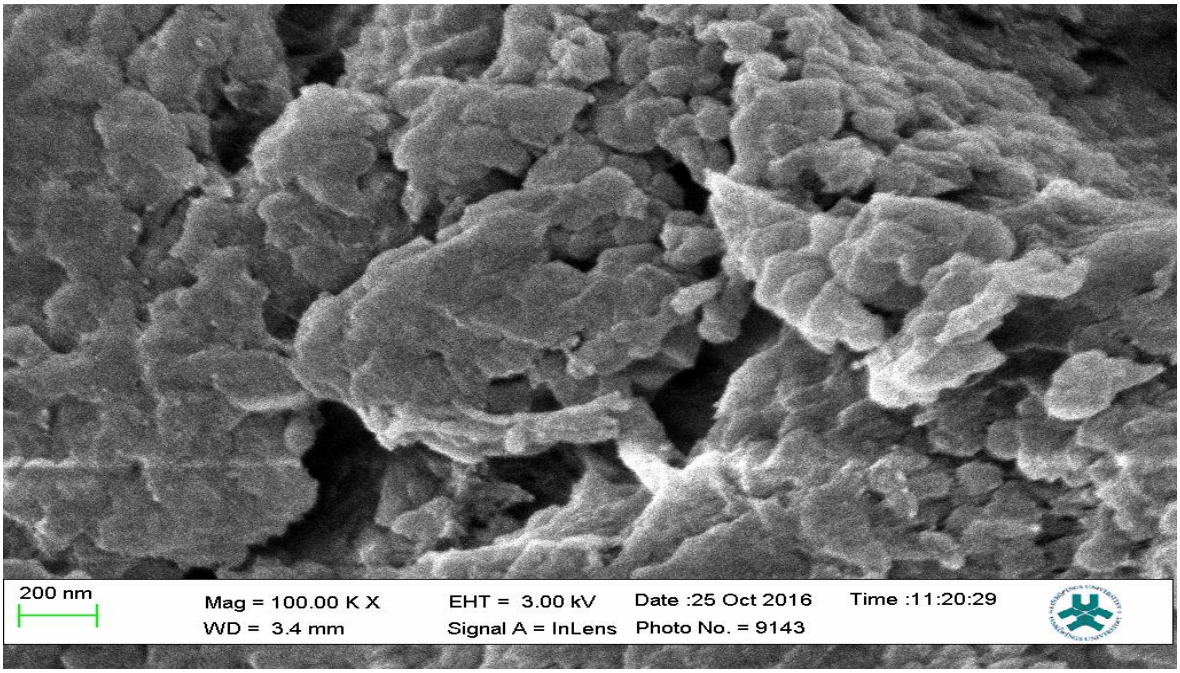

Plate 4.2: MP1Sf

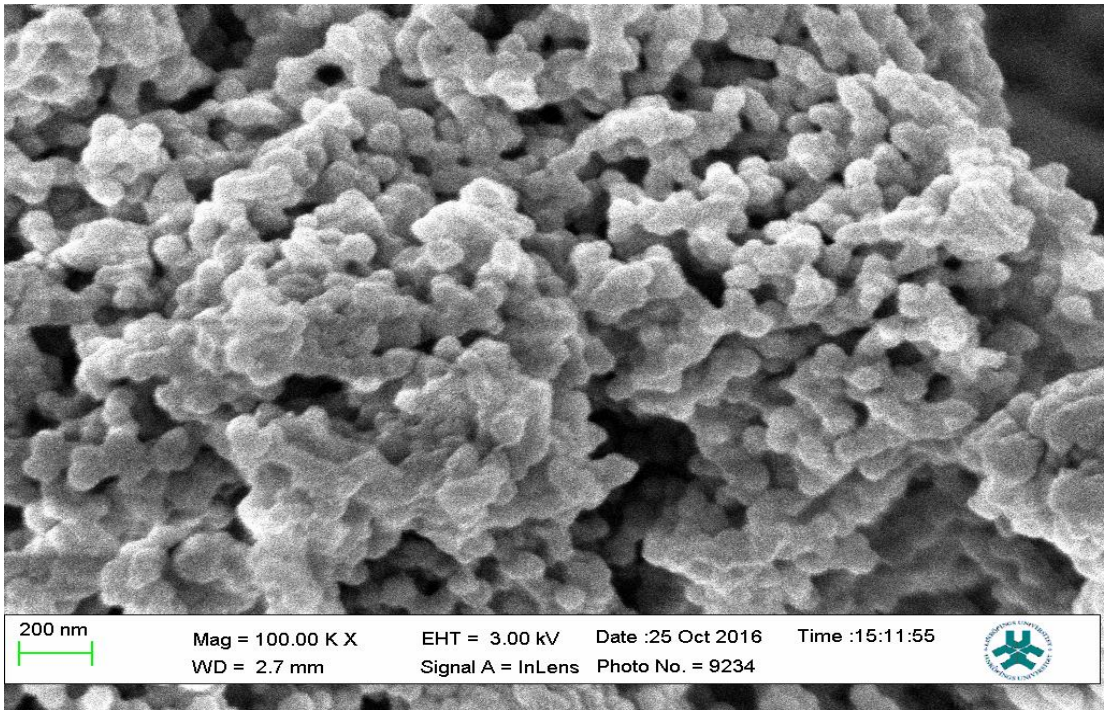

Plate 4.3: MP3Sd

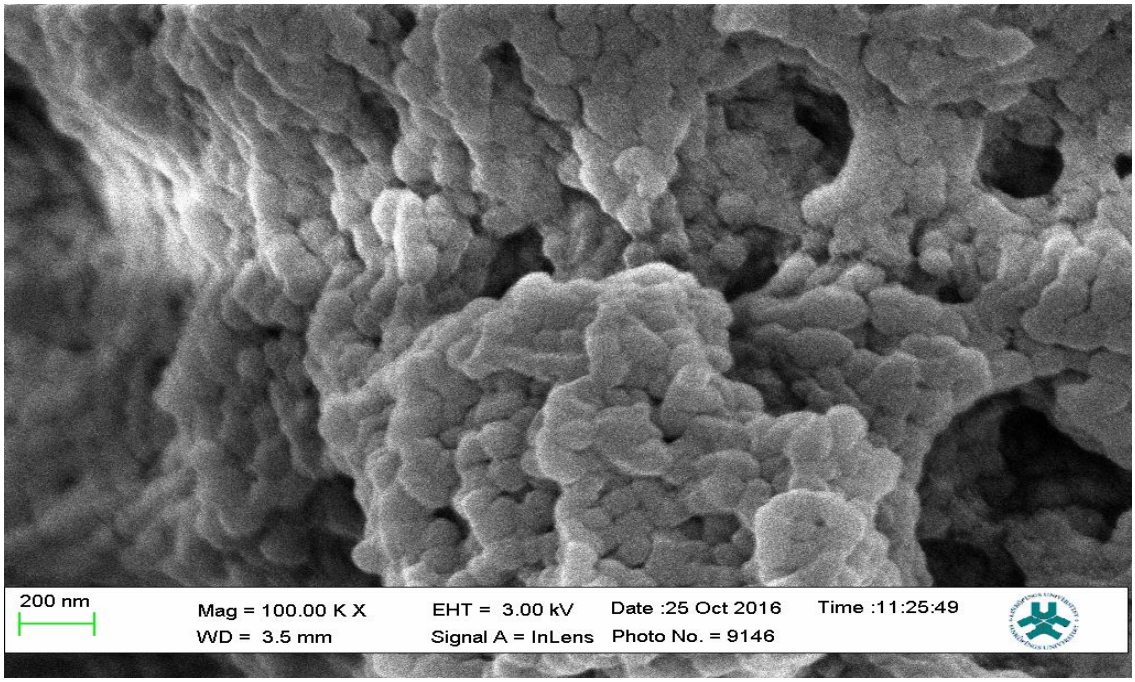

Plate 4.4: MP5Sd

4.9.1.2 Field Emission Scanning Electron Micrographs of Samples from Microwave heated Phenylalanine Templated Geranic acid cross linked MIP.

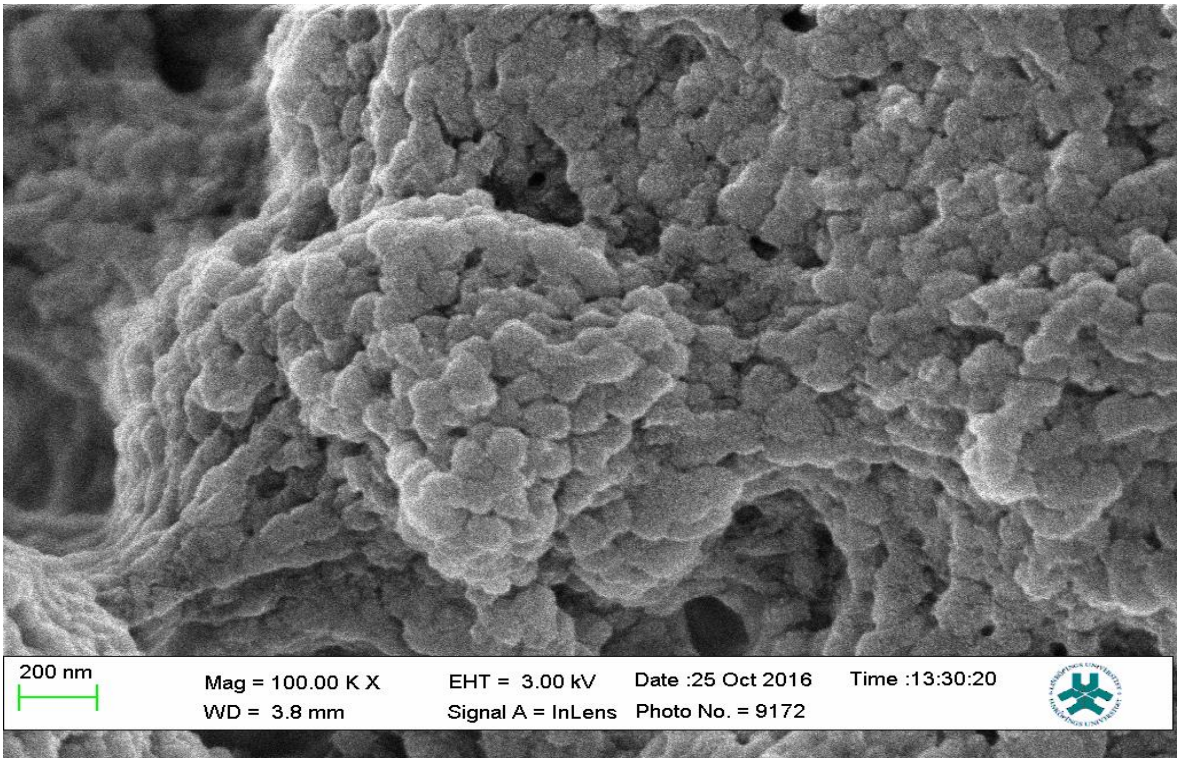

Plate 4.5: MP6Sd

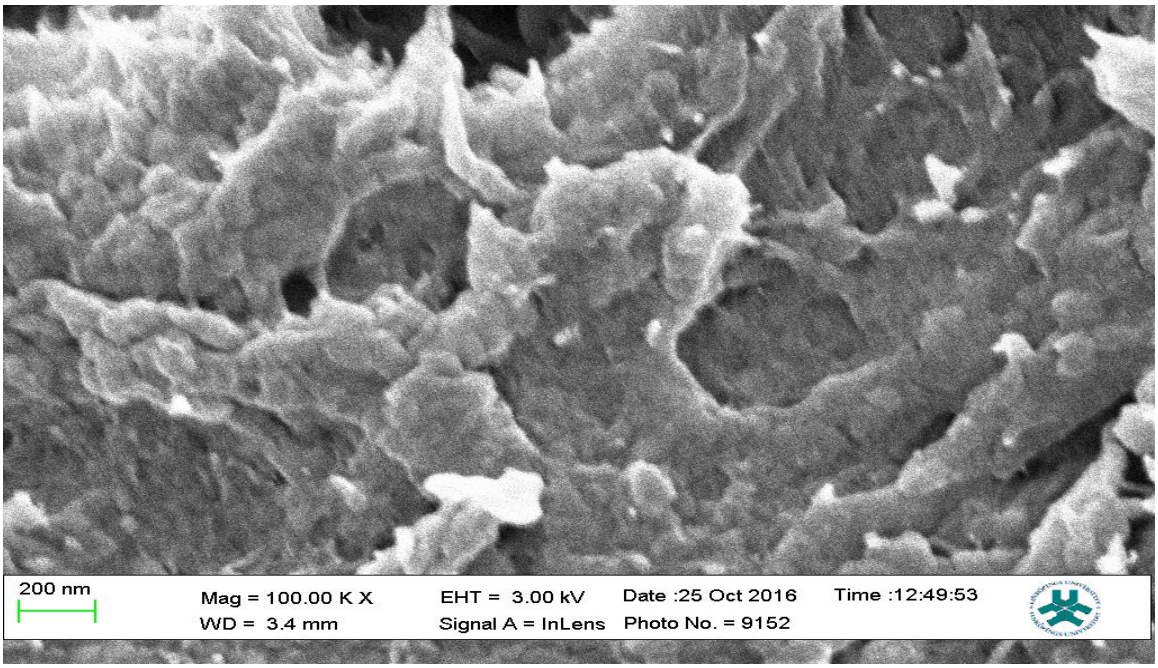

Plate 4.6: MP8Sd

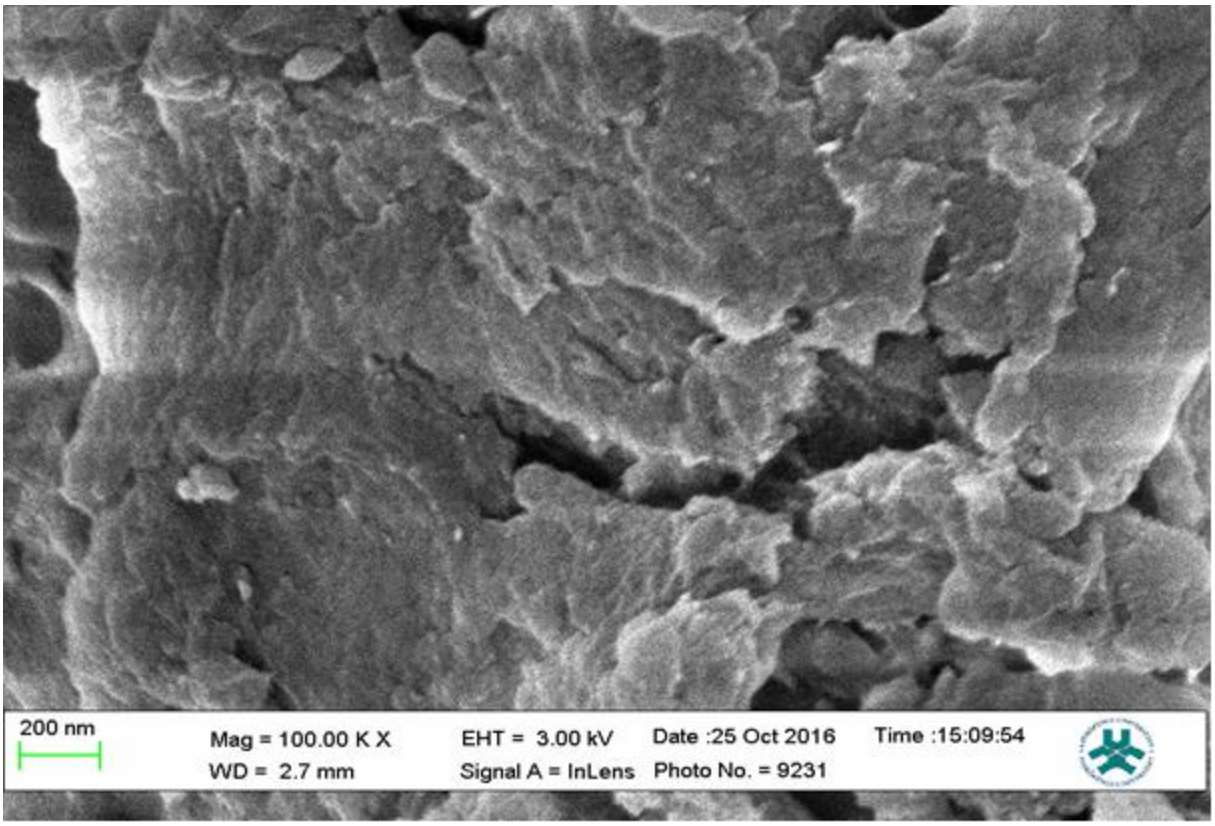

Plate 4.7: MP10Sd

4.9.1.3 Field Emission Scanning Electron Micrographs of Samples from Water bath heated Nicotine Templated BAP cross linked MIP.

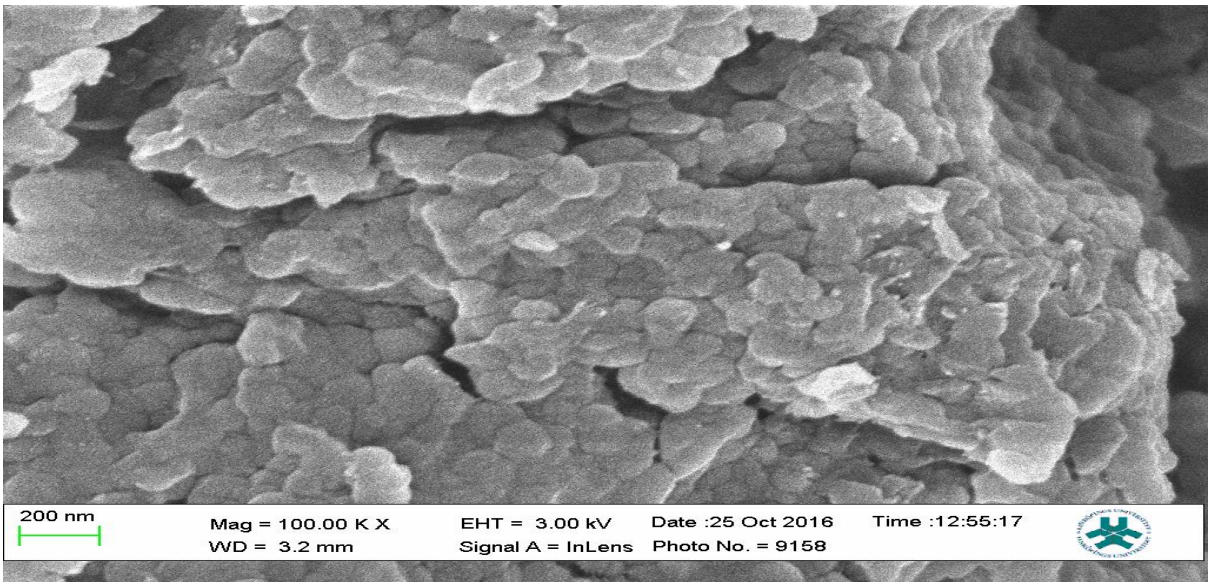

Plate 4.8: P1Sd

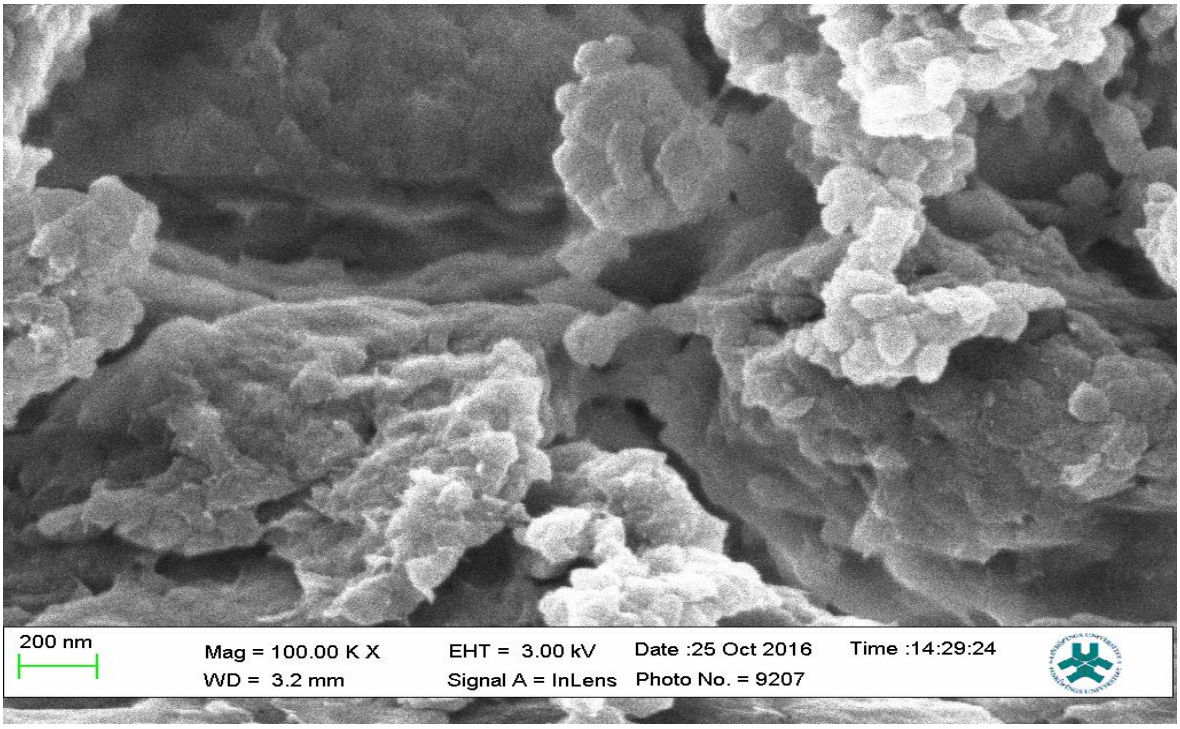

Plate 4.9: P1Sf

4.9.1.4 Field Emission Scanning Electron Micrographs of Samples from Water bath heated Phenylalanine Templated BAP cross linked MIP.

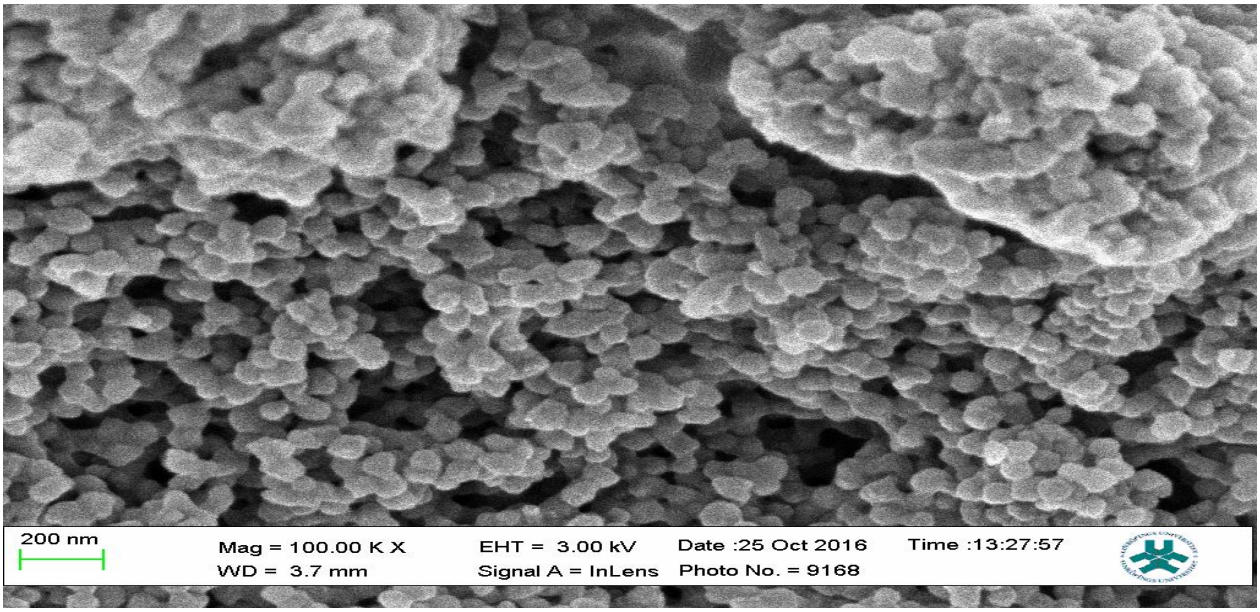

Plate 4.10: P3Sc

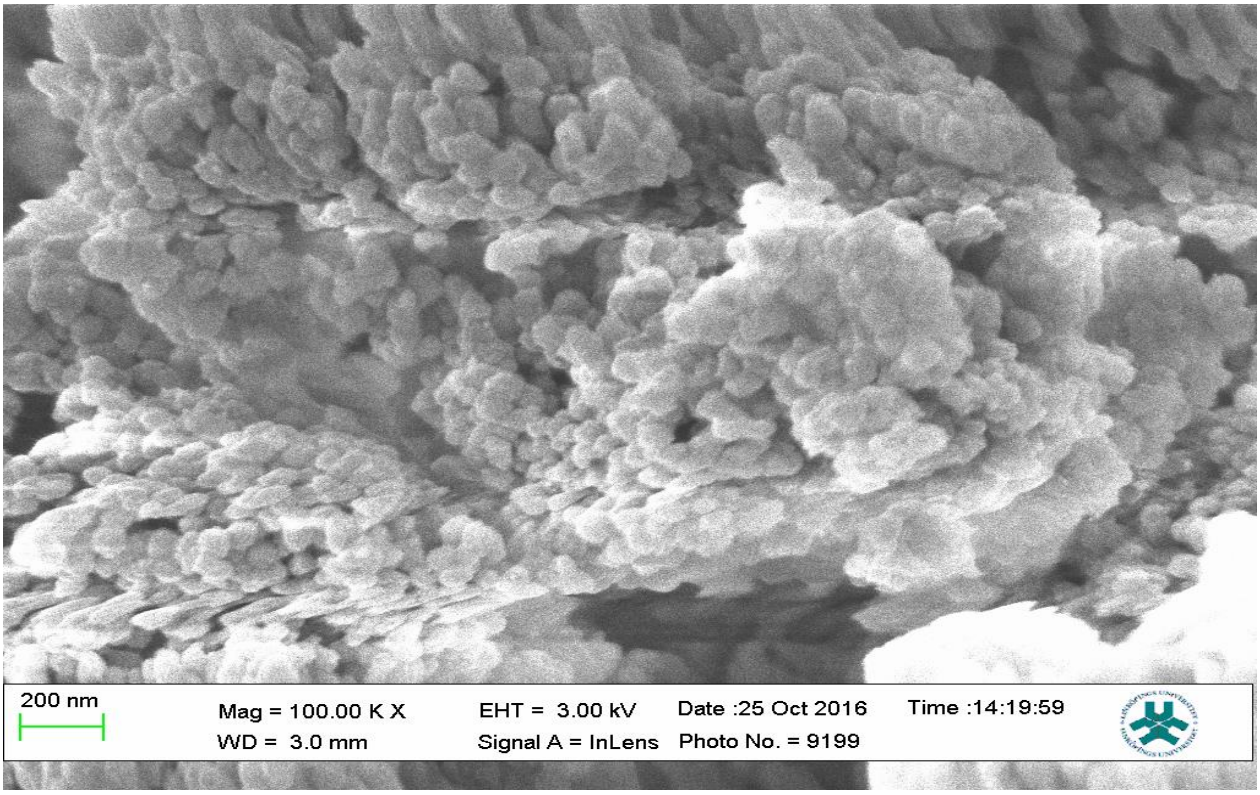

Plate 4.11: P3Sd

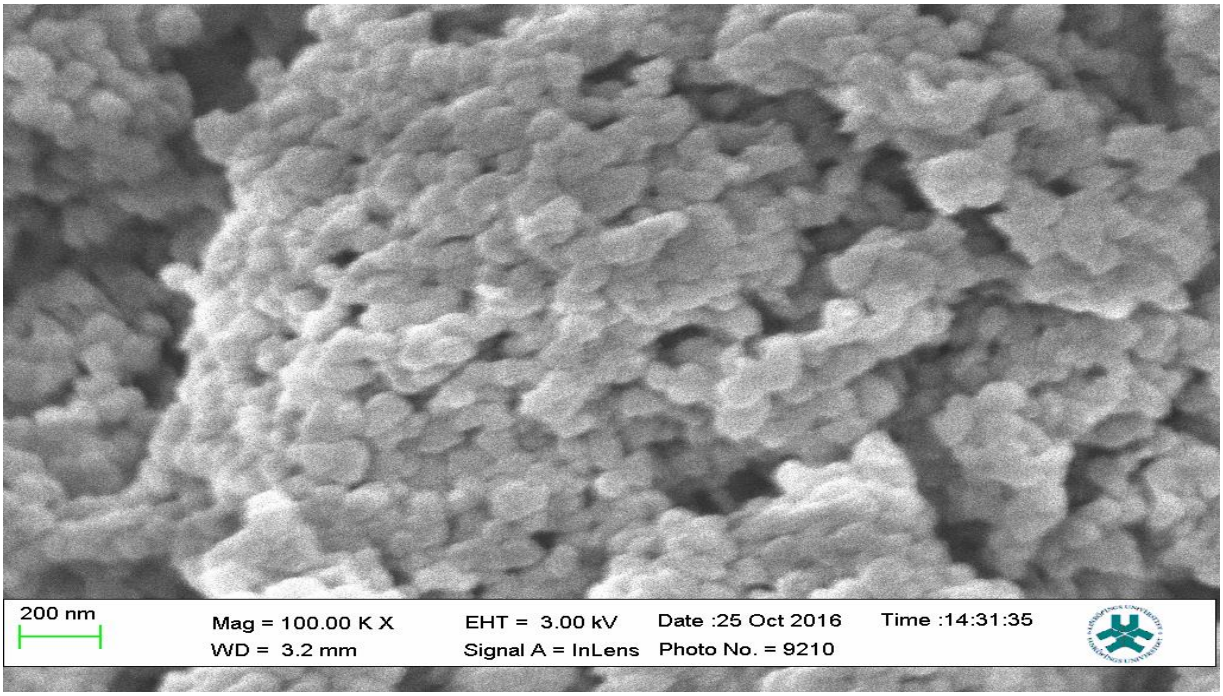

Plate 4.12: P3Sf

4.9.1.5 Field Emission Scanning Electron Micrographs of Samples from Water bath heated Nicotine-Phenylalanine Templated BAP cross linked MIP.

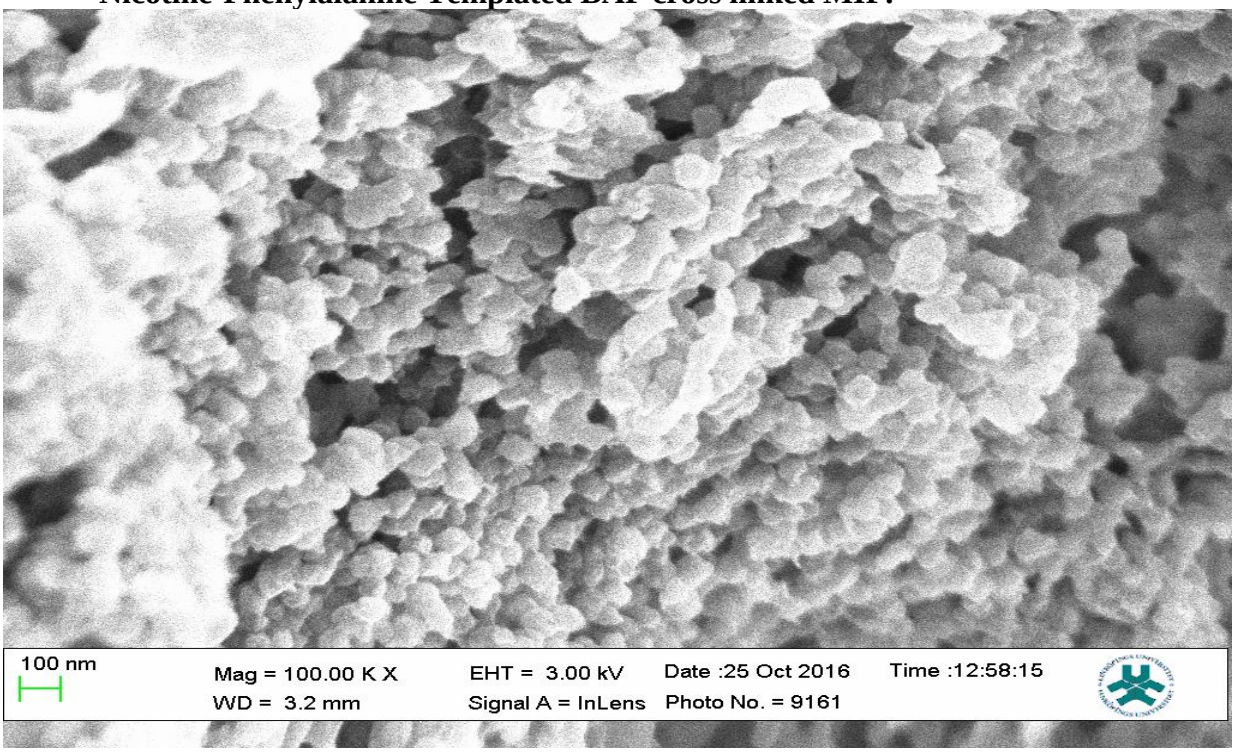

Plate 4.13: P5Sc

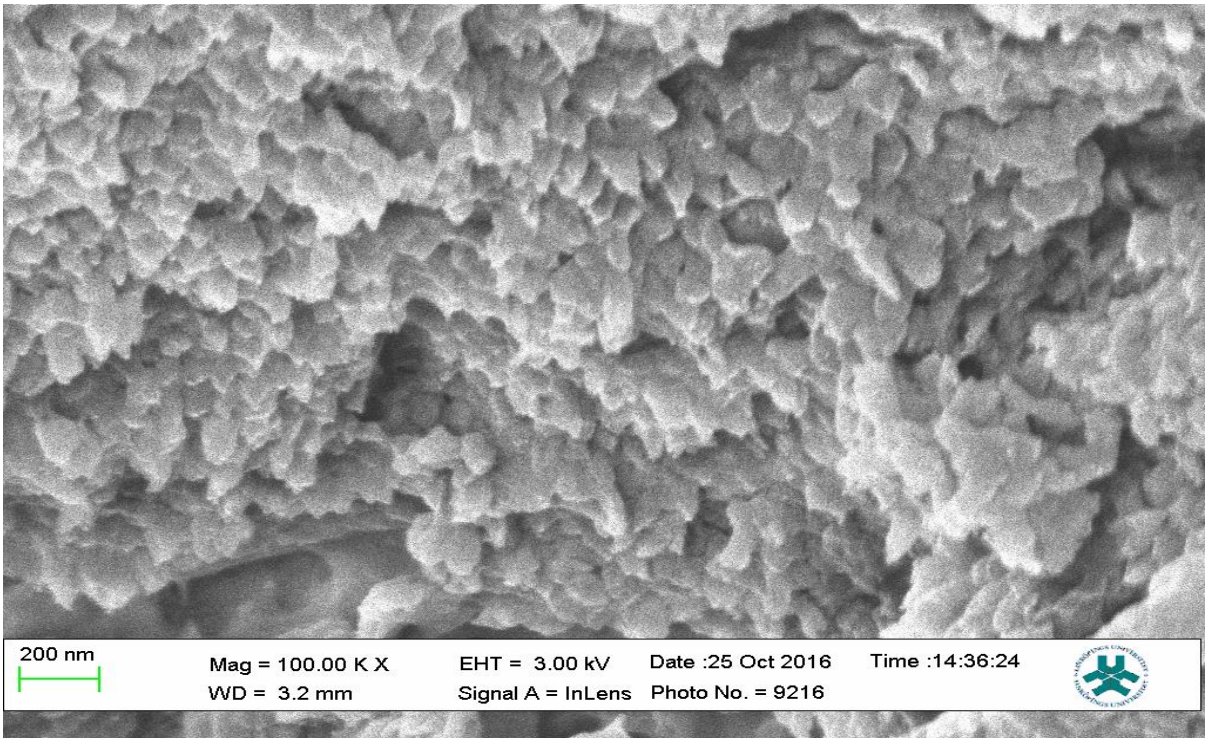

Plate4.14: P5Sf

4.9.1.6 Field Emission Scanning Electron Micrographs of Samples from Water bath heated Nicotine Templated Geranic acid cross linked MIP.

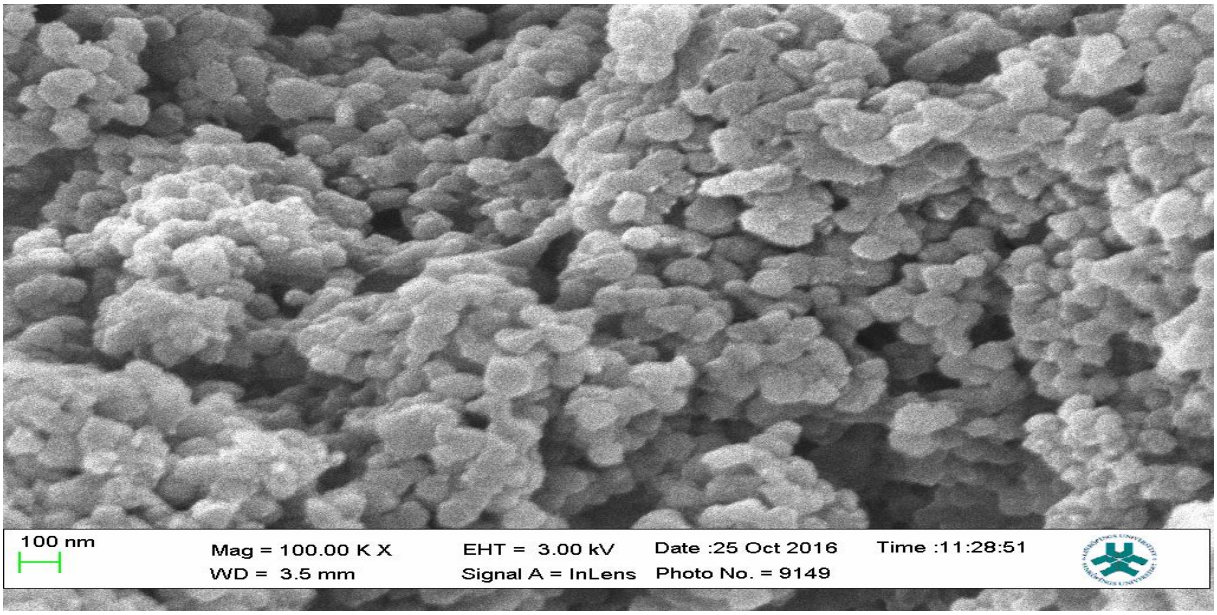

Plate 4.15: P6Sb

4.9.1.7 Field Emission Scanning Electron Micrographs of Samples from Water bath heated Phenylalanine Templated Geranic acid cross linked MIP.

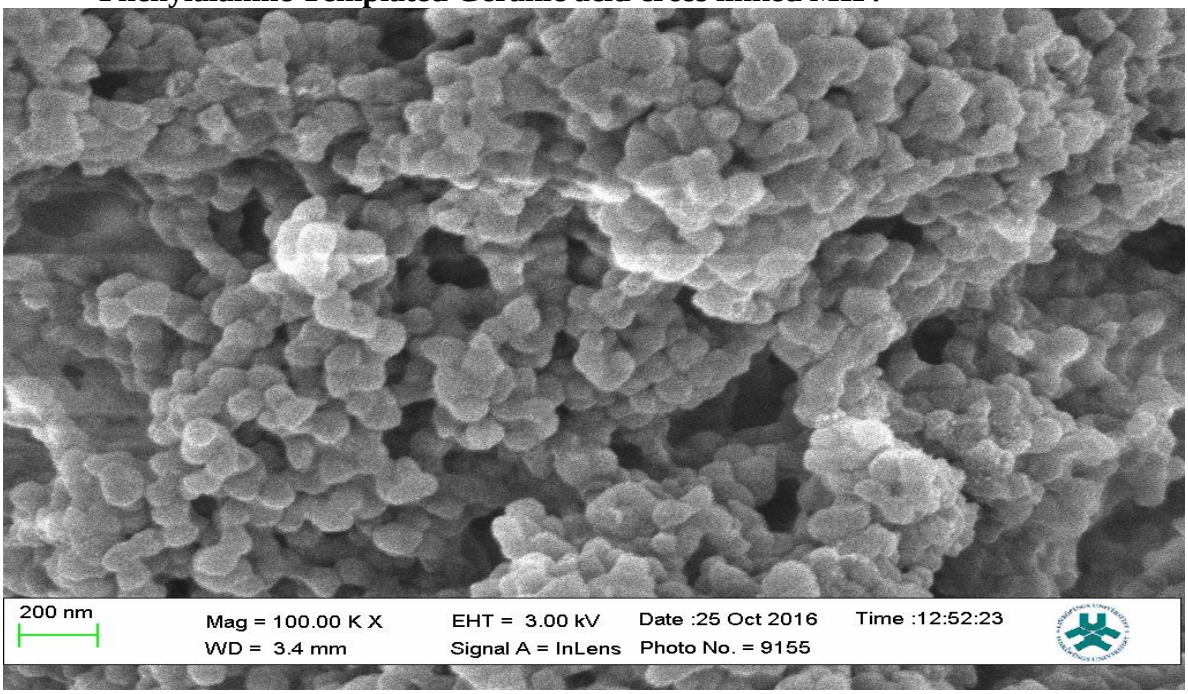

Plate 4.16: P8Sd

4.9.1.8 Field Emission Scanning Electron Micrographs of Samples from Water bath heated Nicotine-Phenylalanine Templated Geranic acid cross linked MIP.

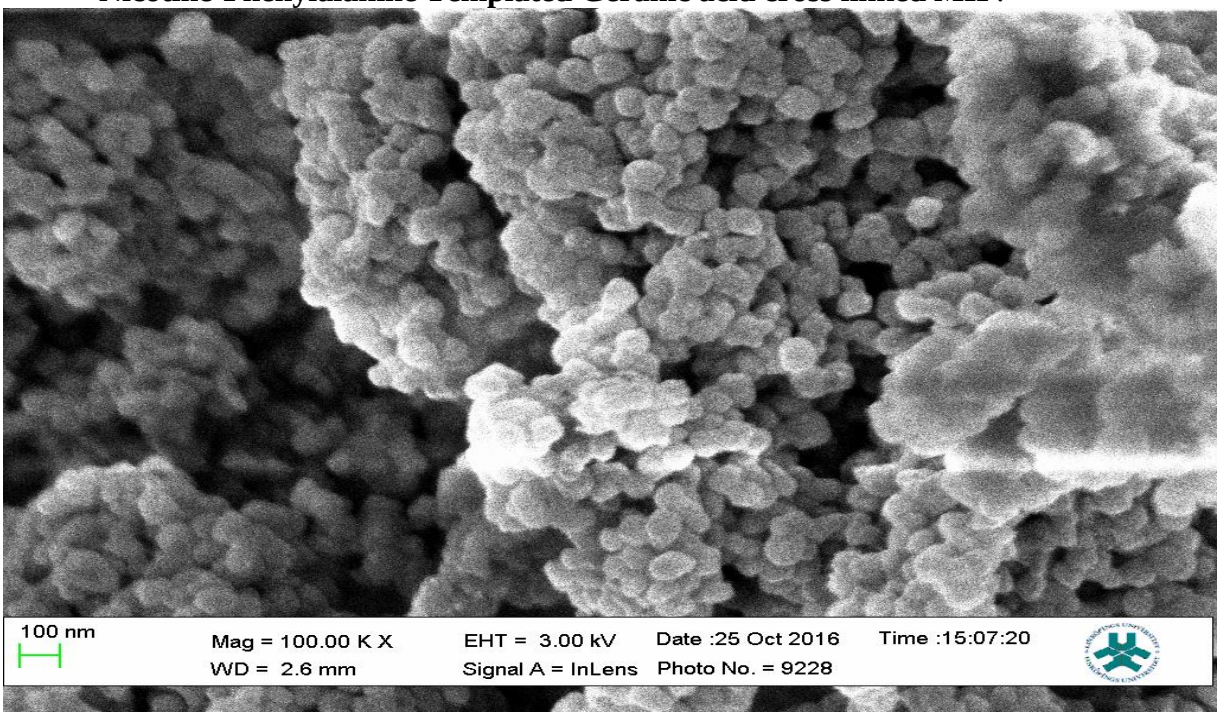

Plate 4.17: P10Sd

The SEM micrographs present the representative samples as being spherical in their morphology. The MIPs (Plates 4.7 and 4.8), are observed to have cavities but with a linked hirachirchal type of network while the NIP (Plate 4.9) does not possess such attribute. This is due to the non-templating of the polymer which ensured that cavities as obtainable with the MIPs are not created. The particles are mesoporous and clustered, presenting a mesh-like framework which is a disadvantage for typical SPE application but acceptable for sequestration of very closely clustered materials as is obtained with fluid cocktails such as smoke streams. The sizes are 200nm for the MIPs and 100nm for the NIP. This difference in size easily implicates the templating and non-templating activities carried out during polymerization. The respective surface area (26.455, 76.635 and 5.339) for 3PhenylPiridine, Nicotine-3PhenylPiridine and the non-templated respectively; Pore volume (0.067, 0.219 and 0.010) and pore diameter (3.411, 3.411and 4.302) values (Table 4.9), align with the observed presentation except for the pore diameter of the NIP which is more than that of the MIPs. The MIPS are polydispersed as indicated by their different aggregate sizes 61and this is in tandem with the micrographs of the TEM. The MIPS are polydispersed as indicated by their different aggregate sizes and this is in tandem with the micrographs of the TEM.

4.9.2 TEM RESULTS:

4.9.2.1 MICROGRAMS FROM TEM ANALYSIS

Plate 4.18: Representative Sample P1Sa

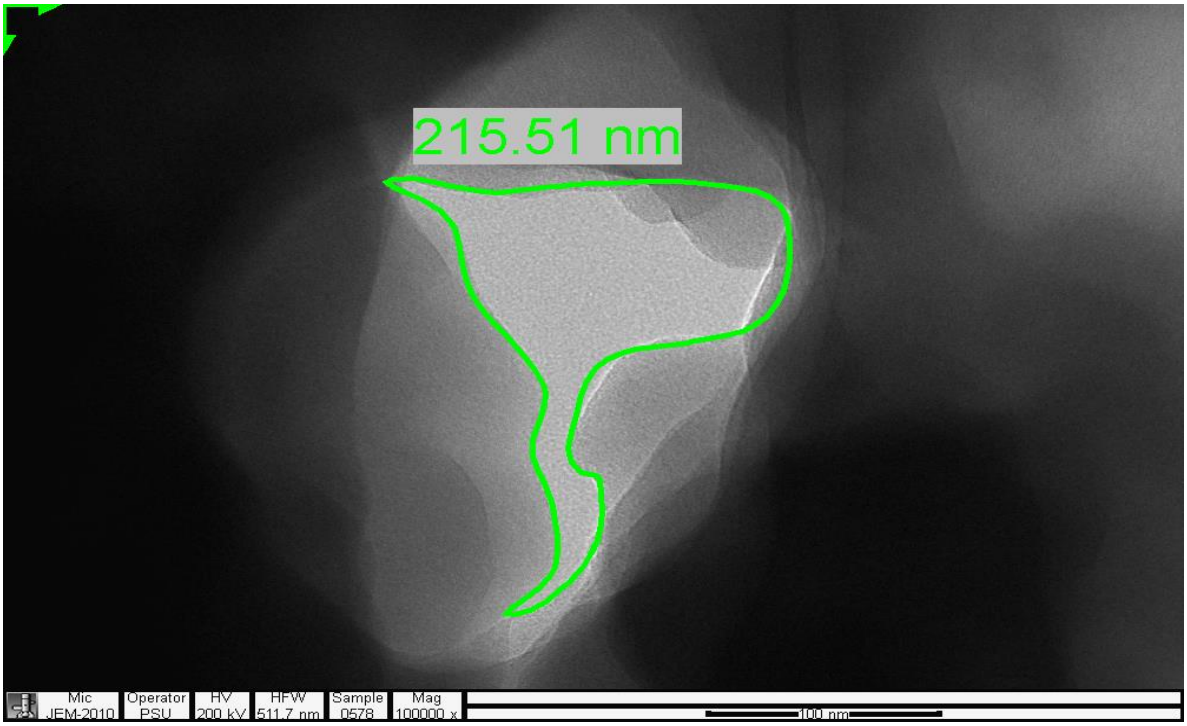

Plate 4.19: Representative Sample P1Sd

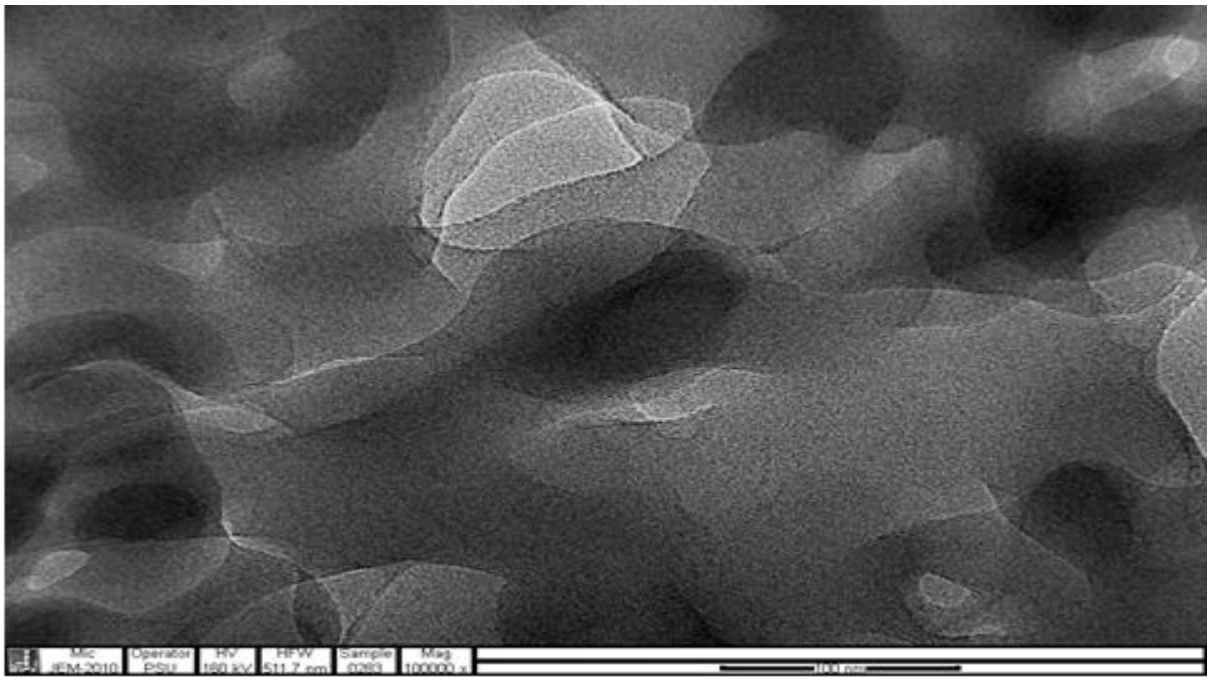

Plate 4.20: Representative Sample P1Sf

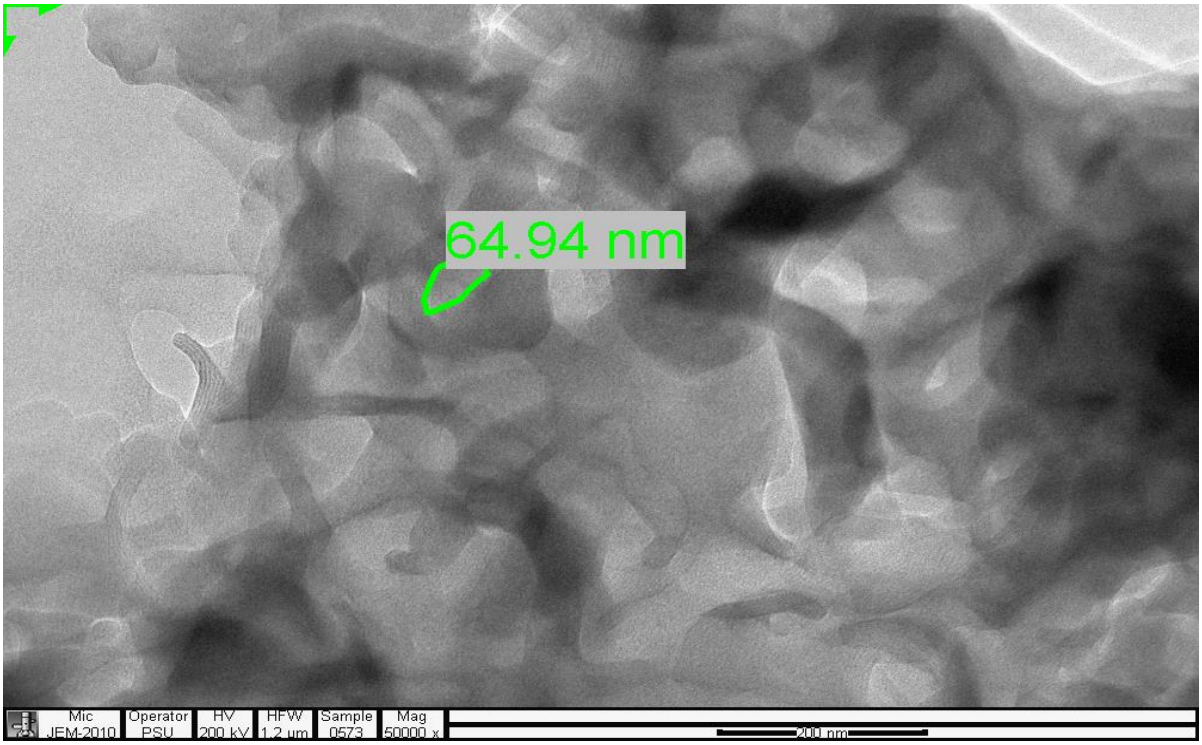

Plate 4.21: Representative P3Sc

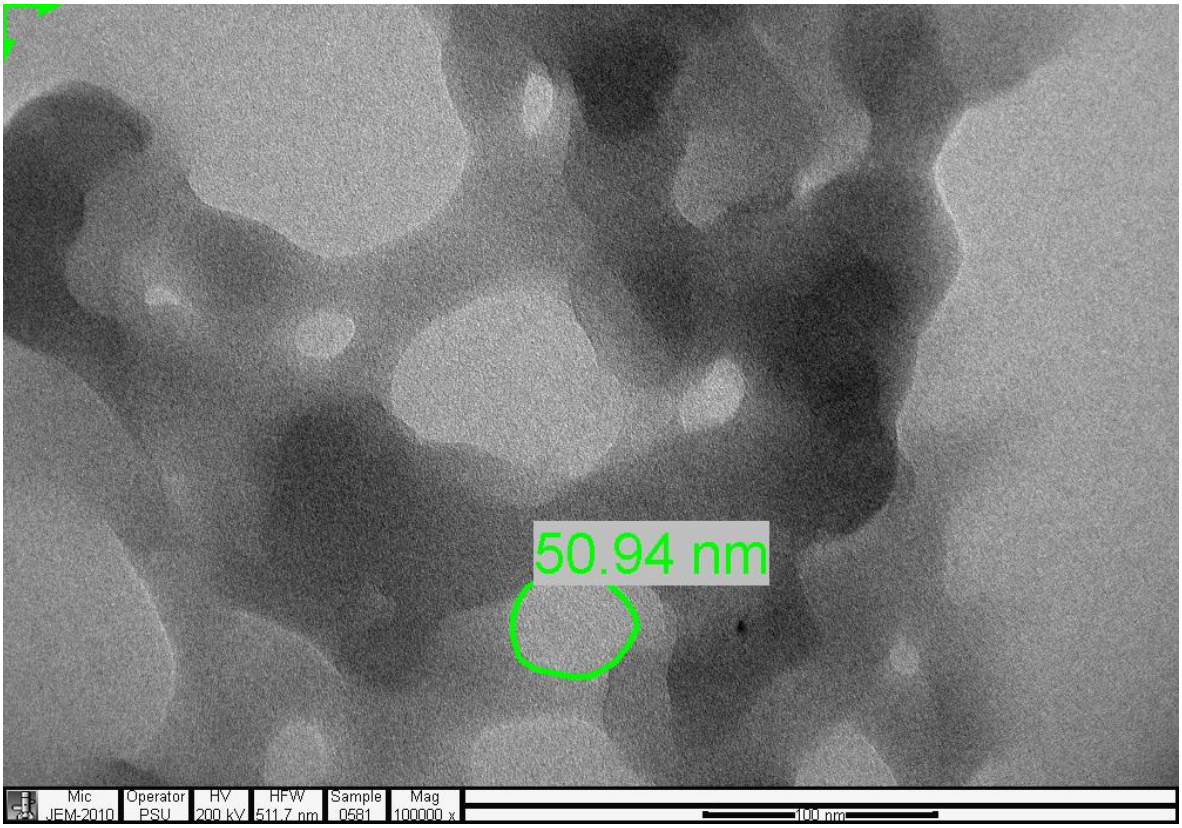

Plate 4.22: Representative Sample P3Sd

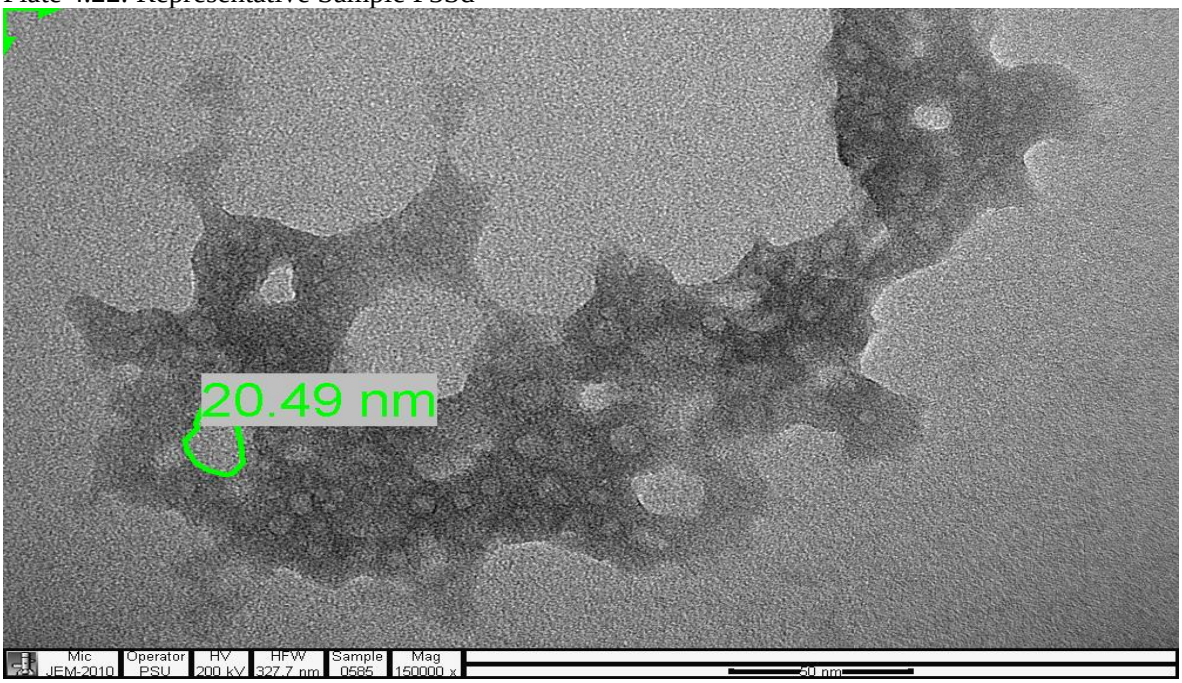

Plate 4.23: Representative Sample P3Sf

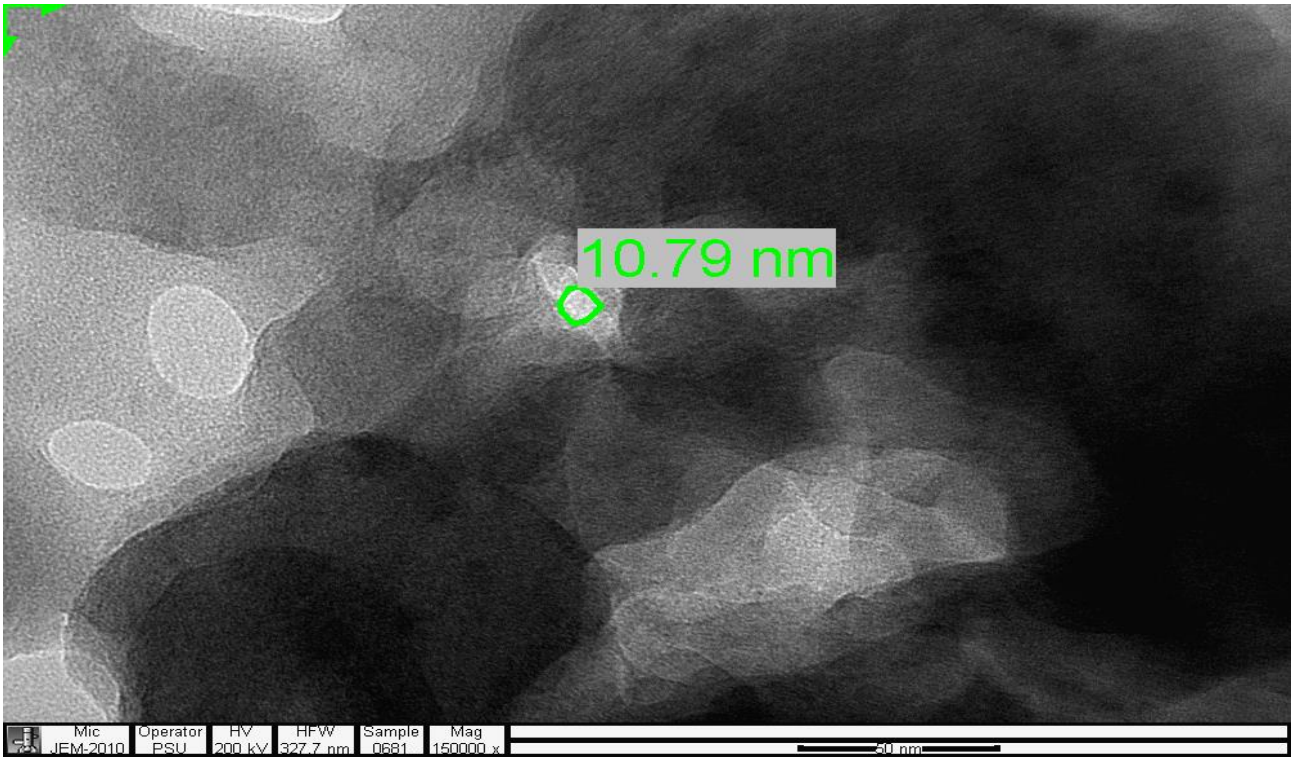

Plate 4.24: Representative Sample P5Se

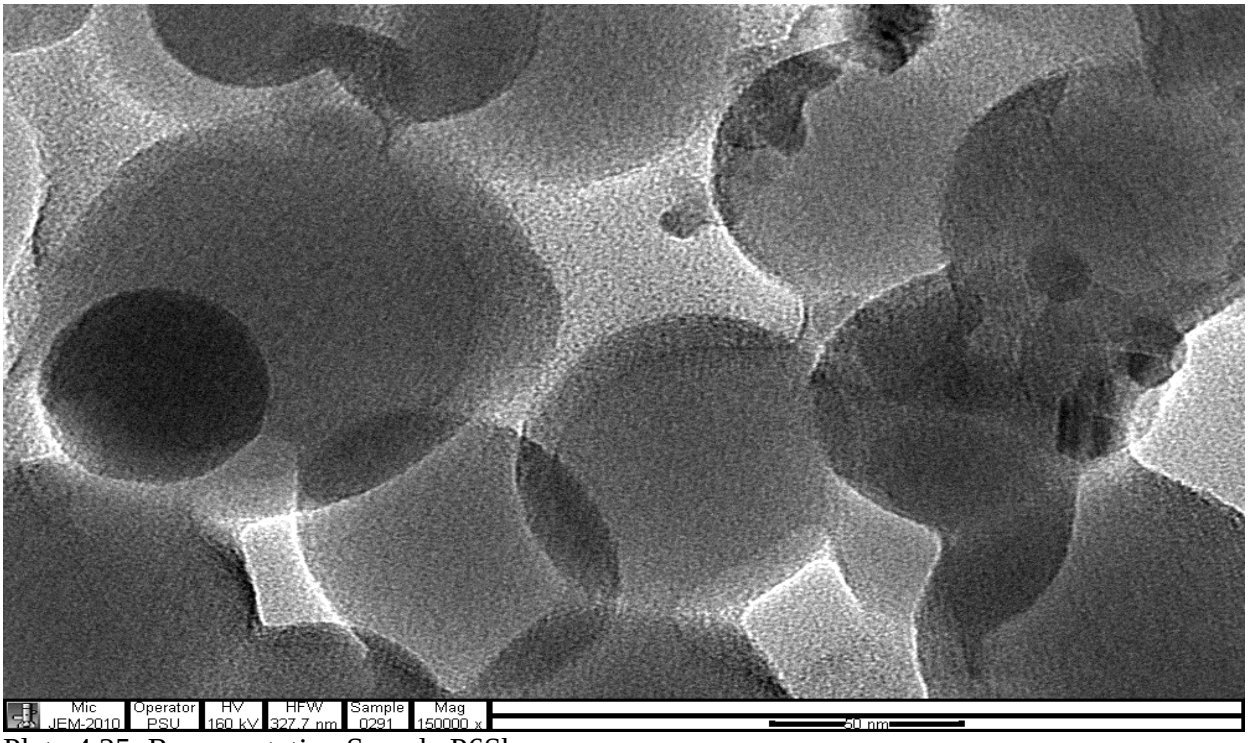

Plate 4.25: Representative Sample P6Sb

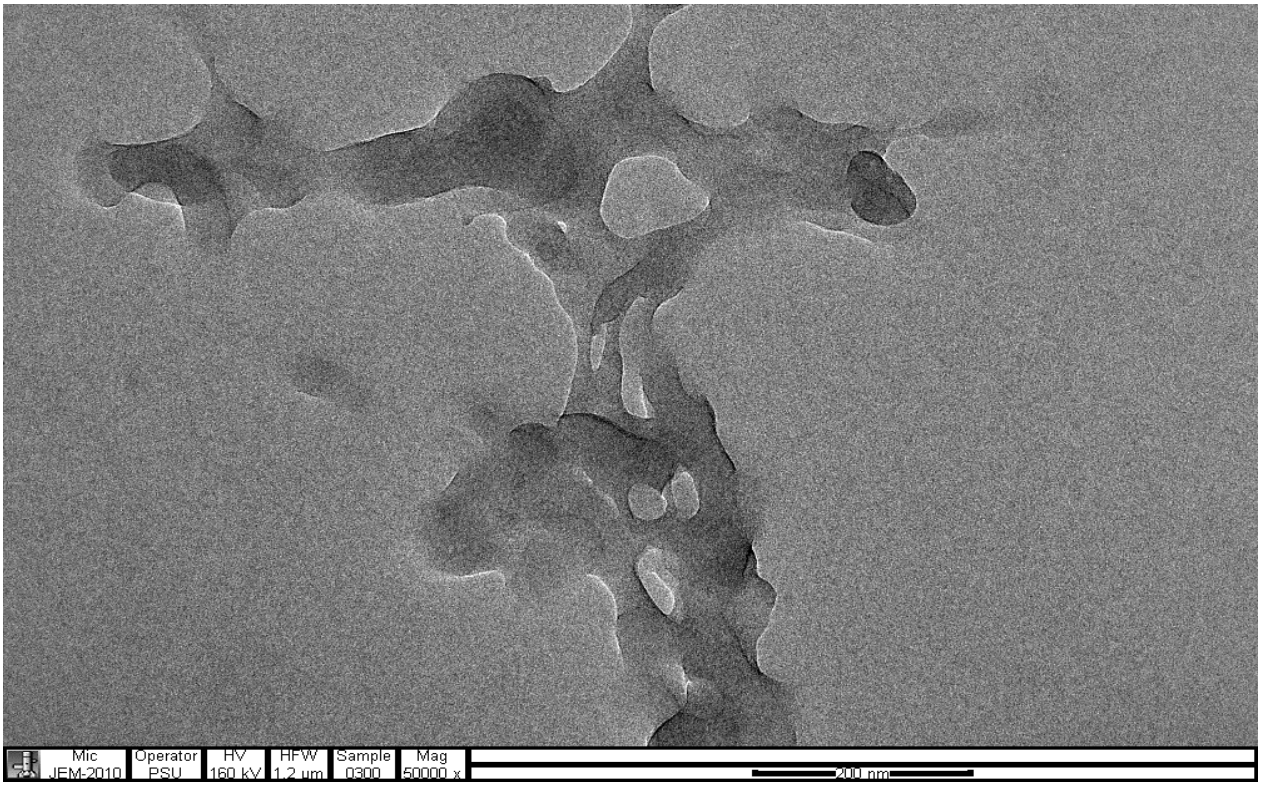

Plate 4.26: Representative Sample MP1Sd

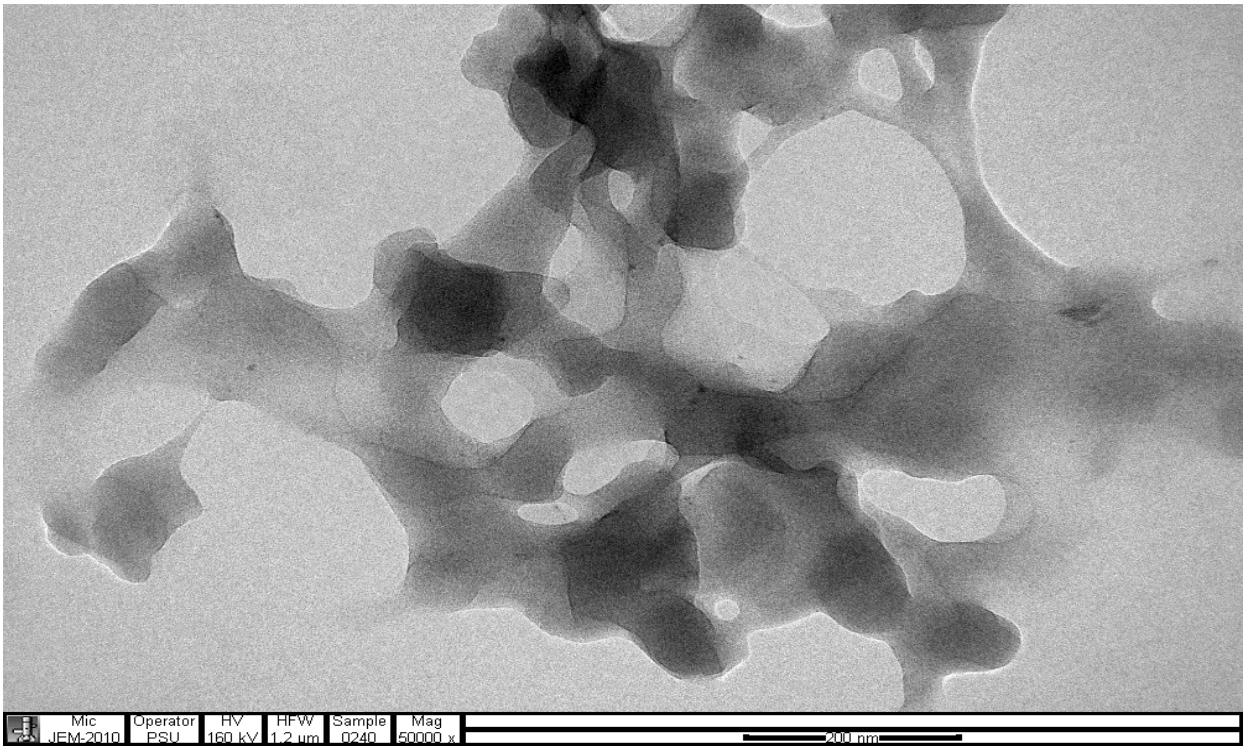

Plate 4.27: Representative Sample MP3Sd

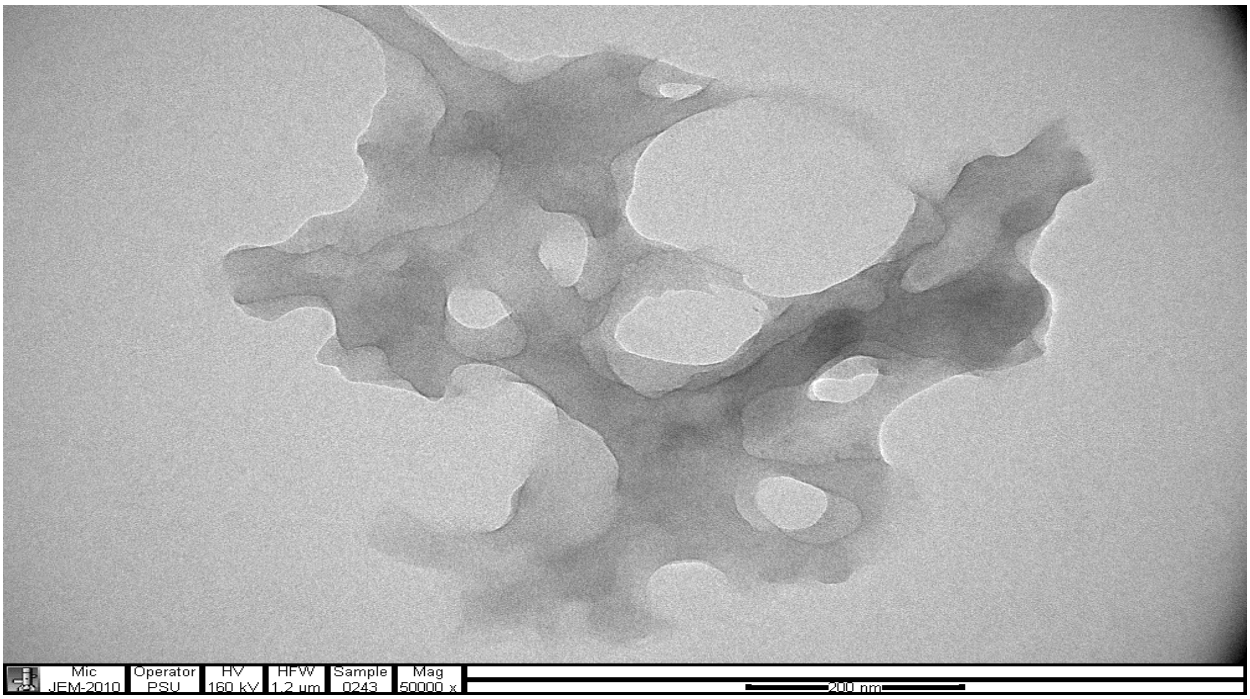

Plate 4.28: Representative Sample MP6Sd

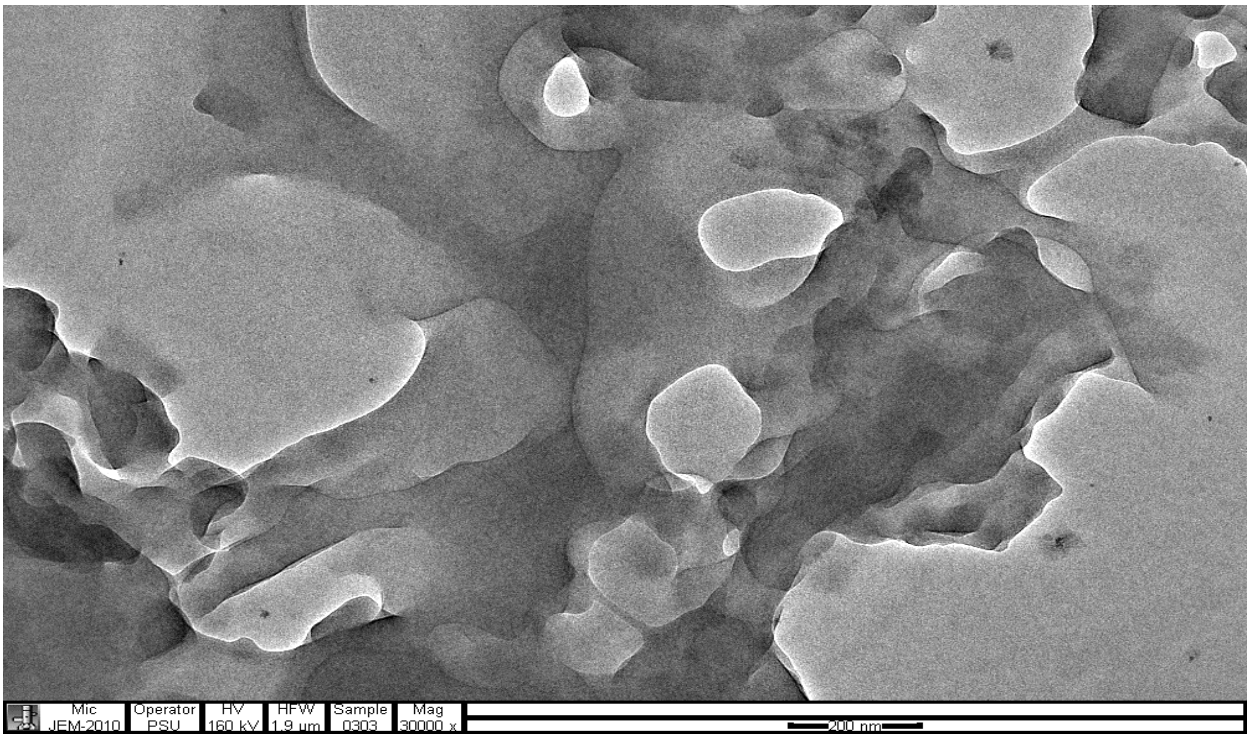

Plate 4.29: Representative Sample MP8Sd

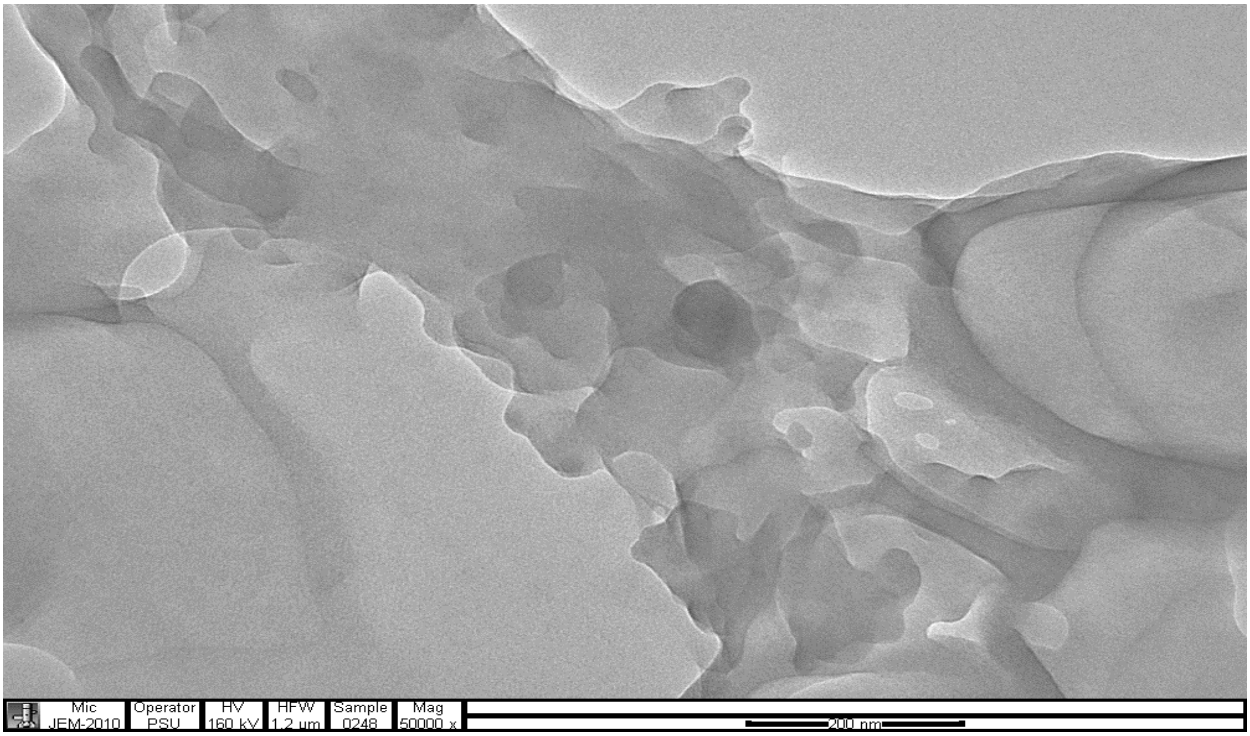

Plate 4.30: Representative Sample MP10Sd

The results from the TEM analysis (Plates 4.18 – 4.30) present the samples as being conical and cylindrical cavities that are tapered. These tapered ends give converging cavity widths of averagely wider than 4nm sizes. This creates the phenomena of sequestration by capilary action.

4.10 SURFACE AREA, PORE SIZE and PORE VOLUME, (BET and BJH ANALYSIS) RESULTS.

Table 4.9: BJH desorption result summary

Sample	Surface Area (m^2g^{-1})	Pore Volume (ccg^{-1})	Pore Diameter (nm)
P3Sd	26.455	0.067	3.411
P5Sd (BAP cross linked blend templated)	**27.072**	**0.112**	**3.823**
P5Sf	76.635	0.219	3.411
P10Sd (Geranic acid cross linked blend templated)	**27.577**	**0.078**	**3.826**
MP3Sd(microwave heating)	5.339	0.010	4.302

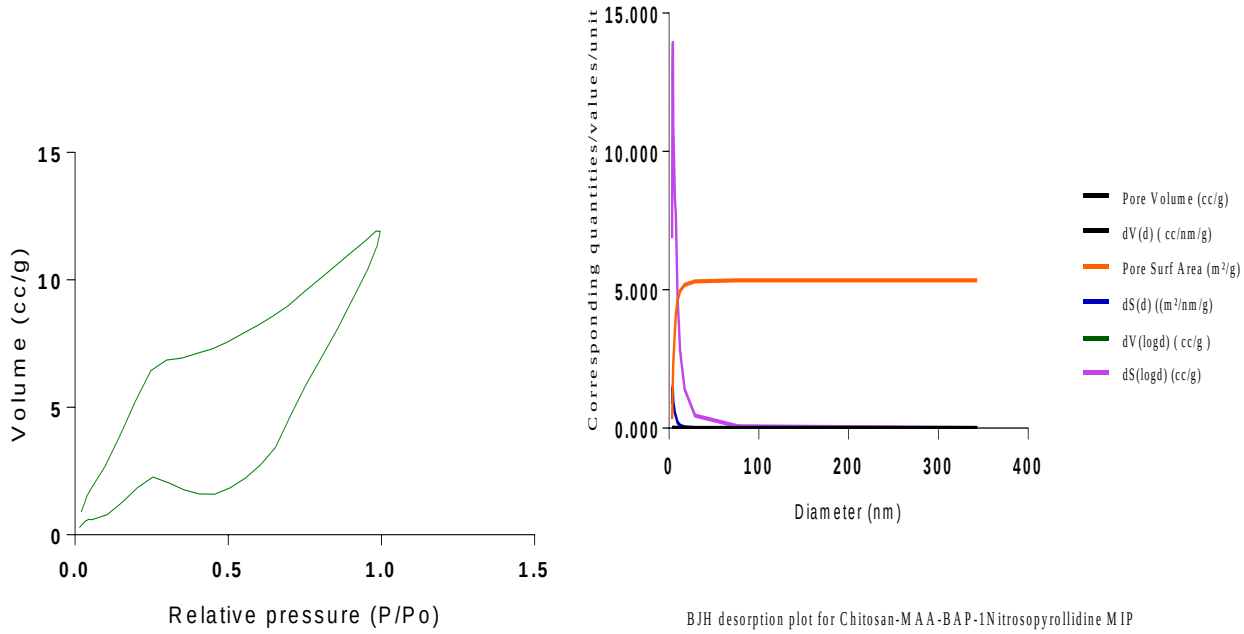

Figure 4.73:BET isotherm for Chitosan-MAA-1Nitrosopyrollidine NIP

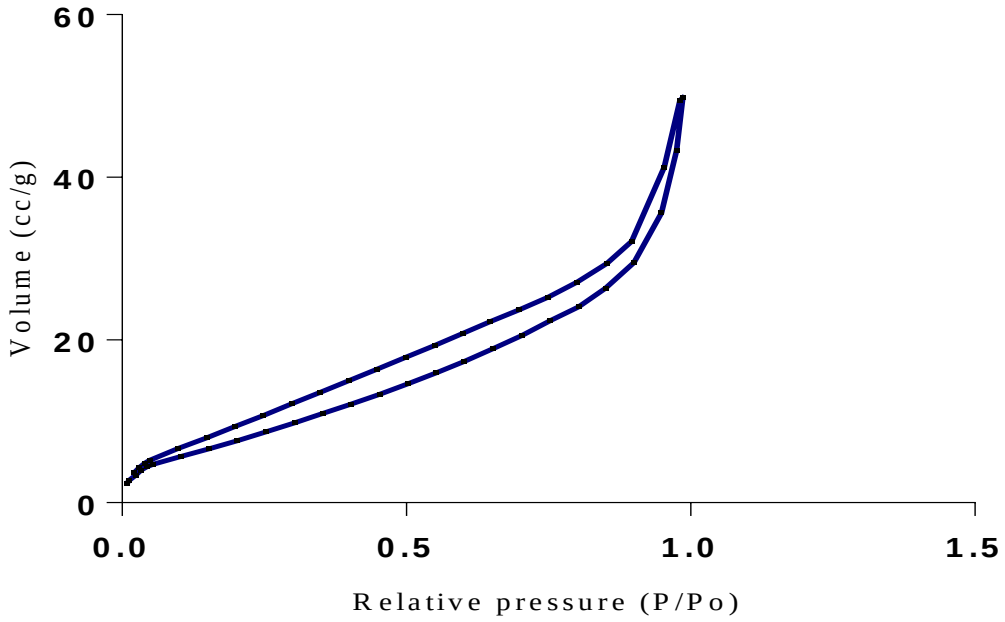

Figure 4.74: BET Isotherm for Chitosan-MAA-BAP-Nicotine-Nitrosopyrollidine MIP.

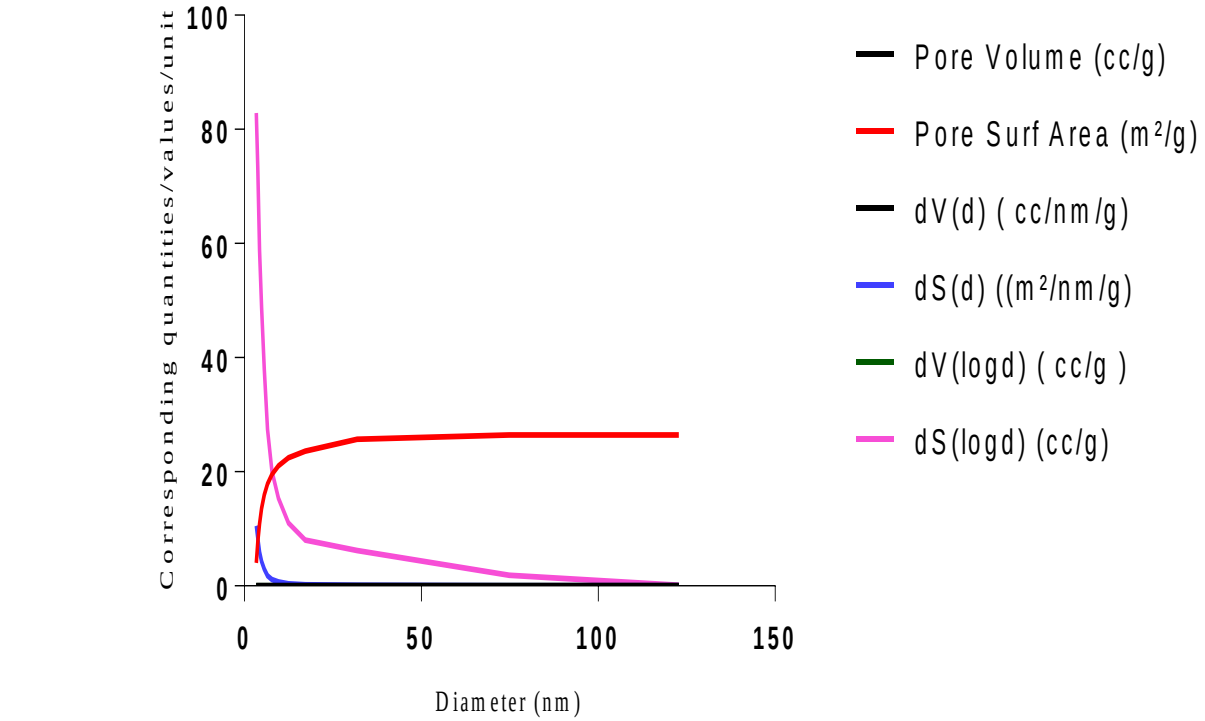

Figure 4.75: BJH desorption plot for Chitosan-MAA-BAP-Nicotine-Nitrosopyrollidine MIP.

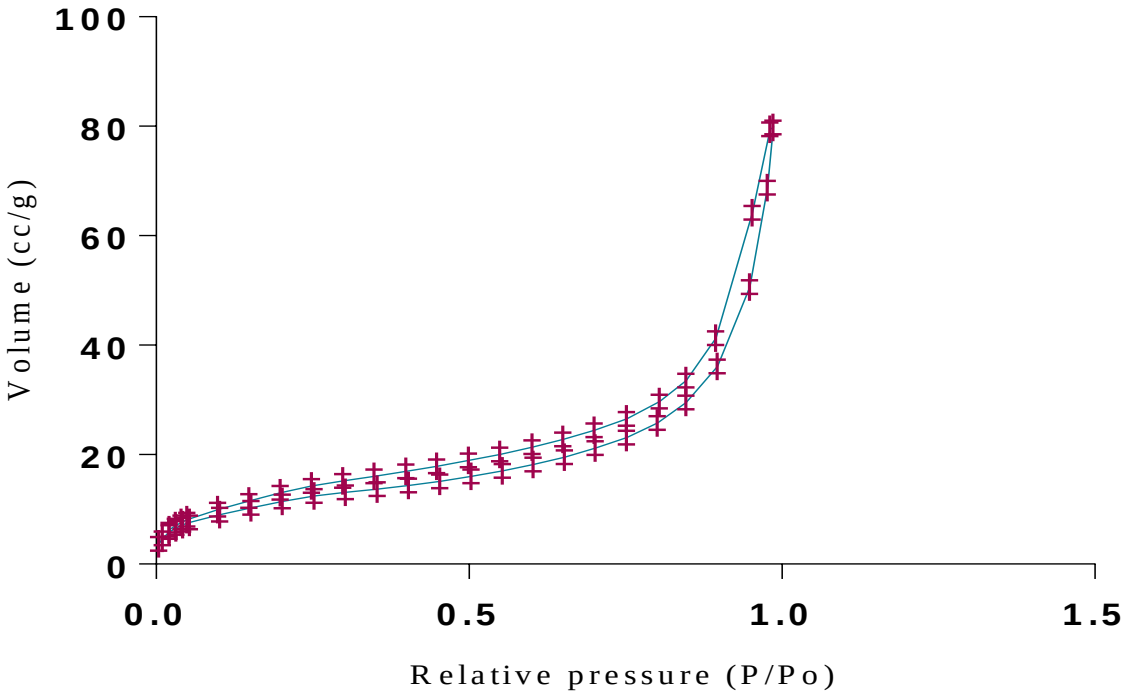

Figure 4.76: BET Isotherm for Chitosan-MAA-BAP-Nicotine-Phenylalanine amide MIP

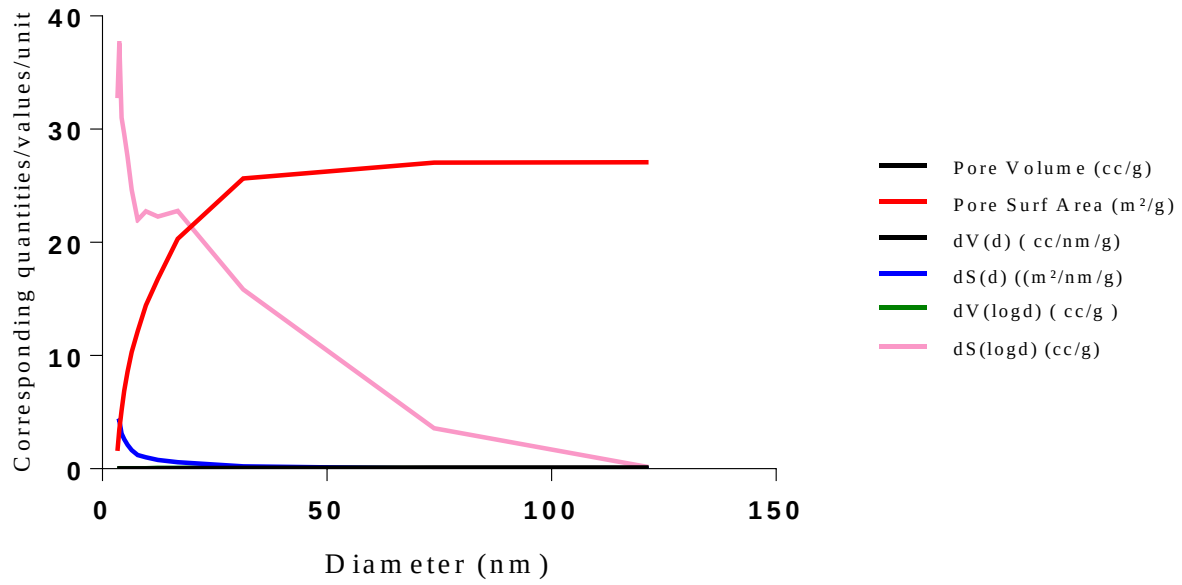

Figure 4.77: BJH desorption plot for Chitosan-MAA-BAP-Nicotine-Phenylalanine amide MIP.

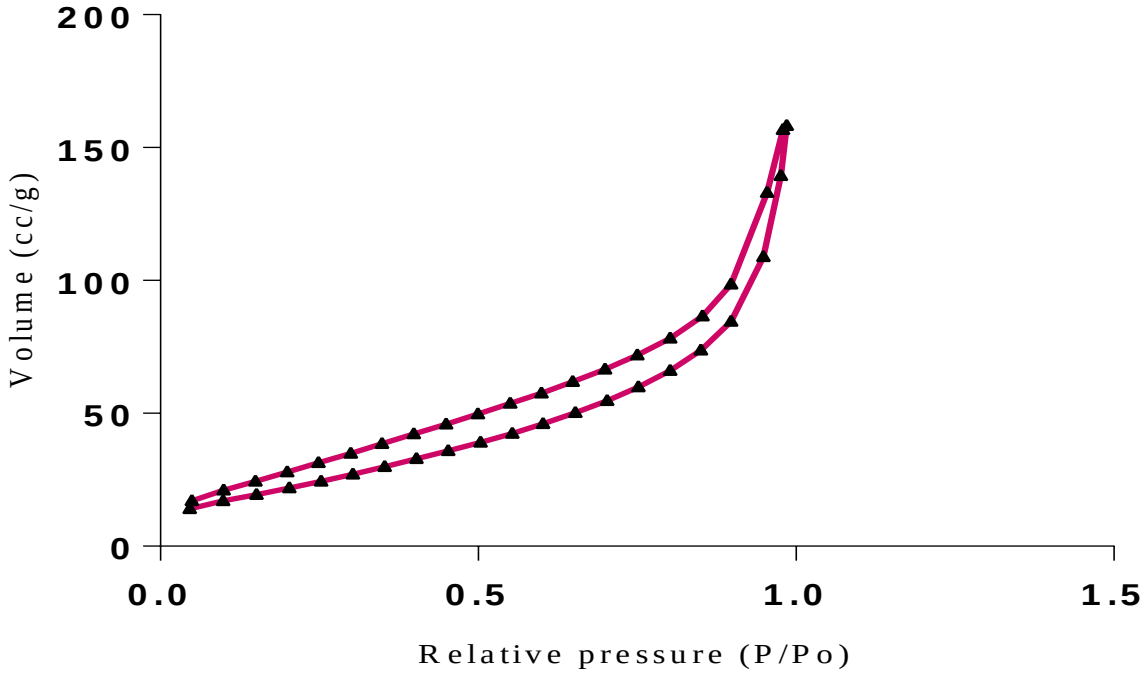

Figure 4.78: BET Isotherm for Chitosan-MAA-BAP-Nicotine-Phenylalanine amide NIP.

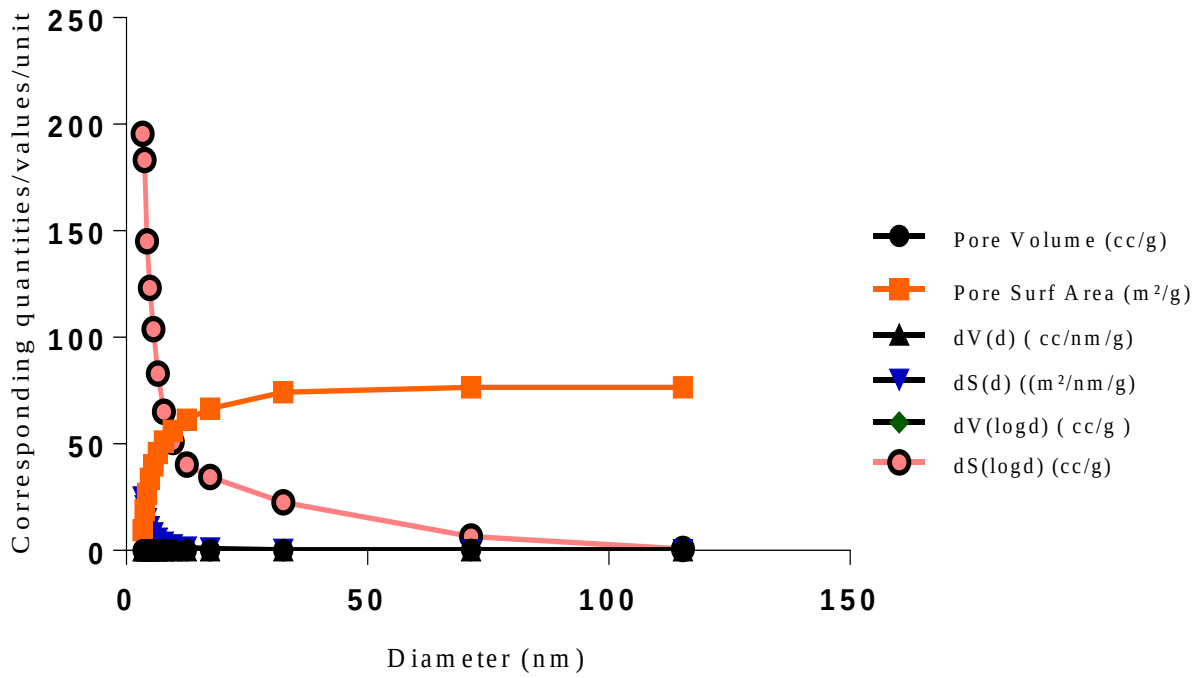

Figure 4.79: BJH desorption plot for Chitosan-MAA-BAP-Nicotine-Phenylaalanine amide NIP.

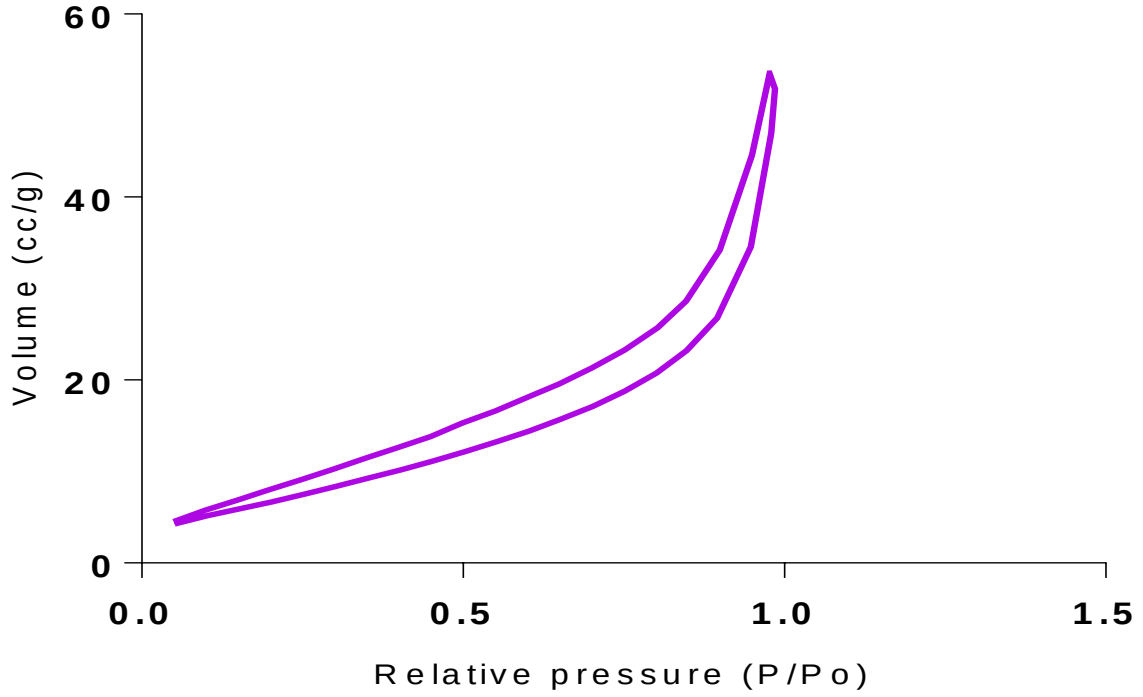

Figure 4.80: BET Isotherm for Chitosan-MAA-Geranic acid-Nicotine-Phenylalanine amide MIP.

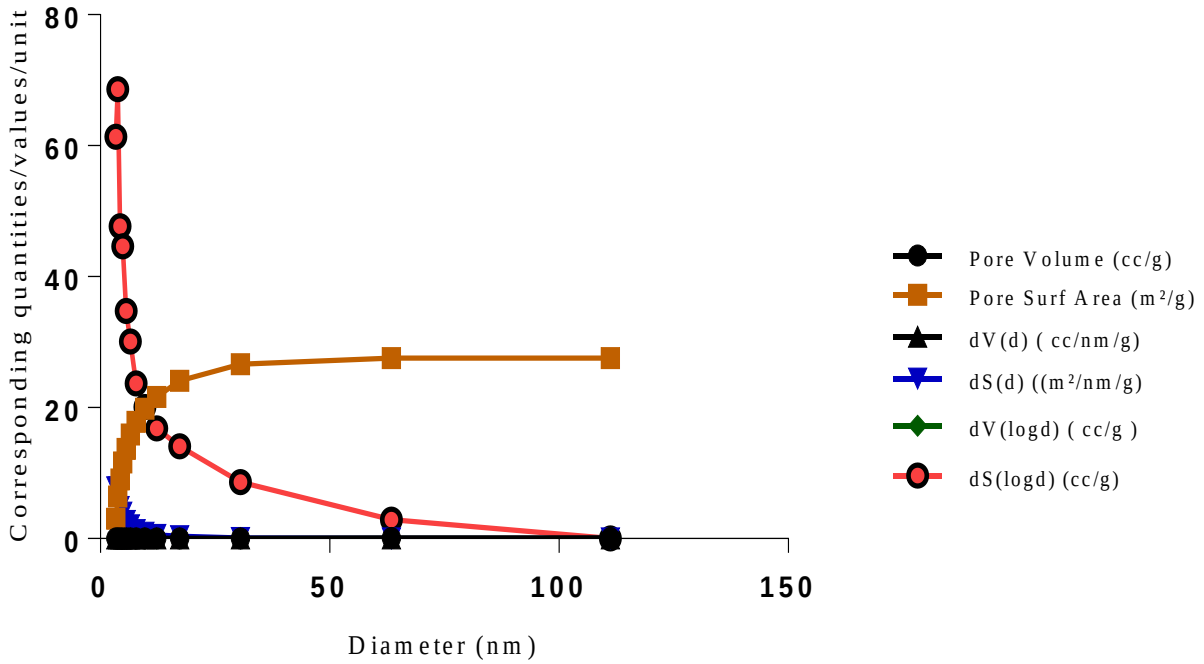

Figure 4.81: BJH desorption plot for Chitosan-MAA-Geranic acid-Nicotine-Phenylalanine amide MIP.

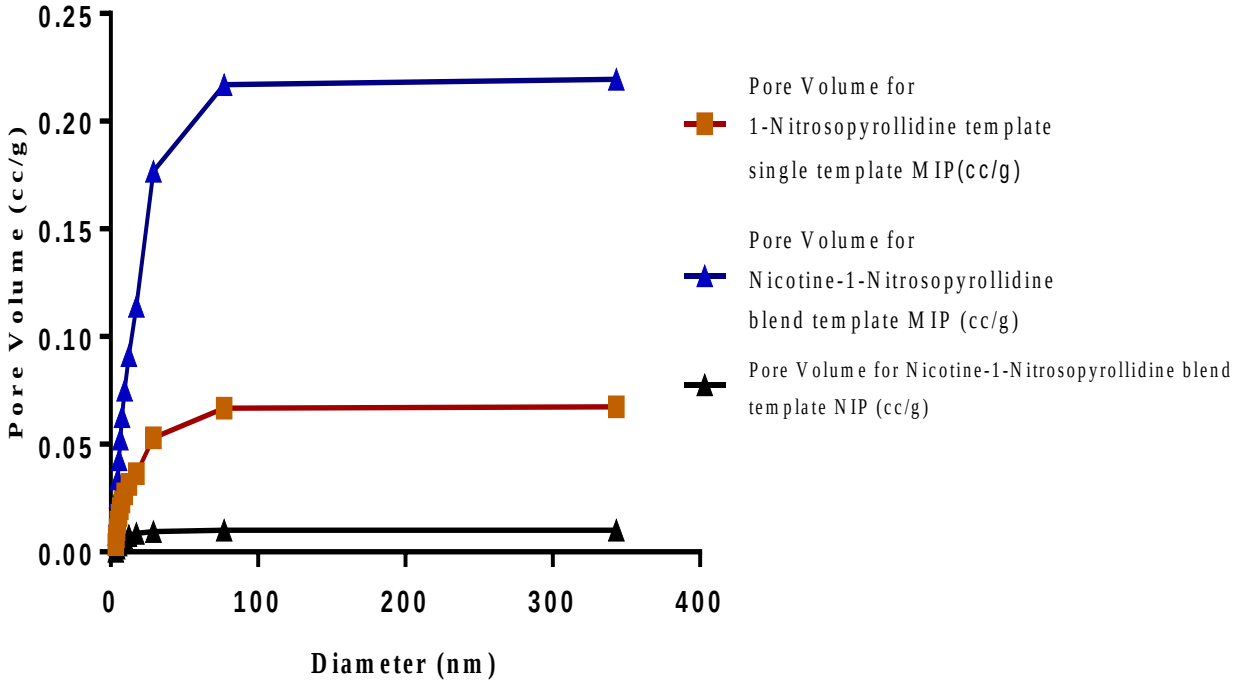

Figure 4.82: Plot of Pore diameter vs Pore volume for Chitosan-MAA-BAP-Nitrosopyrollidine MIP and NIP.

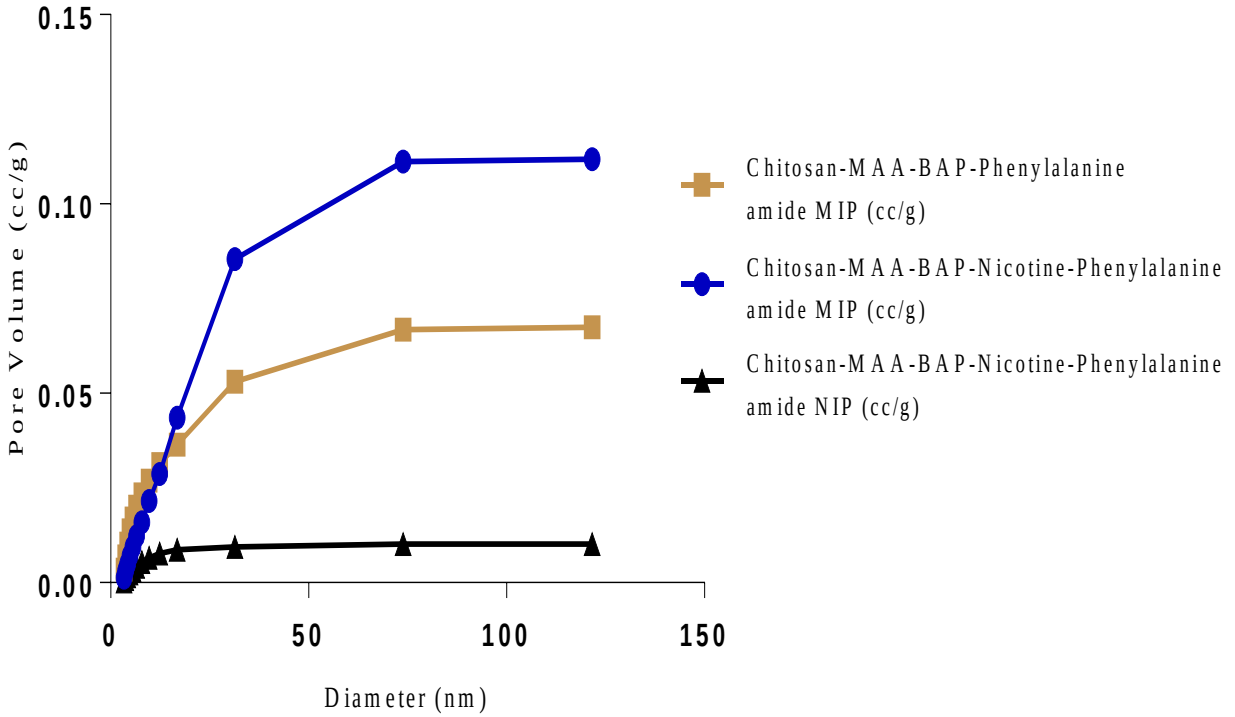

Figure 4.83: Plot of Pore diameter vs Pore volume for Chitosan-MAA-BAP-Phenylalanine amide MIP and NIP.

From the isotherms (Figures 4.73, 4.74, 4.76, 4.78 and 4.80), the samples present a typical composite type IVa and type II isotherm, that is an isotherm having the features of a type II isotherm with potential unrestricted monolayer-multilayer adsorption with characteristic "sharp knee" point 'B',(Figure 4.84). This "sharp knee" point, corresponds to the completion of monolayer coverage. The curve then graduates as a less distinctive curve relative to the 'sharp knee", and this is a proof of substantial degree of overlap of the monolayer coverage and the beginning of a multilayer adsorption. This phenomenon is combined with the type IV isotherm property of being conical and cylindrical mesopores that are closed at the tapered end as seen from results of the TEM analysis (Plates 4.18 - 4.30). The tapered ends of the pores are presented as converging cavities (Figures 4.74, 4.76, 4.78 and 4.80). Because the pores' widths are

averagely wider than 4nm (Plates 4.18, 4.20 – 4.23), the adsorption occurred via capillary condensation, hysteresis was experienced as part of the adsorption mechanism (Eddaoudi, 2005; Thommes and Cychosz, 2014 and Landers, Gor and Neimark, 2014),the samples exhibited the H3 type of hysteresis as contained in IUPAC Classified Standards Sorption Isotherms (IUPAC, 2015).The H3 type of hysteresis, presents characteristic adsorption branching phenomenon of the Type II isotherm, "sharp knee" and this corroborates the earlier deduction of the samples being a type IV isotherm member. It is also characterized by the branching at the lower limit of desorption being normally cited at the cavitation induced pressure point (p/p0).

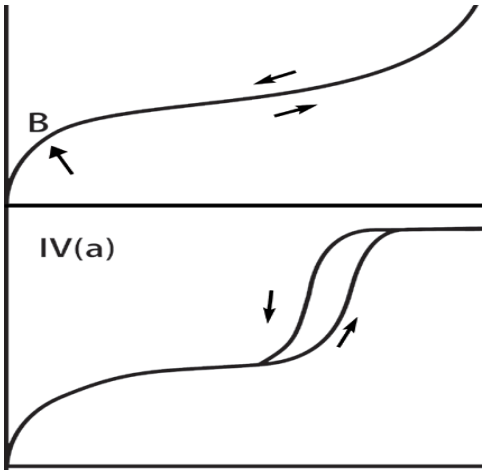

Figure 4.84: The "sharp knee" point (arrow pointed 'B'), adsorption phenomenon of type II and type IV Isotherms. Adapted from (IUPAC, 2015).

The hysteresis loop occurring at relatively high pressure, is distinctive of mesoporous samples and is in agreement with reports by other researchers, (Merino *et al.*, 2013). From the BJH desorption result summary, Table 4.9, the Geranic acid crosslinked blend templated sample (P10Sd), gave a slightly larger surface area at 27.577 m^2g^{-1} but with a smaller pore volume of 0.078 ccg^{-1} for the same value of pore diameter 3.826nm with the BAP crosslinked contemporary (P5Sd). This may be attributed to Geranic acid's larger molecular size/structure imparting the

observed larger surface area to the MIP without necessarily influencing the pore volume and dimensions. This is in agreement with Yoshimatsu *et al.* (2007) and may be pointing to the possible influence of template materials on the MIP's cavity architecture and identity irrespective of cross linker material used. This is at variance with the report from Sun *et al.* (2017), where it is stated that the cross linker impacts on the polymer cavity's physiochemical integrity. None the less no other reason comes readily to mind as to why the observed event between the samples played out. The values of the surface areas, pore volumes and pore diameters were all below 100 m^2g^{-1} for surface, $2ccg^{-1}$ for pore volume and 4nm for pore diameter. This confirms that the MIPs and NIPs are nanoparticle sized materials as is substantiated by the report of Yan *et al.* (2016).

A look at the microwave heated sample (MP3Sd) from Table 4.7 which has 5.339 m^2g^{-1} (surface area), $0.0102ccg^{-1}$ (pore volume) and 4.302nm (pore diameter), when compared to its contemporary MIP of P3Sd with 26.455 m^2g^{-1}(surface area), $0.067ccg^{-1}$(pore volume) and 3.411nm (pore diameter; it becomes evident that the use of microwave heating presents materials with more compact physio-structural attributes. While the values obtained from the NIP sample having a higher amount of cross linker than the MIPs show a larger surface area, pore volume but smaller pore diameter.

Deductions made from the results are in agreement with report by Fu, *et al.* (2015), stating that the formation of cavites is influenced by template-monomer polymerization interactions and not by the porogen employed in the polymerization reaction. The result from the TEM analysis, presents non uniform cavity dimensions for both the MIPs and NIP (due to the weak template-monomer interactions), with peak centers above 4 nm (Figures 4.75, 4.77, 4.79, 4.81 and Table

4.9). This supports the finding that the pore dimensions were generated during the polymerization from template-monomer interactions rather than porogen/solvent influences.

4.11 Particle size results

4.11.1 Particle Size Based On Zeta Potential, Dispersity and Dynamic Viscousity

Table 4.10: Results of Particle Size, Zeta potential, Dispersity, pH and Dynamic Viscosity of representative MIP and NIP Samples**.**

Sample ID	Particle Size (nm)	Zeta potential	Dispersity	pH	Dynamic Viscosity (cp)
Chitosan	238.8	-46.1	0.46	7.4	0.89
P1Sa	545.6	-47.1	0.65	7.4	0.89
P1Sd	342.3	-46.9	0.56	7.4	0.89
P1Se	342.2	-47.2	0.54	7.4	0.89
P1Sf	691.2	-46.5	0.48	7.4	0.89
P3Sa	254.5	-48.6	0.52	7.4	0.89
P3Sb	733.6	-47.7	0.85	7.4	0.89
P3Sc	477.1	-46.8	0.40	7.4	0.89
P3Sd	436.9	-46.7	0.62	7.4	0.89
P3Se	918.2	-47.3	0.61	7.4	0.89
P3Sf	2394.0	-45.7	1.00	7.4	0.89
P5Sa	757.8	-47.1	0.90	7.4	0.89
P5Sb	580.1	-48.5	0.72	7.4	0.89
P5Sc	592.7	-48.6	0.39	7.4	0.89
P5Sd	542.1	-48.5	0.72	7.4	0.89
P5Se	383.7	-49.2	0.68	7.4	0.89
P5Sf	655.2	-47.4	0.48	7.4	0.89
P6Sa	609.7	-43.5	0.95	7.4	0.89
P6Sb	387.8	-47.4	0.81	7.4	0.89
P6Sc	516.3	-80.2		7.4	0.89

P6Sd	526.7	-78.4	0.82	7.4	0.89
P6Se	526.7	-86.2	0.78	7.4	0.89
P6Sf	3676	-75.7	0.57	7.4	0.89
P8Sa	353	-64.0	0.82	7.4	0.89
P8Sb	195.7	-59.4	0.74	7.4	0.89
P8Sd	578.4	-77.6	0.85	7.4	0.89
P8Se	683.5	-80.5	0.86	7.4	0.89
P8Sf	1095	-92.4	0.35	7.4	0.89
P10Sa	2461.7	-106	0.23	7.4	0.89
P10Sb	2099	-82.3	0.80	7.4	0.89
P10Sc	780.1	-81.8	0.65	7.4	0.89
P10Sd	542.1	-86.3	0.91	7.4	0.89
P10Se	2067.3	-93.9	0.39	7.4	0.89
P10Sf	821.9	-81.3	1.00	7.4	0.89
MP1Sd	735.8	-24.7	0.41	7.4	0.89
MP1Sf	786.1	-37.1	0.89	7.4	0.89
MP3Sd	1084.8	-31.6	0.63	7.4	0.89
MP6Sd	979.1	2.2	0.67	7.4	0.89
MP8Sd	852.1	-20.0	0.63	7.4	0.89
MP10Sd	780.1	-21.4	0.65	7.4	0.89

Table 4.11: Results of Particle Size, Zeta potential, Dispersity, pH and Dynamic Viscosity of representative MIP and NIP Samples.

	Sample ID	Native Chitosan	P1Se	P3Sd	P5Sd	P6Se	P8Sd	P10Sd
Particle sizes(nm)	MIPs	238.8	342.3	436.9	542.1	526.7	578.4	542.1
	Corresponding NIPs		P1Sf, 691.2	P3Sf, 2394.0	P5Sf, 655.2	P6Sf, 3676	P8Sf, 1095	P10Sf, 821.9
Zeta potential		-46.1	-47.2	-46.7	-48.5	-86.2	-77.6	-86.3
Dispersity		0.46	0.54	0.62	0.72	0.78	0.85	0.91

From Table 4.11, the samples all have dynamic viscosity (cp) of 0.89 and pH of 7.4. The particle sizes for the non imprinted polymers (NIPs), ranged from between 691.2 to 3676 but interestingly in multiples of that for their respective MIPs. The particle sizes for the MIPs were all higher than that of the native Chitosan (238.8). This is due to the end product of the polymerization reaction. For both the BAP cross linked and Geranic acid cross linked MIPs, the Nicotine templated samples had the least particle size (PISe 342.3 and P6Se 526.7) in comparism with the Phenylalanine and blend templated MIPs. The resultant zeta potentials for all samples were negative. This is an evidence of the cationic nature of the samples when in solution.The dispersity of samples followed a similar trend, increasing from Nicotine sample to Phenylaalanine template and the blend of the two for both cross linkers. The blend templates have the heist for both BAP and Geranic acid cross linked systems with 0.72 and 0.91 respectively. `

4.11.2 Laser Particle Size Result.

Figures 4.85 to 4.89, presents the graphs of differential volume (%) against particle diameter of representative samples of MIPs and NIP. Calculations are from 0.040 1m to 2000 µm

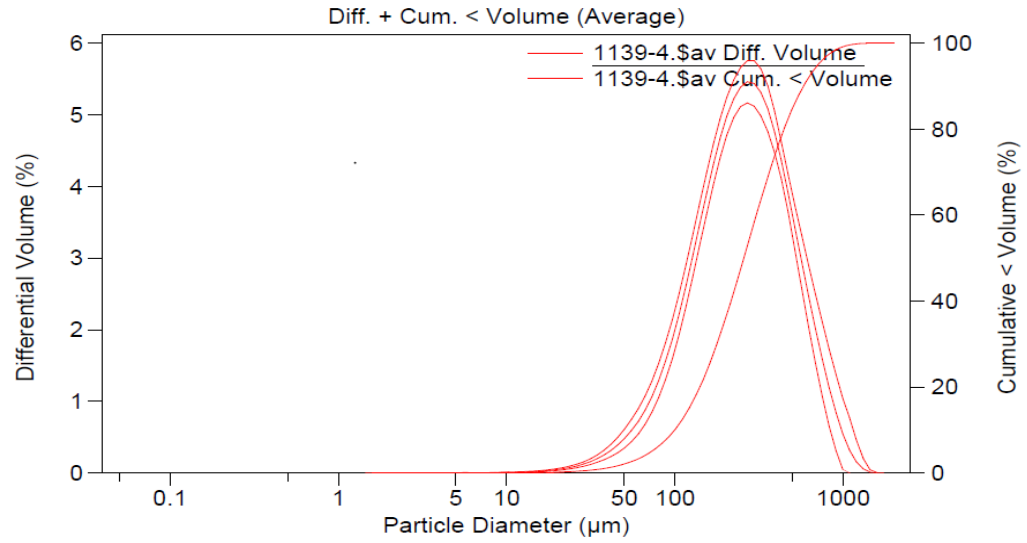

Volume:	100%		
Mean:	304.7 µm	S.D.:	200.2 µm
Median:	256.4 µm	Variance:	40083 µm^2
Mean/Median ratio:	1.188	Skewness:	1.333 Right skewed
Mode:	269.2 µm	Kurtosis:	2.127 Leptokurtic

<10%	<25%	<50%	<75%	<90%
99.57 µm	159.2 µm	256.4 µm	400.5 µm	580.3 µm

Figure 4.85: laser particle size chart of Sample P6 Sa

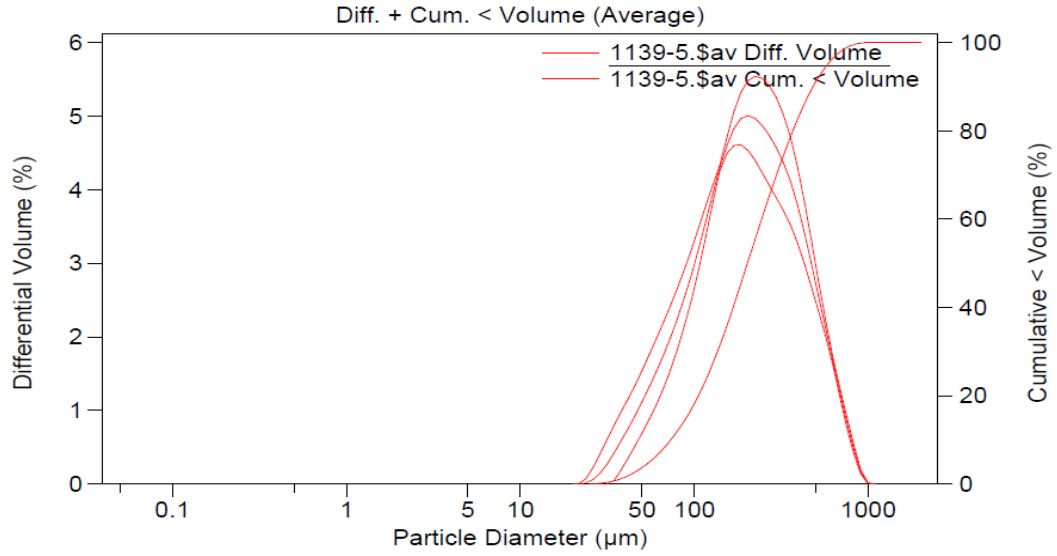

Volume:	100%		
Mean:	244.3 µm	S.D.:	164.0 µm
Median:	201.9 µm	Variance:	26894 µm^2
Mean/Median ratio:	1.210	Skewness:	1.175 Right skewed
Mode:	203.5 µm	Kurtosis:	1.164 Leptokurtic

<10%	<25%	<50%	<75%	<90%
73.31 µm	120.8 µm	201.9 µm	329.3 µm	480.8 µm

Figure 4.86: laser particle size chart of Sample P6 Sb

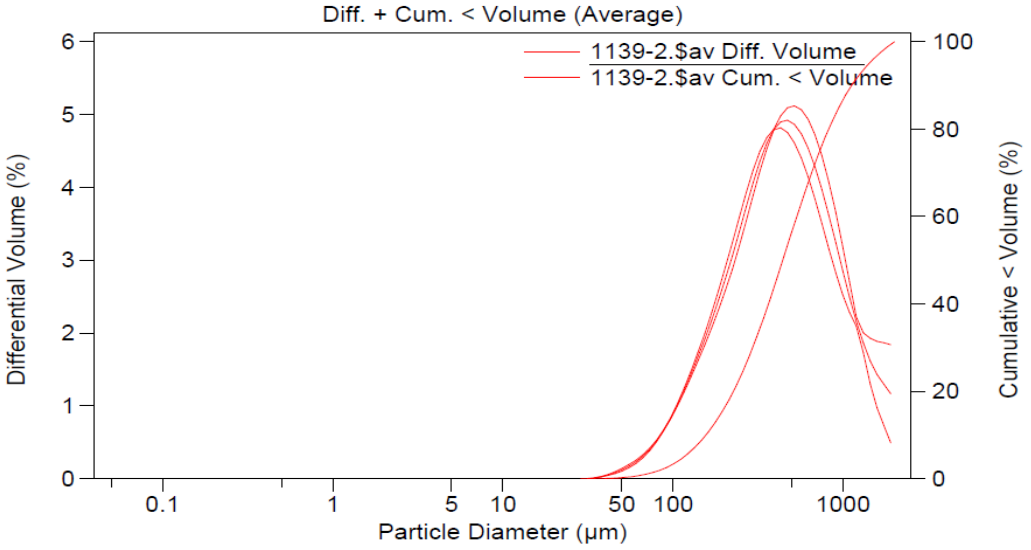

Volume:	100%		
Mean:	552.1 µm	S.D.:	398.1 µm
Median:	442.0 µm	Variance:	158.5e3 µm^2
Mean/Median ratio:	1.249	Skewness:	1.323 Right skewed
Mode:	471.1 µm	Kurtosis:	1.467 Leptokurtic

<10%	<25%	<50%	<75%	<90%
156.3 µm	260.4 µm	442.0 µm	729.5 µm	1123 µm

Figure 4.87: laser particle size chart of Sample P6 Sc

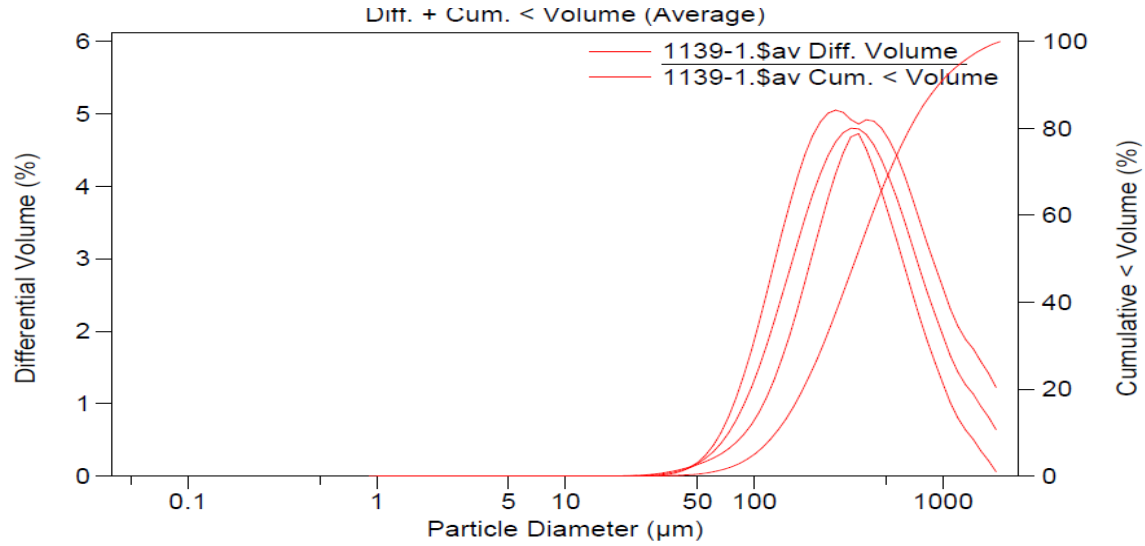

Calculations from 0.040 µm to 2000 µm

Volume:	100%		
Mean:	454.9 µm	S.D.:	358.6 µm
Median:	344.2 µm	Variance:	128.6e3 µm^2
Mean/Median ratio:	1.322	Skewness:	1.681 Right skewed
Mode:	324.4 µm	Kurtosis:	2.911 Leptokurtic

<10%	<25%	<50%	<75%	<90%
130.3 µm	205.3 µm	344.2 µm	583.9 µm	943.0 µm

Figure 4.88: laser particle size chart of Sample P6Se

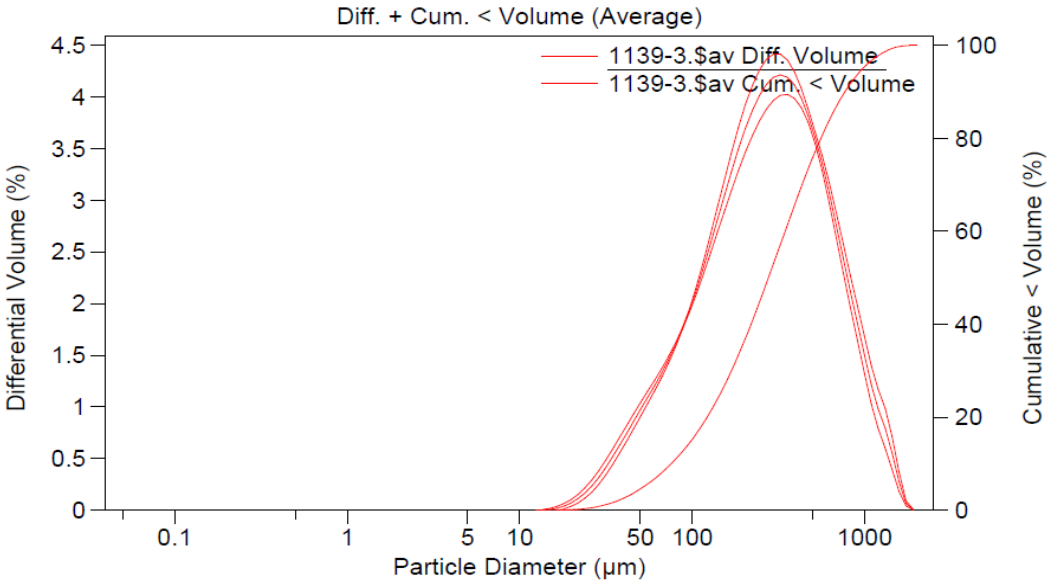

Volume:	100%		
Mean:	360.2 µm	S.D.:	292.9 µm
Median:	276.6 µm	Variance:	85792 µm^2
Mean/Median ratio:	1.303	Skewness:	1.481 Right skewed
Mode:	324.4 µm	Kurtosis:	2.306 Leptokurtic

<10%	<25%	<50%	<75%	<90%
75.58 µm	145.2 µm	276.6 µm	488.7 µm	768.1 µm

Figure 4.89: laser particle size chart of Sample P6 Sf

Discussion

The observed Skewness, (an indication of how far the distribution deviates from the symmetry of a normal Gaussian distribution i.e zero or centrally skewed), leans towards the right hand side from the chart (Figures 4.85 to 4.89). This is interpreted as a positively skewed distribution (Beckman Coulter, 2010). A distribution that "leans" to the right with a long tail at coarse sizes and with mean (454.9 µm, 552.1 µm, 360.2 µm, 304.7 µm and 244.3 µm), greater than the mode (324.4 µm, 471.1 µm, 324.4 µm, 269.2 µm and 203.5 µm) respectively; presents the samples as being positively skewed and the value increases with increasing lean. It is also observed that the "Kurtosis**"** (an indication of how sharply peaked the distribution plot is, compared to a normal 'Gaussian' distribution), is of the leptokurtic class of distribution and "large" because the peak is very narrow and sharp with most particles having a size close to the mean. The Skewness shows a direct linear relationship with the distribution irrespective of the sample type i.e. MIP or NIP. The direction of Skewness (right skew), indicates the relative size of the particles analyzed and its large size can be linked to the ability of Chitosan to swell in the presence of media thereby exhibiting a larger surface area as is evidenced from the SEM and TEM micrographs.

4.12 MIP Swelling Capacity profile result

Table 4.12: Swelling capacity values of MIP and NIP samples indicating initial and final hights in PBS buffer 7.4pH solution after 24Hr.

Sample ID	Height before swelling (a) mm	Height after 24Hr swelling (b) mm	Height Difference (c) mm	Swelling Factor (c/a)
P1Se	1.5	2.5	1.5	1.0
P1Sf	1.5	3.8	2.3	1.5
P3Sd	1.5	3.0	1.5	1.0
P3Sf	1.0	2.5	1.5	1.5
P5Sd	1.0	2.5	1.5	1.5
P5Sf	1.8	3.5	1.5	0.8
P6Se	1.5	2.8	1.3	0.9
P6Sf	1.5	4.0	2.5	1.7
P8Sd	1.0	3.5	2.5	2.5
P10Sd	1.5	2.5	1.0	0.6
P10Sf	1.5	3.0	1.5	1.0
MP1Sd	1.0	2.8	1.8	1.8
MP1Sf	1.0	3.0	2.0	2.0
MP3Sd	1.2	2.8	1.6	1.3
MP6Sd	0.5	1.5	1.0	2.0
MP8Sd	1.2	3.0	1.8	1.5
MP10Sd	1.0	3.5	2.5	2.5

From Table 4.12 the swelling factor for the representativesamples ranged between 0.8 for NIP sample P5Sf to 2.5 for MIP sample P8Sd. A significant inference is that the NIP samples had swelling factor values greater than their MIP counterparts.

4.13 Simultaneous Thermal Analysis Result.

Table 4.13 presents the behaviour of samples in a heated environment. Representative samples with template materials as well as without template materials were studied.

Table 4.13: Values of thermal behaviour of samples from STA analysis

Sample ID	Sample Category	First Onset		Second Onset		Third Onset		Fourth Onset		Fifth Onset	
		% wt retained	Temp. @ onset	% wt retained	Temp. @ onset	% wt retained	Temp. @ onset	% wt retained	Temp. @ onset	% wt retained	Temp. @ onset
TEMPLATE ELUTED SAMPLES											
P1Sd		99.87	32.60	74.50	224.54	66.83	290.03	61.36	368.13	47.22	411.22
P1Sb		99. 98	37.92	78.81	208.84	64.15	371.97				
P3Sb		99.70	33.89	66.42	234.71	60.10	356.97	56.32	404.57	43.77	475.32
P3Sf		99.76	37.69	74.40	216.44	64.09	366.58				
P6Sd		99.92	41.45	62.06	250.40	54.57	363.41	51.38	416.78	42.62	469.91
P6Se(rw)		99.97	49.25	74.56	257.04	62.53	352.88	56.22	417.55	40.93	485.40
P8Sd		99.89	36.04	65.24	249.69	58.59	357.94	56.01	414.93	47.34	476.00
P10Sa		99.95	46.01	64.47	247.24	59.17	355.44	56.01	414.93	47.34	476.00
SAMPLES CONTAINING TEMPLATES											
1(P1Sd)		99.96	42.52	83.23	212.51	64.49	392.17				
2 (P3Sd)		99.89	36.29	71.37	221.01	58.52	364.75				
4 (P6Sd)		99.79	43.74	64.47	250.46	55.23	353.34	48.99	410.15	42.57	433.95
7 (MP1Sf)		99.96	47.25	68.92	222.52	64.10	274.08	54.48	371.91	42.36	415.17

4.14 Rebinding Studies.

Two methods for analyzing the samples were used, gradient elution method and isocratic elution method. Table 4.14 presents the adsorbed concentrations of the templates from the output of the HPLC-MS equipment.

Table 4.14: Concentrations of adsorbed templates by representative sample materials.

Sample ID	Conc. Of Nicotine adsorbed (mM)	Conc. Of Phenylalanine adsorbed (mM)	Conc. Of Nicotine-Phenylalanine adsorbed (mM)	
MIP samples cross-linked with BAP				
P1Se (single wash).	0.179	Not Detected	Not Detected	
PISe(double washing).	0.421	Not Detected	Not Detected	
P1Sf(single wash)	0.421	Not Detected	Not Detected	
P3Sd(single wash)	Not Detected	0.144	Not Detected	
P3Sd (double washing)	Not Detected	0.477	Not Detected	
MP3Sd (microwave heated, single wash)	Not Detected	0.192	Not Detected	
P3Sf(single wash)	Not Detected	0.572	Not Detected	
P5Sd (single washing)	Not Detected as an individual moiety	Not Detected as an individual moiety	0.171(Nic.)	0.067(Phe.)
P5Sd (double washing)	Not Detected as an individual moiety	Not Detected as an individual moiety	0.140(Nic)	0.158(Phe.)
P5Sf(single wash)	Not Detected	Not Detected	0.345	0.577
MIP samples cross-linked with Geranic acid				
P6Se(single wash)	0.076	Not Detected	Not Detected	
P6Se(double washing)	0.153	Not Detected	Not Detected	
MP6Se(double washing)	0.156	Not Detected	Not Detected	
P6Sf(single wash)	0.266	Not Detected	Not Detected	
P8Sd(single wash)	Not Detected	0.142	Not Detected	
MP8Sd(single washing)	Not Detected	0.200	Not Detected	
P8Sf(single wash)	Not Detected	0.477	Not Detected	
P10Sd	Not Detected as an individual moiety	Not Detected as an individual moiety.	0.041(Nic.)	0.108(Phe.)
MP10Sd(single washing)	Not Detected as an individual moiety.	Not Detected as an individual moiety.	0.112(Nic.)	0.113(Phe.)
P10Sf(single wash)	Not Detected	Not Detected	0.112(Nic.)	0.113(Phe.)

Appendix xxvi-xxxv, presents the chromatograms of the samples from the HPLC-MS analysis while Table 4.14 presents the extracted results from the chromatograms. The filtrate from the BAP crosslinked MIP samples (P1, P3 and P5) which contacted the template solutions of initial concentration of 0.600mmol, recorded 0.179mmol of free template material (P1Se) with a single wash with methanol: acetic acid (9:1) as solvent. A duplicate sample of the P1Se with a double cycle of washing recorded a 0.421mmol conc. of template material. This trend played out with the P3Sd (single wash) and P3Sd (double wash) giving 0.144mmol and 0.477mmol for residual template materials. The P5Sd samples with cavity for multi-templating, showed a similar behaviour but with a reversed trend with the Nicotine part of the blend. The Nicotine single wash gave 0.171mmol and 0.140mmol for the double wash. The Phenylalanine counterpart maintained the former trend with the single wash giving a 0.067mmol conc. Conc, and 0.158mmol for the second wash. The geranic acid cross-linked MIP samples performed as well as their BAP crosslinked counterparts with P6Sd (single wash) giving 0.131mmol and the double wash recording 0.153mmol conc. for free template material. The microwave heated P6Sd sample recorded closely related concentration as the water bath counterpart with 0.156mmol of free template material. The P8Sd samples gave 0.198mmol and 0.200mmol respectively for the single wash and double wash samples. A reversal of trend was also observed with the dual templated sample (P10Sd) but on a different template material (Phenylalanine). The single wash gave 0.083mmol (Nicotine), 0.112 (Phenylalanine) and 0.142mmol (Nicotine), 0.113mmol (Phenylalanine) for the double wash sample. This is also the value for the corresponding microwave heated sample. Interestingly, the combined concentration of templates remained the same for both the single wash and the double wash samples (0.225) each. From Table 4.14, the

integrity of the MIPs with respect to selectivity and specificity can be argued in the positive direction. The inability of the samples not to adsorb non-targeted templates based on fabrication design and the ability of the dual-templated samples to selectively adsorb specific amounts of individual templates without the influence of their respective interacting potentials, confirms the selectivity of the MIP samples. The most striking feature is that of the dual templated MIPs not adsorbing single template materials where they are brought into contacts. This is shown by the non-detection of the template materials from the eluates obtained from the elution of adsorbed materials from the contacted MIP samples after introducing the template materials during the experiments.

Table 4.15 presents the various MIPs and NIPs with their corresponding C_i (conc of template solution before adsorption), C_f (conc of template solution after adsorption), K_D(calculated), binding capacities and Imprinting Factors (IF).

Table 4.15: Extracted values of initial concentrations of template solutions from a 3ml volume solution, the concentration of filtrate after contacting with polymer samples; the calculated K_D, binding capacities BC and the imprinting factors (IF)

Sample ID	Initial conc.of template (Ci) mmol	Residual conc. of template in filtrate (Cf).mmol	Conc. of template in MIP mmol	Conc. of template in NIP mmol	Binding Capacity of Polymer	Distribution coefficient (K_D)	Imprinting Factor (IF)
Polymer samples cross-linked with BAP							
P1Se (single wash).	0.6	0.179	0.421	_	2.11	11.76	5.60
PISe(double washing).	0.6	0.421	0.179	_	0.90	2.10	1.00
P1Sf(single wash)	0.6	0.421	_	0.179	0.90	2.10	1.00
P3Sd(single wash)	0.6	0.144	0.456	_	2.28	1.58	6.60
P3Sd (double washing)	0.6	0.477	0.123	_	0.62	1.29	5.38
MP3Sd (microwave	0.6	0.192	0.408	_	2.04	1.06	4.40

heated, single wash)							
P3Sf(single wash)	0.6	0.572	_	0.028	0.14	0.24	1.00
P5Sd (single washing)	0.6	0.2387	0.361	_	1.81	7.57	8.14
P5Sd (double washing)	0.6	0.298	0.302	_	1.51	5.07	5.45
P5Sf(single wash)	0.6	0.590	_	0.010	0.05	0.93	1.00
		Polymer samples cross-linked with Geranic acid					
P6Se(single wash)	0.6	0.076	0.524	_	2.62	34.50	5.40
P6Se(double washing)	0.6	0.153	0.447	_	2.24	14.61	2.33
MP6Se(double washing)	0.6	0.156	0.444	_	2.22	14.23	2.27
P6Sf(single wash)	0.6	0.266	_	0.334	1.67	6.28	1.00
P8Sd(single wash)	0.6	0.142	0.458	_	2.29	16.13	12.50
MP8Sd(single washing)	0.6	0.200	0.400	_	2.00	10.00	7.75
P8Sf(single wash)	0.6	0.477	_	0.123	0.615	1.29	1.00
P10Sd	0.6	0.149	0.451	_	2.26	15.13	1.82
MP10Sd(single washing)	0.6	0.225	0.375	_	1.88	8.33	1.00
P10Sf(single wash)	0.6	0.225	_	0.375	1.88	8.33	1.00

The imprinting factor is used to certify the extent of interaction between the functional monomer and the template. From Table 4.15, imprinting factors of the MIPs ranged from as high as 12.50 for geranic acid cross-linked, phenylalanine templated polymer to as low as 1.82 and 1.00 for geranic acid cross-linked, blend templated polymers (water heated and microwave heated samples respectively). A trend was established between the single washed and double washed samples because of the consistent drop in IF between the single and the double washed. This guides the unnecessary rewashing of templates in a bid to exhaustively elute residual template

material from the MIPs. A possible damage is done to the integrity of the established cavities thereby redering them inefficient. This may be attributed to the presence and activity of the delicate intermolecular bonds of the functional monomer in the presence of the highly poler wash solvent mixture of methanol and acetic acid. Inter and intra-molecular erosion may occur leading to loss of cavity integrity.

There is no direct relationship between the binding capacity and the imprinting factor rather double washing of the polymers reduces their binding capacity as is shown from Table 4.15 and this consequently affects the IF. Examples of this is as shown with P1Se (single wash) having BC of 2.11 while the double washed P1Se had 0.90 and their respective Ifs are 5.60 and 1.00. P3Sd samples have 2.28 and 0.62 as BC with 6.60 and 5.38 as IF respectively.

The geranic acid cross-linked Nicotine templated samples exhibited higher values of BC. K_D and IF (P6Se) than those of BAP cross-linked counterparts (P1Se). This is attributable to the more robust inter and intra molecular bonds inherent with the geranic acid moiety. The more available the bonding activity, the more the binding capacity, K_D and consequent IF; though this does not certify the best molecular interaction but only gurrantees a more robust interacting platform which may give rise to good and acceptable cavity sites depending on the type of bonding involved.

Table 4.16: Concentrations of adsorped degraded products from the machine smoking experiment using representative MIP samples and commercial cigarette Butt filter.

Cigarette smoke constituent	Adsorbent and concentration (mmol) of adsorbed degraded product(s).	
Nicotine	P1	0.572
	P6	0.421
	MP1	0.208
	MP6	0.207
	Commercial filter	0.076
Individually adsorbed TSNA	P3	0.626
	P8	0.572
	MP3	0.514
	MP8	0.477
	Commercial filter	0.144
Combined or blend TSNA products	P10	0.927
	MP10	0.708
	Commercial filter	0.149

The Malboro menthol brand of cigarette contains approximately 0.8mg of nicotine, an average of 65% of which is pyrolyzed or lost from side stream smoke (Ying Liu, Xueliang Liu and Junde Wang, 2003). The rest of the stream delivers approximately 20–80µg of nicotine and TSNAs through the filter butt. This amount exposes the smoker to 0.8mmol of Nicotine/cigarette by conversion alongside the TSNAs. From Table 4.16 the fabricated MIPs adsorbed over 60% (max) and above 25% (min) of the Nicotine content of the smoked cigarette while the commercial filter was only able to adsorb a little above 10% of the Nicotine from the stream. The MIPs with blend template cavities (P10 and MP10) were also able to adsorb much higher amount of the smoke stream toxicants than the commercial filters specifically in a 9:1 concentration ratio. This shows the advantaged utility potential of the fabricated MIPs over the conventional filters currently being used. Figures 4.90 and 4.91 show the specific identification of Nicotine by the MIP sample as displayed on the chromatogram.

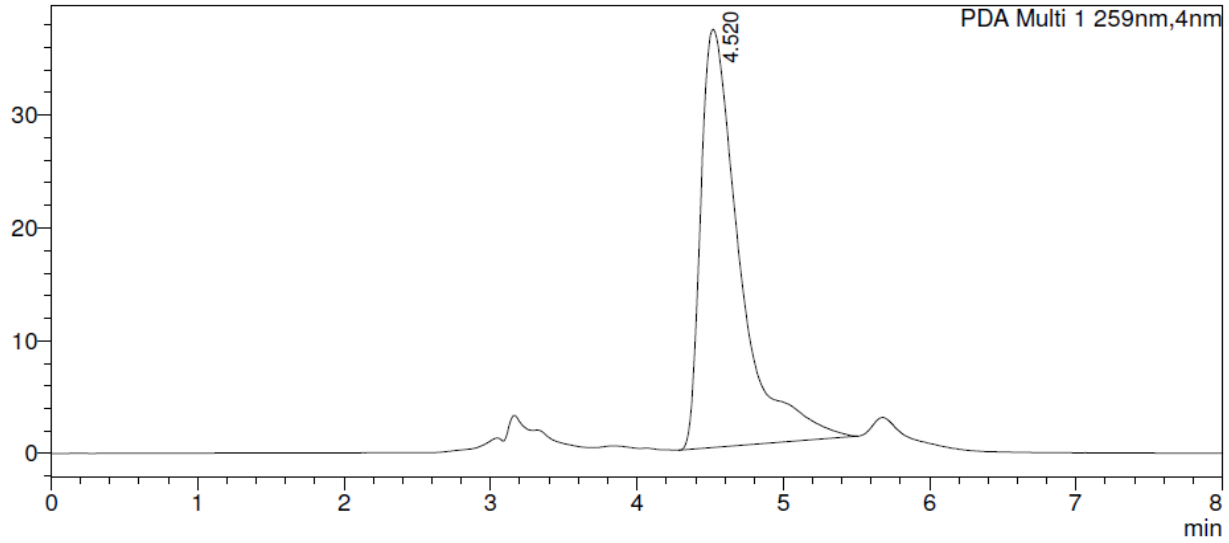

Figure 4.90: Chromatoram of Nicotine from the smoked cigarette stream at 259nm.

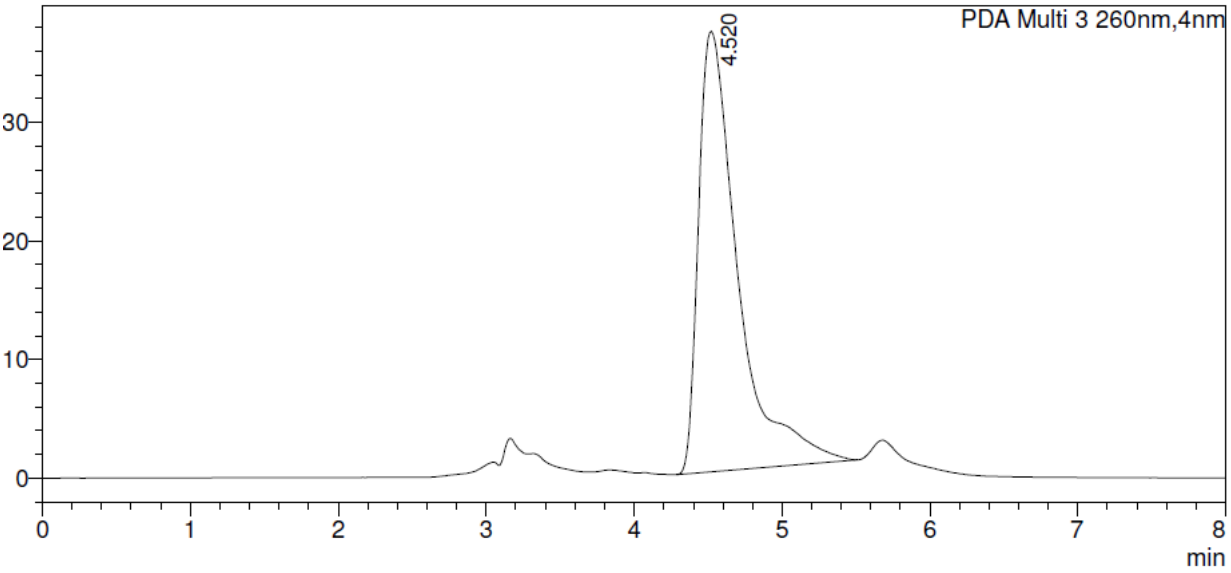

Figure 4.91: Chromatoram of Nicotine from the smoked cigarette stream at 260nm.

Figures 4.90 and 4.91 presents the HPLC chromatogram of the Nicotine from the machine smoked cigarette. The retention time of 4.5min was specific for the nicotine even at the two different wavelengths of 259 and 260nm. This shows the specificity of the separation and identification of the process method and equipment.

CHAPTER FIVE

SUMMARY, CONCLUSION AND RECOMMENDATION

5.1. Summary

The challenges posed by the inherent property of chitosan ie swelling when influenced by certain conditions, for it to be used as a good biomaterial resource for various industrial applications such as is required in thin film sensors, fluid environments and pH influenced set-ups; have been addressed from the result of the experiment carried out in this work. This biofriendly and degradeable material (chitosan) has been used to fabricate filter materials that showed good to excellent adsorption capability for cigarette smoke toxicants. The filter material in the form of molecularly imprinted polymer matrix, showed superior ability over the conventional cellulose acetate filters that are presently used. The good result obtained from the proof-of-concept experiment supports using Chitosan as matrix in thin film biosensing activity for the specific, selective adsorption of nicotine and analogues of TSNAs. This is without the exhibition of the inherent swelability of chitosan when in contact with fluids and protic environments.

Molecularly imprinted polymer fabrication has most times been done with synthetic cross-linking agents such as BAP and this has always hindered the achievement of a 100% biodegradable and benin utility products particularly for areas where *in vivo* applications are needed like in drug delivery systems. This work has utilized the natural product geranic acid as a cross-linker in the fabrication of MIP samples and these samples performed as well as those fabricated using the synthetic cross-linker BAP. This will encourage more research into the use of the wide array of natural products as cross-linking agents in MIP fabrication and consequently expand the scope of this area of science.

5.2 Conclusion

A chitosan based molecularly imprinted polymer fabrication activity has been successfully carried out with good results that substantiated the feasibility of using Chitosan for thin film biosensing, multi-templated hiarachical network and as functional monomer cross-linked with both synthetic and natural cross-linkers. The robustness of chitosan was explored in establishing a multi-templated system capable of sequestering target materials from a cocktail of components.

5.3 Contribution to knowledge

A chitosan based molecularly imprinted polymer fabrication has been successfully carried out with good results that substantiated the feasibility of using Chitosan for thin film biosensing, multi-templated hierarchical network and as functional monomer cross-linkable with both synthetic and natural cross-linkers.

The robustness of chitosan was explored in establishing a multi-templated system capable of sequestering target materials from a cocktail component of a fluid making it feasible to be employed in real-time sequestration activity like cigarette smoking etc.

Biodegradeable filter materials based on Chitosan have been prepared for the sequestration of carcinogenic materials from the smoke of burnt tobacco product. This encourages the possibility of using truly natural and biodegradeable materials in the production of cigarette butt filters which has before now being produced using the difficultly biodegradeable semisynthetic cellulose acetate.

5.4 Recommendation

It is well suited to initiate futher studies into the investigation of the influence of different porogens, functional monomer: template reacting ratios as well as various other natural cross-linker materials on the integrity and recognition potentials of chitosan based molecularly imprinted polymer matrix. Studies on the use of natural polymers like Pullulan and cross-linkers like genipin is already a pivotal focus of further studies and should be vigorously pursued. Enhancement in the robust nature of sequestration materials from this class of MIPs vis-à-vis increasing the number of template blends should also be embarked on. An industrial fabrication and testing of filters based on this research outcome should be vigorously pursued in collaboration with releted industries and stakeholders. The search for other alternative local sources of Chitin and Chitosan should be sustained and extended from the on-going millipede based resource by our research group. Ending it, there should be a probe into the discovery of a suitable alternative to the use of Methacrylic acid in order to increase the economic potential of this process signature.

Reference

Abdou, E., Nagy, K. and Elsabee, M. (2008). Extraction and characterization of chitin and chitosan from local sources. Bioresource Technology, 99(5), 1359-1367. http://dx.doi.org/10.1016/j.biortech.2007.01.051

Abouzeed A. S., Omayma E. Shaltout, Ibrahim S. M., Attia. R. S., Aboul -yazeed A. M. Production and Evaluation of Some Bioactive Compounds Extracted from Squilla (Oratosquilla massavensis) Shells. American Journal of Life Sciences. Special Issue: New Horizons in Basic and Applied Zoological Research. Vol. 3, No. 6-1, 2015, pp. 38-44. doi: 10.11648/j.ajls.s.2015030601.16

Acosta, N., Jiménez, C., Borau, V., and Heras, A. (1993). Extraction and characterization of chitin from crustaceans. Biomass And Bioenergy, 5(2), 145-153. doi: 10.1016/0961-9534(93)90096-m

Adem Y., Handan A., Turan S.E, Mehmet B and Mustafa O.G (2011).Templated-Directed synthesis of silica nanotubes for explosive detection.ACS Appl. Mater. Interfaces; 3: 4159 – 4164.

Ahmed, T., and Aljaeid, B. (2016). Preparation, characterization, and potential application of chitosan, chitosan derivatives, and chitosan metal nanoparticles in pharmaceutical drug delivery. Drug Design, Development and Therapy, 483. http://dx.doi.org/10.2147/dddt.s99651

Aiping, Z., Jianhong, L., & Wenhui, Y. (2006). Effective loading and controlled release of camptothecin by O-carboxymethylchitosan aggregates. *Carbohydrate Polymers*, *63*(1), 89-96. doi: 10.1016/j.carbpol.2005.08.006

Al-Dallal, S., Aljishi, S., Hammam, M., Al-Alawi, S. M., Stutzmann, M., Jin, S., ...and Schwarz, R. (1991). High band-gap hydrogenated amorphous silicon-selenium alloys. *Journal of applied physics*, *70*(9), 4926-4930.

Alberda van Ekenstein, G., and Tan, Y. (1982). A DSC study of the polymerization of Methacrylic acid in dimethylformamide. European Polymer Journal, 18(12), 1061-1065. doi: 10.1016/0014-3057(82)90206-3

Alenus J., Galar P., Ethirajan A., Horemans F., Weustenraed A., Cleij T.J., Wagner P.(2012). Detection of L-nicotine with dissipation mode quartz crystal microbalance using molecular imprinted polymers. Phys. Status Solidi. 209:905–910. doi: 10.1002/pssa.201100768.

Alenus J., Ethirajan A., Horemans F., Weustenraed A., Csipai P., Gruber J., Peeters M., Cleij T.J., Wagner P. (2013). Molecularly imprinted polymers as synthetic receptors for the QCM-D-based detection of l-nicotine in diluted saliva and urine samples. Anal. Bioanal. Chem.; 405:6479–6487. doi: 10.1007/s00216-013-7080-1.

Alexander, C., Andersson, H., Andersson, L., Ansell, R., Kirsch, N., and Nicholls, I. (2006). Molecular imprinting science and technology: a survey of the literature for the years up to and including 2003. *Journal Of Molecular Recognition*, *19*(2), 106-180. doi: 10.1002/jmr.760.

Alves, N., and Mano, J. (2008). Chitosan derivatives obtained by chemical modifications for biomedical and environmental applications. International Journal of Biological Macromolecules, 43(5), 401-414. http://dx.doi.org/10.1016/j.ijbiomac.2008.09.007

Aminabhavi, T., and Munk, P. (1979). Preferential Adsorption onto Polystyrene in Mixed Solvent Systems. Macromolecules, 12(4), 607-613. http://dx.doi.org/10.1021/ma60070a012

Anand, M., Kalaivani, R., Maruthupandy, M., Kumaraguru, A., and Suresh, S. (2014). Extraction And Characterization of Chitosan from Marine Crab and Squilla Collected from the Gulf of Mannar Region, South India. Journal of Chitin and Chitosan Science, 2(4), 280-287. http://dx.doi.org/10.1166/jcc.2014.1053

Andersson, H., Koch-Schmidt, A., Ohlson, S., and Mosbach, K. (1996). Study of the nature of recognition in molecularly imprinted polymers. *Journal Of Molecular Recognition*, *9*(5-6), 675-682. doi: 10.1002/(sici)1099-1352(199634/12)9:5/6<675::aid-jmr320>3.0.co;2-c

Andersson, L. (2002). Selective Solid-Phase Extraction of Bio- and Environmental Samples Using Molecularly Imprinted Polymers. *Cheminform*, *34*(36). doi: 10.1002/chin.200336279

Andersson, L., Sellergren, B., and Mosbach, K. (1984). Imprinting of amino acid derivatives in

` macroporous polymers. *Tetrahedron Letters*, *25*(45), 5211-5214. doi: 10.1016/s0040-4039(01)81566-5

Andersson, H. S., Karlsson, J. G., Piletsky, S. A., Koch-Schmidt, A. C., Mosbach, K., and Nicholls, I. A. (1999). Study of the nature of recognition in molecularly imprinted polymers, II [1]: Influence of monomer–template ratio and sample load on retention and selectivity. Journal of Chromatography A, 848(1-2), 39-49.

Andrea, P., Miroslav, S., Silvia, S., and Stanislav, M. (2001). A solid binding matrix/molecularly imprinted polymer-based sensor system for the determination of clenbuterol in bovine liver using differential-pulse voltammetry. *Sensors And Actuators B: Chemical*, *76*(1-3), 286-294. doi: 10.1016/s0925-4005(01)00586-x

Andrady, A., and Xu, P. (1997). Elastic behavior of chitosan films. *Journal Of Polymer Science Part B: Polymer Physics*, *35*(3), 517-521. doi: 10.1002/(sici)1099-0488(199702)35:3<517::aid-polb10>3.0.co;2-k

Annamma K. M (2008), Ph. D. Thesis, Mahatma Gandhi University, Kottayam.
Of Chitosan from Shrimp Shells Waste. Advanced Materials Research, 1123, 205-208. http://dx.doi.org/10.4028/www.scientific.net/amr.1123.205

Arshady, R., and Mosbach, K. (1981). Synthesis of substrate-selective polymers by host-guest polymerization. *Die Makromolekulare Chemie: Macromolecular Chemistry and Physics*, *182*(2), 687-692.. doi: 10.1002/macp.1981.021820240

ASH. 2009. Tobacco and the developing world. London, United Kingdom: ASH.

ASTM D6400 - 12, 2012, "Standard Specification for Labeling of Plastics designed to be Aerobically Composted in Municipal or Industrial Facilities," ASTM International

Bailey, F., Lundberg, R., and Callard, R. (1964). Some factors affecting the molecular association of poly(ethylene oxide) and poly(acrylic acid) in aqueous solution. *Journal Of Polymer Science Part A: General Papers*, *2*(2), 845-851. doi: 10.1002/pol.1964.100020221

Ballard D.G.H and Bamford C.H (1956) *Proc. Roy. Soc. London.* A236; 384-495.

Bamford, C. H., and Haward, R. N. (1979). Developments in polymerization. *London: Appl Sci Pub*, 215.

Bamford, C. H., and Shiiki, Z. (1968). Free-radical template polymerization. *Polymer*, *9*, 595-

598.

Barrett, E. P., Joyner, L. G., and Halenda, P. P. (1951). The determination of pore volume and area distributions in porous substances. I. Computations from nitrogen isotherms. *Journal of the American Chemical society*, *73*(1), 373-380.

Beckman Coulter Particle Characterization Group, (2011). *LS 13 320 Particle Size Analyzer Manual*, PN 383462 Rev. A., Appendix IV, pp. 117-121.

Binorkar, S., and Jani, D. (2012). Traditional Medicinal Usage of Tobacco and #8211; A Review.Spatula DD - Peer Reviewed Journal On Complementary Medicine And Drug Discovery, 2(2), 127. doi: 10.5455/spatula.20120423103016

Blecher, E. H., and H. Ross. 2013. Tobacco use in Africa: Tobacco control through prevention. Atlanta, GA: American Cancer Society.

Blumstein A, Kakivaya S. R, and Salamone J.C., (1974) *J. Polym. Sci., Polym.Lett.Ed.*, 12, 651.

Blumstein A, Kakivaya S.R, Shah K. R, and Wilkins D. J., (1974) *J. Polym. Sci., Polym.Symp.*, 45, 75.

Bough, W.A., Salter, W.L., Wu, A.C., Perkins, B.E., (1978). Influence of manufacturing variables on the characteristics and effectiveness of chitosan products. 1. Chemical composition, viscosity, and molecular-weight distribution of chitosan products. Biotechnol. Bioeng. 20, 1931–1943

Boris A.(1925). "The History of Filters". tobaccoasia.com. Archived from the original on August 24, 2003. Retrieved 2008-05-18. Accessed 21 February 2017.

Brugnerotto, J., Desbrières, J., Roberts, G., and Rinaudo, M. (2001). Characterization of chitosan by steric exclusion chromatography. Polymer, 42(25), 09921-09927. http://dx.doi.org/10.1016/s0032-3861(01)00557-2

Brunnemann, K., Prokopczyk, B., Djordjevic, M., and Hoffmann, D. (1996). Formation and Analysis of Tobacco-SpecificN-Nitrosamines. *Critical Reviews In Toxicology*, *26*(2), 121-137. doi: 10.3109/10408449609017926

Bundi, A., and Wüthrich, K. (1977). 1H NMR titration shifts of amide proton resonances in Polypeptide chains. FEBS Letters, 77(1), 11-14. http://dx.doi.org/10.1016/0014-5793(77)80182-8

Bunermann H, Duttagupta N, Schuetz J, and Muller W., (1981), *Biochemistry***,** 20, 2664.

Carreno-Gomez, B. and A. Duncan. 1997. Evaluation of the biological properties of soluble Chitosan and chitosan microspheres. International Journal of Pharmaceutical **148**: 231-240.Carter S. New frontier, new power: the retail environment in Australia's dark market. Tob Control. 2003 Dec; 12(Suppl 3):iii95–101.

Cerrai P, Guerra G. D., Maltinti S, Tricoli M, Giusti P, Petarca L, and Polacco G (1994), *Macromol. Chem., Rapid Comm.*, 15, 983.

Challa, G., and Tan, Y. (1981). Template polymerization. *Pure and Applied Chemistry*, *53*(3), 627-641. doi: 10.1351/pac198153030627

Chaouachi, K. (2009). Hookah (Shisha, Narghile) Smoking and Environmental Tobacco Smoke (ETS). A Critical Review of the Relevant Literature and the Public Health Consequences International Journal of Environmental Research and Public Health. 6(2), 798-843; https://doi.org/10.3390/ijerph6020798

Chen, G.; Guan, Z.; Chen, C.; Fu, L.; Sundaresan, V.; Arnold, F.Chen, Lingxin, Shoufang Xu, and Jinhua Li (2011): "Recent Advances In Molecular Imprinting Technology: Current Status, Challenges And Highlighted Applications". Chemical Society Reviews 40.5 2922.

Chen P, Song L, Liu Y, Fang Y-e (2007). Synthesis of silver nanoparticles by [gamma]-ray irradiation in acetic water solution containing chitosan. Radiat Phys Chem; 76(7):1165-8.

Chen, S., Rotaru, A. E., Liu, F., Philips, J., Woodard, T. L., Nevin, K. P., and Lovley, D. R. (2014). Carbon cloth stimulates direct interspecies electron transfer in syntrophic co-cultures. *Bioresource technology*, *173*, 82-86.

Chen Y and Tan HM. (2006). Crosslinked carboxymethylchitosang-poly (acrylic acid) copolymer as a novel superabsorbent polymer. Carbohydr Res. 341: 887-96.

Chen, L., Wang, X., Lu, W., Wu, X., and Li, J. (2016). Molecular imprinting: perspectives and Applications. Chemical Society Reviews, 45(8), 2137-2211. http://dx.doi.org/10.1039/c6cs00061d

Chouwatat, P., Hirai, T., Higaki, K., Higaki, Y., Sue, H. J., and Takahara, A. (2017). Aqueous lubrication of poly (etheretherketone) via surface-initiated polymerization of electrolyte monomers. *Polymer*, *116*, 549-555.

Chuekachang, S., Janmanee, R., Baba, A., Phanichphant, S., Sriwichai, S., Shinbo, K., ...and

Ushijima, H. (2013). Fabrication of thin film from conducting polymer/single wall carbon nanotube composites for the detection of uric acid. *Molecular Crystals and Liquid Crystals*, *580*(1), 1-6.

Chun HK and Kyu SC (1998): Synthesis and properties of carboxyalkyl chitosan and its derivative. Journal of Ind & Eng chemistry; 4: 19-25.

Cityofhope.org. (2014). https://www.cityofhope.org/about-city-of-hope/news-and-media/blogs-and-publications. Accessed 12/3/2016 by 4:23pm.

Coates, J. (2000). Interpretation of Infrared Spectra, A Practical Approach. *Encyclopedia Of Analytical Chemistry*. http://dx.doi.org/10.1002/9780470027318.a5606

Coggins, C. and Gaworski, C.L. (2008). Could charcoal filtration of cigarette smoke reduce smoking-induced disease? A review of the literature. Journal of Regulatory toxicology and pharmacology.50 Vol. pp 359-365. Doi: 10.1016/j.yrtph.2008.01.001

Corsi, K., F. Chellat, L. Yahia and J.C. Farnandes. 2003. Mesenchymak sten cells, MG63 and HEK293 transfaction using chitosan-DNA nanoparticles. Biomaterials **24**: 1255-1261.

Counts M.E., Morton M.J., Laffoon S.W., Cox R.H., Lipowicz, P.H. (2005). Smoke composition and Predicting relationships for international commercial cigarettes smoked with three machine-smoking conditions. Regulatory Toxicology and Pharmacology; 41(3):185–227.

Croux D., Weustenraed A., Pobedinskas P., Horemans F., Diliën H., Haenen K., Cleij T., Wagner P., Thoelen R., De Ceuninck W. (2012). Development of multichannel quartz crystal microbalances for MIP-based biosensing. Phys. Status Solidi Appl. Mater. Sci.; 209:892–899. doi: 10.1002/pssa.201100715.

Dai, C., Zhang, J., Zhang, Y., Zhou, X., Duan, Y., and Liu, S. (2012). Selective removal of acidic pharmaceuticals from contaminated lake water using multi-templates molecularly imprinted polymer. Chemical Engineering Journal, 211-212, 302-309. http://dx.doi.org/10.1016/j.cej.2012.09.090

Despond S, Espuche N, Cartier N, Domard A. (2005). Barrier properties of paper-chitosan and Paper-chitosan-carnauba wax films. J Appl Polym Sci 98:704–10.

Dickert, F. L.; Halikias, K.; Hayden, O.; Piu, I.; Sikorski, R (2001)**.***Sens. Actuat. B., 76,* 295.

Dickert F.L., Hayden O. (2002). Bio imprinting of polymers and sol-gel phases. Selective

detection of yeasts with imprinted polymers. Anal. Chem.; 74:1302–1306. doi:10.1021/ac010642k.

Dickey, F. H. (1949). The preparation of specific adsorbents *Proc. Natl. Acad. Sci. U.S.A.*, *35*, 227-229. doi: 10.1073/pnas.35.5.227

Ding, M., Wu, X., Yuan, L., Wang, S., Li, Y., and Wang, R. (2011). Synthesis of core–shell magnetic molecularly imprinted polymers and detection of sildenafil and vardenafil in herbal dietary supplements. Journal Of Hazardous Materials, 191(1-3), 177-183. http://dx.doi.org/10.1016/j.jhazmat.2011.04.058

Djordjevic M.V, Doran K.A (2009). Nicotine content and delivery across tobacco products. Handbook of Experimental Pharmacology; 192:61–82.

Dong, H., Tong, A., and Li, L. (2003). Syntheses of steroid-based molecularly imprinted polymers and their molecular recognition study with spectrometric detection. Spectrochimica Acta Part A: Molecular and Biomolecular Spectroscopy, 59(2), 279-284. http://dx.doi.org/10.1016/s1386-1425 (02)00179-8

Drewnowska, O., Turek, B., Carstanjen, B., and Gajewski, Z. (2013). Chitosan – a promising biomaterial in veterinary medicine. Polish Journal of Veterinary Sciences, 16(4). http://dx.doi.org/10.2478/pjvs-2013-0119

Drozd NN, Sher A.I, Makarov V.A, Galbraikh LS, Vikhoreva G.A and Gorbachiova I.N (2001): Comparison of antithrombin activity of polysulfate chitosan derivatives in vivo and in vitro system, Thrombosis Research; 102: 445-55.

Du W, Zhou H, Luo Z, Zheng P, Guo P, Chang R.2014. Molecular Imprinting.2(1).

Duan, Y., Dai, C., Zhang, Y., & Ling-Chen. (2013). Selective trace enrichment of acidic pharmaceuticals in real water and sediment samples based on solid-phase extraction using multi-templates molecularly imprinted polymers. Analytica Chimica Acta, 758, 93-100. http://dx.doi.org/10.1016/j.aca.2012.11.010

Duarte, M. L., Ferreira, M. C., Marva ˜o, M. R., and Rocha, J. (2001). Determination of the degree of acetylation of chitin materials by 13C CP/MAS NMR spectroscopy. International Journal of Biological Macromolecules, 28, 359–363.

Dutta, P.K., J. Dutta and V.S. Tripathi. (2004). Chitin and chitosan: Chemistry, properties and applications. Journal of Scientific and Industrial Research 63: 20-31.

Eddaoudi, M. (2005). Characterization of Porous Solids and Powders: Surface Area, Pore Size and Density By S. Lowell (Quantachrome Instruments, Boynton Beach), J. E. Shields (C. W. Post Campus of Long Island University), M. A. Thomas, and M. Thommes (Quantachrome In-struments). Kluwer Academic Publishers: Dordrecht, the Netherlands. 2004. Xiv 348 pp. ISBN 1-4020-2302-2. Journal of the American Chemical Society, 127(40), 14117-14117. http://dx.doi.org/10.1021/ja041016i

Ekberg, B.and Mosbach, K. (1989). Molecular imprinting: A technique for producing specific separation materialsTrends Biotechnolog.7, 92-96

Elena R, Lupei M, Ciolacu FL and Desbrières J (2011): Synthesis and characterization of n-alkyl Chitosan for papermaking applications. Cellulose Chem. Technol; 45: 619-25.

Elena, V.; Piletska, A.R.; Guerreiro, M.J.; Whitcombe, J.; Sergey, A.P (2009).*Macromolecules* 42, 4921.

Elias H.G., (1977) Ed., Polymerization of Organized Systems, *Gordon & Breach Sci. Pub*., New York.

Elzein, A.R., F. Dabbarh and C. Chaput. (2002). Injectable self-setting calcium phosphate cement. In: Chitosan in pharmacy and chemistry (Eds. R.A.A. Muzzareli & C. Muzzareli) ATEC: Grottammare. Italy, Pp.365- 370.

Erbahar, D., Harbeck, M., Gümüş, G., Gürol, I., and Ahsen, V. (2014). Self-assembly of phthalocyanines on quartz crystal microbalances for QCM liquid sensing applications. Sensors and Actuators B: Chemical, 190, 651-656. http://dx.doi.org/10.1016/j.snb.2013.09.034

Eriksen, M., J. Mackay, and H. Ross.(2012). The tobacco atlas, 4th ed. Atlanta, GA: American Cancer Society

Espinosa-García B.M, Argüelles-Monal W.M, Hernández J, FélixValenzuela L, Acosta N, Goycoolea F.M (2007). Molecularly imprinted Chitosan - Genipin hydrogels with recognition capacity toward Oxylene. Biomacromolecules; 8(11): 3355-64. 230 Current Chemical Biology, 2009, Vol. 3, No. 2

Esson, K. M., and S. R. Leeder. (2004). The millennium development goals and tobacco control: An opportunity for global partnership. Geneva, Switzerland: Tobacco Free Initiative, WHO.

Fang L., Wen G.L and Kang D.Y (2002): Preparation of oxidized glucose-crosslinked N-alkylated Chitosan membrane and in vitro studies of pH-sensitive drug delivery behaviour. Biomaterials; 23: 343-47.

Farramae C. Francisco, Rhoda Mae C. Simora, Sharon N. Nuñal. (2015). Deproteination and Demineralization of shrimp waste using lactic acid bacteria for the production of crude chitin and chitosan. AACL Bioflux. Volume 8, Issue 1. http://www.bioflux.com.ro/aacl

Farrington, K., Magner, E., and Regan, F. (2006). Predicting the performance of molecularly imprinted polymers: selective extraction of caffeine by molecularly imprinted solid phase extraction. *Analytica chimica acta*, *566*(1), 60-68

Faucher, J. A., Koleske, J. V., Santee Jr, E. R., Stratta, J. J., and Wilson Iii, C. W. (1966). Glass transitions of ethylene oxide polymers. *Journal of Applied Physics*, *37*(11), 3962-3964

Federal Ministry of Health. (2012a). GATS Nigeria. Global Adult Tobacco Survey: Country report 2012. Abuja, Nigeria: Federal Ministry of Health.

Federal Ministry of Health, (2012b). Global Adult Tobacco Survey: Country report 2012 part II. Abuja, Nigeria: Federal Ministry of Health.

Ferguson J and Shah S. A. O (1968), *Eur. Polym. J*., 4, 343.

Ferguson J. and Shah S. A. O., (1968) *Eur. Polym.J*, 4, 611.

Ferguson, J., and Eboatu, A. (1989). Redox-initiated template polymerization of acrylic acid by means of Fenton's reagent: initiator complexation. European Polymer Journal, 25(7-8), 731-735. http://dx.doi.org/10.1016/0014-3057(89)90038-4

Ferrer, I., Lanza, F., Tolokan, A., Horvath, V., Sellergren, B., Horvai, G., and Barceló, D. (2000). Selective Trace Enrichment of Chlorotriazine Pesticides from Natural Waters and Sediment Samples Using Terbuthylazine Molecularly Imprinted Polymers. Analytical Chemistry, 72(16), 3934-3941. http://dx.doi.org/10.1021/ac000015f

Fu, G., Zhao, J., Yu, H., Liu, L., and He, B. (2007). Bovine serum albumin-imprinted polymer gels prepared by graft copolymerization of acrylamide on chitosan. Reactive and Functional Polymers, 67(5), 442-450.

Fu, X., Xu, L., Qi, L., Tian, H., Yi, D., and Yu, Y. (2017). BMH-21 inhibits viability and induces apoptosis by p53-dependent nucleolar stress responses in SKOV3 ovarian cancer cells. Oncology Reports, 38(2), 859-865. doi: 10.3892/or.2017.5750

Fu, X., Yang, Q., Zhou, Q., Lin, Q., and Wang, C. (2015). Template-Monomer Interaction in

Molecular Imprinting: Is the Strongest the Best? Open Journal of Organic Polymer Materials, 05(02), 58-68. http://dx.doi.org/10.4236/ojopm.2015.52007.

GATS (2012). https://www.afro.who.int/sites/default/files/2017-09/tob-gats-in-nigeria-a-sucess-story-in-afr.pdf. accessed 15 May 2016.

Gately, Iain (2004). Tobacco: A Cultural History of How an Exotic Plant Seduced Civilization. Diane. pp. 3–7. ISBN 0-8021-3960-4.

Gavhane, Y.N., A.S. Gaurav and A.V. Yadav. (2013). Chitosan and its application: A review of literature. *International Journal of Research in Pharmaceutical and Biomedical* **4**: 312-331.

George W.(2009). https://www.politifact.com/truth-o-meter/statements/2009/jun/29/george-will/claims-smoking-kills-more-people-annually-other-da/. Accessed 10 July 2017.

Golker, K., Karlsson, B., Olsson, G., Rosengren, A., and Nicholls, I. (2013). Influence of Composition and Morphology on Template Recognition in Molecularly Imprinted Polymers. Macromolecules, 46(4), 1408-1414. http://dx.doi.org/10.1021/ma3024238

Goosen, M. (1997). Applications of chitin and chitosan. Lancaster [u.a.]: Technomic Publ. Co.

Gregg, S. J. and Sing, K. S. W (1982). Adsorption: Surface Area and Porosity, *Second edition, London,*

Guo T.Y, Xia Y.Q, Hao G.J, Song M.D, Zhang B.H. (2004); Adsorptive separation of hemoglobin by molecularly imprinted chitosan beads. Biomaterials; 25(27): 5905-12.

Guo T.Y, Xia Y.Q, Wang J, Song M.D, Zhang B.H. (2005); Chitosan beads as molecularly imprinted polymer matrix for selective separation of proteins. Biomaterials; 26(28): 5737-45.

Ham-Pichavant F, Sèbe G, Pardon P, Coma V. (2005). Fat resistance properties of chitosan-based paper packaging for food applications. Carbohydr Polym 61:259–65.

Han, J.H. 2000. Antimicrobial food packaging. Food Technology 54: 56-65.

Hang, T.T., D.E. Dunstan and D.R. Crispin. (2010); Anticancer activity and therapeutic applications of chitosan nanoparticles. In: Chitin, chitosan, oligosaccharides and their derivatives, biological activities and applications. (Eds. S.K. Kim), New York, CRC Press. UK, Pp. 271-282.

Haupt, K., and Mosbach, K. (2006). Molecularly imprinted polymers and their use in biomimetic

sensors. *Chemical reviews*, *100*(7), 2495-2504.

Hayashida, N., Fujimoto, M., Ke, T., Prakasam, R., Shinkawa, T., Li, L., Ichikawa, H., Takii, R.and Nakai, A. (2015). Heat shock factor 1 ameliorates proteotoxicity in cooperation with the transcription factor NFAT. EMBO J 2010 .

Health New Zealand (2009). Annual Summary Of Outbreaks In New Zealand in 2009. https://surv.esr.cri.nz/PDF_surveillance/AnnualRpt/AnnualOutbreak/2009/2009OutbreakRpt.pdf. Accessed 14 of April 2018.

Healton, C. G., Cummings, K. M., O'connor, R. J., and Novotny, T. E. (2011). Butt really? The environmental impact of cigarettes. *Tobacco Control*, *20*(Suppl 1), i1-i1

Henningfield J.E., Fant R.V., Radzius A, Frost S. (1999) Nicotine concentration, smoke pH and whole tobacco aqueous pH of some cigar brands and types popular in the United States. Nicotine Tobacco Research; 1(2):163–168.

Higashi, F., Nakano, Y., Goto, M., and Kakinoki, H. (1980). High-molecular-weight polyterephthalamide by direct polycondensation reaction in the presence of poly(ethylene oxide). *Journal Of Polymer Science: Polymer Chemistry Edition*, *18*(3), 1099-1104. doi: 10.1002/pol.1980.170180328

Higashi F.; Sano K, and Kakiniki H., (1980) *J. Polym. Sci., J. Chem. Ed.*, 18, 1841.

Hoffmann, D., Rivenson, A., and Hecht, S. (1996). The Biological Significance of Tobacco-SpecificN-Nitrosamines: Smoking and Adenocarcinoma of the Lung. *Critical Reviews In Toxicology*, *26*(2), 199-211. doi: 10.3109/10408449609017931

Hon, D.N.S. 1(996) Chitin and chitosan: Medical applications In Polysaccharides in medicinal application (Eds. S.Dumitriu). New York: Marcel Dekker. pp.631-651 *Applications of Chitin and Chitosan in... (PDF Download Available).* Available from: https://www.researchgate.net/publication/291174564_Applications_of_Chitin_and_Chitosan_in_Industry_and_Medical_Science_A_Review [accessed May 28 2018].

Huang, H., Yuan, Q., and Yang, X. (2004). Preparation and characterization of metal–chitosan nanocomposites. *Colloids And Surfaces B: Biointerfaces*, *39*(1-2), 31-37. doi: 10.1016/j.colsurfb.2004.08.014

Hudson, S.M. and C. Smith. (1998). Polysaccharide: Chitin and chitosan: Chemistry and

technology of their use as structrual materials. In: *Biopolymers from Renewable Resources* (Eds. D. L. Kaplan). Pp.96-118.

Hung, C., & Hwang, C. (2008). Analysis of Ketoprofen and Mefenamic Acid by High-Performance Liquid Chromatography with Molecularly Imprinted Polymer as the Stationary Phase. Journal Of Chromatographic Science, 46(9), 813-818. http://dx.doi.org/10.1093/chromsci/46.9.813

Husain, K., Scott, B. R., Reddy, S. K., and Somani, S. M. (2001). Chronic ethanol and nicotine interaction on rat tissue antioxidant defense system. *Alcohol*, *25*(2), 89-97.

Inaki Y, and Takemoto K., (1987). in Current Topics in Polymer Science, R. M. Ottenbrite,L. A. Utracki, and S. Inoue, Eds., *Hanser Pub*., Munich, Vol. 1, 79.

Ineichen, B. (2005). Smoke: A Global History of Smoking. Social History Of Medicine, 18(3), 508-509. doi: 10.1093/shm/hki061

Intorp, M., Purkis, S., and Wagstaff, W. (2012). Determination of Tobacco Specific Nitrosamines in Cigarette Mainstream Smoke: The CORESTA 2011 Collaborative Study. Beiträge Zur Tabakforschung International/Contributions To Tobacco Research, 25(4), 507-519. doi: 10.2478/cttr-2013-0926

IUPAC. (2015). Physisorption of gases, with special reference to the evaluation of surface area and pore size distribution (IUPAC Technical Report) (pp. 1-19). De Gruyter.

Jain, A., Gulbake, A., Shilpi, S., Jain, A., Hurkat, P., and Jain, S. (2013). A New Horizon in Modifications of Chitosan: Syntheses and Applications. *Critical Reviews In Therapeutic Drug Carrier Systems*, *30*(2). doi: 10.1615/critrevtherdrugcarriersyst.2013005678

Janshoff, A., Galla, H., and Steinem, C. (2000). Piezoelectric Mass-Sensing Devices as Biosensors—An Alternative to Optical Biosensors?. Angewandte Chemie, 39(22), 4004-4032.http://dx.doi.org/10.1002/1521-3773(20001117)39:22<4004::aid-anie4004>3.0.co;2-2

Jha, P. (2009). Avoidable global cancer deaths and total deaths from smoking. *Nature Reviews Cancer*, *9*(9), 655-664. doi: 10.1038/nrc2703

Jianglian, D. and Z. Shaoying. (2013). Application of chitosan based coating in fruits and vegetables preservation: A review. *Food Processing and Technology* **4**: 227-230. doi:10.472/2157-7110.1000227

Jing, T., Wang, J., Liu, M., Zhou, Y., Zhou, Y., and Mei, S. (2013). Highly effective removal of 2, 4-dinitrophenolic from surface water and wastewater samples using hydrophilic molecularly imprinted polymers. Environmental Science and Pollution Research, 21(2), 1153-1162. http://dx.doi.org/10.1007/s11356-013-2007-0

Jing, T., Xia, H., Niu, J., Zhou, Y., Dai, Q., and Hao, Q. et al. (2011). Determination of trace 2, 4-dinitrophenol in surface water samples based on hydrophilic molecularly imprinted polymers/nickel fiber electrode. Biosensors and Bioelectronics, 26(11), 4450-4456. http://dx.doi.org/10.1016/j.bios.2011.05.001

Kabanov V.A, Topchiev D.A, Karaputadze T.M, (1973) *J. Polym. Sci Symp*.42, 173 (with Mkrtchian L.A) *Eur. Polym. J.* 11; 153.

Kai Z, Dieter P, Johanna H, Thomas G and Steffen F: (2011). FT Raman investigation of novel chitosan sulfates exhibiting osteogenic capacity. Carbohydr Polym; 83: 60-65.

Kamiński, W., and Modrzejewska, Z. (1997). Application of Chitosan Membranes in Separation of Heavy Metal Ions. Separation Science and Technology, 32(16), 2659-2668. http://dx.doi.org/10.1080/01496399708006962

Kanazawa, K. and Cho, N.J. (2009). Quartz Crystal Microbalance as a Sensor to Characterize. Macromolecular Assembly Dynamics. Journal of Sensors doi:10.1155/2009/824947

Kanazawa, K. K., and Gordon II, J. G. (1985). The oscillation frequency of a quartz resonator in contact with liquid. *Analytica Chimica Acta*, *175*, 99-105.

Kasaai, M., Arul, J., and Charlet, G. (2013). Fragmentation of Chitosan by Acids. The Scientific World Journal, 2013, 1-11. http://dx.doi.org/10.1155/2013/508540

Kathleen Register. (2001). Underwater Naturalist, Bulletin of the American Littoral Society. http://www.longwood.edu/cleanva/ciglitterarticle.htm Accessed 12 July 2017.

Katz, A., and Davis, M. (1999). Investigations into the Mechanisms of Molecular Recognition with Imprinted Polymers. *Macromolecules*, *32*(12), 4113-4121. doi: 10.1021/ma981445z

Kempe, M., and Mosbach, K. (1995). Separation of amino acids, peptides and proteins on molecularly imprinted stationary phases. *Journal Of Chromatography A*, *691*(1-2), 317-323. doi: 10.1016/0021-9673(94)00820-y.

Khor, E., and Lim, L. (2003). Implantable applications of chitin and chitosan. *Biomaterials*, *24*(13), 2339-2349. doi: 10.1016/s0142-9612(03)00026-7

Kim, H., and Spivak, D. (2003). New Insight into Modeling Non-Covalently Imprinted Polymers. Journal Of The American Chemical Society, 125(37), 11269-11275. doi: 10.1021/ja0361502

Kim, S.K. and P. Dewapriya. (2014). Biologically active compounds from seafood processing by-products. In: Biotransformation of waste biomass into high value 249iochemical (Eds. S.K. Brar, G.S. Dhillon & C.R. Soccol). New York, Heidelberg Dordrecht London. Pp. 299-313.

Kjellgren, H., Gällstedt, M., Engström, G., and Järnström, L. (2006). Barrier and surface properties of chitosan-coated greaseproof paper. *Carbohydrate Polymers*, *65*(4), 453-460. doi: 10.1016/j.carbpol.2006.02.005

Klotzbach, T. L., Watt, M., Ansari, Y., and Minteer, S. D. (2008). Improving the microenvironment for enzyme immobilization at electrodes by hydrophobically modifying chitosan and Nafion® polymers. Journal of Membrane Science, 311(1-2), 81-88.

Knorr, D. (1991) Recovery and utilization of chitin and chitosan in food processing waste management. Food Technology. International Development Research Centre.26, 114–122.

Krupadam, R., Venkatesh, A., and Piletsky, S. (2013). Molecularly Imprinted Polymer Receptors for Nicotine Recognition in Biological systems. Molecular Imprinting, 1. doi: 10.2478/molim-2012-0004

Kullmann W., (1987) in Enzymatic Peptide Synthesis, *CRC Press*, Boca Raton.

Kumar, M. N. R. (2000). A review of chitin and chitosan applications. *Reactive and functional polymers*, *46*(1), 1-27.

Kumari, S., Rath, P., Sri Hari Kumar, A., and Tiwari, T. (2015). Extraction and characterization of Chitin and chitosan from fishery waste by chemical method. Environmental Technology & Innovation, 3, 77-85. http://dx.doi.org/10.1016/j.eti.2015.01.002

Kurita, K. (2006). Chitin and Chitosan: Functional Biopolymers from Marine Crustaceans. *Marine Biotechnology*, *8*(3), 203-226. doi: 10.1007/s10126-005-0097-5

Kyzas, G., and Bikiaris, D. (2015). Recent Modifications of Chitosan for Adsorption

Applications: A Critical and Systematic Review. Marine Drugs, 13(1), 312-337. http://dx.doi.org/10.3390/md13010312

Kyzas, G., and Bikiaris, D. (2015). Recent Modifications of Chitosan for Adsorption Applications: A Critical and Systematic Review. Marine Drugs, 13(1), 312-337. http://dx.doi.org/10.3390/md13010312

Lachova, M., Lehotay, J., and Cizmarik, J. (2008). ChemInform Abstract: Applications of Molecularly Imprinted Polymers in Analytical and Pharmaceutical Chemistry. *Cheminform*, *39*(12). doi: 10.1002/chin.200812280

Landers, J., Gor, G., and Neimark, A. (2014). ChemInform Abstract: Density Functional Theory Methods for Characterization of Porous Materials. Cheminform, 45(6), doi: 10.1002/chin.201406276

Langmuir, I. (1916). The constitution and fundamental properties of solids and liquids. part i. solids. Journal of the American Chemical Society, 38(11), 2221-2295. http://dx.doi.org/10.1021/ja02268a002

Lavignac, N., Allender, C.J. and Brain, K.R. (2004). Current status of molecularly imprinted polymers as alternatives to antibodies in sorbent assays. Analytica Chimica Acta 510: 139-145.

Lee, H., Yee, M., Eckmann, Y., Hickok, N., Eckmann, D., and Composto, R. (2012). Reversible swelling of chitosan and quaternary ammonium modified chitosan brush layers: effects of pH and counter anion size and functionality. Journal Of Materials Chemistry, 22(37), 19605. http://dx.doi.org/10.1039/c2jm34316a

Leonhardt, A., and Mosbach, K. (1987). Enzyme-mimicking polymers exhibiting specific substrate binding and catalytic functions. *Reactive Polymers, Ion Exchangers, Sorbents*, *6*(2-3), 285-290. doi: 10.1016/0167-6989(87)90099-7

Levi, R., McNiven, S., Piletsky, S., Cheong, S., Yano, K., and Karube, I. (1997). Optical Detection of Chloramphenicol Using Molecularly Imprinted Polymers. *Analytical Chemistry*, *69*(11), 2017-2021. doi: 10.1021/ac960983b

Li, D., Wei, H., Liang, W., Zhang, Z., and Stokke, B. (2015). Oriental reed warbler

(Acrocephalus orientalis) nest defence behaviour towards brood parasites and nest predators. Behaviour, 152(12-13), 1601-1621. doi: 10.1163/1568539x-00003295

Lim, L., Auras, R., and Rubino, M. (2008). Processing technologies for poly(lactic acid). Progress In Polymer Science, 33(8), 820-852. doi: 10.1016/j.progpolymsci.2008.05.004

Lin, H. Y., Hsu, C. Y., Thomas, J. L., Wang, S. E., Chen, H. C., & Chou, T. C. (2006). The microcontact imprinting of proteins: The effect of cross-linking monomers for lysozyme, ribonuclease A and myoglobin. Biosensors and Bioelectronics, 22(4), 534-543.

Lin, K. C., Chung, H. Y., Wu, C. Y., Liu, H. L., Hsieh, Y. W., Chen, I. H., ...and Wai, Y. Y. (2010). Constraint-induced therapy versus control intervention in patients with stroke: a functional magnetic resonance imaging study. *American journal of physical medicine & rehabilitation*, *89*(3), 177-185.

Liu, B., Zheng, H., Deng, X., Xu, B., Sun, Y., Liu, Y., and Liang, J. (2017). Formation of cationic hydrophobic micro-blocks in P(AM-DMC) by template assembly: characterization and application in sludge dewatering. RSC Advances, 7(10), 6114-6122. doi: 10.1039/c6ra27400e

Liu L, Li Y, Li S, Hu N, He Y, Pong R, Law M (2012). Comparison of next-generation Sequencing systems. [Review]. BioMed. Res. Int. 251364.

Liu, H., Du, Y., Wang, X., and Sun, L. (2004). Chitosan kills bacteria through cell membrane damage. *International Journal Of Food Microbiology*, *95*(2), 147-155. doi: 10.1016/j.ijfoodmicro.2004.01.022

Liu, J. Q., and Wulff, G. (2008). Functional mimicry of carboxypeptidase A by a combination of transition state stabilization and a defined orientation of catalytic moieties in molecularly imprinted polymers. *Journal of the American Chemical Society*, *130*(25), 8044-8054.

Liu, Y., Liu, X., and Wang, J. (2003). Molecularly Imprinted Solid-Phase Extraction Sorbent for Removal of Nicotine from Tobacco Smoke. Analytical Letters, 36(8), 1631-1645. doi: 10.1081/al-120021554

Lopez, A., Collishaw, N., and Piha, T. (1994). A descriptive model of the cigarette epidemic in developed countries. *Tobacco Control*, *3*(3), 242-247. doi: 10.1136/tc.3.3.242

Lohmeyer, J., Tan, Y., and Challa, G. (1980). Polymerization of Methacrylic Acid in the

Presence of Isotactic Poly(methyl Methacrylate) as Possible Template. Journal Of Macromolecular Science: Part A-Chemistry, 14(6), 945-957. doi: 10.1080/00222338008068122

Lok, C. M. and Son, R. (2009). Application of molecularly imprinted polymers in food sample analysis – a perspective. *International Food Research Journal* 16: 127-140

Luo, X., Zhan, Y., Tu, X., Huang, Y., Luo, S., and Yan, L. (2011). Novel molecularly imprinted polymer using 1-(α-methyl acrylate)-3-methylimidazolium bromide as functional monomer for simultaneous extraction and determination of water-soluble acid dyes in wastewater and soft drink by solid phase extraction and high performance liquid chromatography. Journal of Chromatography A, 1218(8), 1115-1121. http://dx.doi.org/10.1016/j.chroma.2010.12.081

Luo, J., Wang, X., Xia, B., and Wu, J. (2010). Preparation and Characterization of Quaternized Chitosan Under Microwave Irradiation. *Journal Of Macromolecular Science, Part A*, *47*(9), 952-956. doi: 10.1080/10601325.2010.501310

Madikizela, L., and Chimuka, L. (2016). Determination of ibuprofen, naproxen and diclofenac in aqueous samples using a multi-template molecularly imprinted polymer as selective adsorbent for solid-phase extraction. Journal Of Pharmaceutical And Biomedical Analysis, 128, 210-215. http://dx.doi.org/10.1016/j.jpba.2016.05.037

Mahdy Samar, M., El-Kalyoubi, M., Khalaf, M., and Abd El-Razik, M. (2013). Physicochemical, functional, antioxidant and antibacterial properties of chitosan extracted from shrimp wastes by microwave technique. Annals Of Agricultural Sciences, 58(1), 33-41. doi:10.1016/j.aoas.2013.01.006

Mahony, J., Molinelli, A., Nolan, K., Smyth, M., and Mizaikoff, B. (2005). Towards the rational development of molecularly imprinted polymers: 1H NMR studies on hydrophobicity and ion-pair interactions as driving forces for selectivity. *Biosensors And Bioelectronics*, *20*(9), 1884-1893. Doi: 10.1016/j.bios.2004.07.036

Manzo, V., Ulisse, K., Rodríguez, I., Pereira, E., and Richter, P. (2015). A molecularly imprinted polymer as the sorptive phase immobilized in a rotating disk extraction device for the determination of diclofenac and mefenamic acid in wastewater. Analytica Chimica Acta, 889, 130-137. http://dx.doi.org/10.1016/j.aca.2015.07.038

Marthe, S.; Vasquez. D.S. (2003). Improving the Strategy and Performance of Molecularly Imprinted Polymers Using Cross-Linking Functional Monomers Journal of Organic Chemistry, 68, 9604-9611.

Marx, K. A. (2003). Quartz Crystal Microbalance: A Useful Tool for Studying Thin Polymer Films and Complex Biomolecular Systems at the Solution−Surface Interface. Biomacromolecules, 4, 1099-1120, doi: 10.1021/bm020116i.

Maslova, G. V. (2001). Theory and practice of producing chitin by electrochemical method. In Chitin and Chitosan (T. Uragami, K. Kurita and T. Fukamizo, eds.), Kodansha Scientific Ltd.pp. 325-327

Maslova G.V. (2003). Electrochemical method of obtaining chitin: the essence and physicochemical aspects of electrochemical activation. In Advances in Chitin Science Vol. VI (K. M. Varum, A. Domard and 0. Smidsred, Eds.) pp.263-264, NTNU Trondheim.

Maslova G.V. Kuprina E.E, Bogeruk A.K. and Ezjov V.G. (1996). Russian Patent No. 2059390.

Masahira H, Hiroshi N, and Masayoshi K (1980). Template polycondensation of active esters containing nucleic acid bases with diamines Macromol.Chem...181, C11, 2325 (1980).

Masque, N. (2001). Molecularly imprinted polymers: new tailor-made materials for selective solid-phase extraction. *Trac Trends In Analytical Chemistry*, *20*(9), 477-486. doi: 10.1016/s0165-9936(01)00062-0

MCAT study discussions, (2017).

Méndez, D., Alshanqeety, O., and Warner, K. (2012). The potential impact of smoking control policies on future global smoking trends. *Tobacco Control*, *22*(1), 46-51. Doi: 10.1136/tobaccocontrol-2011-050147

Merino, E., Verde-Sesto, E., Maya, E., Iglesias, M., Sánchez, F., and Corma, A. (2013). Synthesis of Structured Porous Polymers with Acid and Basic Sites and Their Catalytic Application in Cascade-Type Reactions. Chemistry Of Materials, 25(6), 981-988. Doi: 10.1021/cm400123d

Michael A. C, Justice J. B., Neill D. B. (1985). In vivo voltammetric determination of the kinetics of dopamine metabolism in the rat..Neuroscience Letters 56: 365-369,

Ming-chun, L. I., LIU, C., XIN, M. H., ZHAO, H., WANG, M., FENG, Z., and SUN, X. L. (2005). Preparation and characterisation of acylated chitosan. *Chem Res Chinese U*, *21*, 114-16.

Ministry of Health. 2009. Tobacco Trends 2008: A brief update of tobacco use in New Zealand. Wellington: Ministry of Health. http://www.moh.govt.nz accessed 12/5/2016, by 2:30am.

Mohammad R.S, Roya M.T, Abel M and Mohammad A.R. (2010). Synthesis and in vitro evaluation of thiolated chitosandextran sulphate nanoparticles for the delivery of letrozole. Journal of Pharmaceutical Education & Research; 1: Vol. 1 Issue 2, p62-67. 6

Mirmohseni, A., Shojaei, M., and Farbodi, M. (2008). Application of a quartz crystal nanobalance to the molecularly imprinted recognition of phenylalanine in solution. Biotechnology And Bioprocess Engineering, 13(5), 592-597. doi: 10.1007/s12257-008-0028-1

Moraes, L., Rocha, R., Menegazzo, L., Araújo, E., Yukimito, K., and Moraes, J. (2008). Infrared spectroscopy: a tool for determination of the degree of conversion in dental composites. Journal Of Applied Oral Science, 16(2), 145-149. doi: 10.1590/s1678-77572008000200012

Monardes N.1574. First and second and third parts of medical history,of things. https://archive.org/details/primeraysegunda01monagoog.Accessed,28-5-2019by 1015pm.

Mosbach K and Ramstrom O. (1996). The emerging technique of molecular imprinting and its future impact on biotechnology. Nature Biotechnology, 14, 163–170.

Mourya, V. K., and Inamdar, N. N. (2008). Chitosan-modifications and applications: opportunities galore. Reactive and Functional polymers, 68(6), 1013-1051.

Mukherjee-Roy, M., Kurihara, M., and Penn, L. S. (1995). Multi-step derivatization and analysis of the surface of nonporous silicate glass. *Journal of adhesion science and technology*, *9*(7), 953-969.

Mullett, W., Lai, E. and Sellergren, B. (1999). Determination of nicotine in tobacco by molecularly imprinted solid phase extraction with differential pulsed elution. Analytical Communications, 36(6), 217-220. Doi: 10.1039/a902509jW

Munnia, A., Giese, R. W., Polvani, S., Galli, A., Cellai, F. and Peluso, M. E. (2017). Bulky DNA adducts, tobacco smoking, genetic susceptibility, and lung cancer risk. In *Advances in clinical chemistry* (Vol. 81, pp. 231-277). Elsevier

Murakami, K., Ishihara, M., Aoki, H., Nakamura, S., Nakamura, S.and Yanagibayashi, S. (2010). Enhanced healing of mitomycin C-treated healing-impaired wounds in rats with hydrosheets composed of chitin/chitosan, fucoidan, and alginate as wound dressings. *Wound Repair And Regeneration*, *18*(5), 478-485. Doi: 10.1111/j.1524-475x.2010.00606.x

Murugadoss, A.and Chattopadhyay, A. (2007). A 'green' chitosan–silver nanoparticle composite as a heterogeneous as well as micro-heterogeneous catalyst. *Nanotechnology*, *19*(1), 015603. Doi: 10.1088/0957-4484/19/01/015603

Muzzarelli, R. (1988). Chitins and Chitosans as Immunoadjuvants and Non-Allergenic Drug Carriers. *Marine Drugs*, *8*(2), 292-312. Doi: 10.3390/md8020292

Muzzarelli, R.A. (1977). *Chitin*. Pergamon Press Ltd. Headington Hill Hall, Oxford, England Pp.5-37.

Nicholls, I., Adbo, K., Andersson, H., Andersson, P., Ankarloo, J.and Hedin-Dahlström, J. (2001). Can we rationally design molecularly imprinted polymers?. *Analytica Chimica Acta*, *435*(1), 9-18. Doi: 10.1016/s0003-2670(01)00932-1

Nilsson, K., Lindell, J., Norrlöw, O.and Sellergren, B. (1994). Imprinted polymers as antibody mimetics and new affinity gels for selective separations in capillary electrophoresis. *Journal Of Chromatography A*, *680*(1), 57-61. Doi: 10.1016/0021-9673(94)80052-9

Nishi, S.and Kotaka, T. (1985). Complex-forming poly(oxyethylene)/poly(acrylic acid) interpenetrating polymer networks. 2. Function as a chemical valve. *Macromolecules*, *19*(4), 978-984. Doi: 10.1021/ma00158a007

Nishimura, S., Kai, H., Shinada, K., Yoshida, T., Tokura, S.and Kurita, K. (1998). Regioselective syntheses of sulfated polysaccharides: specific anti-HIV-1 activity of novel chitin sulfates. *Carbohydrate Research*, *306*(3), 427-433. Doi: 10.1016/s0008-6215(97)10081-7

Nomura, T.and Okuhara, M. (1982). Frequency shifts of piezoelectric quartz crystals immersed in organic liquids. *Analytica Chimica Acta*, *142*, 281-284.

Nong, S., Lin, F., Huang, X.and Yuan, D. (2013). Preparation of a stir bar sorptive extraction coating based on molecularly imprinted polymer and its application in the extraction of dienestrol and hexestrol in complicated samples. Chinese Journal of Chromatography, 30(11), 1133-1142. http://dx.doi.org/10.3724/sp.j.1123.2012.08034

Norio N, Akir E and Shin IN, Highly phosphorylated chitin, partially deacetylated chitin and chitosan as new functional polymers synthesis and characterisation. Int J Macromol 1986; 8: 311-17.

Nunthanid, J., Luangtana-anan, M., Sriamornsak, P., Limmatvapirat, S., Huanbutta, K.and Puttipipatkhachorn, S. (2009). Use of spray-dried chitosan acetate and ethylcellulose as compression coats for colonic drug delivery: Effect of swelling on triggering in vitro drug release. *European Journal Of Pharmaceutics And Biopharmaceutics*, *71*(2), 356-361.doi: 10.1016/j.ejpb.2008.08.002

O'Brien C. P.Drug addiction and abuse, in J. G. Hardman, L. E. Limbird, Eds. (2001) Goodman and Gilman's The Pharmacological Basis of Therapeutics, 10th ed., Pregamon, New York, pp. 621–642.

O'Connor, C., Rees, G.and Joffe, H. (2012). Neuroscience in the Public Sphere. Neuron, 74(2), 220-226. doi: 10.1016/j.neuron.2012.04.004.

O'Connor, M., Selig, E., Pinsky, M.and Altermatt, F. (2011). Toward a conceptual synthesis for climate change responses. Global Ecology And Biogeography, 21(7), 693-703. doi: 10.1111/j.1466-8238.2011.00713.x

Obinna.Ofoegbu, Patrice A.C. Okoye, Augustine. N. Eboatu and Roongnapa S. Srichana. (2019). Preparation Of Dual-Templated Filter Material Using Grafted Molecularly Imprinted Chitosan For Sequestration Of Toxic Tobacco Smoke Products. International Journal of Research and Scientific Innovation (IJRSI) vol.6 issue 5, pp.01-12.

Odukoya, O., Odeyemi, K., Oyeyemi, A.and Upadhyay, R. (2013). Determinants of Smoking Initiation and Susceptibility to Future Smoking among School-Going Adolescents in Lagos State, Nigeria. *Asian Pacific Journal Of Cancer Prevention*, *14*(3), 1747-1753. Doi: 10.7314/apjcp.2013.14.3.1747

Ogata, N., Sanui, K., Nakamura, H.and Kishi, H. (1980). Polycondensation of diethyl mucate with hexamethylenediamine in the presence of poly(vinyl pyridine). *Journal Of Polymer Science: Polymer Chemistry Edition*, *18*(3), 933-938. Doi: 10.1002/pol.1980.170180314

Ogata, N., Sanui, K., Nakamura, H.and Kuwahara, M. (1980). Polycondensation reaction of dimethyl tartrate with hexamethylenediamine in the presence of various matrices. *Journal Of Polymer Science: Polymer Chemistry Edition*, *18*(3), 939-948. Doi: 10.1002/pol.1980.170180315

Papisov I.M. Konscleva O.E., Markov S.V., Litmanouch A.A (1984). *Eur. Polym. J.* 20; 195.

Park HJ, Chinnan MS, Shewfelt R, L. Edible corn-zein filmcoatings to extend storage life of tomatoes. J Food Process Pres.; 18:317–331. Doi: 10.1111/j.1745-4549.1994.tb00255.

Parfitt, G. D. (1981). The role of the surface in the dispersion of powders in liquids. Pure Appl. Chem., 1981, Vol. 53, No. 11, pp. 2233-2240 http://dx.doi.org/10.1351/pac198153112233

Park, H., Suzuki, T.and Lennarz, W. (2001). Identification of proteins that interact with mammalian peptide:N-glycanase and implicate this hydrolase in the proteasome-dependent pathway for protein degradation. Proceedings Of The National Academy Of Sciences, 98(20), 11163-11168. doi: 10.1073/pnas.201393498

Park, S., Marsh, K.and Rhim, J. (2002). Characteristics of Different Molecular Weight Chitosan Films Affected by the Type of Organic Solvents. *Journal Of Food Science*, *67*(1), 194-197. Doi: 10.1111/j.1365-2621.2002.tb11382.x

Peng, Y. (2011). *Fluoro-silane as a functional monomer for protein conformational imprinting*. [Place of publication not identified]: Proquest, Umi Dissertatio.

Phan T.H.D., Brouwer R and Davidson M. (2014).The economic costs of avoided deforestation in the developing world: a meta-analysis. J. For. Econ., 20, pp. 1-16

Piletsky, S., Piletskaya, E., Yano, K., Kugimiya, A., Elgersma, A.and Levi, R. (1996). A Biomimetic Receptor System for Sialic Acid Based on Molecular Imprinting. *Analytical Letters*, *29*(2), 157-170. Doi: 10.1080/00032719608000997

Piletsky, S. A.and Turner, A. P. (2002). Electrochemical sensors based on molecularly imprinted polymers. *Electroanalysis: An International Journal Devoted to Fundamental and Practical Aspects of Electroanalysis*, *14*(5), 317-323.

Piletsky, S., Turner, N.and Laitenberger, P. (2005). Molecularly imprinted polymers in clinical Diagnostics: Future potential and existing problems. *Medical Engineering & Physics*, *28*(10), 971-977. Doi: 10.1016/j.medengphy.2006.05.004

Ping Qu, Jianping Lei, Ruizhuo Ouyang and Huangxian Ju. (2009). Enantioseparation and Amperometric Detection of Chiral Compounds by in Situ Molecular Imprinting on the Microchannel Wall. Anal. Chem., 2009, 81 (23), pp 9651–9656. DOI: 10.1021/ac902201a

Dolinnaya N. G, Drusta V. L, and Shabarova Z.A (1981). DNA-like duplexes with repetitions. I. Efficient template-guided chemical polymerization of d(TGGCCAAGCTp). Nucleic Acid Nucleic Acids Res. 9, 5747-5761.

Połowiński S. (1984). Composition equation for matrix copolymerization. *Journal Of Polymer Science: Polymer Chemistry Edition*, *22*(11), 2887-2894. Doi: 10.1002/pol.1984.170221113

Polowinski S. (1994). In: Bloor D, Brook R.J., Flemmings M.C., Mahaja S. ed. *The encyclopedia of advanced materials* oxford: pergamon press p.2784. Polymerization: The Preparation of a Fluorescent Sensor ford-Fructose. Organic Letters, 1(8), 1209-1212. http://dx.doi.org/10.1021/ol9908732

Polyakov, M.V. (1931). Adsorption properties and structure of silica gel. Zhurnal fizicheskoi khimii 2S, 799–804.

Prasad BB, Srivastava S, Tiwari K, Sharma PS (2009) Trace-level sensing of dopamine in real samples using molecularly imprinted polymer-sensor. Biochem Eng J 2–3:232–239

Przekora, A., Palka, K.and Ginalska, G. (2014). Chitosan/β-1, 3-glucan/calcium phosphate ceramics composites—Novel cell scaffolds for bone tissue engineering application. Journal of Biotechnology,182-183, 46-53. http://dx.doi.org/10.1016/j.jbiotec.2014.04.022

Qu, P., Lei, J., Ouyang, R.and Ju, H. (2009). Enantioseparation and amperometric detection of chiral compounds by in situ molecular imprinting on the microchannel wall. Analytical chemistry, 81(23), 9651-9656.

Rahman, A., Shanta, Z. S., Rashid, M. A., Parvin, T., Afrin, S., Khatun, M. K.and Sattar, M. A. (2016). In vitro antibacterial properties of essential oil and organic extracts of Premna integrifolia Linn. *Arabian Journal of Chemistry*, *9*, S475-S479.

Rajasree R. and Rahate K.P. (2013). An overview on various modifications of chitosan and its applications. International journal of pharmaceutical sciences and research. Vol. 4(11): 4175-4193. DOI: http://dx.doi.org/10.13040/IJPSR.0975-8232.

Ramstroem, O., Andersson, L.and Mosbach, K. (1993). Recognition sites incorporating both pyridinyl and carboxy functionalities prepared by molecular imprinting. *The Journal Of Organic Chemistry*, *58*(26), 7562-7564. doi: 10.1021/jo00078a041

Ratzsch M., (1985). Abstracts of the 30th IUPAC symposium on macromolecules, the Hague; the Netherlands; Aug 18-23; p.37.

Regent Court Technologies. (2001). Method of treating tobacco to reduce nitrosamine content, and products produced thereby. United States of America. US 6202649 B1.

Reito S, and Hiriako K, (2002).Synthesis of polymers by template polymerization. 2. Effects of solvents and polymerization temperature. Macromolecules; 35: 7207 -7213.

Reza Arshady Klaus Mosbach.(1981). Synthesis of substrate-selective polymers by host-guest polymerization. Makromol. Chem..182 (5), 687. https://doi.org/10.1002/macp.1981.021820240

Rinaudo, M. (2006). Chitin and Chitosan — Properties and Applications. *Cheminform*, *38*(27). doi: 10.1002/chin.200727270

Robinson, D.and Mosbach, K. (1989). Molecular imprinting of a transition state analogue leads to a polymer exhibiting esterolytic activity. *Journal Of The Chemical Society, Chemical Communications*, (14), 969. doi: 10.1039/c39890000969

Rodahl M.and Kasemo B. (1996). On the measurement of thin liquid overlayers with the quartz-crystal microbalance. *Sensors and Actuators A: Physical*, *54*(1-3), 448-456.

Ronghua, H, Polinnaya N. G, Drusta V. L, and Shabarova Z.A (1981). *Nucleic Acid Symp.Ser.*, 9,255 (1981).

Rosengren, A., Karlsson, B.and Nicholls, I. (2013). Consequences of Morphology on Molecularly Imprinted Polymer-Ligand Recognition. *International Journal Of Molecular Sciences*, *14*(1), 1207-1217. doi: 10.3390/ijms14011207

Ruth H, Inmaculada A, and Angeles H. (2010). Chitosan amphiphilic derivatives chemistry properties and applications. Curr Org Chem.14: 308-30.

Ruthven, D. M. (1984). *Principles of adsorption and adsorption processes*. John Wiley & Sons

Saha, S.and Sarkar, P. (2013). Arsenic mitigation by chitosan-based porous magnesia-

impregnated alumina: performance evaluation in continuous packed bed column. *International Journal Of Environmental Science And Technology*, *13*(1), 243-256. doi: 10.1007/s13762-015-0806-1

Saifuddin, N.and Yasumira, A. A. (2010). Microwave Enhanced Synthesis of Chitosan-graft Molecularly Imprinted Polymer (MIP) for Selective Extraction of Antioxidants. *Journal of Chemistry*, *7*(4), 1362-1374.

Saito, R., and Kobayashi, H. (2002). Synthesis of polymers by template polymerization. 2. Effects of solvent and polymerization temperature. Macromolecules, 35(19), 7207-7213.

Sanagi, M., Salleh, S., Ibrahim, W., Naim, A., Hermawan, D.and Miskam, M. (2013). Molecularly imprinted polymer solid-phase extraction for the analysis of organophosphorus pesticides in fruit samples. *Journal Of Food Composition And Analysis*, *32*(2), 155-161. doi: 10.1016/j.jfca.2013.09.001

Santora, B. P.and Gagné, M. R.(2000). "A wolf in sheep's clothing". Chemical Innovation. 23-29.

Sastry, Kalpana & Shrivastava, A and Gudipati, Venkateshwarlu. (2015). Assessment of current trends in R&D of chitin-based technologies in agricultural production-consumption systems using patent analytics. *Journal of Intellectual Property Rights*. 20. 19-38.

Sato, T., Nemoto, K., Moei, S.and Oteu, T (1979). Radical Polymerization of Maleic Acid by Potassium Persulfate in the Presence of Polyvinylpyrrolidone in Water. J. Macromol. Sci., Chem., A12; 751 – 766.

Satyamoorthy KMarshall A., (2011) Holographic sensor. US 7998639 B2, 2011. Cambridge Enterprise Limited.. Holographic sensor. US.

Sauerbrey, G. (1959). *The use of quartz crystal oscillators for weighing thin layers and for microweighing applications*. Zeitschrift für Physik, Vol. 155, No. 2, pp. 206-222.

Seifner A., Lieberzeit P., Jungbauer C., Dickert F.L. (2009). Synthetic receptors for selectively detecting erythrocyte ABO subgroups. Anal. Chim. Acta. 651:215–219. doi: 10.1016/j.aca.2009.08.021.

Sellergren, B.and Andersson, L. (1990). Molecular recognition in macroporous polymers prepared by a substrate analog imprinting strategy. *The Journal Of Organic Chemistry*, *55*(10), 3381-3383. doi: 10.1021/jo00297a074

Sellergren, B.and Shea, K. (1993). Influence of polymer morphology on the ability of imprinted network polymers to resolve enantiomers. *Journal Of Chromatography A*, *635*(1), 31-49. doi: 10.1016/0021-9673(93)83112-6

Sellergren, B. (1997). Noncovalent molecular imprinting: antibody-like molecular recognition in polymeric network materials. *Trac Trends In Analytical Chemistry*, *16*(6), 310-320. doi: 10.1016/s0165-9936(97)00027-7

Severin, K. (2001). ChemInform Abstract: Imprinted Polymers with Transition Metal Catalysts. *Cheminform*, *32*(20). doi: 10.1002/chin.200120301

Sha, X., Xu, X., Sohlberg, K., Loll, P.and Penn, L. (2014). Evidence that three-regime kinetics is inherent to formation of a polymer brush by a grafting-to approach. *RSC Adv.*, *4*(79), 42122-42128. doi: 10.1039/c4ra05663a

Shafey, O., S. Dolwick, and G. E. Guindon, eds. (2003).Tobacco control country profiles, 2nd ed. Atlanta, GA: UICC with the WHO and the American Cancer Society.

Shavit N. and Cohen J., (1977). Polymerization in Organized Systems, Ed. H. G. Elias, p. 213, *Gordon & Breach*, London.

Shea, K. (1994). Molecular Imprinting of Synthetic Network Polymers: The de Novo Synthesis of Macromolecular Binding and Catalytic Sites," Trends in Polymer Science, Vol. 2, No. 5, 166-173.

Shea K. and Sasaki, D. (1991). An analysis of small-molecule binding to functionalized synthetic polymers by 13C CP/MAS NMR and FT-IR spectroscopy. *Journal Of The American Chemical Society*, *113*(11), 4109-4120. doi: 10.1021/ja00011a009

Shun Li, Shen, D., Shao, J., Crowder, R., Liu, W.and Prat, A. (2013). Endocrine-Therapy-Resistant ESR1 Variants Revealed by Genomic Characterization of Breast-Cancer-Derived Xenografts. Cell Reports, 4(6), 1116-1130. doi: 10.1016/j.celrep.2013.08.022

Sila, A., Ghlissi, Z., Kamoun, Z., Makni, M., Nasri, M., Bougatef, A., and Sahnoun, Z. (2014). Astaxanthin from shrimp by-products ameliorates nephropathy in diabetic rats. European Journal Of Nutrition, 54(2), 301-307. doi: 10.1007/s00394-014-0711-2

Silvia B. (2012). "American Association for Cancer Research (AACR) Strong oral carcinogen identified in smokeless tobacco. *ScienceDaily*. Retrieved May 15, 2018 from www.sciencedaily.com/releases/2012/04/120402093140.htm

Simha, R., Zimmerman, J.and Moacanin, J. (1963). Polymerization Kinetics of Biological Macromolecules on Templates. *The Journal Of Chemical Physics*, *39*(5), 1239-1246. doi: 10.1063/1.1734422

Sing K. S. W.(1985). Reporting physisorption data for gas/solid systems with special reference to the determination of surface area and porosity. Pure and Appl. Chem., Vol. 57, No. 4, pp. 603-619 http://dx.doi.org/10.1351/pac198557040603

Smid, J., Tan, Y.and Challa, G. (1983). Effects of poly(2-vinylpyridine) as a template on the radical polymerization of methacrylic acid—I. Influence of atactic poly(2-vinylpyridine) concentration. *European Polymer Journal*, *19*(10-11), 853-858. doi: 10.1016/0014-3057(83)90037-x

Smith, K., Winslow, A.and Petersen, D. (1959). Association Reactions for Poly(alkylene Oxides) and Polymeric Poly(carboxylic Acids). *Industrial & Engineering Chemistry*, *51*(11), 1361-1364. doi: 10.1021/ie50599a029

Song, M., Benowitz, N., Berman, M., Brasky, T., Cummings, K., & Hatsukami, D. (2017). Cigarette Filter Ventilation and its Relationship to Increasing Rates of Lung Adenocarcinoma. JNCI: Journal Of The National Cancer Institute, 109(12). http://dx.doi.org/10.1093/jnci/djx075

Spivak, D. A.(2005). "Selectivity in molecularly imprinted matrices", Molecularly Imprinted Materials: Science and Technology. Yan, M.; Ramstrom, O., Eds.; (Marcel Dekker, New York). Chapter 15, 395-417.

Sridhari, T. R. and P. K. Dutta. (2000). Synthesis and characterization of maleilated chitosan for dye house effluent. *Indian Journal of Chemical Technology* **7**: 198-201.

Stefan, M., and Murray, R. (1997). Schizophrenia: developmental disturbance of brain and mind? Acta Paediatrica, 86(S422), 112–116. doi:10.1111/j.1651-2227.1997.tb18358.x

Stefan, R., Aboul-Enein, H.and Van S. J. (2002). Enantioselective Electrochemical Sensors. Sensors Update, 10(1), 123-141. doi: 10.1002/1616-8984(200201)10:1<123::aid-seup123>3.0.co;2-y

Suhrcke, M., R. A. Nugent, and D. S. L. Rocco. 2006. Chronic disease: An economic perspective. London, United Kingdom: The Oxford Health Alliance.www.oxha.org. Accessed 12 June 2018, by 2:35pm.

Sumathi.N, Vignesh.R and Madhusudhanan.J. (2017). Extraction, characterization and applications of chitosan from fish scales. International Journal Of Modern Trends In Engineering and Research, 4(4), 137-141. http://dx.doi.org/10.21884/ijmter.2017.4131.q8njr

Sun, Y., Frankenberg, C., Wood, J., Schimel, D., Jung, M., and Guanter, L.(2017). OCO-2 advances photosynthesis observation from space via solar-induced chlorophyll fluorescence. Science, 358(6360), eaam5747. doi: 10.1126/science.aam5747

Sunday E. A. (2006). Tobacco Specific Nitrosamines in Nigerian Cigarettes.UICCWorld Cancer Congress Washington, DC, USA. Atawodi, S., Preussmann, R. and Spiegelhalder, B. (1995). Tobacco-specific nitrosamines in some Nigerian cigarettes. Cancer Letters, 97(1), pp.1-6.

Surini, S., Akiyama, H., Morishita, M., Nagai, T.and Takayama, K. (2003). Release phenomena of insulin from an implantable device composed of a polyion complex of chitosan and sodium hyaluronate. *Journal Of Controlled Release*, *90*(3), 291-301. doi: 10.1016/s0168-3659(03)00196-2

Svenson, J.and Nicholls, I. (2001). On the thermal and chemical stability of molecularly imprinted polymers. *Analytica Chimica Acta*, *435*(1), 19-24. doi: 10.1016/s0003-2670(00)01396-9

Svenson, J., Karlsson, J.and Nicholls, I. (2004). Nuclear magnetic resonance study of the molecular imprinting of (−)-nicotine: template self-association, a molecular basis for cooperative ligand binding. *Journal Of Chromatography A*, *1024*(1-2), 39-44. doi:10.1016/j.chroma.2003.09.064

Tada, M.and Iwasawa, Y. (2003). Design of Molecular-Imprinting Metal-Complex Catalysts. *Cheminform*, *34*(43). doi: 10.1002/chin.200343254

Taghavi, S., Khashyarmanesh, Z., Moalemzadeh-Haghighi, H., Nassirli, H., Eshraghi, P., Jalali, N.and Hassanzadeh-Khayyat, M. (2012). Nicotine content of domestic cigarettes, imported cigarettes and pipe tobacco in Iran. *Addiction & health*, *4*(1-2), 28.

Takeda, K.and Kobayashi, T. (2005). Bisphenol A imprinted polymer adsorbents with selective recognition and binding characteristics. *Science And Technology Of Advanced Materials*, *6*(2), 165-171. doi: 10.1016/j.stam.2004.11.008

Takeuchi, T., Fukuma, D., and Matsui, J. (1999). Combinatorial molecular imprinting: an approach to synthetic polymer receptors. Analytical Chemistry, 71(2), 285-290. doi: 10.1021/ac980858v

Takeuchi, T.,and Haginaka, J. (1999). Separation and sensing based on molecular recognition using molecularly imprinted polymers. *Journal of Chromatography B: Biomedical Sciences and Applications*, *728*(1), 1-20.

Tamara K, Michelle W, Yasmin A and Shelley DM:(2008). Improving the microenvironment for enzyme immobilization at electrodes by hydrophobically modifying chitosan and Nafion polymers, J Membr Sci; 311: 81-88.

Tan Y.Y and Challa G., (1989) in *Encyclopedia of Polymer Science and Engineering*, Mark, Bikales, Overberger, and Menges Eds, *John Wiley & Sons*, Vol. 16, 554.

Tan Y.Y and G. Challa G., (1987) *Makromol. Chem., Macromol.Symp*.,10/11, 215 (1987).

Thakur, V., and Thakur, M. (2014). Recent Advances in Graft Copolymerization and Applications of Chitosan: A Review. ACS Sustainable Chemistry & Engineering, 2(12), 2637-2652. http://dx.doi.org/10.1021/sc500634p

Thommes, M.and Cychosz, K. (2014). Physical adsorption characterization of nanoporous materials: progress and challenges. Adsorption, 20(2-3), 233-250. doi: 10.1007/s10450-014-9606-zM. Thommes, K. A. Cychosz. Adsorption 20, 233 (2014).

Thanou, M., Nihot, M., Jansen, M., Verhoef, J., & Junginger, H. (2001). Mono-N-carboxymethyl chitosan (MCC), a polyampholytic chitosan derivative, enhances the intestinal absorption of low molecular weight heparin across intestinal epithelia in vitro and in vivo. *Journal Of Pharmaceutical Sciences*, *90*(1), 38-46. doi: 10.1002/1520-6017(200101)90:1<38::aid-jps5>3.3.co;2-v.

Thanou, M., Kotzé, A., Scharringhausen, T., Lueßen, H., de Boer, A., Verhoef, J.and Junginger, H. (2000). Effect of degree of quaternization of N-trimethyl chitosan chloride for enhanced transport of hydrophilic compounds across intestinal Caco-2 cell monolayers. Journal Of Controlled Release, 64(1-3), 15-25. http://dx.doi.org/10.1016/s0168-3659(99)00131-5

Toan, N. V. (2009). Production of chitin and chitosan from partially autolyzed shrimp shell materials. *The open biomaterials journal*, *1*(1).

Tomoi, M., Oda, H., & Kakiuchi, H. (1987). *Die Makromolekulare Chemie, Rapid Communications*, *8*(7), 339-343. doi: 10.1002/marc.1987.030080705

Townsend, L., Flisher, A., Gilreath, T.and King, G. (2006). A systematic literature review of tobacco use among adults 15 years and older in sub-Saharan Africa. *Drug And Alcohol Dependence*, *84*(1), 14-27. doi: 10.1016/j.drugalcdep.2005.12.008.

Tronci, G., Ajiro, H., Russell, S. J., Wood, D. J.and Akashi, M. (2014). Tunable drug-loading capability of chitosan hydrogels with varied network architectures. *Acta biomaterialia*, *10*(2), 821-830.

Trubetskoy, V. S., Hanson, L. J., Slattum, P. M., Hagstrom, J. E., Budker, V. G.and Wolff, J. A. (1998). Self-assembly of DNA—polymer complexes using template polymerization. *Nucleic acids research*, *26*(18), 4178-4185.

Tsuchida, E.and Osada, Y. (1975). Effects of macromolecular matrix on the process of radical polymerization of ionizable monomers. *Journal Of Polymer Science: Polymer Chemistry Edition*, *13*(3), 559-569. doi: 10.1002/pol.1975.170130303

Tsuchida, E.and Osada, Y. (1974). *Die Makromolekulare Chemie*, *175*(2), 593-601. doi: 10.1002/macp.1974.021750220

Twu, Y., Chen, Y.and Shih, C. (2008). Preparation of silver nanoparticles using chitosan suspensions. *Powder Technology*, *185*(3), 251-257. doi: 10.1016/j.powtec.2007.10.025...

Uragami, T., Yoshida, F.and Sugihara, M. (1983). Studies of synthesis and permeabilities of special polymer membranes. LI. Active transport of halogen ions through chitosan membranes. *Journal of Applied Polymer Science*, *28*(4), 1361-1370.

Vankatesan, J.and Kim, S. (2010). Chitosan Composites for Bone Tissue Engineering—An Overview. *Marine Drugs*, *8*(8), 2252-2266. doi: 10.3390/md8082252

Vargas, M., Albors, A., Chiralt, A.and González-Martínez, C. (2009). Characterization of chitosan–oleic acid composite films. *Food Hydrocolloids*, *23*(2), 536-547. doi: 10.1016/j.foodhyd.2008.02.009

Varum, K. M. and Smidsrod, 0. (1994) Chitosan Preparation. World Patent Application No. W003011912.

Varun, T., Senani, W., Kumar, N., Gautam, M., Gupta, R.and Gupta, M. (2017). Extraction and characterization of chitin, chitosan and chitooligosaccharides from crab shell waste. *Indian Journal Of Animal Research*, (OF). doi: 10.18805/ijar.v0iof.8456

Veras C.A.G., Carvalho Jr J.A., Rabelo E.R.C., Alvarado E.C., Sandberg D.V.and Santos J.C.(2002). Log smoldering after an amazonian deforestation fire. Technology & Engineering. 22(4):283–294

Vendamme, R., Eevers, W., Kaneto, M.and Minamizaki, Y. (2009). Influence of Polymer Morphology on the Capacity of Molecularly Imprinted Resins to Release or to Retain their Template. Polymer Journal, 41(12), 1055-1066. http://dx.doi.org/10.1295/polymj.pj2009098

Venter, J., Kotze, A., Auzelyvelty, R.and Rinaudo, M. (2006). Synthesis and evaluation of the mucoadhesivity of a CD-chitosan derivative. *International Journal Of Pharmaceutics*, *313*(1-2), 36-42. doi: 10.1016/j.ijpharm.2006.01.016

Vincent, T.; Remcho, Z.; Jessica,T (1999). Analytical Chemistry News & Features**.***1*, 248.

Vladimir S.T, Vladimir G.B, Lisa J.H, Paul M.S, Jon A.W, and James E.H, (1998).Self-assembly of DNA-polymer complexes using Template polymerization.Nuclei Acid Res; Vol 26, No 18, 4178 – 4185.

Vlatakis, G., Andersson, L., Müller, R.and Mosbach, K. (1993). Drug assay using antibody mimics made by molecular imprinting. *Nature*, *361*(6413), 645-647. doi: 10.1038/361645a0

Vongchan, P., Sajomsang, W., Subyen, D.and Kongtawelert, P. (2002). Anticoagulant activity of a sulfated chitosan. *Carbohydrate Research*, *337*(13), 1239-1242.

Wang, H., Jiang, J., Ma, L.and Pang, Y. (2006). Syntheses of molecularly imprinted polymers and their molecular recognition study for benzotriazole. Reactive and Functional Polymers, 66(10), 1081-1086. http://dx.doi.org/10.1016/j.reactfunctpolym.2006.01.022

Wang, W., Gao, S.and Wang, B. (1999). Building Fluorescent Sensors by Template Polymerization: The Preparation of a Fluorescent Sensor ford-Fructose. *Organic Letters,1* (8), 1209-1212. doi: 10.1021/ol9908732

Watson Jr J.D., Hopkins N.H., Roberts J.W., Steitz J.A., and Weiner A.M., (1987) in Molecular Biology of the Gene, *The Benjamin/Cummings Pub. Comp*., Menlo Park.

Weltrowski, M., Martel, B.and Morcellet, M. (1996). ChitosanN-benzyl sulfonate derivatives as sorbents for removal of metal ions in an acidic medium. *Journal Of Applied Polymer Science*, *59*(4), 647-654. doi: 10.1002/(sici)1097-4628(19960124)59:4<647::aid-app10>3.0.co;2-n

Whidby, J., Edwards, W.and Pitner, T. (1979). Cheminform Abstract: Isomeric Nicotines. Their Solution Conformation And Proton, Deuterium, Carbon-13, And Nitrogen-15 Nuclear Magnetic Resonance. Chemischer Informationsdienst, 10(28). doi: 10.1002/chin.197928091

Whitcombe, M., Rodriguez, M., Villar, P.and Vulfson, E. (1995). A New Method for the Introduction of Recognition Site Functionality into Polymers Prepared by Molecular Imprinting: Synthesis and Characterization of Polymeric Receptors for Cholesterol. *Journal Of The American Chemical Society*, *117*(27), 7105-7111. doi: 10.1021/ja00132a010

Whitcombe, M., Alexander, C.and Vulfson, E. (2000). ChemInform Abstract: Imprinted Polymers: Versatile New Tools in Synthesis. *Cheminform*, *31*(36), no-no. doi: 10.1002/chin.200036278

WHO. (2004). Tobacco increases the poverty of individuals and families. Geneva, Switzerland: WHO. (Accessed 11July (2017).

WHO (2009). World Health Organization. WHO global health risks. Mortality and burden of global health risks. Mortality and burden of disease attributable to selected major risks. Geneva, Switzerland: WHO; 2009 Available from: http://www.who.int/healthinfo/global_burden_disease/GlobalHealthRisks_report_full.pd.

WHO (2010a). Guidelines for implementation of Article 14 of the WHO FCTC. Geneva, World Health Organization Framework Convention on Tobacco Control (http://www.who.int/fctc/guidelines.pdf, accessed 13 June 2016).

WHO (2010b). Gender, women, and the tobacco epidemic. Geneva, World Health Organization (http://whqlibdoc.who.int/publications/2010/9789241599511_eng.pdf, accessed 19 June (2017).

WHO. 2010c. Global health observatory data repository: Tobacco control. http://gamapserver.who.int/gho/interactive_charts/tobacco/policies/atlas.html?indicator=i 1 (accessed May 7, 2017).

WHO (2011a). WHO report on the global tobacco epidemic, 2011: warning about the dangers of tobacco. Geneva, World Health Organization (http://whqlibdoc.who.int/publications/2011/9789240687813_eng.pdf, accessed 11July (2017).

WHO. 2011b. Global status report on noncommunicable diseases 2010. Geneva, Switzerland: WHO. accessed 19 July (2017).

WHO (2013a). Review of evidence on health aspects of air pollution – REVIHAAP project: technical report. Copenhagen, WHO Regional Office for Europe (http://www.euro.who.int/__data/assets/pdf_file/0004/193108/REVIHAAP-Finaltechnical-report.pdf, accessed 12 November 2017).

WHO. 2013b. WHO report on the global tobacco epidemic, 2013: Enforcing bans on tobacco advertising, promotion and sponsorship. Geneva, Switzerland: WHO. accessed 21July (2017).

WHO (2013c). European mortality database (MDB) [online database]. Copenhagen, WHO Regional Office for Europe (http://data.euro.who.int/hfamdb/, accessed 14 November (2017).

WHO. 2013d. WHO report on the global tobacco epidemic, 2013: Enforcing bans on tobacco advertising, promotion and sponsorship. Published data set. Geneva, Switzerland: Tobacco Free Initiative, WHO. accessed 11 October (2017).

Wu C, Amrani N, Jacobson A, Sachs MS. (2007).The use of fungal in vitro systems for studying translational regulation. Methods Enzymol 429:203-25

Wu, K., Sukumar, N., Lanzillo, N. A., Wang, C., "Rampi" Ramprasad, R., Ma, R. and Breneman, C. (2016). Prediction of polymer properties using infinite chain descriptors (ICD) and machine learning: Toward optimized dielectric polymeric materials. *Journal of Polymer Science Part B: Polymer Physics*, *54*(20), 2082-2091.

Wu, L., Shi, C., Tian, L.and Zhu, J. (2008). A One-Pot Method to Prepare Gold Nanoparticle Chains with Chitosan. *The Journal Of Physical Chemistry C*, *112*(2), 319-323. doi:

10.1021/jp076733o

Wu, Y., Ma, H., Gu, D.and He, J. (2015). A quartz crystal microbalance as a tool for biomolecular interaction studies. RSC Adv., 5(79), 64520-64525. http://dx.doi.org/10.1039/c5ra05549k

Wu, Y., Liu, X., Cui, J., Meng, M., Dai, J., Li, C.and Yan, Y. (2017). Bioinspired synthesis of high-performance nanocomposite imprinted membrane by a polydopamine-assisted metal-organic method. Journal Of Hazardous Materials, 323, 663-673. http://dx.doi.org/10.1016/j.jhazmat.2016.10.030

Wulff, G. (1972). The use of polymers with enzyme-analogous structures for the resolution of racemates. *Angrew. Chem. Internat. Edit.*, *11*(4), 341.

Wulff P., Vallon V., Huang D.Y. , Völkl H., Yu F., Richter K., Jansen M., Schlünz M., Klingel K., Loffing J., Kauselmann G., Bösl M.R. , Lang F.and Kuhl D. (2002). Impaired renal Na(+) retention in the sgk1-knockout mouse. J Clin Invest November 1, 2002; 110 (9): 1263-8.

Wulff, G. (2002). Enzyme-like Catalysis by Molecularly Imprinted Polymers. *Chemical Reviews*, *102*(1), 1-28. doi: 10.1021/cr980039a; Templates— A Way towards Artificial Antibodies. *Angewandte Chemie International Edition In English*, *34*(17), 1812-1832. doi: 10.1002/anie.199518121

Wulff, G., Sarhan, A.and Zabrocki, K. (1973). Enzyme-analogue built polymers and their use for the resolution of racemates. *Tetrahedron Letters*, *14*(44), 4329-4332. doi: 10.1016/s0040-4039(01)87213-0

Wulff, G., Vesper, W., Grode-Einsler, R. and Sarhan, A. (1977). Enzyme-analogue built polymers. On the specificity distribution of chiral cavities prepared in synthetic polymersMakromol. Chem., 178, 2817-2825.

Wynder, E. L.and Hoffmann, D. (1994). Smoking and lung cancer: scientific challenges and opportunities. *Cancer Research*, *54*(20), 5284-5294.

Xie, J., Cai, C., Lai, S., Yang, L., Luo, L.and Yang, H. (2013). Synthesis and application of a molecularly imprinted polymer as a filter to reduce polycyclic aromatic hydrocarbon levels in mainstream cigarette smoke. Reactive And Functional Polymers, 73(12), 1606-1611. doi: 10.1016/j.reactfunctpolym.2013.09.00310.

Xie, J., Zhou, B., Zhang, T., Zeng, X., Yang, M., Wang, W.and Yang, J. (2018). Preparation of nicotine surface molecularly imprinted polymers for selective solid-phase extraction of nicotine from zero-level refill liquids of electronic cigarettes. Analytical Methods, 10(29), 3637-3644. doi: 10.1039/c8ay00616d

Xu, C., Zeng, Y., Rui,X., Xiao, N., Zhu, J., Zhang, W., Chen, J., W Liu, W. and Tan, H (2011). Controlled soft-template synthesis of ultrathin C@ FeS nanosheets with high-Li-storage performance. Acs Nano 6 (6), 4713-4721

Xu, L., Huang, Y., Zhu, Q.and Ye, C. (2015). Chitosan in Molecularly-Imprinted Polymers: Current and Future Prospects. International Journal Of Molecular Sciences, 16(8), 18328-18347. http://dx.doi.org/10.3390/ijms160818328

Xu, Y., Kim, K., Hanna, M.and Nag, D. (2005). Chitosan–starch composite film: preparation and characterization. *Industrial Crops And Products*, *21*(2), 185-192. doi: 10.1016/j.indcrop.2004.03.002

Yamazaki, N.and Higashi, F. (1981). Studies on reactions of N-phosphonium salts of pyridines. VIII. Preparation of polyamides by means of diphenyl phosphite in pyridine. *Journal Of Polymer Science: Polymer Letters Edition*, *12*(4), 185-191. doi: 10.1002/pol.1974.130120402Yanti,

Yang, K., Wang, X., Zhou, Z., Xu, J., Weng, J.and Zhang, Q. (2007). One-step synthesis and characterisation of chitosan-mediated micro-sized gold nanoplates through a thermal process. *IET Nanobiotechnology*, *1*(6), 107. doi: 10.1049/iet-nbt:20070018

Yanti, N.T., Royani, I., Widayani K. (2016). Synthesis and characterization of MAA-based molecularly-imprinted polymer (MIP) with D-glucose template. Journal Of Physics: Conference Series, 739, 012143. doi: 10.1088/1742-6596/739/1/012143

Yilmaz, E., Mosbach, K.and Haupt, K. (1999). Influence of functional and cross-linking monomers and the amount of template on the performance of molecularly imprinted polymers in binding assays. Analytical Communications, 36(5), 167-170.

Yilmaz, E., Haupt, K., and Mosbach, K. (2000). The use of immobilized templates—A new approach in molecular imprinting. *Angewandte Chemie International Edition*, *39*(12), 2115-2118.

Yilmaz, A., Memon, S., and Yilmaz, M. (1999). Synthesis and binding properties of calix[4]arene telomers. Journal Of Polymer Science Part A: Polymer Chemistry, 37(23), 4351-4355. doi: 10.1002/(sici)1099-0518(19991201)37:23<4351::aid-pola11>3.0.co;2-l

Ying L., Xueliang L. and Junde W. (2003) Molecularly Imprinted Solid-Phase Extraction Sorbent for Removal of Nicotine from Tobacco Smoke. Analytical Letters, 36:8, 1631-1645, DOI: 10.1081/AL-120021554

Yoshimatsu, K., Reimhult, K., Krozer, A., Mosbach, K., Sode, K.and Ye, L. (2007). Uniform molecularly imprinted microspheres and nanoparticles prepared by precipitation polymerization: The control of particle size suitable for different analytical applications. *Analytica chimica acta*, *584*(1), 112-121.

Younes, I.and Rinaudo, M. (2015). Chitin and Chitosan Preparation from Marine Sources. Structure, Properties and Applications. *Marine Drugs*, *13*(3), 1133-1174. doi: 10.3390/md13031133

Yu, C., Ramström, O.and Mosbach, K. (1997). Enantiomeric Recognition by Molecularly Imprinted Polymers Using Hydrophobic Interactions. *Analytical Letters*, *30*(12), 2123-2140. doi: 10.1080/00032719708001728

Yu, Q., Deng, S.and Yu, G. (2008). Selective removal of perfluorooctane sulfonate from aqueous solution using chitosan-based molecularly imprinted polymer adsorbents. *Water Research*, *42*(12), 3089-3097. doi: 10.1016/j.watres.2008.02.024

Zander, Å., Findlay, P., Renner, T., Sellergren, B.and Swietlow, A. (1998). Analysis of Nicotine and Its Oxidation Products in Nicotine Chewing Gum by a Molecularly Imprinted Solid-Phase Extraction. Analytical Chemistry, 70(15), 3304-3314. doi: 10.1021/ac971272w

Zhang, K., Peschel, D., Helm, J., Groth, T.and Fischer, S. (2011). FT Raman investigation of novel chitosan sulfates exhibiting osteogenic capacity. Carbohydrate polymers, 83(1), 60-65.

Zhang, J., Ni, Y., Wang, L., Ma, J.and Zhang, Z. (2015). Selective solid-phase extraction of artificial chemicals from milk samples using multiple-template surface molecularly imprinted polymers. *Biomedical Chromatography*, *29*(8), 1267-1273. doi: 10.1002/bmc.3416

Zhang, M.and Hirano, S. (1995). Novel N-unsaturated fatty acyl and N-trimethylacetyl derivatives of chitosan. *Carbohydrate polymers*, *26*(3), 205-209.

Zhang, M., Yu, M., Li, F., Zhu, M., Li, M., Gao, Y.and Yi, T. (2007). A highly selective fluorescence turn-on sensor for cysteine/homocysteine and its application in bioimaging. *Journal of the American Chemical Society*, *129*(34), 10322-10323.

Zhang,Y.and Zhang, M. (2001). Synthesis and characterization of macroporous chitosan/calcium phosphate composite scaffolds for tissue engineering. *Journal Of Biomedical Materials Research*, *55*(3), 304-312. doi: 10.1002/1097-4636(20010605)55:3<304::aid-jbm1018>3.0.co;2-j

Zhou, Y., Yang, Y., Guo, X.and Chen, G. (2003). Effect of molecular weight and degree of deacetylation of chitosan on urea adsorption properties of copper chitosan. *Journal Of Applied Polymer Science*, *89*(6), 1520-1523. doi: 10.1002/app.12235

Zhou, H., Qian, J., Wang, J., Yao, W., Liu, C., Chen, J.and Cao, X. (2009). Enhanced bioactivity of bone morphogenetic protein-2 with low dose of 2-N, 6-O-sulfated chitosan in vitro and in vivo. *Biomaterials*, *30*(9), 1715-1724. doi: 10.1016/j.biomaterials.2008.12.016

Zou, Y.and Khor, E. (2009). Preparation of sulfated-chitins under homogeneous conditions. *Carbohydrate Polymers*, *77*(3), 516-525.

Zvezdova, D. (2010). Synthesis and characterization of chitosan from marine sources in black sea. *Scientific Works of the Russia University* 49: 65-69.

APPENDIX

Proton Nuclear Magnetic Resonance Spectra of Hydrogen shift from the titration of varied volumes of functional monomer (Chitosan) against fixed volume of templates (Nicotine, Phenylalanine and Nicotine-Phenylalanine 50:50 blend).

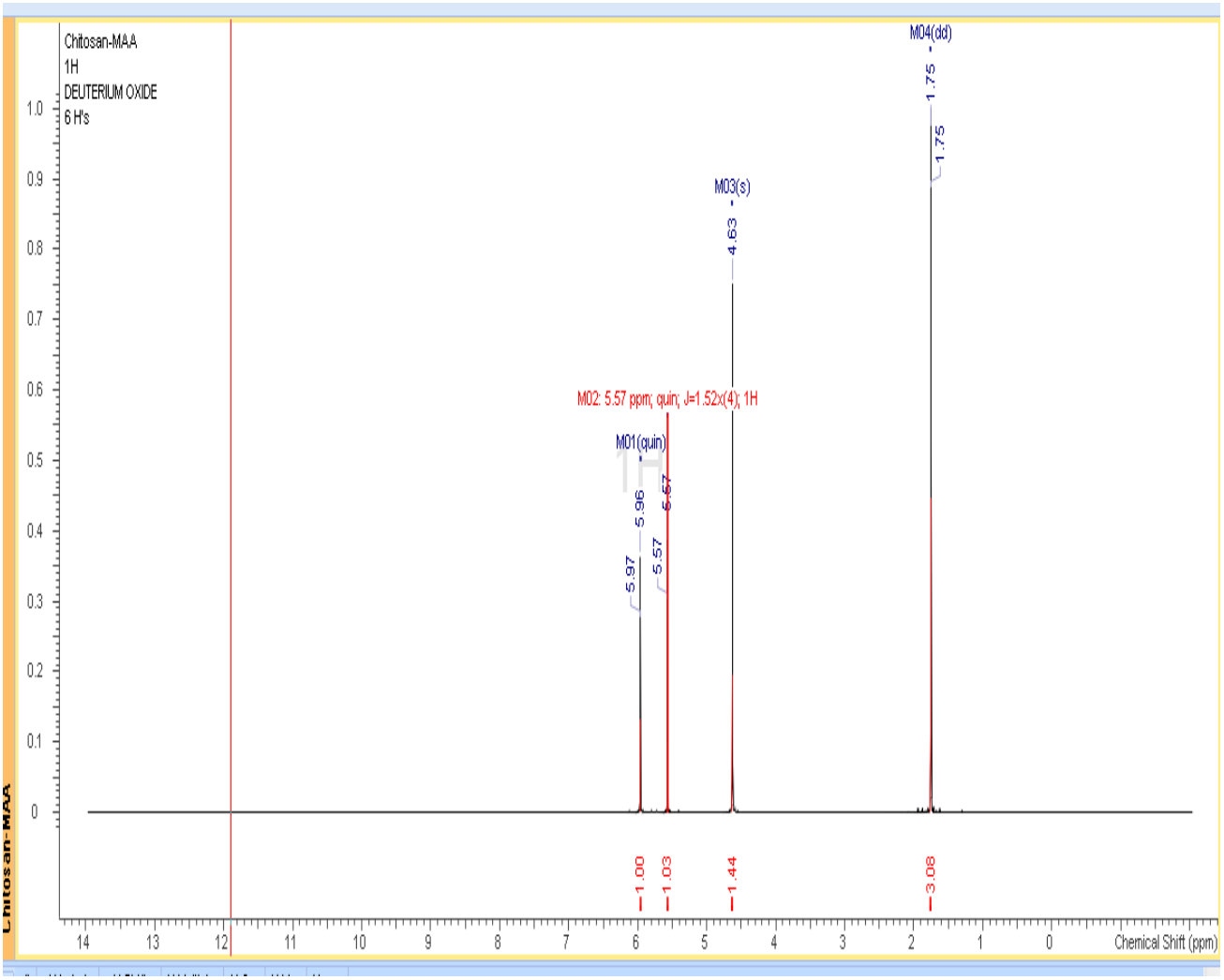

Appendix i**:** Proton Spectra for Chitosan-Methacrylic acid.

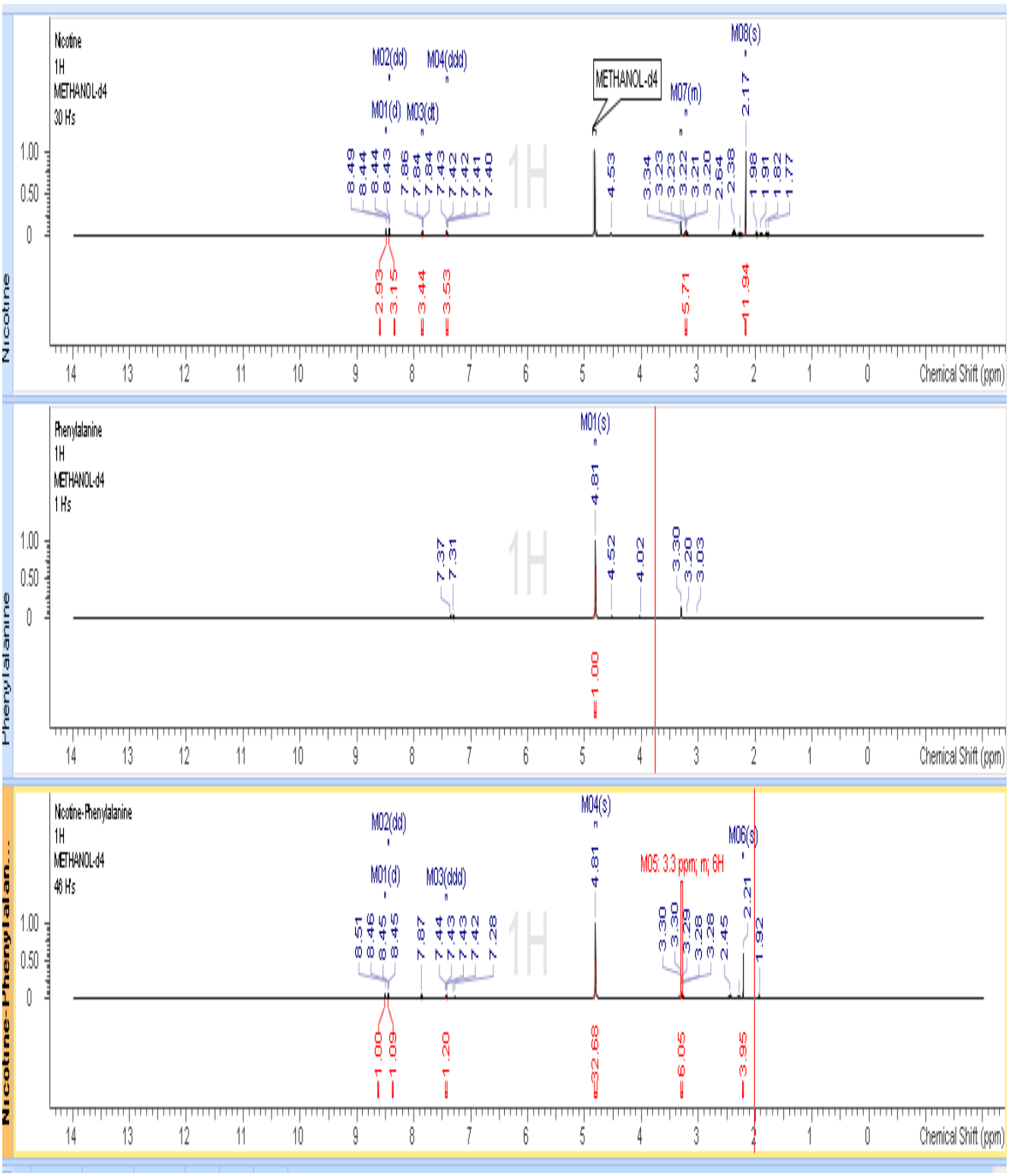

Appendix ii Stacked Proton Spectra for the respective templates that were used (Nicotine, Phenylalanine and their blends).

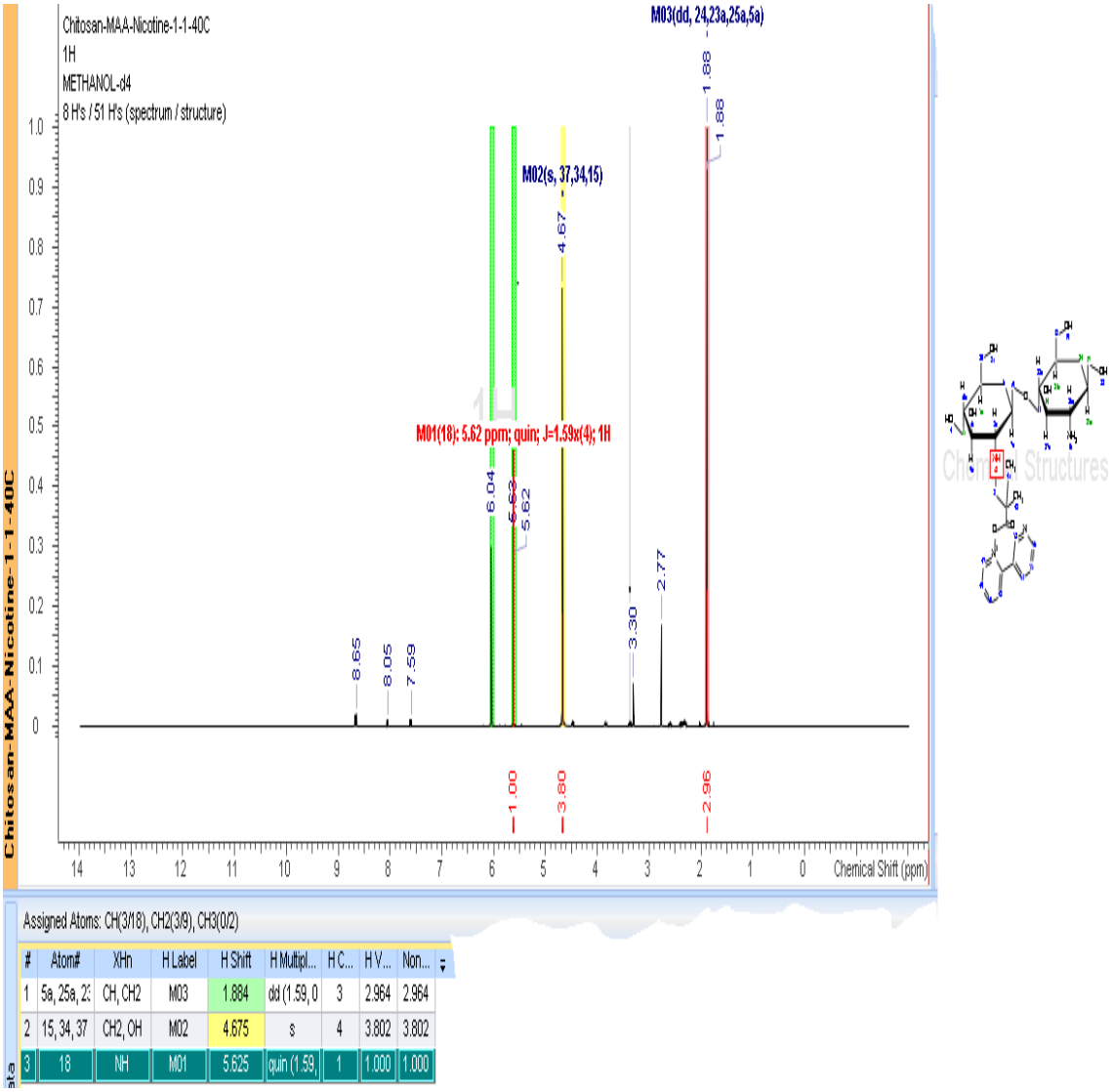

Assigned Atoms: CH(3/18), CH2(3/9), CH3(0/2)

#	Atom#	XHn	H Label	H Shift	H Multipl...	H C...	H V...	Non...
1	5a, 25a, 2:	CH, CH2	M03	1.884	dd (1.59, 0	3	2.964	2.964
2	15, 34, 37	CH2, OH	M02	4.675	s	4	3.802	3.802
3	18	NH	M01	5.625	quin (1.59,	1	1.000	1.000

Appendix iii: Characteristic peaks of the amine proton in the functional monomer (Chitosan) on interaction with template Nicotine.

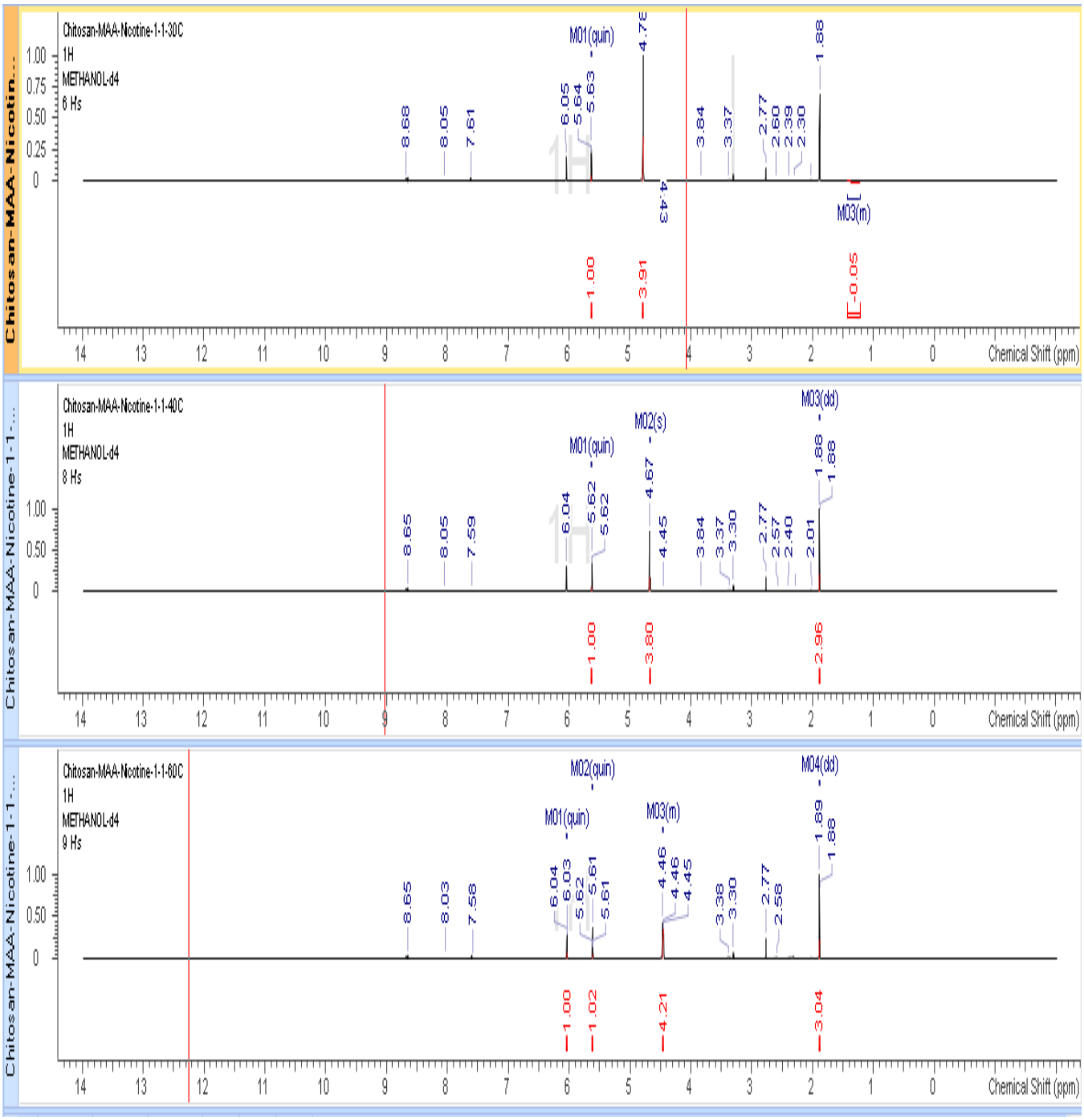

Appendix iv**:** Stacked Proton spectra of 1:1 reacting ratio of functional monomer vs Nicotine template in Methanol-d4 at temperatures of 30^{O}C, 40^{O}C and 60^{O}C.

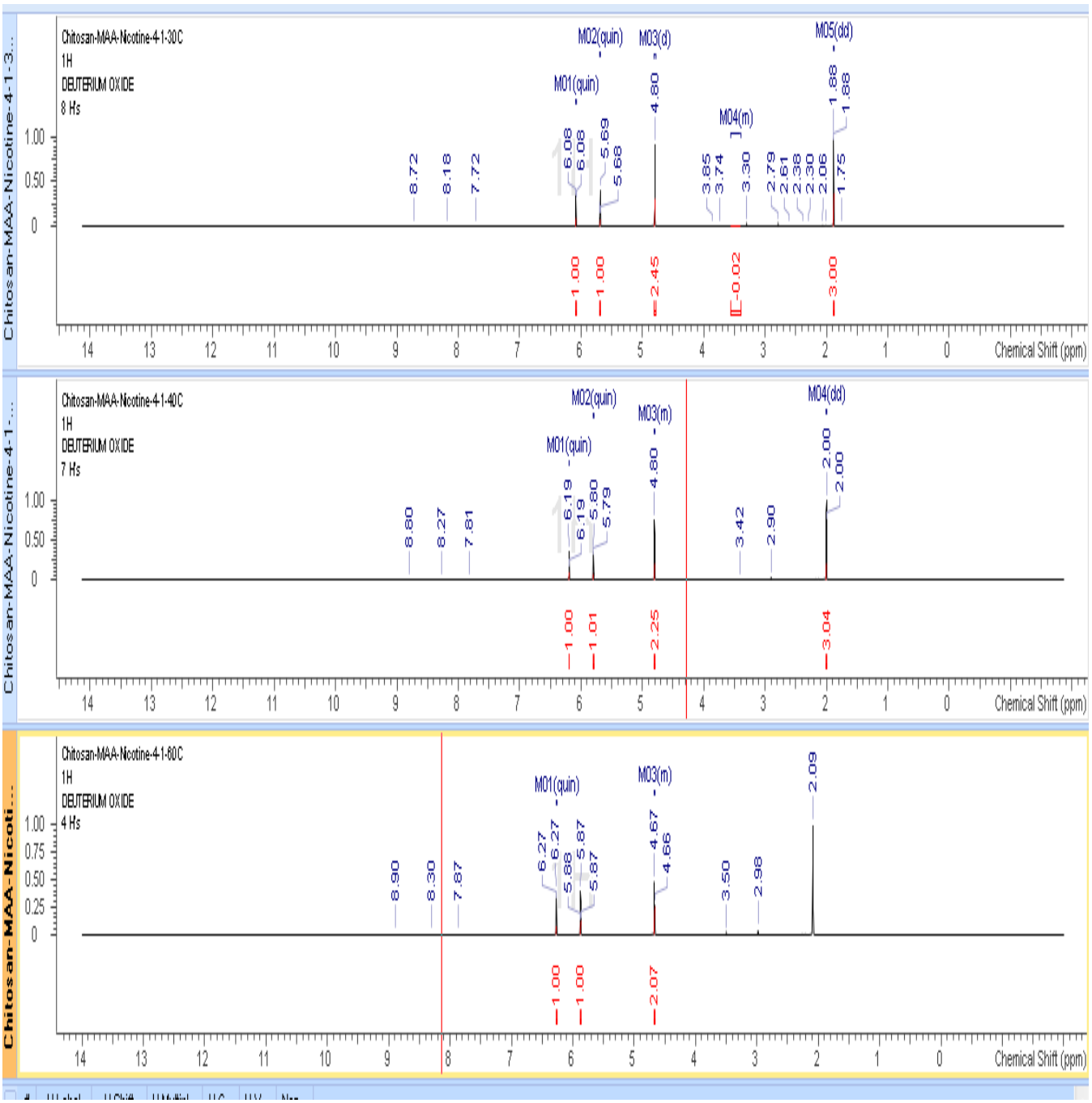

Appendix v: Stacked Proton spectra of 4:1 reacting ratio of functional monomer vs Nicotine template in Deutrium oxide at temperatures of 30^{O}C, 40^{O}C and 60^{O}C.

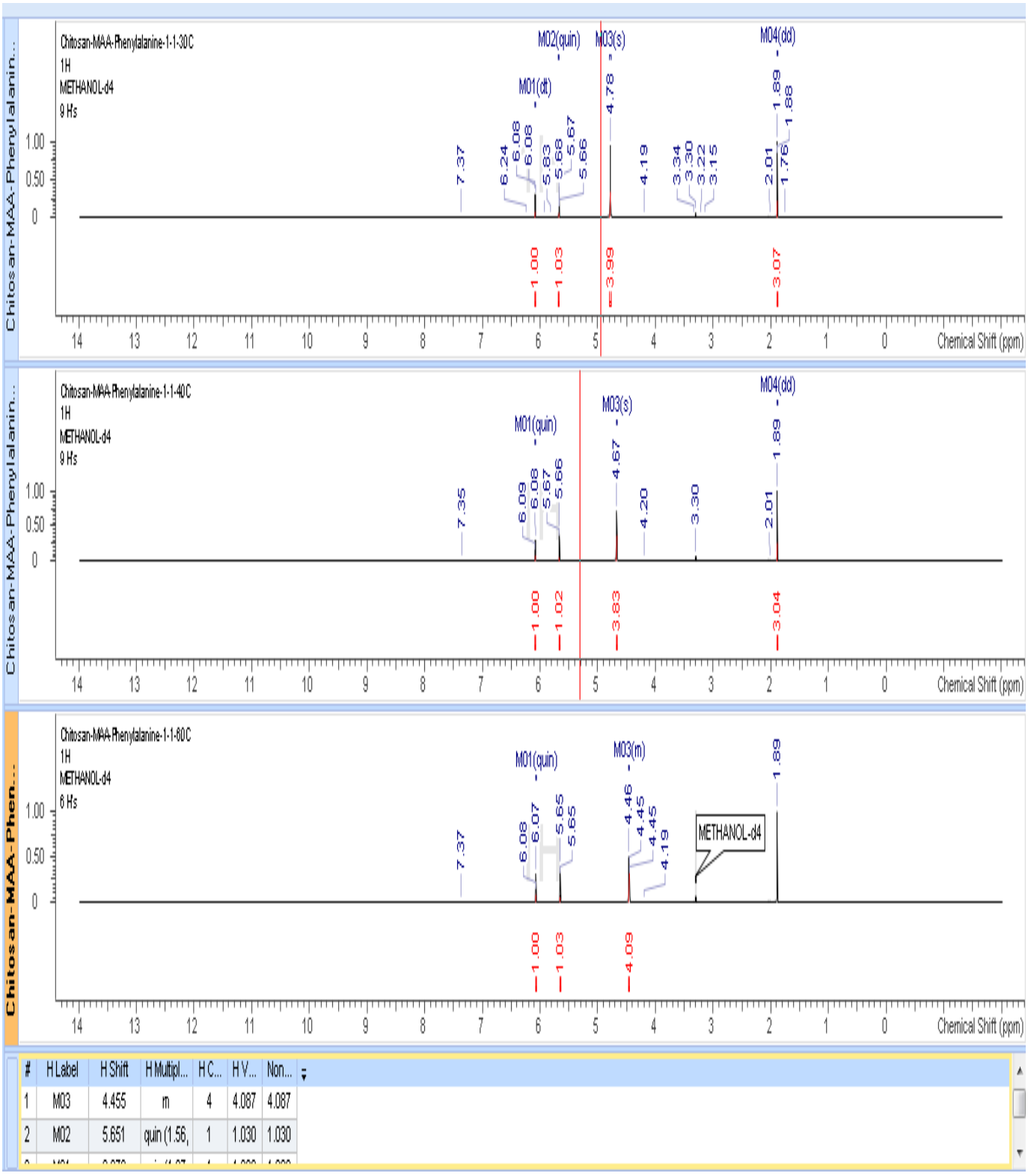

Appendix vi: Stacked Proton spectra of 1:1 reacting ratio of functional monomer vs Phenylalanine template in Methanol-d4 at temperatures of 30^{O}C, 40^{O}C and 60^{O}C**.**

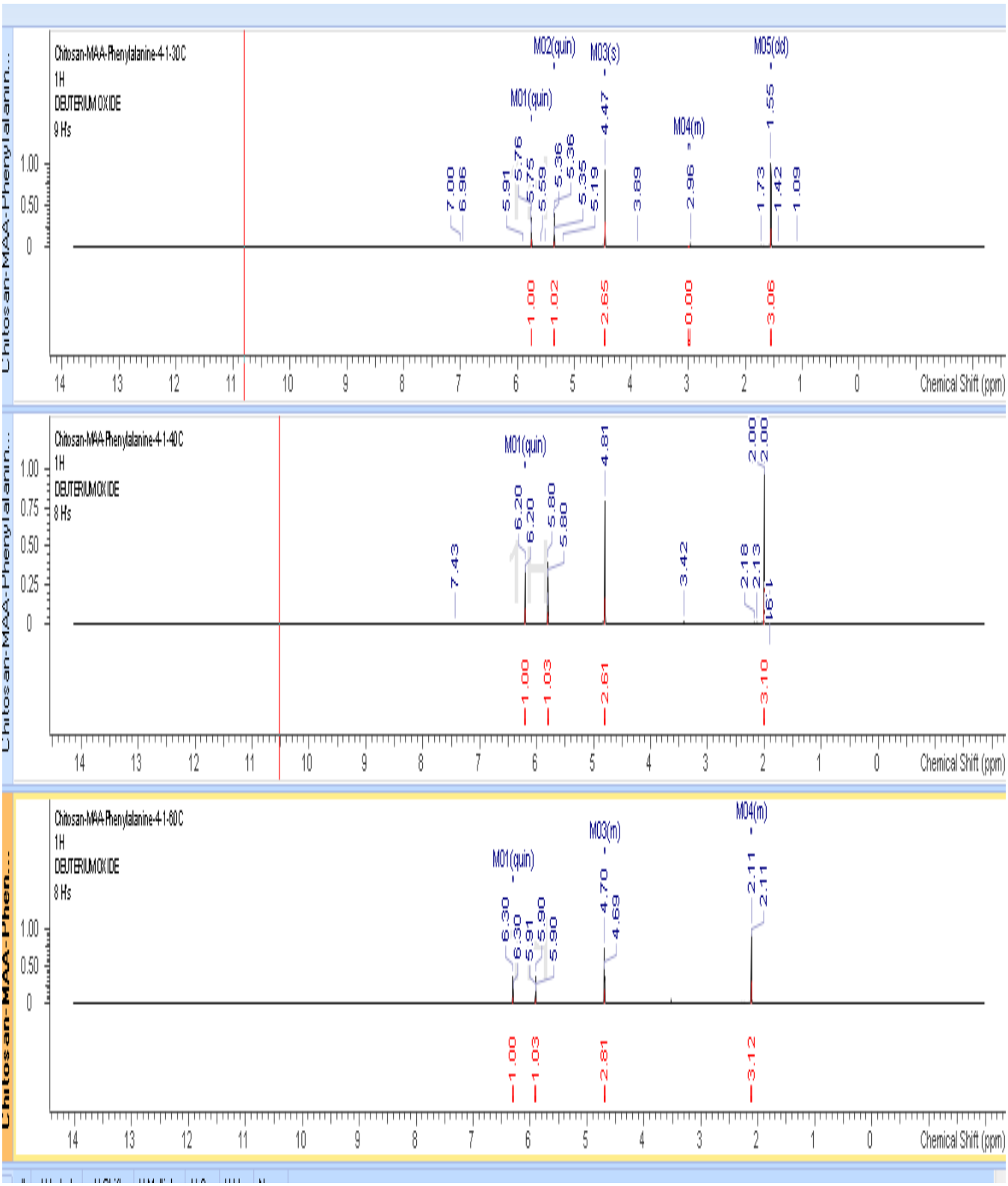

Appendix vii: Stacked Proton spectra of 4:1 reacting ratio of functional monomer vs Phenylalanine template in Deutrium oxide at temperatures of 30^{O}C, 40^{O}C and 60^{O}C.

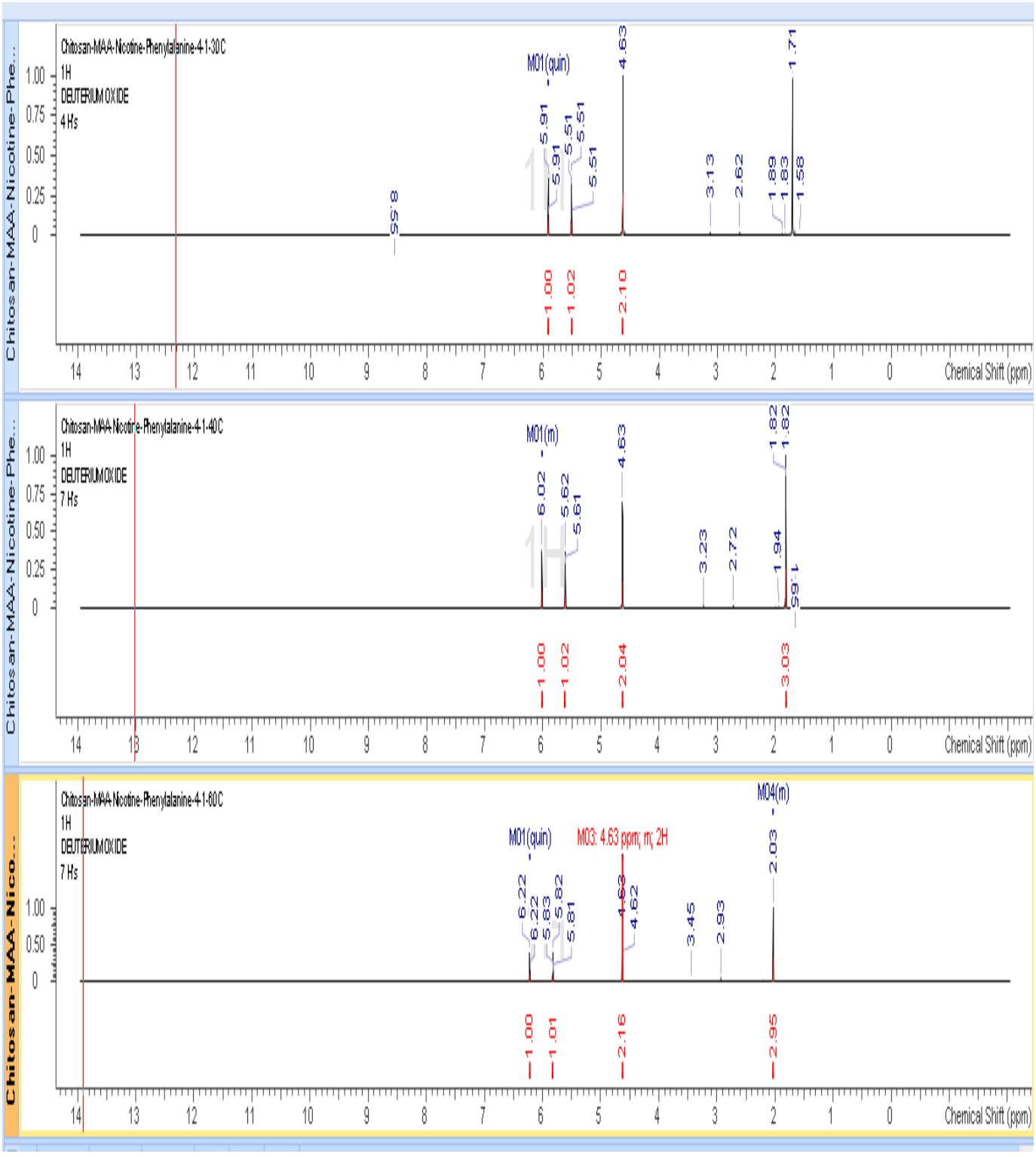

Appendix viii: Stacked Proton spectra of 4:1 reacting ratio of functional monomer vs Nicotine-Phenylalanine template in Deutrium oxide at temperatures of 30^{O}C, 40^{O}C and 60^{O}C.

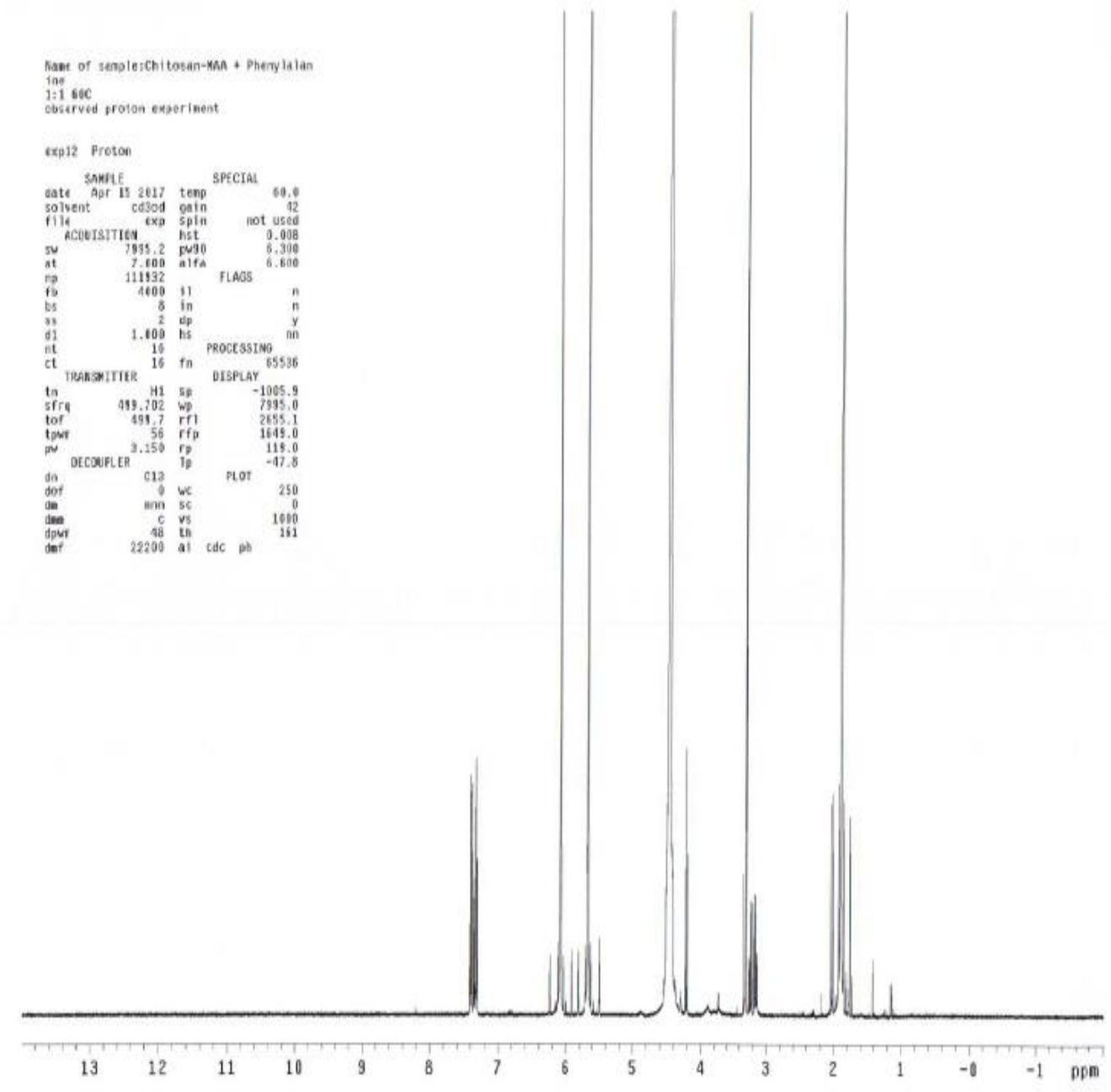

Appendix ix: Spectra of 1:1blend of Chitosan-MAA: Phenylalanine @ a reaction temp. of 60^{O}C.

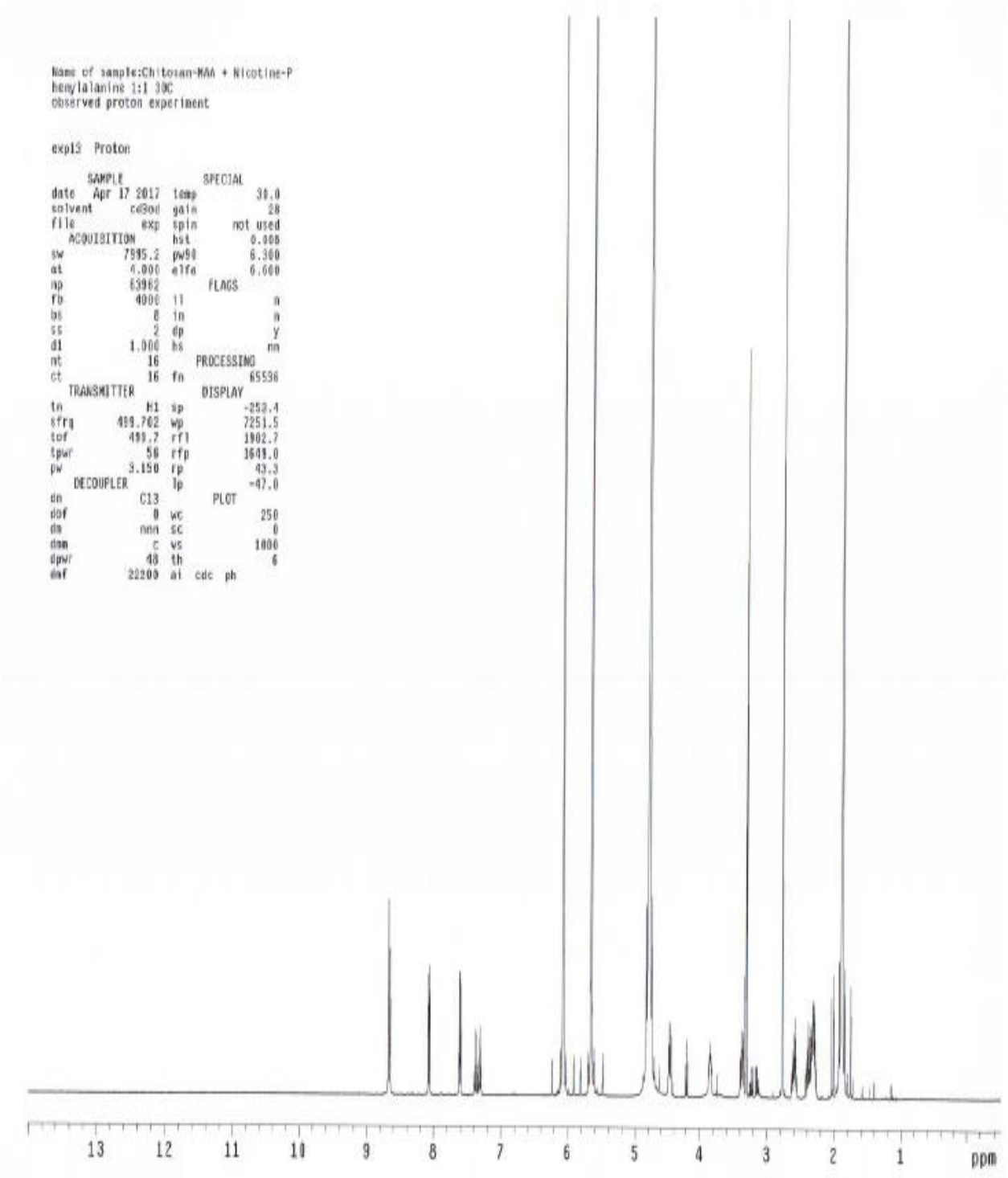

Appendix x: Spectra of 1:1blend of Chitosan-MAA: Nicotine-Phenylalanine @ a reaction temp. of 30^{O}C.

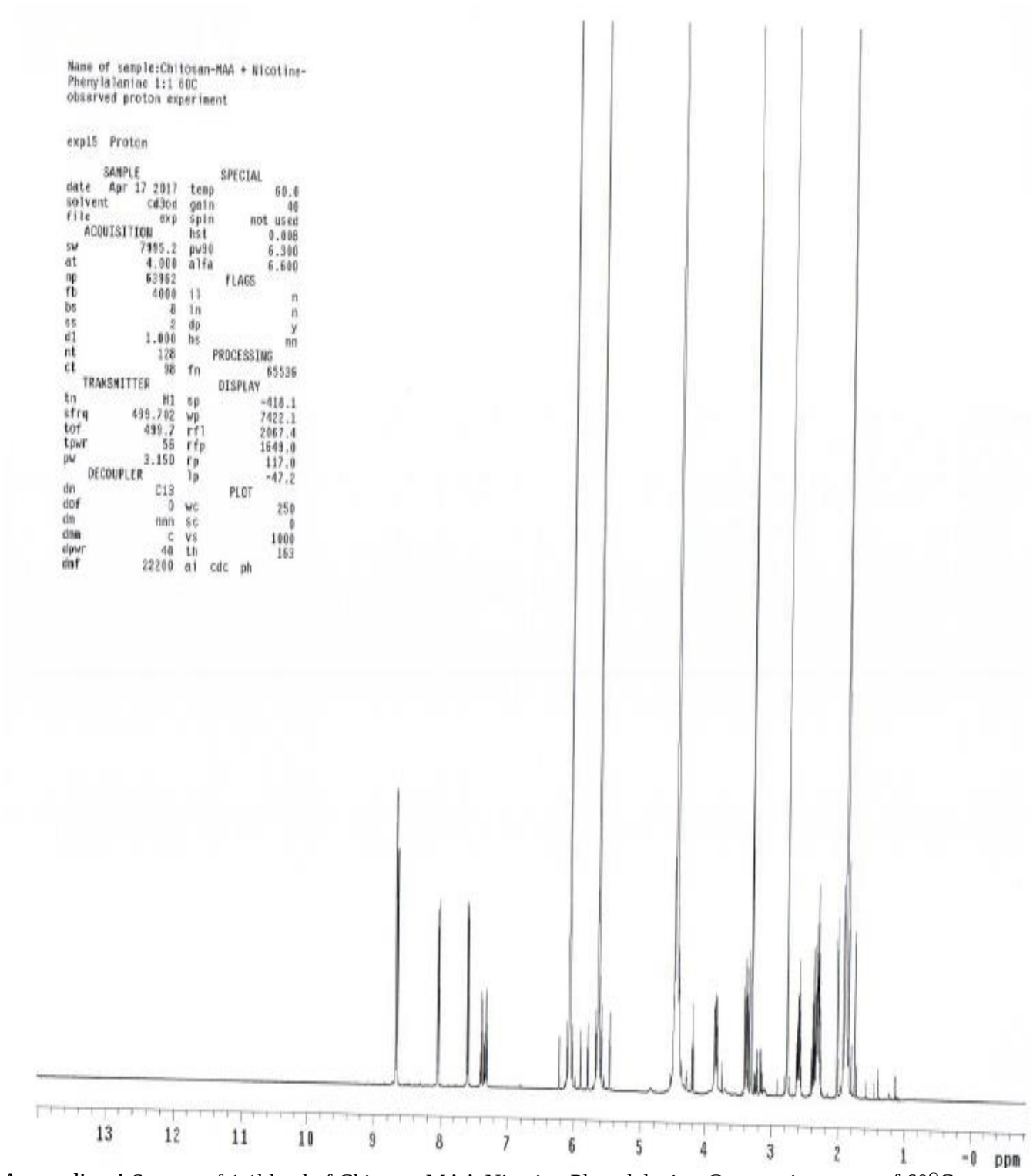

Appendix xi:Spectra of 1:1blend of Chitosan-MAA:Nicotine-Phenylalanine @ a reaction temp. of 60^{O}C

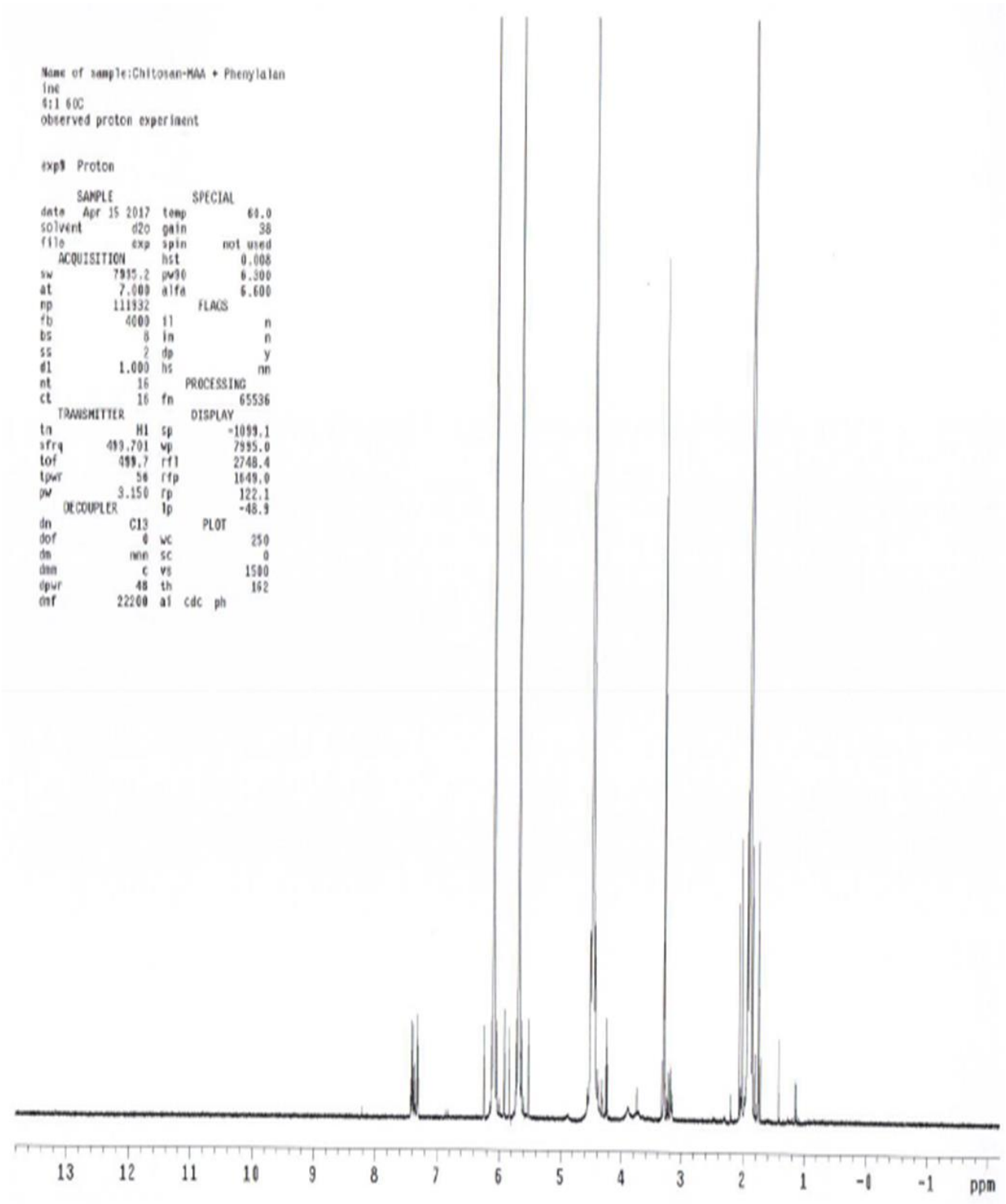

Appendix xii: Spectra of 4:1blend of Chitosan-MAA:Phenylalanine @ a reaction temp. of 60^{O}C

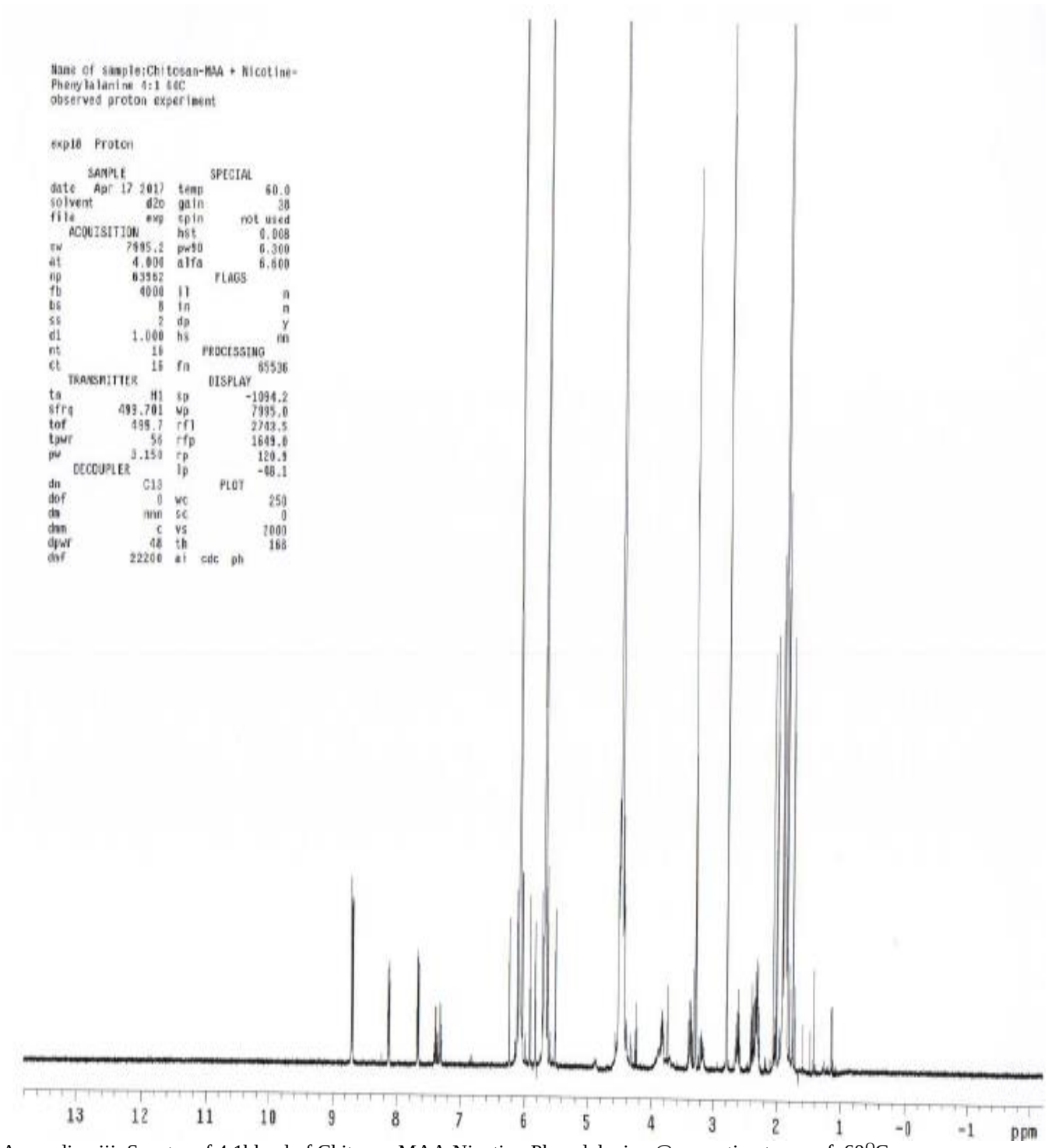

Appendix xiii: Spectra of 4:1blend of Chitosan-MAA:Nicotine-Phenylalanine @ a reaction temp. of $60^{O}C$

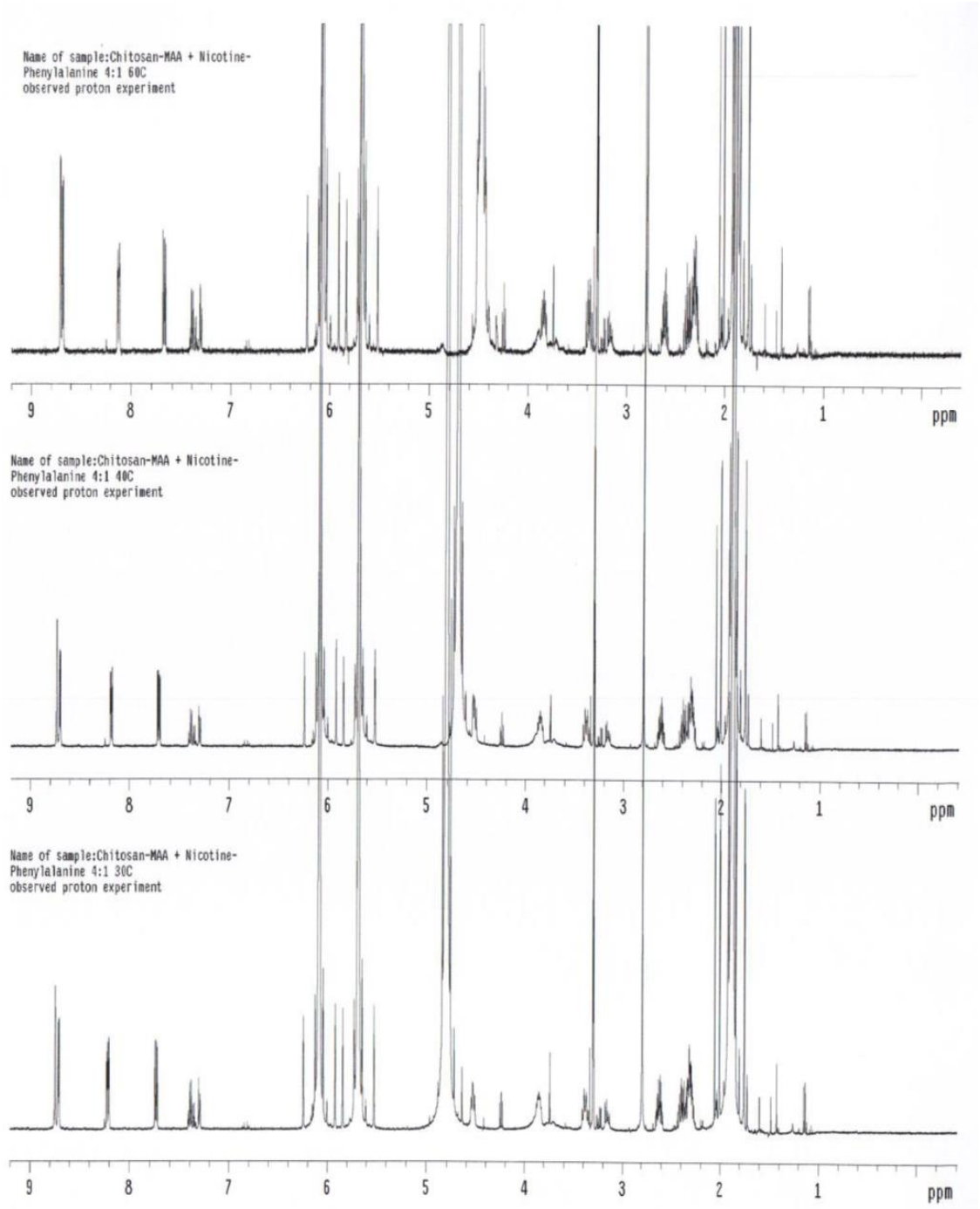

Appendix xiv: Stacked H'NMR titration spectra of a 4:1 functional monomer vs. template ratio at three different temperatures of $30^{O}C$, $40^{O}C$ and $60^{O}C$.

Spectra Results from the FTIR spectroscopy of the proof-of-concept experiment.
Prepolymerized sample of CS-Nic-3Pp MIP

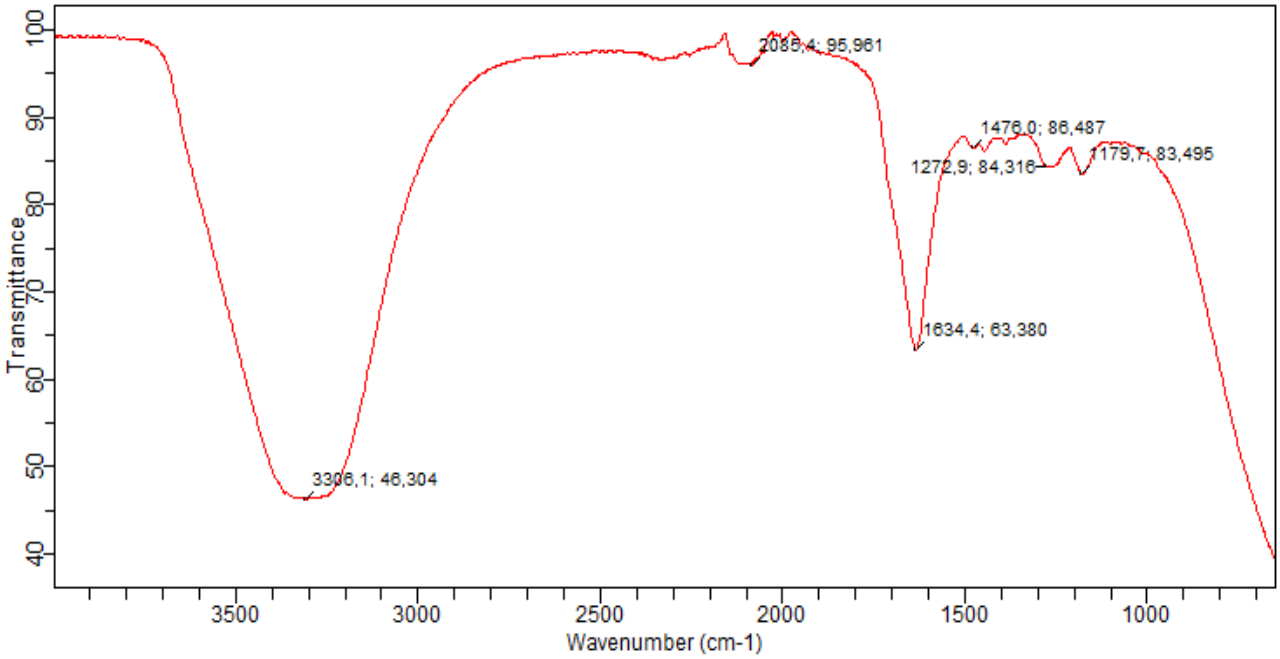

Appendix xv: Spectra of Prepolymerized and polymerized MIP samples

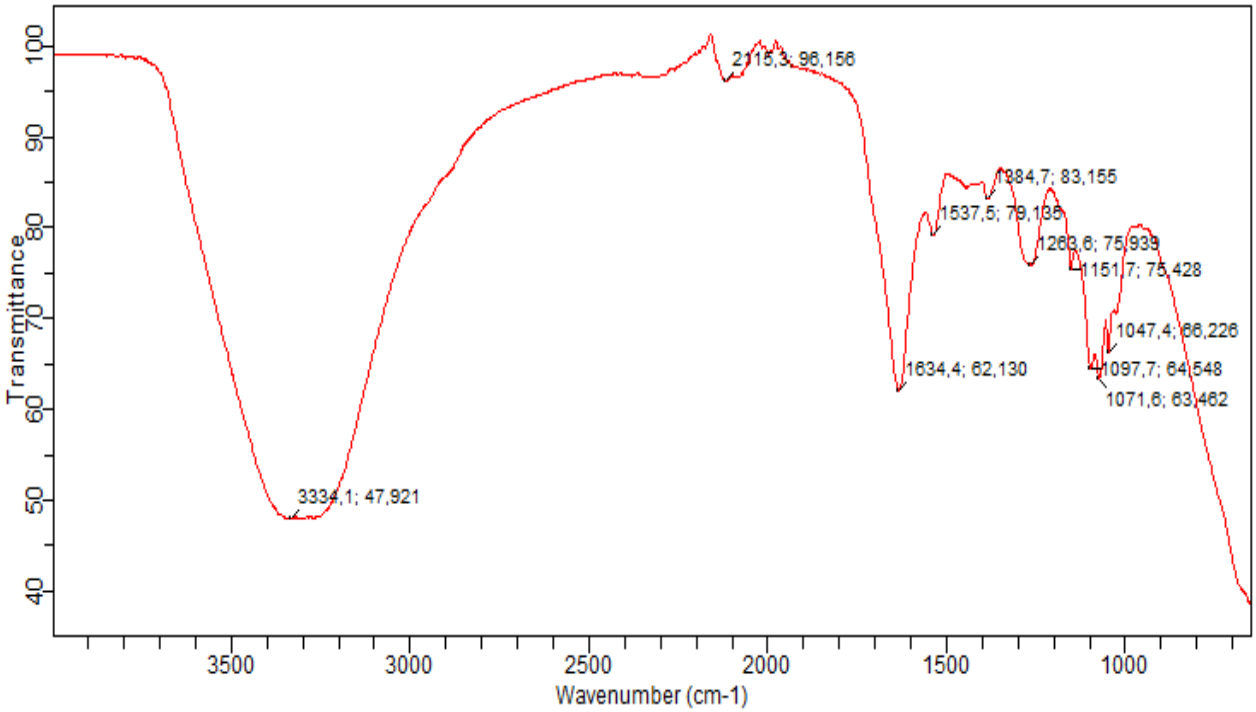

Appendix xvi: Spectra of Prepolymerized and polymerized NIP Sample

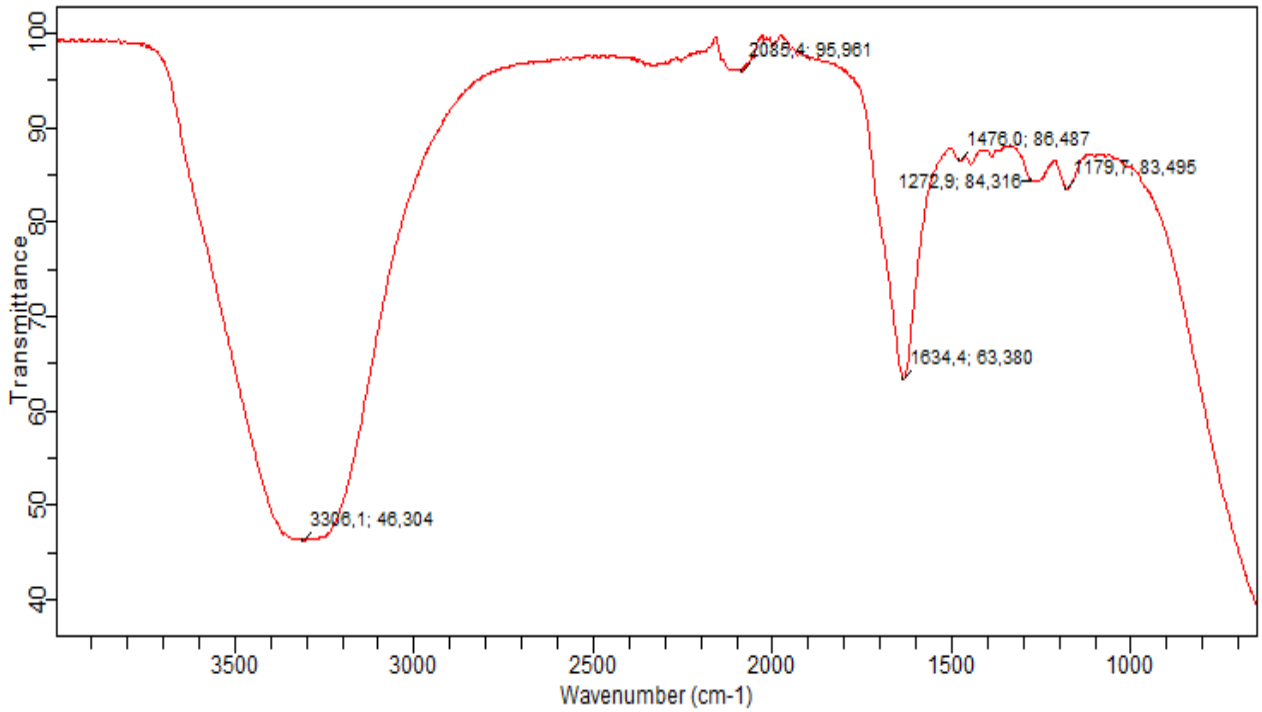

Appendix xvii: Spectra of Nicotine templated MIP Sample

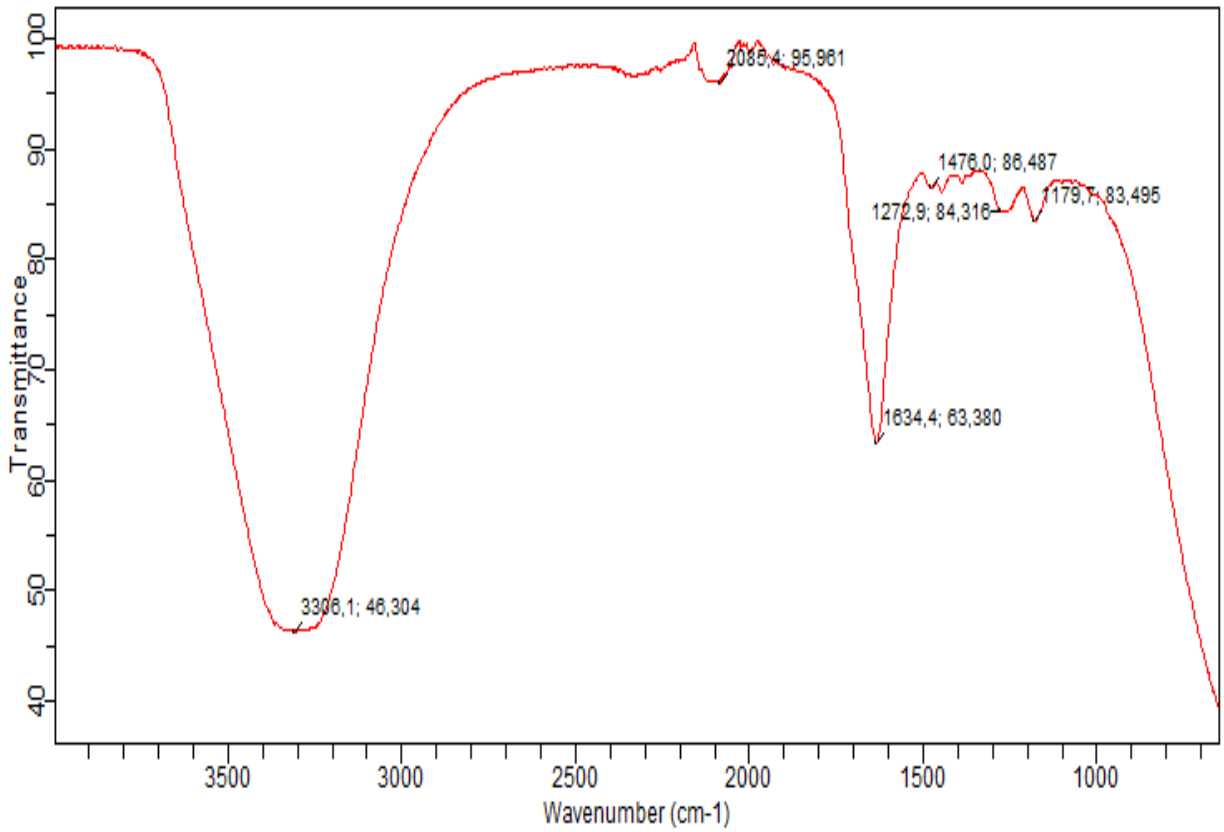

Appendix xviii: Spectra of 3-PhenylPiridine MIP Sample

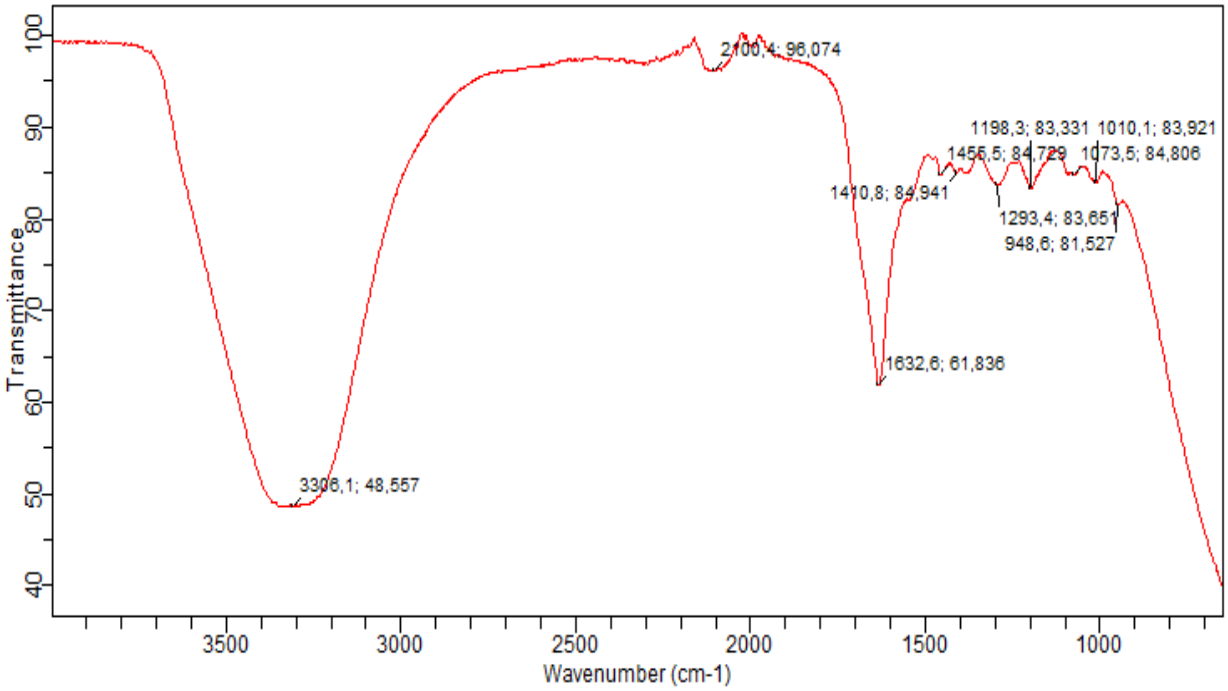

Appendix xix: Spectra of 3-PhenylPiridine-Nicotine MIP Sample

Spectra Results from the FTIR spectroscopy of the bulk experiment.

A FTIR Charts of BAP cross linked polymers:

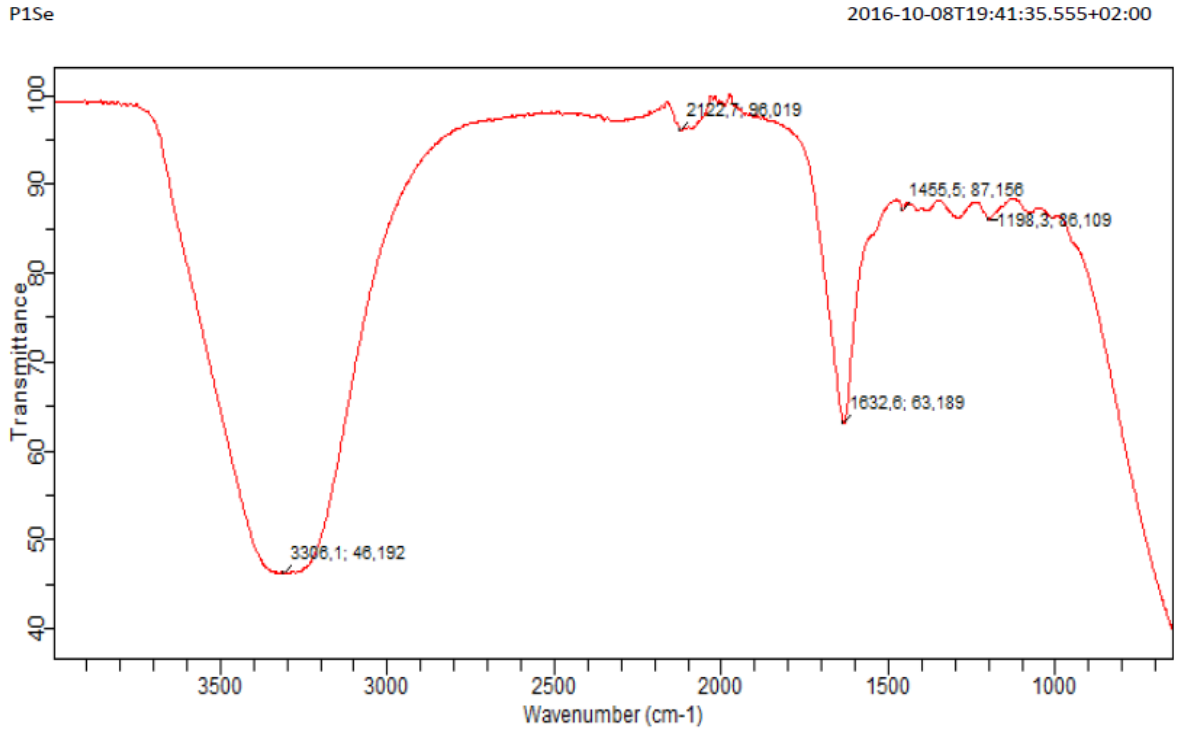

Appendix xx: Spectra of Nicotine templated MIP.(P1Se)

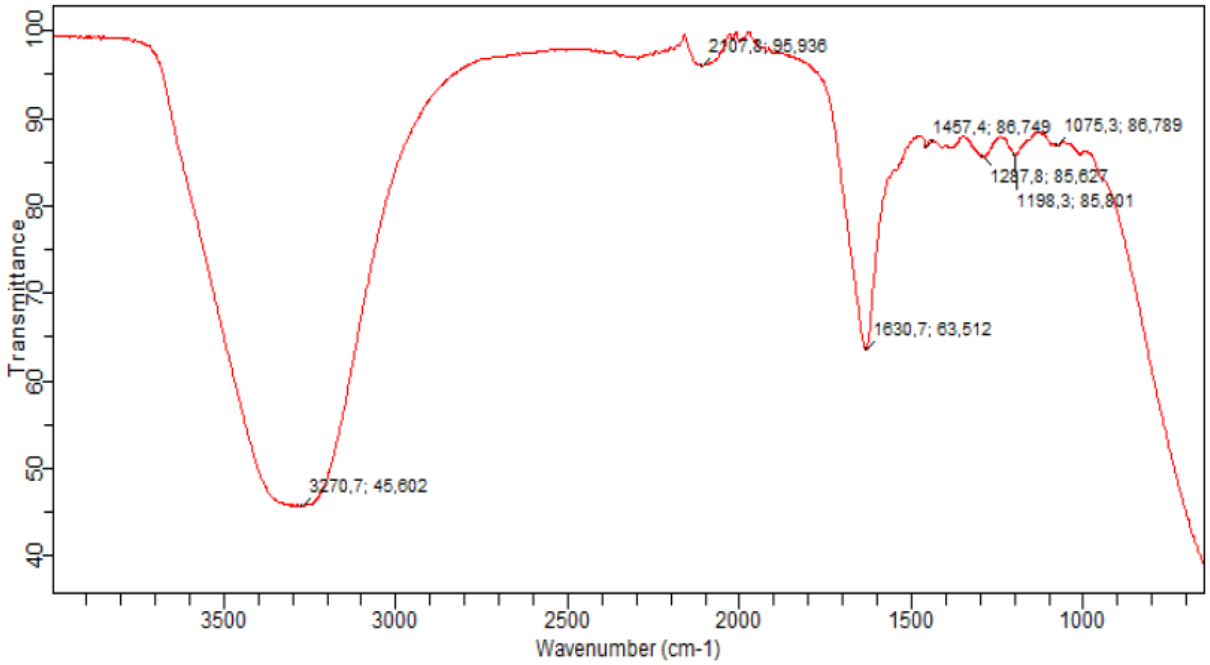

Appendix xxi: Spectra of Nicotine templated MIP.(P1Sf)

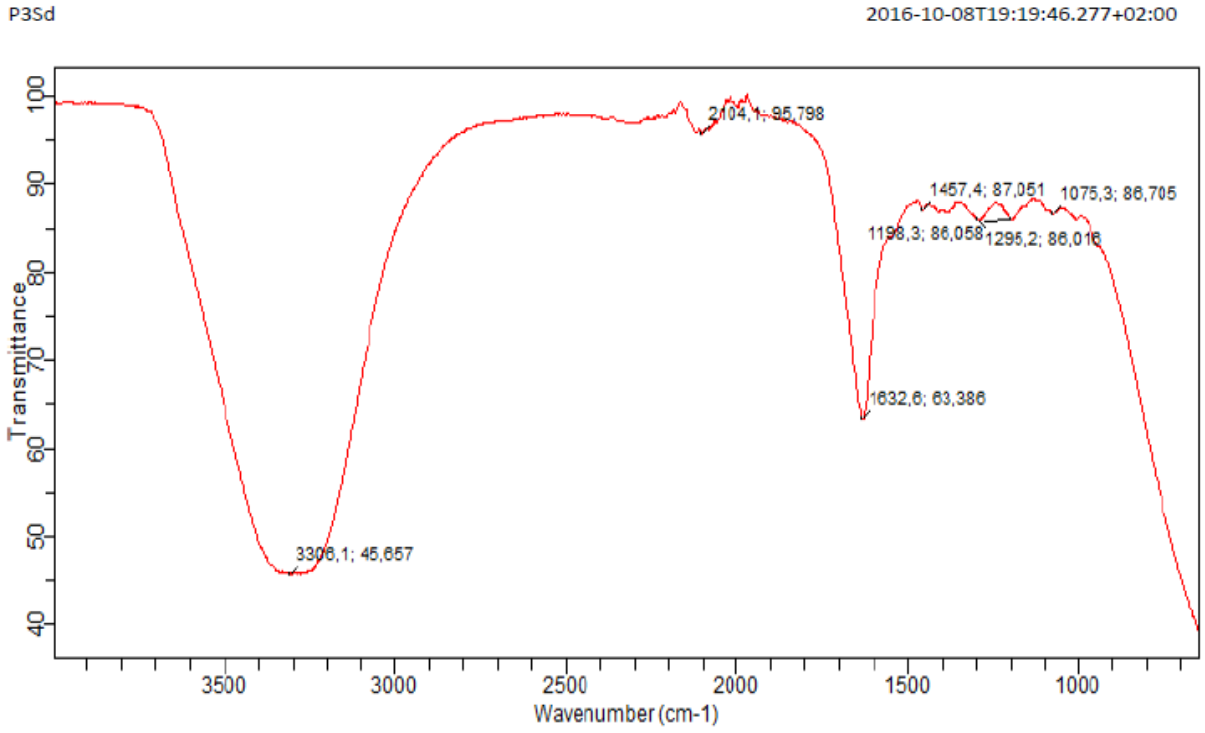

Appendix xxii: Spectra of Nicotine templated MIP.(P3Sd)

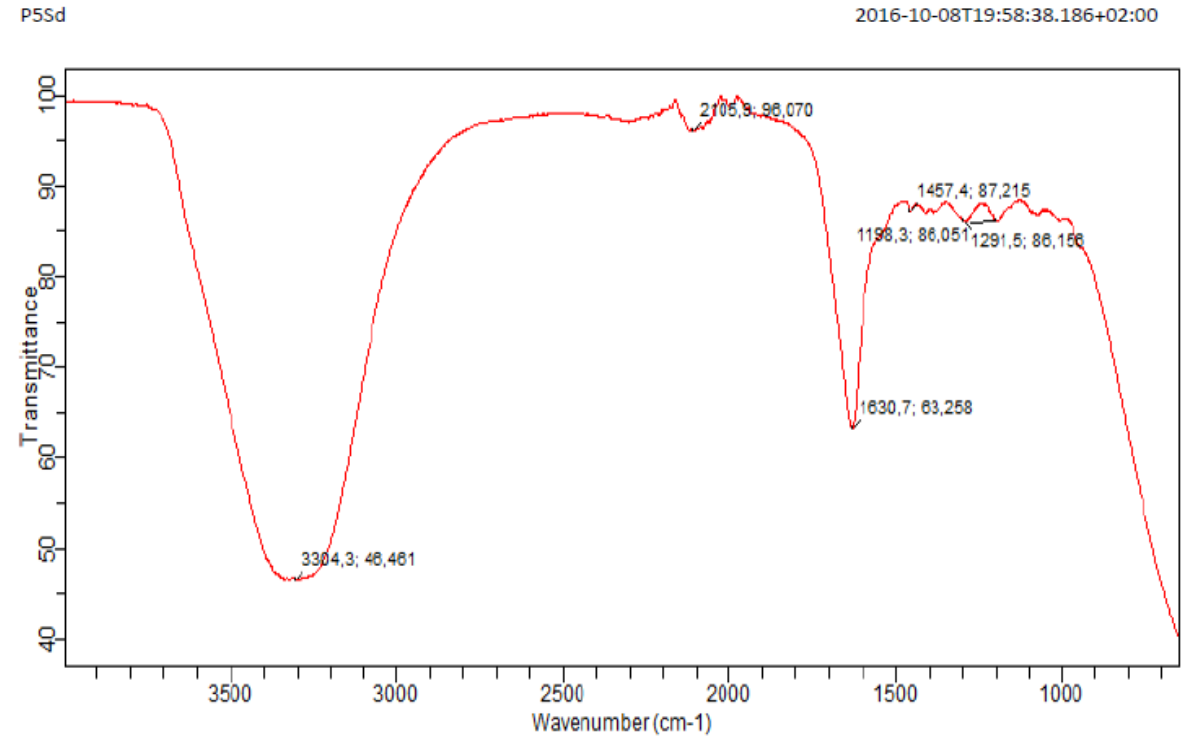

Appendix xxiii: Spectra of Nicotine templated MIP.(P5Sd)

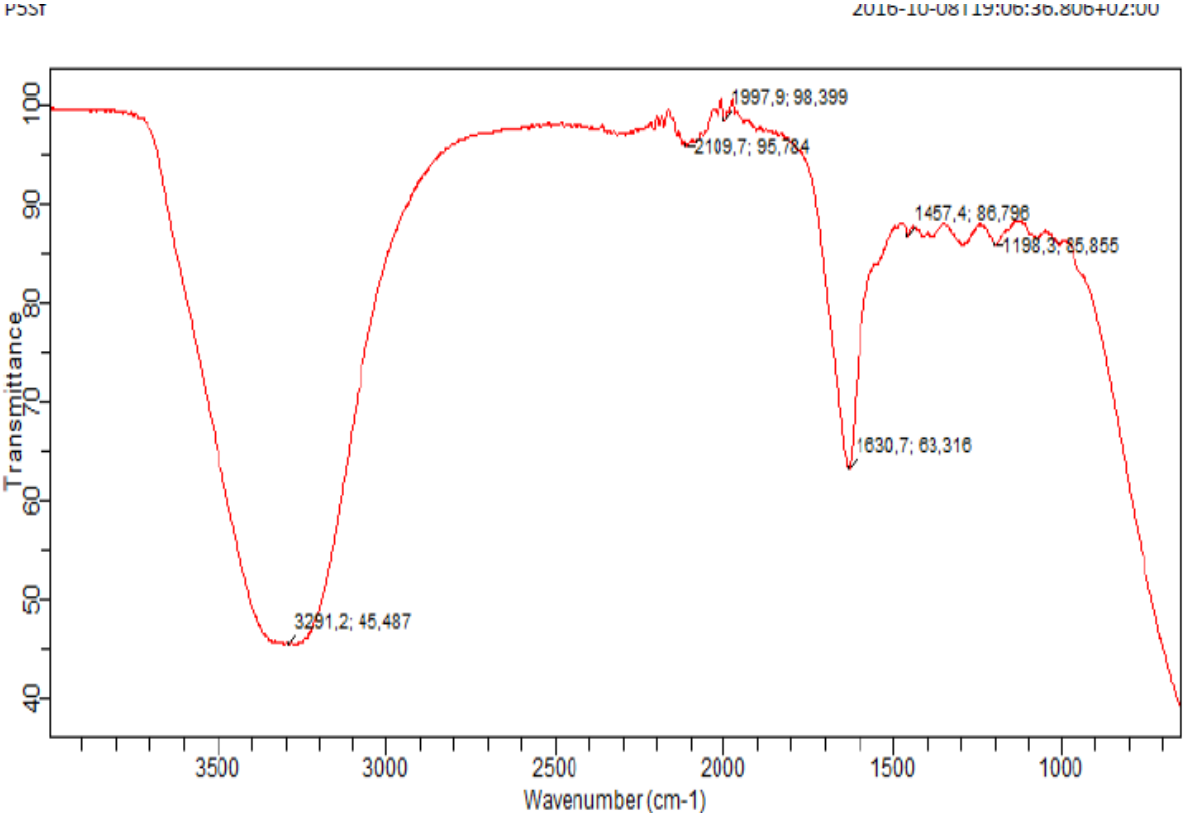

Appendix xxiv: Spectra of Nicotine templated NIP.(P5Sf)

Thermograms of Template Eluted Samples:

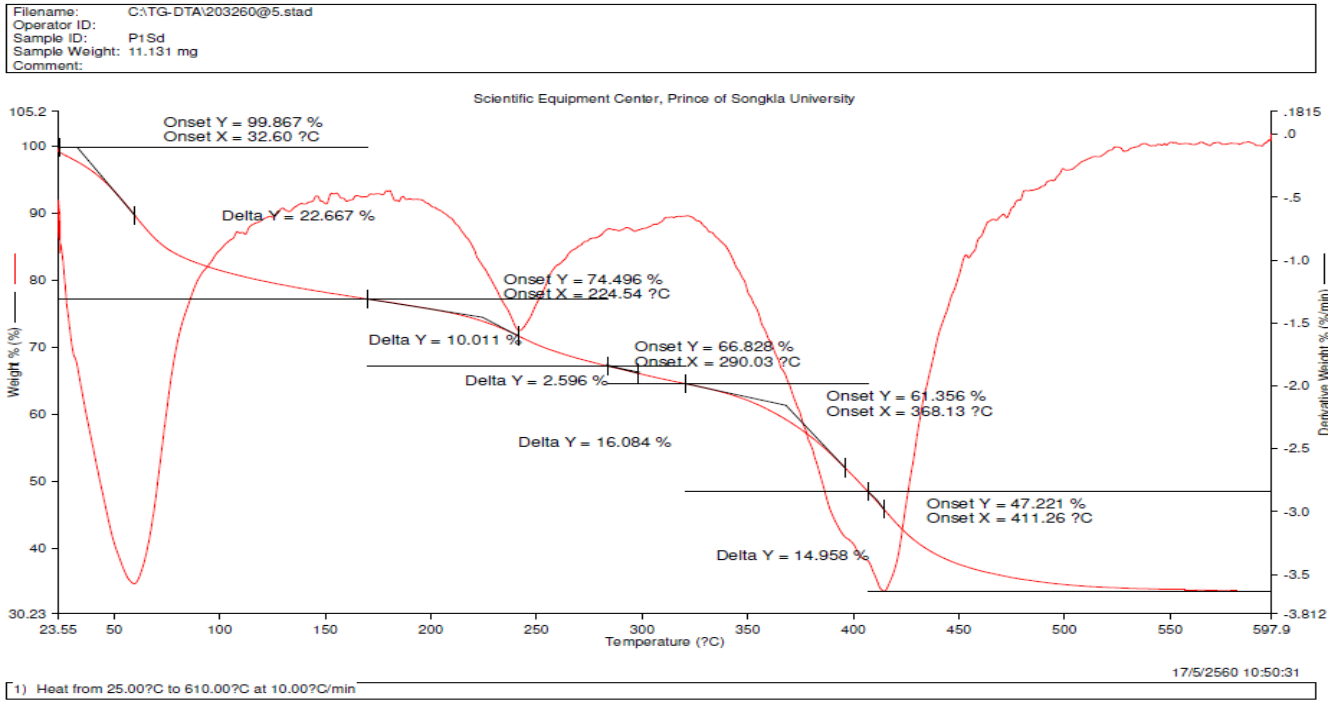

Appendix xxv: Simultaneouse Thermal Analysis thermogram of of Nicotine templated MIP.(P1Sd)

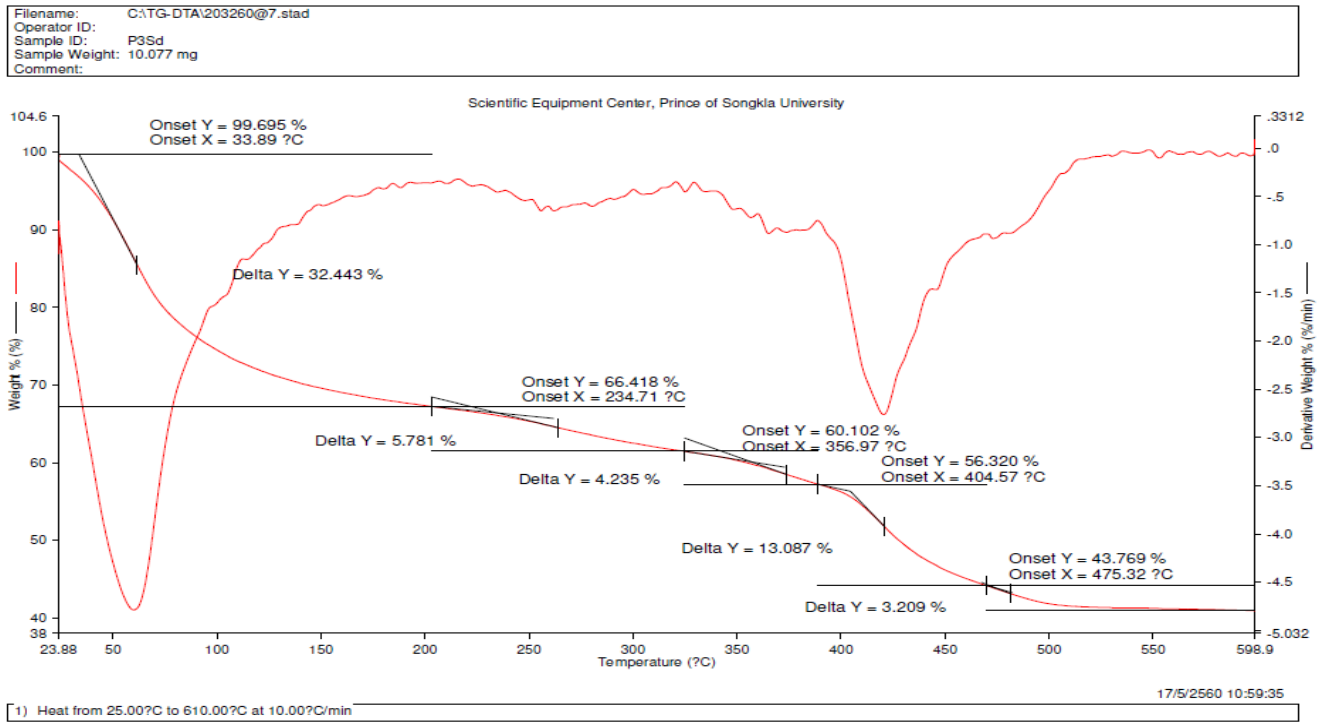

Appendix xxvi: Simultaneouse Thermal Analysis thermogram of Phenylalanine templated MIP. (P3Sd)

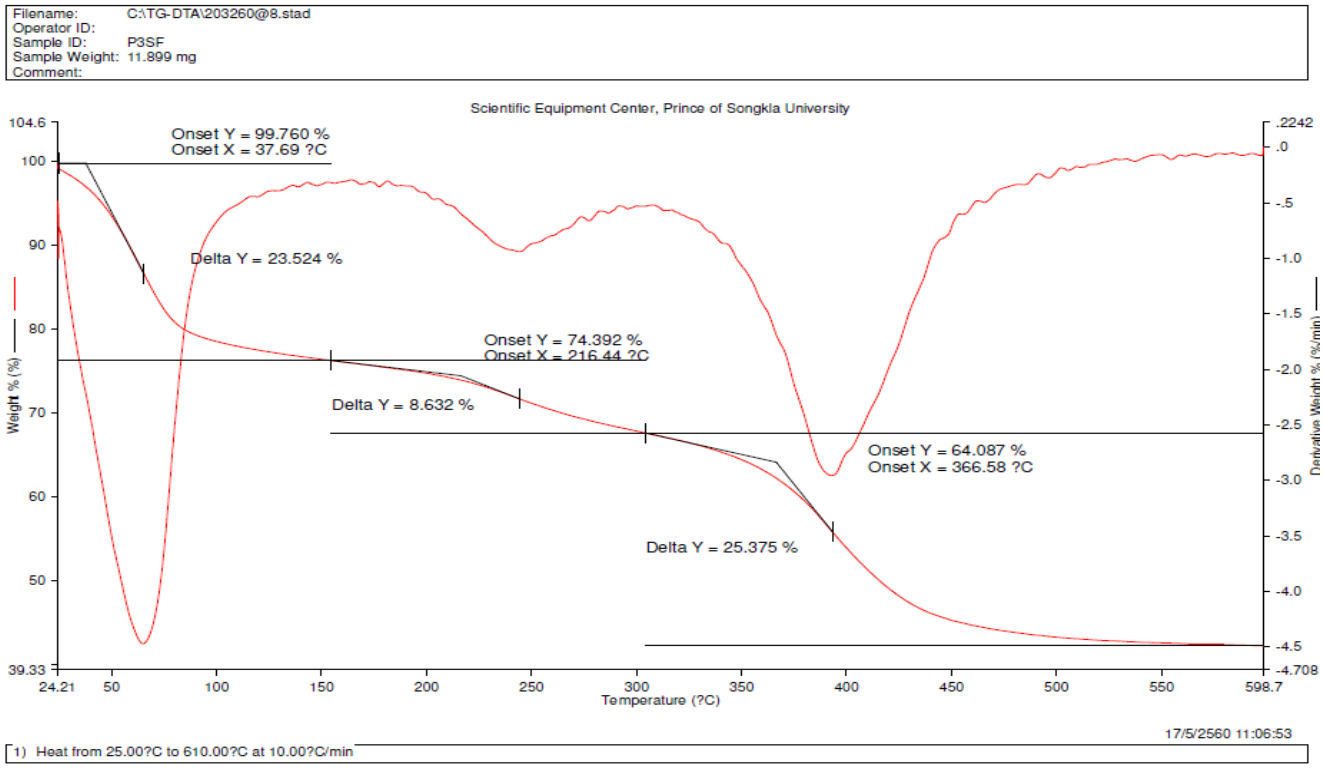

Appendix xxvii: Simultaneouse Thermal Analysis thermogram of Phenylalanine templated NIP. (P3SF)

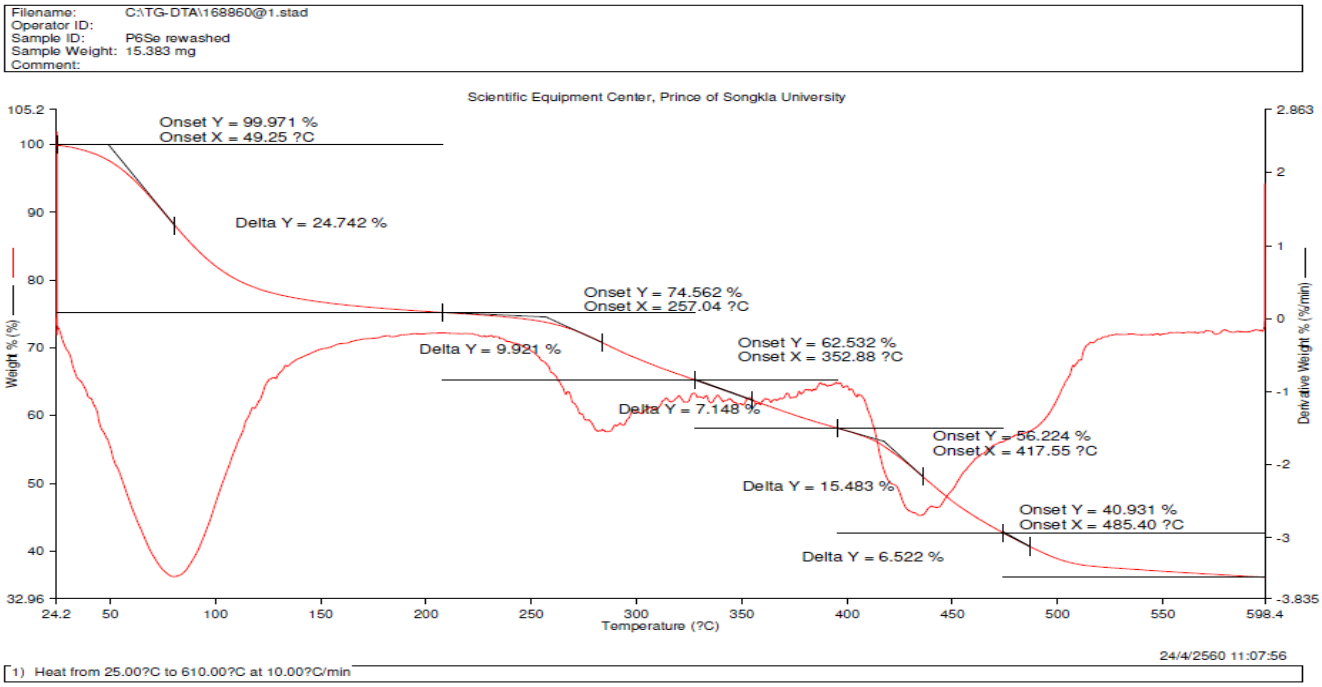

Appendix xxviii: Simultaneouse Thermal Analysis thermogram of Phenylalanine templated MIP. (P6Se)

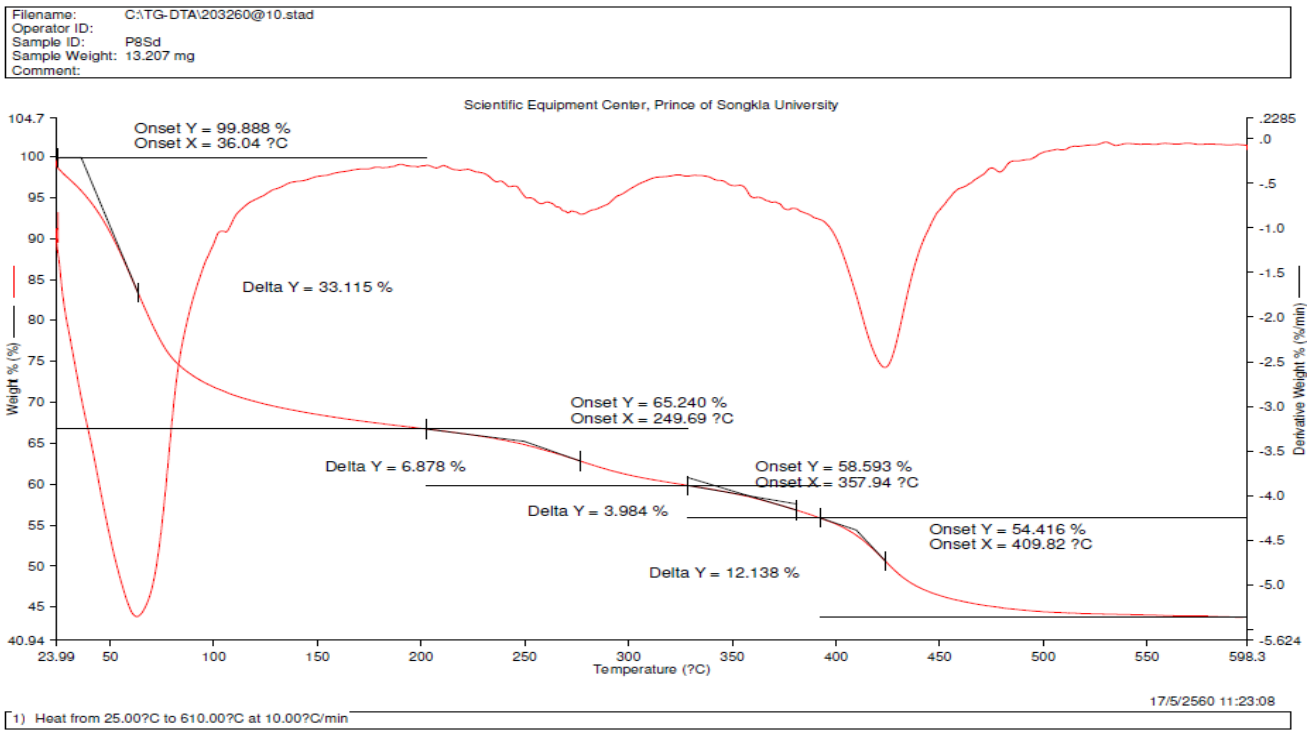

Appendix xxix: Simultaneouse Thermal Analysis thermogram of Phenylalanine templated MIP. (P8Sd)

Thermograms of Representative Template containing Samples:

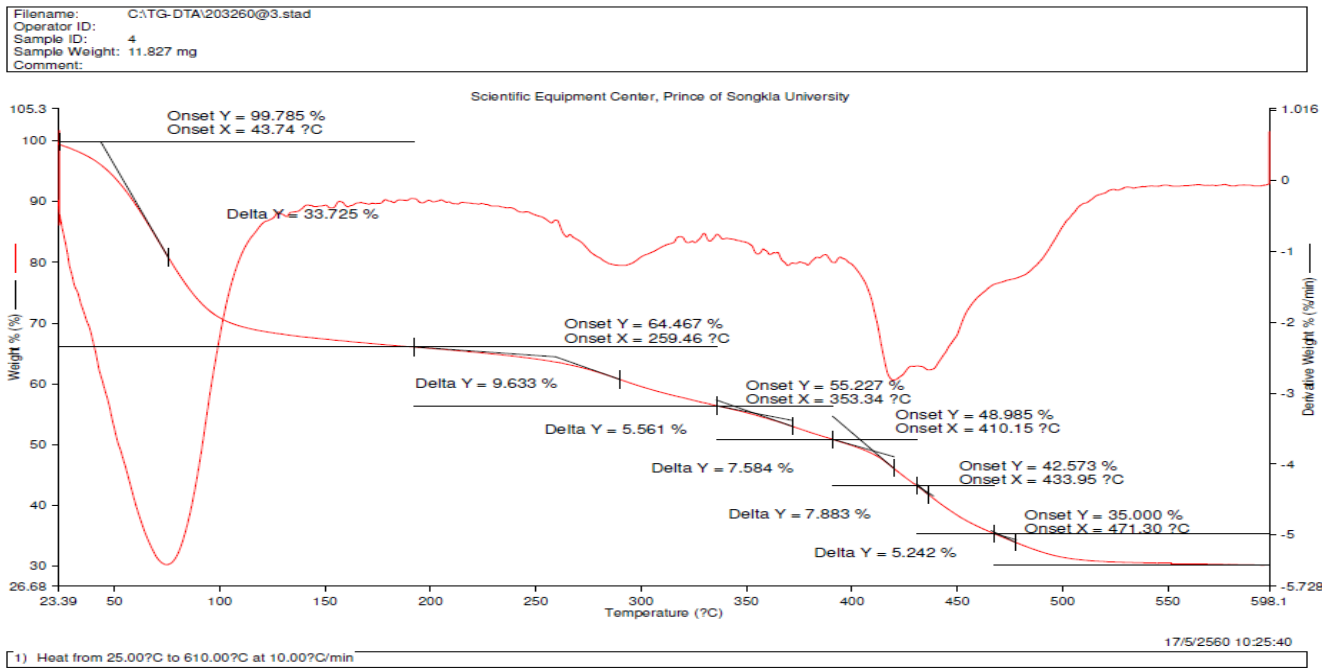

Appendix xxx: Simultaneouse Thermal Analysis thermogram of Nicotine-Phenylalanine templated MIP.(P5Sd).

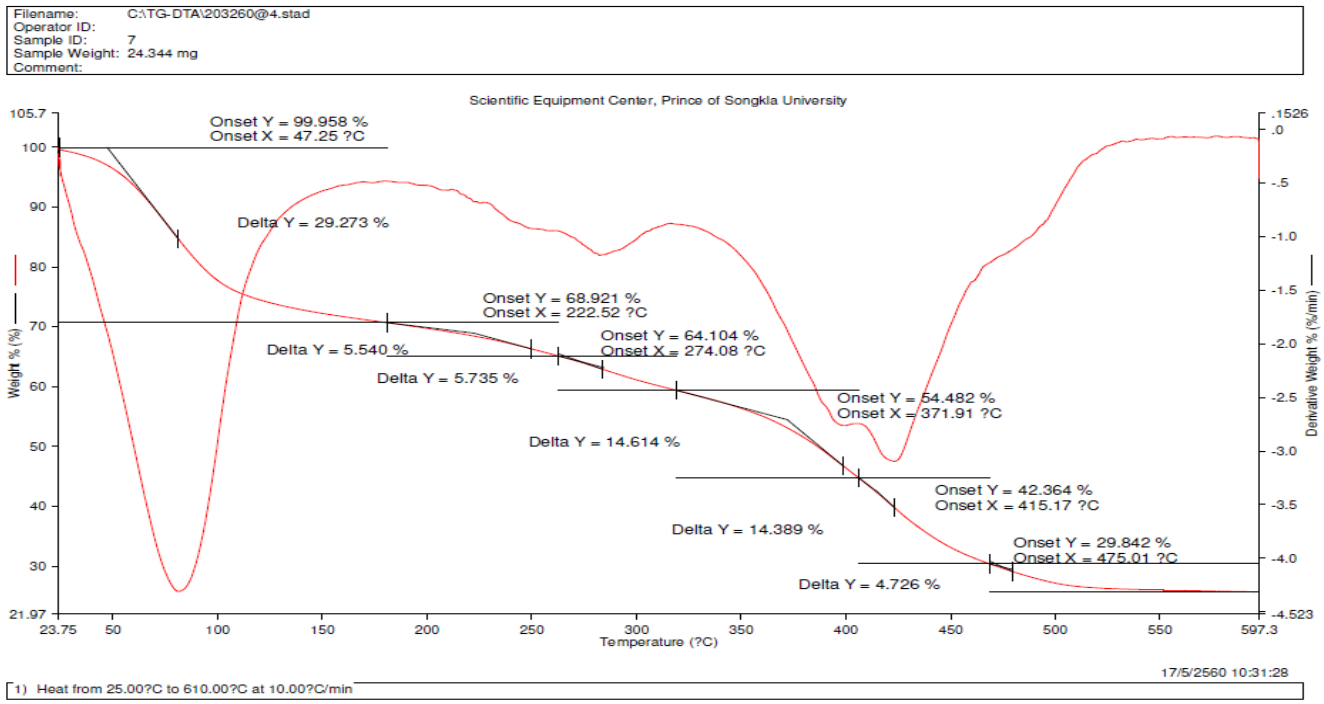

Appendix xxxi: Simultaneouse Thermal Analysis thermogram of Nicotine-Phenylalanine templated MIP. (P10Sd).

Chromatograms from rebinding studies using LC-MS analytical method.

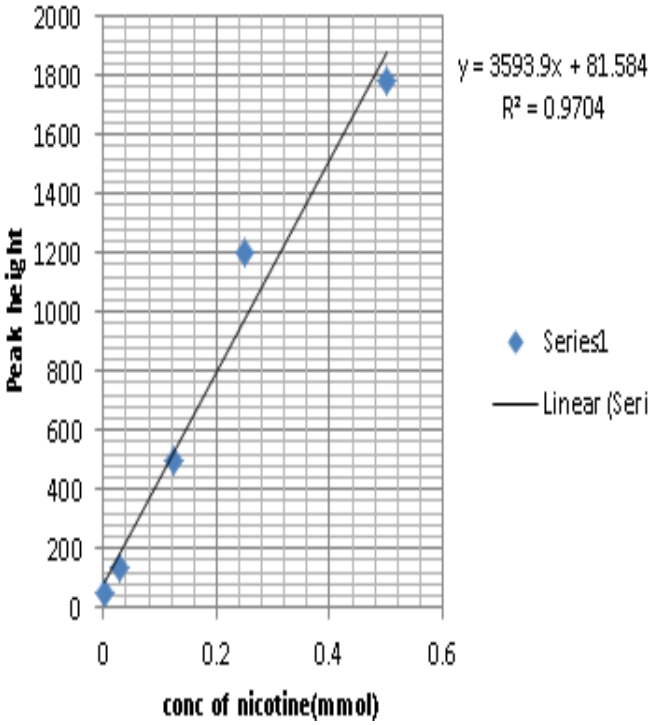

Appendix xxxii: Calibration curve for Nicotine

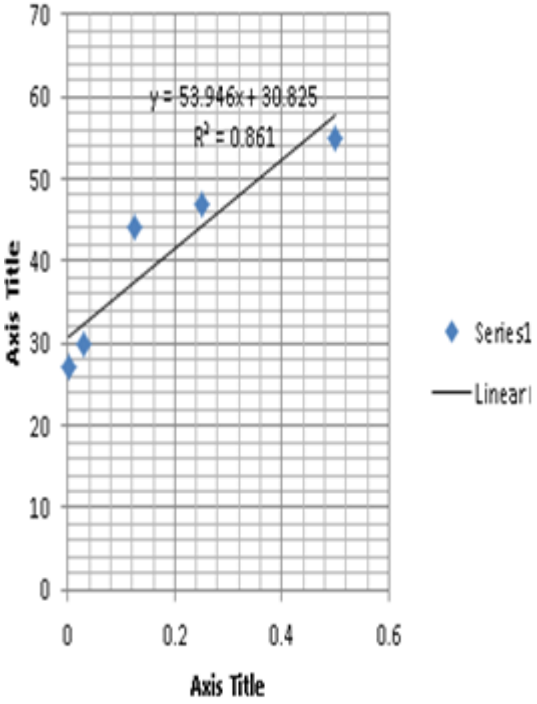

Calibration curve for Phenylalanine amide

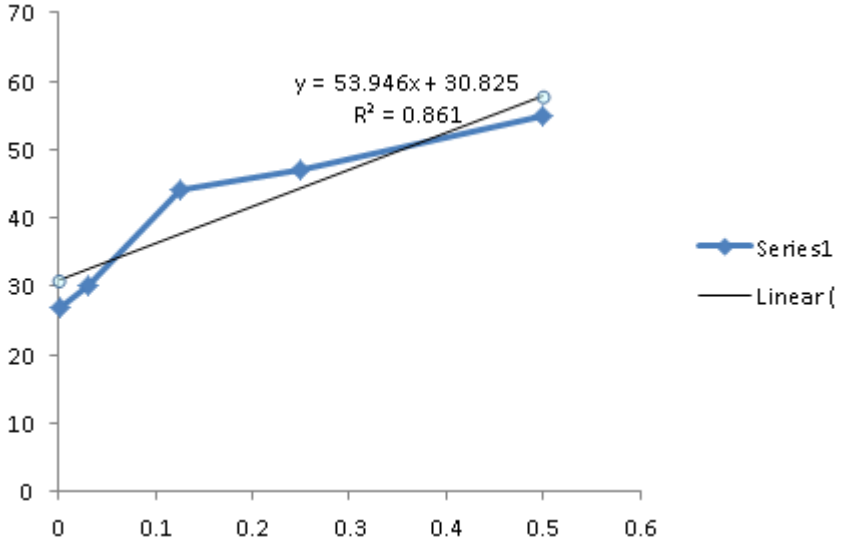

Appendix xxxiii: Calibration curve for Nicotine-Phenylalanine 50:50 blend.

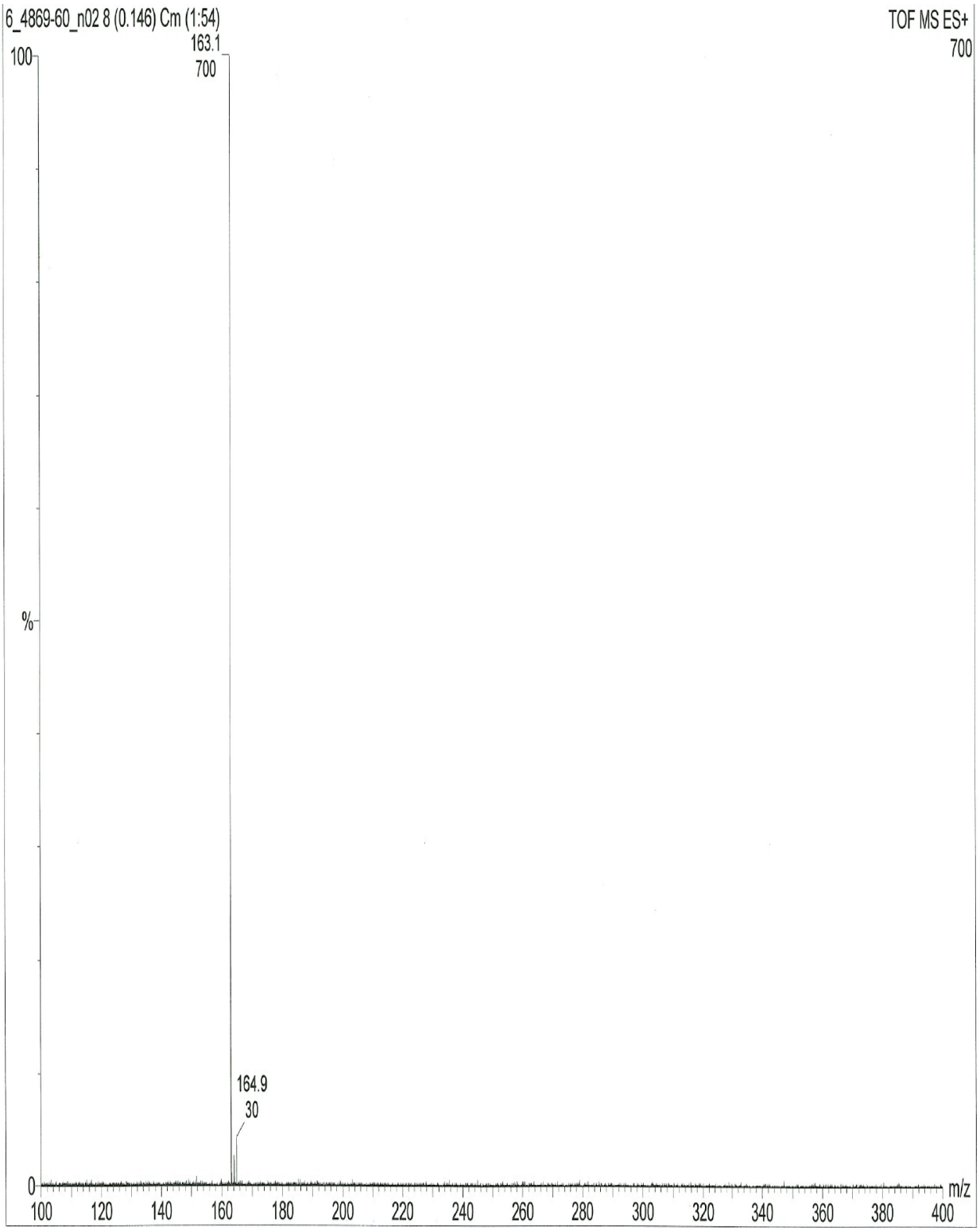

Appendix xxxiv : LC-MS Chromatogram of P1Se (5)

Appendix xxxv: LC-MS Chromatogram of P1Se (5R)

Appendix xxxvi: LC-MS Chromatogram of P1Sf (9R)

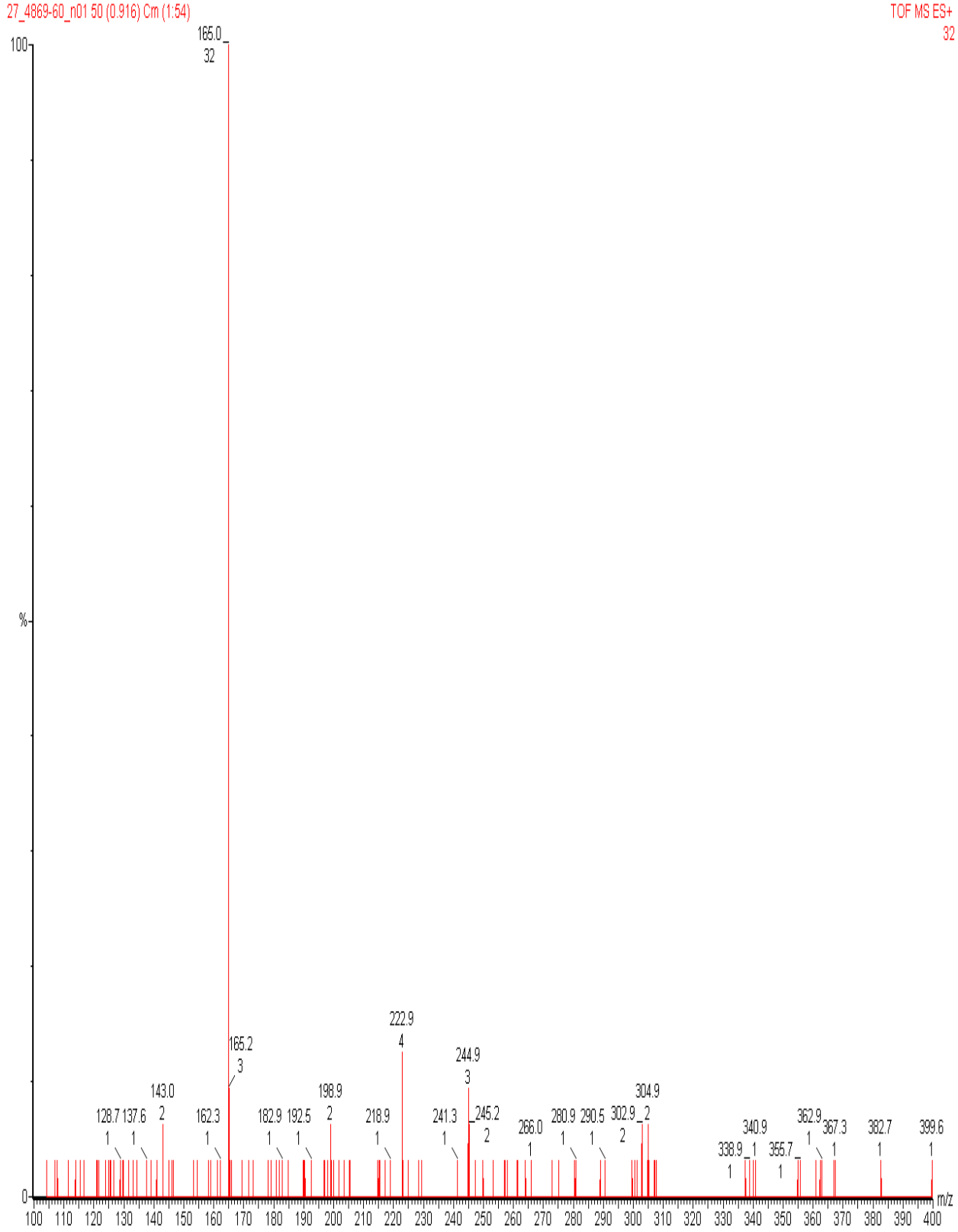

Appendix xxxvii: LC-MS Chromatogram of P3Sd (19)

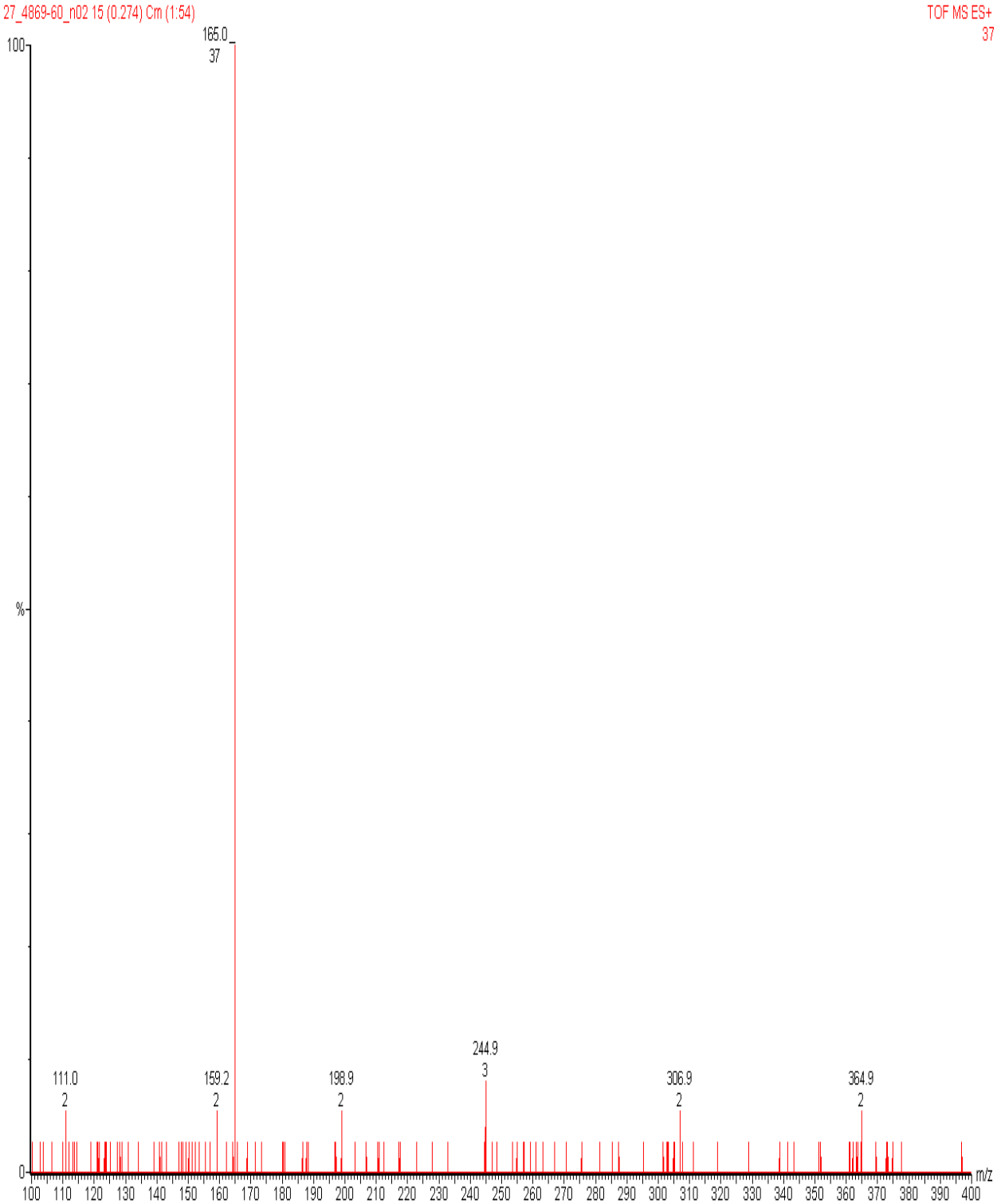

Appendix xxxviii: LC-MS Chromatogram of P3Sd (19R).

Appendix xxxix: LC-MS Chromatogram of P3Sf (18R)

ppendix xl: LC-MS Chromatogram of P5Sf (31)

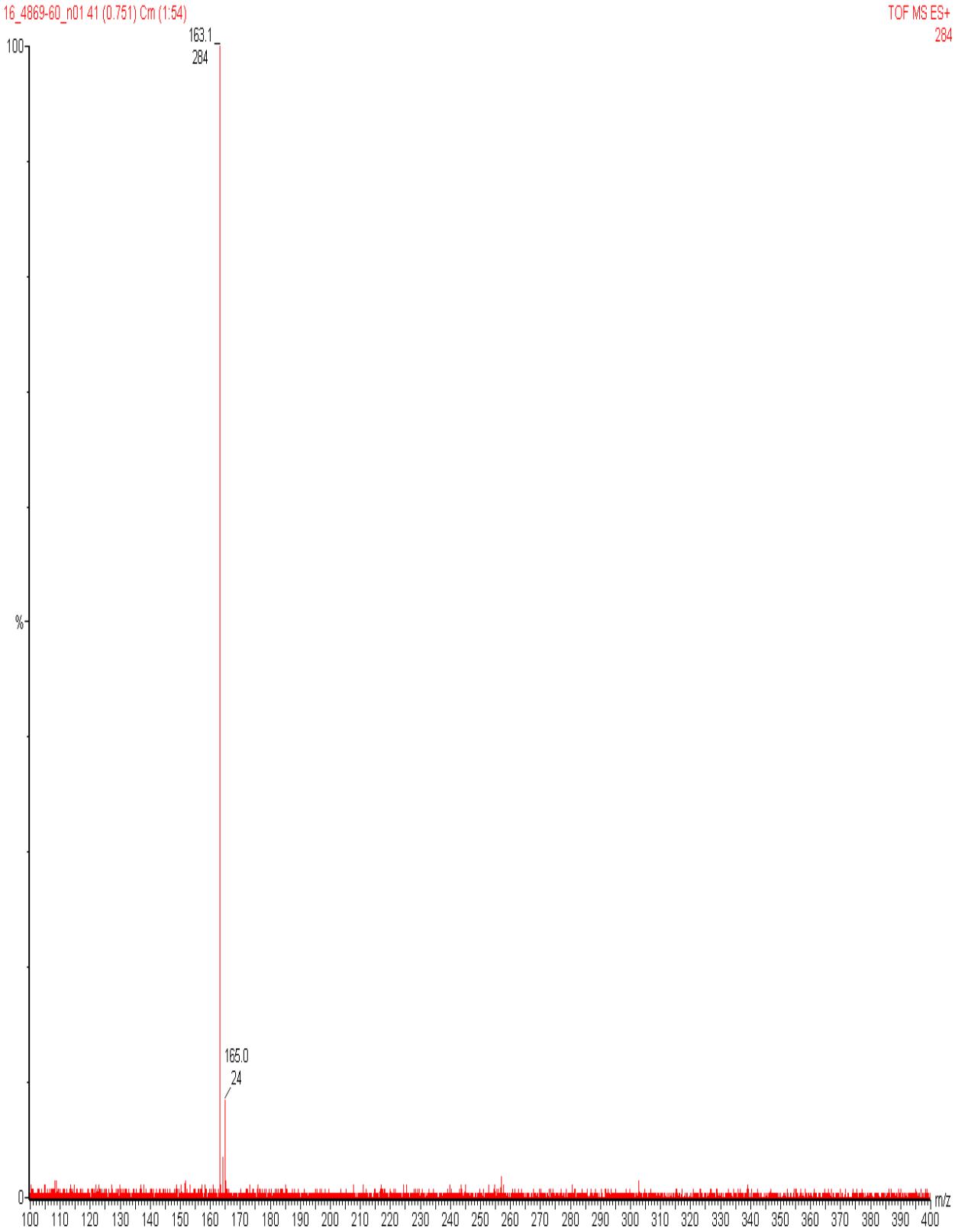

Appendix xli: LC-MS Chromatogram of P6Se (13)

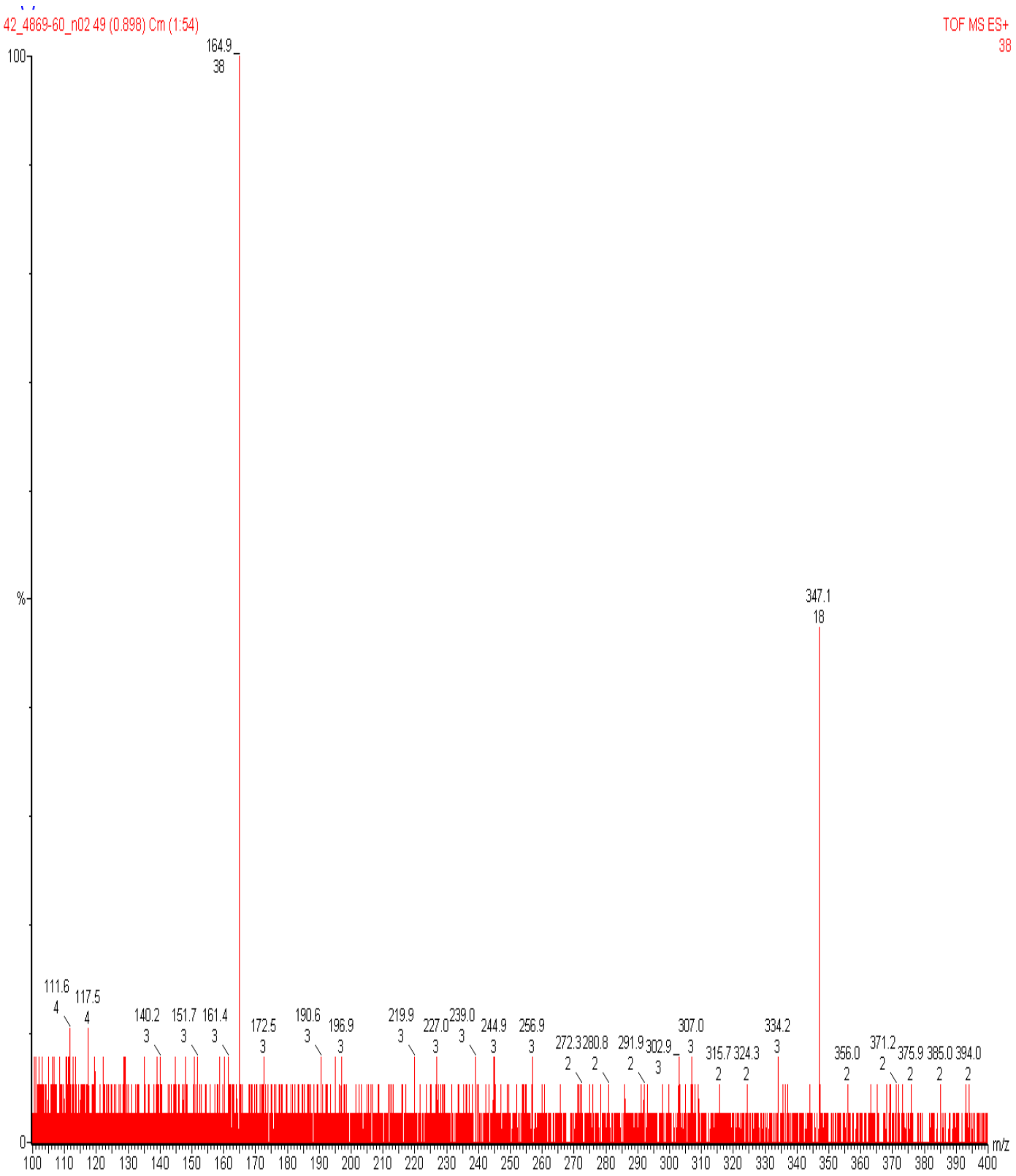

Appendix xlii: LC-MS Chromatogram of P8Sd (27)

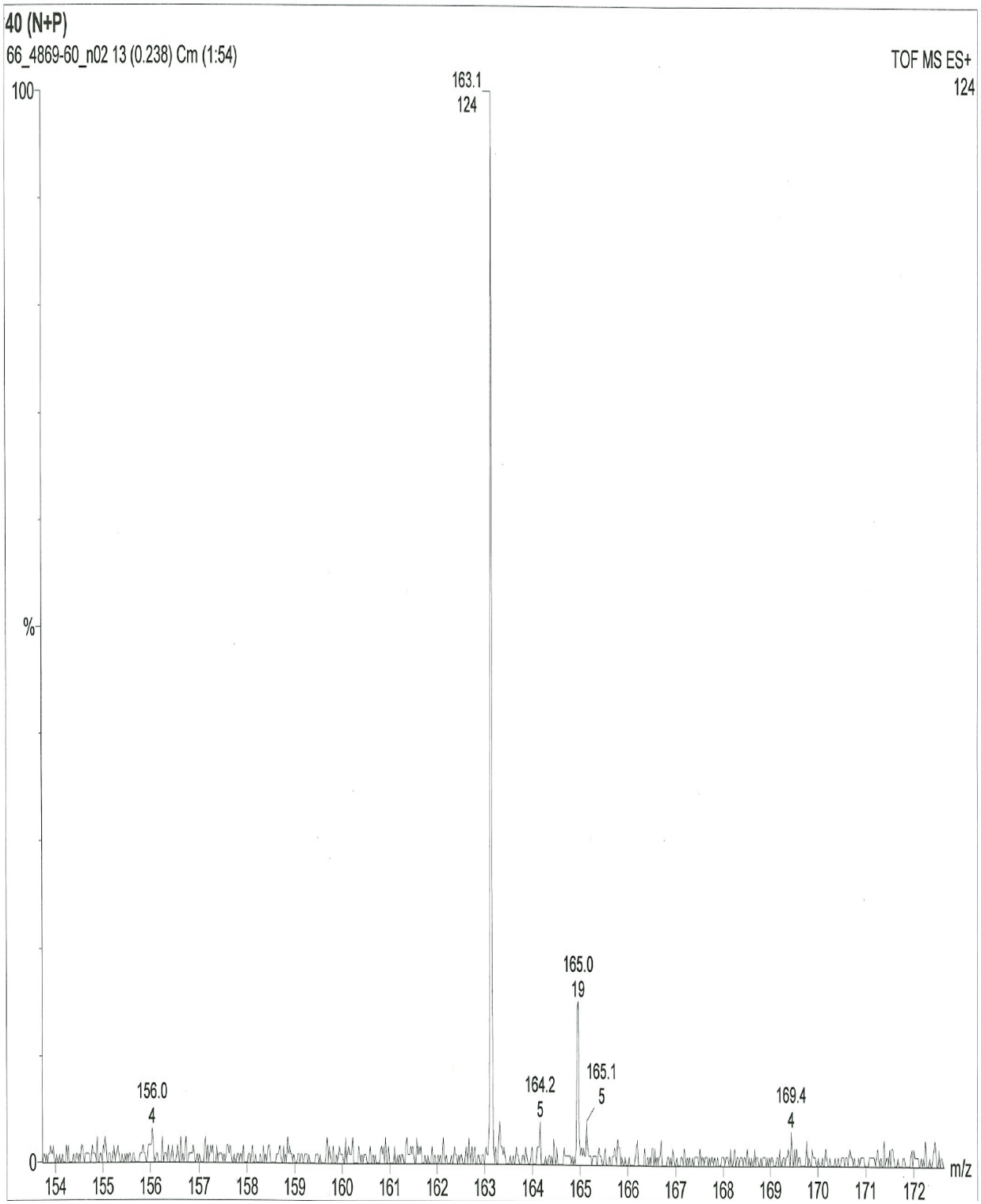

Appendix xliii: LC-MS Chromatogram of P10Sd (38)